

**Environmental processes that control the chemical recovery of
arsenic impacted northern landscapes**

by

Michael John Palmer

A thesis submitted to the
Faculty of Graduate and Postdoctoral Affairs
in partial fulfillment of the requirements for the degree of
Doctor of Philosophy in Geography

Carleton University

Ottawa, Ontario

© 2022

Michael John Palmer

Abstract

Arsenic (As) is a contaminant of global concern because of its toxic and carcinogenic properties. Waste streams associated with gold mining activities have resulted in extensive As pollution of landscapes worldwide. The Yellowknife area in the Northwest Territories, Canada was contaminated by more than half a century of As-bearing atmospheric mining emissions from the roasting of arsenopyrite ore during historical gold ore processing (1938-1999). The environmental footprint from legacy mining emissions persists on the landscape and questions remain about the distribution and fate of As in the local environment. The principal objective of this thesis was to improve our understanding of the environmental processes that control the chemical recovery of As impacted landscapes. Individual field studies were designed to address: a) the distribution, source, and solid-phase speciation of As in Yellowknife area soils; b) the seasonal variation of As in surface waters of shallow lakes; c) the influence of contrasting winter hydrology on the geochemical cycling of As in a shallow lake; and d) the seasonal contributions of terrestrial and aquatic fluxes of As in a contaminated watershed. The combination of mineralogical, geospatial, and statistical tools provided a novel method for determination of geochemical background in soils for areas impacted by legacy mining emissions, including recent unambiguous identification of anthropogenically impacted soils. Year-round investigations of surface waters, sediments, and sediment porewaters provided new insights into seasonal and under-ice processes that influence the mobility and geochemical cycling of As. The evaluation of terrestrial and aquatic As fluxes across a contaminated watershed revealed continued transport of legacy arsenic from catchment soils to lakes, and hydrology mediated within-lake processing and export of arsenic. Thus, climate and hydrology were found to play a fundamental role in the chemical recovery of As impacted lakes.

Acknowledgements

This thesis was supported by many incredible people and organizations. Looking back, I am overwhelmed by the amount of support and encouragement that I received from friends, family, and colleagues when I (ahem, we....) decided, at the age of 40, to abandon a cushy government job, relocate our family from Yellowknife to Ottawa and back to Yellowknife, to pursue something that would probably not make us any richer (financially...).

I blame a lot of this on Heather Jamieson, who fostered my early interest in arsenic and mentored me throughout my pre-PhD and PhD career. Heather has also been a great role model as a scientist and in ensuring that our research addresses relevant questions to society. Supervision from Murray Richardson and John Chételat supported my growth as a scientist and encouraged me through the PhD process. I am indebted to them for their support, guidance, and mentorship. I am looking forward to many future collaborations.

The financial and in-kind support provided by the Department of Environment and Natural Resources (ENR) of the Government of the Northwest Territories (GNWT) was instrumental in developing this project. I am grateful to the Cumulative Impact Monitoring Program (CIMP) and the Water Management and Monitoring divisions of the GNWT for funding the core proposal for this work and for providing warehouse space to conduct all of our field work. Staff at the Taiga Environmental Laboratory provided analytical support, space to prepare samples and equipment, and general laboratory advice. Specific thanks need to be directed to Judy Mah, Glen Hudy, Shalene Manickum, Bruce Stuart, and Brad Koswan for being incredibly helpful and supportive in all of the analytical work. The Northwest Territories Geological Survey hosted me as a visiting student for two years and I thank Steve Kokelj and John Ketchum for making this happen and providing a stimulating work environment.

I greatly appreciate the personal financial support that I received from the W. Garfield Weston Foundation, the Province of Ontario through the Ontario Graduate Scholarship (OGS) program, the Department of Geography and Environmental Studies at Carleton University through the Duncan M. Anderson and Martin Bergmann scholarships, the NSERC Discovery Grants to Murray Richardson and John Chételat, the Aurora Research Institute (ARI) Fellowship Program, and the Northern Scientific Training Program. The support from Aurora College in my final two years was essential to the completion of this project and specific thanks are directed to Joel McAlister, Pippa Seccombe-Hett, and the Professional Development Committee chaired by Dave Porter.

The field work for this project required an incredible amount of horsepower and I am indebted to the many people that joined me in the field, including: Michael Gilday, Ty Hamilton, Jonathon Mackenzie, Dwayne Wohlgemuth, Stefan Goodman, Mike Palmer (a different one!), Jack Panayi, Yvonne Pike, Tim Ensom, Angus Smith, and Claire Marchildon.

The research community in Yellowknife was incredibly supportive and provided much appreciated collegiality, advice, and discussions when I was so far away from my home academic institution. In particular, I extend thanks to Steve Kokelj, Tim Ensom, Ashley Rudy, Kumari Karunaratne, and Ryan Connon.

William Lines and Johanne Black from the Land and Environment Department at the Yellowknives Dene First Nation (YKDFN) supported this project from the beginning and helped to guide this research towards answering questions that matter for the YKDFN.

Many students and staff from Heather Jamieson's lab at Queen's University helped with this project. Thanks are extended to Agatha Dobosz, Chris Schuh, and Anežka Radková for

support and advice during SEM-MLA work in this thesis. Soil sample collection by Kirsten Maitland and Jon Oliver to support the work in Chapter 3 is gratefully acknowledged.

Finally, many, many thanks are due to my family who supported me through this degree. Mom and Dad (James and Liz Palmer) fostered my early curiosities and gave me the confidence to strive for new things. My sister, Ali Fluevog, was a great resource for PhD advice (and laughs). Our kids, Charlie and Pippa, deserve appreciation for putting up with all this arsenic talk and even collecting a few samples. Wendy Lahey was a source of strength that held our young family together and supported my journey as a northern-based scientist.

Thesis supervisor and co-author statements

The authors of each article have read and signed the following statements outlining the role of Michael Palmer as the principal investigator and main author for each publication:

- a) I, John Chételat, as a co-author of “Seasonal variation of arsenic and antimony in surface waters of small subarctic lakes impacted by legacy mining pollution near Yellowknife, NT, Canada”, and “Hydrologic control on winter dissolved oxygen mediates arsenic cycling in a small subarctic lake” acknowledge Mike Palmer as the principal investigator and lead contributing author to these manuscripts. Mike designed the study, conducted the field work, and he was responsible for the data analyses, writing and revisions of the manuscripts. I, John Chételat, contributed to the published articles in the thesis as his supervisor during his doctoral studies in geography. My contribution comprised of advice, assistance and editorial remarks related to the experimental design, field work, analyses and writing of these manuscripts. My activities were entirely consistent with the role of thesis supervisor.

- b) I, Murray Richardson, as a co-author of “Mineralogical, geospatial, and statistical methods combined to estimate geochemical background of arsenic in soils for an area impacted by legacy mining pollution”, “Seasonal variation of arsenic and antimony in surface waters of small subarctic lakes impacted by legacy mining pollution near Yellowknife, NT, Canada”, and “Hydrologic control on winter dissolved oxygen mediates arsenic cycling in a small subarctic lake” acknowledge Mike Palmer as the principal investigator and lead contributing author to these manuscripts. Mike designed the study, conducted the field

work, and he was responsible for the data analyses, writing and revisions of the manuscripts. I, Murray Richardson, contributed to the published articles in the thesis as his supervisor during his doctoral studies in geography. My contribution comprised of advice, assistance and editorial remarks related to the experimental design, field work, analyses and writing of these manuscripts. My activities were entirely consistent with the role of thesis supervisor.

c) I, Heather Jamieson, as a co-author of “Mineralogical, geospatial, and statistical methods combined to estimate geochemical background of arsenic in soils for an area impacted by legacy mining pollution”, “Seasonal variation of arsenic and antimony in surface waters of small subarctic lakes impacted by legacy mining pollution near Yellowknife, NT, Canada”, and “Hydrologic control on winter dissolved oxygen mediates arsenic cycling in a small subarctic lake” acknowledge Mike Palmer as the principal investigator and lead contributing author to these manuscripts. Mike designed the study, conducted the field work, and he was responsible for the data analyses, writing and revisions of the manuscripts. I, Heather Jamieson, contributed to the published articles in the thesis as his supervisor during his doctoral studies in geography. My contribution comprised of advice, assistance and editorial remarks related to the experimental design, field work, analyses and writing of these manuscripts. My activities were entirely consistent with the role of thesis supervisor.

d) I, Marc Amyot, as a co-author of “Hydrologic control on winter dissolved oxygen mediates arsenic cycling in a small subarctic lake” acknowledge Mike Palmer as the principal

investigator and lead contributing author to this manuscript. Mike was responsible for study design, data collection, data analyses, writing and revisions of the manuscript. I, Marc Amyot, was involved in this research as a research partner and investigator. This involvement has included help with the study design, laboratory work and editorial revision of the manuscript. These activities have been entirely consistent with the roles of research partner and investigator.

e) I, Hendrik Falck, as a co-author of “Mineralogical, geospatial, and statistical methods combined to estimate geochemical background of arsenic in soils for an area impacted by legacy mining pollution” acknowledge Mike Palmer as the principal investigator and lead contributing author to this manuscript. Mike was responsible for study design, data collection, data analyses, writing and revisions of the manuscript. I, Hendrik Falck, was involved in this research as a research partner and investigator. This involvement has included help with the study design and editorial revision of the manuscript. These activities have been entirely consistent with the roles of research partner and investigator.

f) I, Jennifer Galloway, as a co-author of “Seasonal variation of arsenic and antimony in surface waters of small subarctic lakes impacted by legacy mining pollution near Yellowknife, NT, Canada” acknowledge Mike Palmer as the principal investigator and lead contributing author to this manuscript. Mike was responsible for study design, data analyses, writing and revisions of the manuscript. I, Jennifer Galloway, was involved in this research as a research partner and investigator. This involvement has included field

collection of data and editorial revision of the manuscript. These activities have been entirely consistent with the roles of research partner and investigator.

g) I, Kirsten Maitland, as a co-author of “Mineralogical, geospatial, and statistical methods combined to estimate geochemical background of arsenic in soils for an area impacted by legacy mining pollution” acknowledge Mike Palmer as the principal investigator and lead contributing author to this manuscript. Mike was responsible for study design, data analyses, writing and revisions of the manuscript. I, Kirsten Maitland, was involved in this research as a research partner and investigator. This involvement has included field collection of data, laboratory work, and editorial revision of the manuscript. These activities have been entirely consistent with the roles of research partner and investigator.

h) I, Jon Oliver, as a co-author of “Mineralogical, geospatial, and statistical methods combined to estimate geochemical background of arsenic in soils for an area impacted by legacy mining pollution” acknowledge Mike Palmer as the principal investigator and lead contributing author to this manuscript. Mike was responsible for study design, data analyses, writing and revisions of the manuscript. I, Jon Oliver, was involved in this research as a research partner and investigator. This involvement has included field collection of data, laboratory work, and editorial revision of the manuscript. These activities have been entirely consistent with the roles of research partner and investigator.

- i) I, Anežka Radková, as a co-author of “Mineralogical, geospatial, and statistical methods combined to estimate geochemical background of arsenic in soils for an area impacted by legacy mining pollution” acknowledge Mike Palmer as the principal investigator and lead contributing author to this manuscript. Mike was responsible for study design, data collection, data analyses, writing and revisions of the manuscript. I, Anežka Radková, was involved in this research as a research partner and investigator. This involvement has included help with the laboratory work and editorial revision of the manuscript. These activities have been entirely consistent with the roles of research partner and investigator.

Copyrighted material and citing material in this thesis

The copyright for all figures from Chapters 3 and 4 is held jointly by the authors and Elsevier Inc. The copyright for all figures from Chapter 5 is held jointly by the authors and the Association for the Sciences of Limnology and Oceanography (ASLO). Elsevier and ASLO allow authors to use their works for teaching and scholarly purposes without having to seek special permission. Authors rights comprise the allowance to include published material in an academic thesis or dissertation, provided that citations and DOI links to the formal publications on ScienceDirect or ASLO are included.

Any citation to the material in this thesis should use the original published article as source.

Material appearing exclusively in this thesis should be cited as follows:

Palmer, M.J. 2022. Environmental processes that control the chemical recovery of arsenic impacted northern landscapes, PhD. Thesis, Carleton University, Ottawa, ON.

Table of contents

Abstract	ii
Acknowledgements	iii
Thesis supervisor and co-author statements.....	vi
Copyrighted material and citing material in this thesis.....	x
Table of contents	xi
List of tables	xvii
List of figures	xviii
Chapter 1: Introduction.....	1
1.1 Mining pollution, landscape recovery, and research justification.....	1
1.2 Purpose	5
1.3 Thesis structure and chapter overview	6
Chapter 2: Background on arsenic mobility and transport	9
2.1 Arsenic speciation in soils, lake sediments and surface waters	9
2.2 Arsenic mobility and transport in terrestrial and aquatic environments	14
2.2.1 Catchment soils as a reservoir and source of arsenic	14
2.2.2 Terrestrial fluxes of As.....	17
2.2.2.1 Metal(loid) catchment transport with snow melt.....	17
2.2.2.2 Metal(loid) catchment transport during the thawing season	19
2.2.2.3 Metal(loid) fluxes during winter and the impact of climate change.....	20
2.2.2.4 Mass export of As from terrestrial catchments.....	20
2.2.3 Aquatic pools and fluxes	22
2.2.3.1 Lakes as reservoirs and sources of arsenic	22
2.2.3.2 Fluxes of As across the sediment-water boundary	24
2.2.3.3 Seasonal variation in lake water arsenic concentrations	26
2.3 Lake hydrology and chemical recovery of lake waters.....	28
2.4 Climate change and the fate of As in aquatic environments.....	29
2.5 Summary and connection with thesis objectives.....	31
Chapter 3: Arsenic in soils of the Yellowknife area: Regional distribution, attribution of source, and estimation of geochemical background	33
Abstract	33

3.1 Introduction	34
3.2 Background	38
3.2.1 Mining history and previous work on soils in the region	38
3.2.2 Study area	40
3.3 Material and methods:.....	41
3.3.1 Origin and distribution of As in soils near legacy point sources of mining emissions	41
3.3.1.1 Field collection	42
3.3.1.2 Total metal(loid) analyses	44
3.3.1.3 Mineralogical analysis.....	45
3.3.2 Estimation of natural background in the Slave Geological Province.....	46
3.3.3 Data analysis.....	46
3.3.3.1 Spatial distribution of As and As mineralogy across the Yellowknife area.....	46
3.3.3.2 Estimating geochemical background for the Slave Geological Province.....	49
3.4 Results	50
3.4.1 Relationships between soil As and distance from legacy mining emission sources	50
3.4.2 Variability in Public Health layer As by terrain type, wind direction, and underlying bedrock geology	52
3.4.3 Solid-phase As speciation in Public Health layer samples.....	55
3.4.4 Geochemical background in the Slave Geological Province.....	57
3.5 Discussion	60
3.5.1 Impacts from legacy mining emissions persist in soils near Yellowknife	60
3.5.2 Variability in Yellowknife area soil As driven by regional and local factors	65
3.5.3 Estimation of geochemical background for the Slave Geological Province	66
3.6 Concluding remarks	68
Chapter 4: Seasonal variation of arsenic and antimony in surface waters of small subarctic lakes impacted by legacy mining pollution near Yellowknife, NT, Canada	70
Abstract	70
4.1 Introduction.....	71
4.2 Materials and Methods.....	74
4.2.1 Environmental setting and background	74
4.2.1.1 Arsenic and antimony pollution in the Yellowknife area, NT, Canada	76
4.2.1.2 Study lakes.....	77
4.2.2 Lake morphometry	78

4.2.3 Water and sediment sampling.....	79
4.2.3.1 Frequent surface water sampling of the four study lakes	79
4.2.3.2 Regional lake water and sediment surveys.....	81
4.2.4 Water column oxygen depletion.....	82
4.2.5 Measuring solute exclusion from lake ice	82
4.2.6 Data analysis.....	83
4.2.6.1 Assessing the relative influence of summer and winter processes in Handle Lake ..	84
4.3 Results	85
4.3.1 Seasonal changes in water column dissolved oxygen	88
4.3.2 The concentration of arsenic and major ions in lake ice	89
4.3.3 Seasonal changes in surface water chemistry.....	89
4.3.4 Seasonal As and Sb mass loading in Handle Lake.....	91
4.3.5 Seasonal changes in inorganic arsenic speciation of surface waters	95
4.3.6 Potential influence of snowmelt on surface water As concentrations and speciation ..	95
4.3.7 Seasonal differences in As, Sb, Fe, and major ions in the regional lake surveys.....	96
4.3.8 Relationship between surface water and near-surface sediment chemistry	96
4.4 Discussion	97
4.4.1 Seasonal changes in surface water As influenced by a combination of physical and biogeochemical processes.....	98
4.4.1.1 The relative influence of biogeochemical processes vs cryo- and evapoconcentration in controlling As concentration and loading in Handle Lake.....	102
4.4.2. Periods of seasonal anoxia alter the oxidation state of surface water arsenic.	102
4.4.3 Changes in surface water Sb concentrations across seasonal redox transitions.....	103
4.5 Conclusions and directions for future research.....	104
Chapter 5: Hydrologic control on winter dissolved oxygen mediates arsenic cycling in a small subarctic lake	107
Abstract	107
5.1 Introduction	108
5.2 Materials and methods	110
5.2.1 Site description	110
5.2.2 Instrumentation.....	112
5.2.3 Sample collection	113
5.2.3.1 Water column samples.....	113

5.2.3.2 Sediment porewaters.....	114
5.2.3.3 Sediment cores.....	116
5.2.4 Lake water and sediment porewater analyses.....	117
5.2.5 Sediment geochemistry and As mineralogy	118
5.3 Results.....	119
5.3.1 Contrasting winter streamflow between 2017-18 and 2018-19.....	119
5.3.2 Dissolved oxygen	120
5.3.3 Depth-weighted mean concentrations of As and Fe.....	121
5.3.4 Water column profiles of As, Fe, and S	123
5.3.5 Water column As during the anoxic to oxic lake water transition in spring 2018	125
5.3.6 Porewater profiles across seasons.....	126
5.3.7 Solid-phase bulk chemistry and changes in As mineralogy at the sediment-water boundary	129
5.4 Discussion	132
5.4.1 Seasonal As cycling coupled with biogeochemical cycling of Fe and S.....	132
5.4.2 The magnitude of winter increase in lake water As is controlled by the position of redox boundaries within the water column.....	135
5.4.3 Oxidation of the water column during the spring transition from anoxic to oxic lake water conditions.....	138
5.5 Conclusions and implications for climate change.....	139
Chapter 6: Terrestrial and aquatic fluxes of arsenic in a subarctic landscape during years with contrasting hydrological conditions.....	141
Abstract	141
6.1 Introduction.....	143
6.2 Materials and Methods	145
6.2.1 Site description	145
6.2.2 Field methods	147
6.2.2.1 Lake and stream water measurements	147
6.2.2.2 Catchment runoff.....	148
6.2.2.3 Sediment fluxes	149
6.2.2.3.1 Mesocosm experiments	149
6.2.2.3.2 Sediment porewater analysis and Fick's First Law of Diffusion	151
6.2.3 Lake water, stream water, catchment runoff and sediment porewaters analysis.....	151

6.2.4 Lower Martin Lake water budget	151
6.2.5 Data analysis.....	153
6.2.5.1 Mass balance estimation.....	153
6.2.5.2 Calculation of sediment As fluxes from field incubations and sediment porewater gradients.....	154
6.3 Results.....	155
6.3.1 Rainfall and streamflow generation.....	155
6.3.2 Stream chemistry and arsenic loading via lake inlet and outlet	156
6.3.3 As inputs from terrestrial catchments.....	156
6.3.4 Changes in lake storage	159
6.3.5 Sediment As fluxes.....	160
6.3.6 Long-term patterns in As fluxes	163
6.4 Discussion	165
6.4.1 Annual fluxes dominated by regional stream hydrology.....	166
6.4.2 Seasonality of watershed As fluxes	169
6.4.2.1 Autumn as a period of watershed quiescence?	169
6.4.2.2 Contrasting winter hydrology drives major differences in watershed fluxes of As	170
6.4.2.3 Spring as a period of major watershed flux of As	171
6.4.2.4 Summer fluxes dominated by streamflow and internal loading from contaminated sediments	172
6.5 Implications for recovery of impacted lakes	172
Chapter 7: Conclusions and directions for future research.....	174
7.1 Key findings and contributions	174
7.2 Future research directions	179
7.3 Concluding statement.....	183
References.....	185
Appendices.....	205
Appendix A: Supporting information for Chapter 3 - Arsenic in soils of the Yellowknife area: Regional distribution, attribution of source, and estimation of geochemical background.....	205
Appendix B: Supporting information for Chapter 4 - Seasonal variation of arsenic and antimony in surface waters of small subarctic lakes impacted by legacy mining pollution near Yellowknife, NT, Canada.....	217
Appendix C: Supporting information for Chapter 5 - Hydrologic control on winter dissolved oxygen mediates arsenic cycling in a small subarctic lake	231

Appendix D: Supporting information for Chapter 6 - Terrestrial and aquatic fluxes of arsenic
in a subarctic landscape during years with contrasting hydrological conditions 240

List of tables

Table 2.1	List of common As-bearing minerals and compounds and their chemical formulae. A more complete list can be found in Table 2 from Drahota and Fillipi (2009).....	12
Table 3.1.	Summary statistics for till As concentrations (mg kg^{-1}) from Kerr and Knight (2005) excluding samples within 20 km of Yellowknife, representing natural background in the region. Upper fence is calculated as the 3 rd quartile + 1.5 x IQR (interquartile range).....	60
Table 4.1.	Physical characteristics of the four study lakes.....	77
Table 4.2.	Summary statistics for select elements and water quality parameters at the four detailed study sites.....	88
Table 4.3.	Mass balance and sediment-water flux estimates in Handle Lake for As and Sb.....	94
Table 6.1.	Seasonal mass fluxes of As (kg) in the Lower Martin Lake watershed partitioned into the following seasons: fall (Sep. 1 – Oct. 31), winter (Nov. 1 – Mar. 31), spring (Apr. 1 – May 31), and summer (June 1 – Aug. 31). Annual values in parentheses refer to the percentage of individual annual fluxes of the total input or output of As in the watershed.....	162
Table 6.2.	Measured fluxes for select elements during experimental sediment incubations. Treatments include exposure to different temperature and redox conditions. See supplemental information for plots for each element during each treatment.....	162
Table 6.3.	Theoretical sediment fluxes calculated using porewater As measurements and Fick's Law. As fluxes represent the mean flux \pm 1 standard deviation.....	163

List of figures

Figure 2.1: Conceptual diagram illustrating seasonal watershed pools and fluxes of As in a subarctic shield environment.....	10
Figure 2.2: Conceptual diagram outlining the main biogeochemical processes controlling As cycling within lakes.....	25
Figure 3.1: Arsenic concentrations in Public Health layer samples (0-5 cm) within a 30 km radius of Yellowknife (N = 407).....	43
Figure 3.2: The concentration of arsenic in soils with distance from the historical Giant Mine roaster colour coded by underlying bedrock classification for: a) the Public Health layer (0-5 cm); and b) soils 10 – 40 cm below the soil surface. Panel c) The presence and absence of As ₂ O ₃ in a subset of Public Health layer soils (N = 82) as determined by SEM.....	51
Figure 3.3: Soil core As profiles from sites along a distance gradient from Giant Mine in 5 km intervals: a) < 5 km; b) 5-10 km; c) 10-15 km; and d) 15-20 km.....	53
Figure 3.4: Arsenic concentrations in Public Health layer samples by terrain unit, wind direction, and bedrock lithology.....	55
Figure 3.5: Total As and As ₂ O ₃ (mg kg ⁻¹) in Public Health layer samples (0-5 cm) with distance from the historic Giant Mine roaster.....	56
Figure 3.6: Distribution of As in soils and till in: a) the Slave Geological Province; and b) the Yellowknife area. All samples collected between 10 and 70 cm below the soil surface.....	58
Figure 3.7: Tukey boxplots for As in silt and clay fraction of till (data > 20 km from YK) from the Kerr and Knight (2005) dataset.....	61
Figure 4.1: Study area (left panel) and bathymetry of the four study lakes: a) BC-20; b) Handle Lake; c) Lower Martin Lake; and d) Long Lake.....	75
Figure 4.2: The seasonal variation in As, Fe, Mn, and dissolved oxygen (saturation %) and the proportion of inorganic arsenic species in surface waters of the four study lakes, July 2014 to September 30, 2016.....	86
Figure 4.3: Concentrations of As, Sb and the sum of major ions in the filtered fraction (< 0.45 µm) of surface waters for each of the study sites, July 2014 to November 2016...	87
Figure 4.4: Relationships between selected elements (As, Fe, and the sum of major ions) and dissolved oxygen in surface waters for: a) BC-20; b) Handle Lake; c) Lower Martin Lake; and d) Long Lake.....	92

Figure 4.5:	Relationships between seasonal change in surface water concentrations of elements (as the percent change in water chemistry between fall and late winter) and maximum lake depth in 31 lakes within 30 km of Yellowknife, including: a) As; b) Fe; c) Sb; and d) sum of major ions.....	97
Figure 5.1:	Map of study area and sampling locations. LMLA and LMLB are locations of sediment coring, sediment porewater sampling and lake-water chemistry profiles.....	112
Figure 5.2:	Daily mean streamflow ($\text{m}^3 \text{s}^{-1}$) at the outlet of Lower Martin Lake (ECCC, 2019; station 07SB013) and dissolved oxygen levels (mg L^{-1}) measured at the lake inlet, September 2017 to October 2019.....	120
Figure 5.3:	Time-series of a) total filtered As and dissolved oxygen; and c) total filtered Fe at two locations in Lower Martin Lake, September 2017 to July 2019.....	121
Figure 5.4:	Water column profiles of: a) filtered As, b) inorganic As speciation, and c) filtered Fe during consecutive years at LMLA.....	124
Figure 5.5:	Water column concentrations of filtered: a) S(-II); b) Fe(II); and c) As(III) during winter 2019 at LMLA and LMLB. Note the water column did not fully reach anoxia in 2019.....	125
Figure 5.6:	a) Dissolved oxygen measured 30 cm above the sediment boundary and the specific conductivity of surface waters. b) Water column measurements of filtered As, the proportion of inorganic As species, dissolved oxygen and specific conductivity at LMLB during the snowmelt period. c) The proportion of total inorganic As as As(III) and the particulate fraction of total As during the snowmelt period at LMLA.....	127
Figure 5.7:	Mean and standard deviation of porewater concentrations of: a) filtered As; and b) filtered Fe in the open-water season (2017: N = 4; 2018: N = 6), early winter (2017: N = 2; 2018: N = 3), and late winter (2018: N = 4; 2019: N = 2). Bottom panels represent: c) open-water; and D) late-winter SO_4 and $\sum\text{H}_2\text{S}$ concentrations in porewaters during the second year of the study (2018-19).....	128
Figure 5.8:	Solid-phase chemistry of duplicate sediment cores (LMLA and LMLB) during the open-water season (September 2017) and under ice (April 2018), including a) As; b) Fe; and c) S. Error bars represent the standard deviation of concentrations at discrete intervals from duplicate cores. Inset panels highlight near surface (0-5cm) concentrations of elements. D) The mass distribution of As in solid-phase host minerals in surface sediments collected in September 2017 and April 2018 and at the As maxima for April 2018.....	130
Figure 5.9:	Conceptual model of the geochemical cycling of As in Lower Martin Lake and the influence of contrasting winter hydrological conditions.....	137

Figure 6.1: Maps of the study area. The left panel includes bathymetric data for Lower Martin Lake, the perimeter of the local catchment area, and the location of the lake inlet and outlet. The top right panel shows the location of Lower Martin Lake in relation to Yellowknife, Pocket Lake, Great Slave Lake, and the historical mine roasters at Giant and Con mines..... 146

Figure 6.2: a) Mean daily streamflow and approximately bi-weekly measurements of total As in surface waters at the inlet and outlet of Lower Martin Lake, September 2017 to September 2019; b) annual cumulative inflow and As mass at the inlet of Lower Martin Lake for September 2017-18 and September 2018-19; annual cumulative discharge and As mass at the outflow of Lower Martin Lake, September 2017-18 and September 2018-19..... 157

Figure 6.3: The hydrology and runoff chemistry from the Pocket Lake subcatchment..... 158

Figure 6.4: Lake volume (m³), depth-integrated lake water As concentration (µg L⁻¹) and the mass of As (kg) stored in the water column of Lower Martin Lake September 2017 to September 2019..... 160

Figure 6.5: Cumulative mass fluxes in Lower Martin Lake for the two consecutive study years..... 161

Figure 6.6: a) Hydrograph, As concentration, and annual As loading in Baker Creek, near the outlet of Lower Martin Lake, May 2010 to May 2021. Annual As loads were calculated from interpolated daily As concentration and daily mean streamflow measurements from May 1- April 30; b) Relationship between annual As export and total annual discharge in Baker Creek (near the outlet of Lower Martin Lake); and c) Relationship between mean annual As concentration in Baker Creek and WRT in Lower Martin Lake..... 164

Chapter 1: Introduction

The research presented in this thesis enhances our understanding of the environmental processes that control the chemical recovery of arsenic (As) impacted landscapes. All of the studies were undertaken in the Yellowknife area of the Northwest Territories, Canada, a region that was impacted by more than 60 years of As-rich atmospheric emissions from ore processing associated with gold mining (1938-1999). Although atmospheric As emissions ended in 1999, the legacy of As pollution continues to persist in the environment. This introductory chapter provides justification for the specific research objectives in the thesis and outlines the four primary research chapters of the thesis. A brief overview of the mining history in the Yellowknife region is included, and this is described in more detail in the study area sections of the individual research chapters.

1.1 Mining pollution, landscape recovery, and research justification

Arsenic is one of the World Health Organization's ten chemicals of major public health concern due to its widespread occurrence and its toxic and carcinogenic properties (WHO, 2010). The greatest threats to public health are through exposure to contaminated drinking water and the use of contaminated water for irrigation of food crops (Chatterjee et al., 1995). Consequently, there has been considerable attention directed at understanding the extent of contamination in global water resources and the processes that control the mobility and fate of As in these environments (Smedley and Kinniburgh, 2002; Wang and Mulligan, 2006). While many of these source water impacts are the result of natural processes, such as the dissolution of As-bearing minerals in groundwater aquifers (Ahmed et al., 2004), there has also been substantial contamination of

surface waters from the pollution streams of resource extraction industries, such as mining, oil and gas production, and the historical application of As-bearing pesticides and fertilizers. In many cases, particularly prior to the implementation of improved treatment technologies and tighter environmental regulations in the 1970's, As-bearing waste from these operations was distributed broadly across the landscape, resulting in enduring environmental legacies in many parts of the world, including northern Canada (Houben et al., 2016; McMartin et al., 1999; Nriagu, 1983; Wagemann et al., 1978).

The Yellowknife region in the Northwest Territories, Canada, represents one of the largest environmental legacies of As pollution in the world. More than 20,000 tonnes of As-bearing emissions were dispersed atmospherically across the Yellowknife area from 1938 to 1999 from ore processing activities associated with two gold mines in the region (Giant Mine (1948-2004) and Con Mine (1938-2003)). The majority (85%) of As-bearing emissions were released between 1948 and 1958, when daily emissions from Giant Mine ranged from 2 to 7 tonnes per day (Bromstad et al., 2017; Jamieson, 2014). The implementation of pollution control technologies, starting with a baghouse in 1958, led to substantial reduction in As emissions, and by the 1990s emissions were limited to less than 4 tonnes per year (Bromstad et al., 2017; Wrye, 2008). The extensive atmospheric As pollution in the Yellowknife region left an enduring environmental legacy on the landscape and elevated concentrations of As remain in soils (Jamieson et al., 2017), lake waters (Houben et al., 2016), and lake sediments (Galloway et al., 2017) more than 50 years after the bulk of emissions were released.

Globally, there has been considerable research dedicated to delineating the distribution of pollutants in areas impacted by point source emissions (e.g. Blais et al., 1999; McMartin et al., 1999). Typically, these studies focus on the geospatial distribution of pollutants through

concentration-distance relationships and mapping of regional survey data (e.g. Reimann and De Caritat, 2005). The regional impact of As-bearing mining emissions in the Yellowknife area has been documented since vegetation and soil surveys by Hocking et al. (1978). The regional distribution of As in soils has been recently revisited by Jamieson et al. (2017). Additional regional surveys have explored the contemporary distribution of As in lake waters and lake sediments (Galloway et al., 2017; Houben et al., 2016; Palmer et al., 2015), with impacts from mining emissions recorded in lake sediments at least as far as 80 km downwind (Jasiak et al., 2021). While geospatial characterization of pollutant distribution in areas of point sources of pollution is a powerful tool, there is often ambiguity surrounding the source of elevated pollutant levels in areas where natural geological enrichments of elements may be co-located with point sources emissions. This is particularly evident in the Yellowknife area, where elevated concentrations of As have typically been attributed to natural sources associated with As enrichment in underlying bedrock geology (Cheney et al., 2020; GNWT, 2003). Additional approaches to differentiate between geogenic and industrial sources of As are required in the Yellowknife area and would be relevant to other regions impacted by point sources of pollution.

Understanding and managing the chemical recovery of landscapes that have been impacted by As pollution requires identification of the factors that control the mobility and transport of As within and between the various environmental compartments on the landscape. A considerable amount of attention has been paid to the physical and biogeochemical processes that influence As mobility within individual ecosystem compartments, including soils (e.g. *Bowell 1994; Peryea & Creger 1994; Smith et al. 1998*), lake sediments (e.g. *Kneebone et al. 2002; Root et al. 2007*), and lake waters (e.g. *Barrett et al., 2019; Martin and Pedersen, 2002*), however, very little attention has been directed at understanding seasonal variations in the mobility and flux of As within and

between individual environmental compartments. Seasonality is a central characteristic of northern environments, where lakes are ice covered and catchment soils can be frozen for much of the year. While there has been substantial research directed at understanding the geochemical cycling of As in aquatic environments, including fluxes of As across the sediment-water boundary (Andrade et al., 2010; Kneebone et al., 2002; Martin and Pedersen, 2002), there is little published literature on the role that winter ice cover plays on the geochemical cycling of As in lakes. To date, most research related to the cycling of As in aquatic environments near Yellowknife has taken place in the open water season (Andrade et al., 2010; Leclerc et al., 2021; Schuh et al., 2018; Van Den Berghe et al., 2018). In light of recent work highlighting the importance of under ice conditions on the cycling of redox sensitive metal species (Joung et al., 2017; Schroth et al., 2015), under-ice investigations are warranted to develop our understanding of seasonal As dynamics in the Yellowknife area.

A holistic understanding of landscape recovery requires studies that integrate processes across watersheds, including terrestrial-aquatic fluxes, within-lake processes, and stream inflow and export. Integrative mass balance studies provide essential insights into the transport, fate, and recovery of landscapes from metal pollution (Landre et al., 2010; Semkin et al., 2005). While there have been individual studies focused on the export of As from contaminated terrestrial catchments (e.g. Erbanova et al., 2008; Novak et al., 2011) or along lake chains (e.g. Aurilio et al., 1994; Hemond, 1995), there is a paucity of studies that use a whole watershed approach and evaluate the seasonal importance of these partitioned processes. There is a particular need for an integrative watershed approach in northern environments as these area are undergoing rapid change through shifts in hydrological processes and pathways (McKenzie et al., 2020; Walvoord and Kurylyk, 2016), and lake thermal regimes and productivity (Woolway et al., 2020).

Limnological and hydrological change will likely alter the cycling and transport of As in impacted environments. Evaluating the seasonality and relative importance of watershed fluxes will be critical in furthering our understanding of the recovery trajectory for As impacted landscapes near Yellowknife in a changing climate.

1.2 Purpose

The overarching purpose of this thesis is to improve our understanding of environmental processes that influence the recovery of lakes from As pollution. This information will be useful for resource managers tasked with continued monitoring of As impacted landscapes, particularly in the Yellowknife region. The individual research studies in this thesis span terrestrial and aquatic compartments across the landscape, but are linked by their common goal to improve our understanding of the mobility, cycling, and fate of As along the landscape continuum from catchment soils to lake outlets.

The seven objectives of this thesis are outlined below. The associated thesis chapters are included in parentheses.

- 1) Describe the distribution and mineralogy of As in near-surface soils in the Yellowknife area to determine the geogenic and mining associated contributions of As to soils (*Chapter 3, Arsenic in soils of the Yellowknife area: Regional distribution, attribution of source, and estimation of geochemical background*);
- 2) Develop new approaches to estimate the range of geochemical background for As in areas impacted by legacy As emissions (*Chapter 3, Arsenic in soils of the Yellowknife area: Regional distribution, attribution of source, and estimation of geochemical background*);

- 3) Contrast the seasonal variation of two roaster derived pollutants (As and Sb) in surface waters of shallow lakes near Yellowknife, NT (*Chapter 4, Seasonal variation of arsenic and antimony in surface waters of small subarctic lakes impacted by legacy mining pollution near Yellowknife, NT*);
- 4) Investigate seasonal controls on the geochemical cycling of As in shallow subarctic lakes (*Chapter 4 and Chapter 5: Hydrologic control on winter dissolved oxygen mediates arsenic cycling in a small subarctic lake*);
- 5) Investigate the influence of winter hydrology on the geochemical cycling of As in shallow lakes (*Chapter 5: Hydrologic control on winter dissolved oxygen mediates arsenic cycling in a small subarctic lake*);
- 6) Compare the magnitude and timing of terrestrial and aquatic As fluxes to a lake under different hydrological conditions (*Chapter 6: Terrestrial and aquatic watershed fluxes of arsenic in a subarctic landscape during years with contrasting hydrological conditions*);
- 7) Describe long-term patterns in As export from a contaminated watershed to elucidate how changing hydrological conditions associated with climate change may influence the recovery of As impacted watersheds (*Chapter 6: Terrestrial and aquatic watershed fluxes of arsenic in a subarctic landscape during years with contrasting hydrological conditions*).

1.3 Thesis structure and chapter overview

This thesis is structured in an integrated manuscript format. Chapters 1 and 2 provide introductory and background material that form the scientific basis for the studies presented in chapters 3, 4, 5, and 6. These research study chapters are composed of standalone manuscripts that are published works or are intended for publication soon after the completion of the thesis. Each of the four

independent studies improves our knowledge regarding the origin, distribution, mobility, and fate of arsenic in subarctic landscapes. Chapter 7 provides a summary of the main findings in the specific chapters and highlights areas in need of future research. Specific details on the publication status of the research chapters are provided below:

Chapter 3: Arsenic in soils of the Yellowknife area: Regional distribution, attribution of source, and estimation of geochemical background: This chapter was published as a journal article in *Science of the Total Environment* and the original material should be cited as:

Palmer, M.J., Jamieson, H.E., Radková, A, Richardson, M., Maitland, K., Oliver, J., Falck, H. 2021. Mineralogical, geospatial, and statistical methods combined to estimate geochemical background of arsenic in soils for an area impacted by 60 years of mining pollution. *Science of the Total Environment*, 776. <https://doi.org/10.1016/j.scitotenv.2021.145926>

Chapter 4: Seasonal variation of arsenic and antimony in surface waters of small subarctic lakes impacted by legacy mining pollution near Yellowknife, NT: This chapter was published as a journal article in *Science of the Total Environment* and the original material should be cited as:

Palmer, M.J., Chételat, J., Richardson, M., Jamieson, H.E., Galloway, J. 2019. Seasonal variation of arsenic and antimony in surface waters of small subarctic lakes impacted by legacy mining pollution near Yellowknife, NT, Canada. *Science of the Total Environment*, 684: 326-339. <https://doi.org/10.1016/j.scitotenv.2019.05.258>

Chapter 5: Hydrologic control on winter dissolved oxygen mediates arsenic cycling in a small subarctic lake: This chapter was published as a journal article in *Limnology and Oceanography* and the original material should be cited as:

Palmer, M.J., Chételat, J., Jamieson, H.E., Richardson, M., and Amyot, M. 2020. Hydrologic control on winter dissolved oxygen mediates arsenic cycling in a small subarctic lake. *Limnology and Oceanography*, 66: 30-46. <https://doi.org/10.1002/lno.11556>

Chapter 6: Terrestrial and aquatic fluxes of arsenic in a subarctic landscape during years with contrasting hydrological conditions: This chapter is being prepared for journal publication with a series of co-authors and will be submitted shortly after completion of this thesis. The expected citation is:

Palmer, M.J., Richardson, M., Chételat, J., Spence, C., Jamieson, H.E., and Connon, R. Terrestrial and aquatic fluxes of arsenic in a subarctic landscape during years with contrasting hydrological conditions. Journal to be determined.

Chapter 2: Background on arsenic mobility and transport

This chapter provides background on the processes that influence the mobility and transport of As in terrestrial and aquatic environments which are investigated in subsequent manuscript-based chapters. Focus is directed to published literature from subarctic shield environments where available. Particular emphasis is devoted to exploring the role of winter conditions on As mobility in lakes, since this has been generally underexplored, yet recent studies have highlighted the dynamic and important role that winter plays in annual lake processes for other elements (e.g. Block et al., 2019; Denfeld et al., 2018). Chapter 2 ends with a description of how specific research gaps will be addressed by this thesis. The mass flux diagram in Figure 2.1 provides a framework for the chapter and presents a conceptual transport model for As in a Precambrian shield environment that has been impacted by atmospheric As pollution. The Precambrian shield is used as the landscape for discussion since this is the area of focus for this thesis and the mining of metal sulfide ores in this region has resulted in some of the most widespread contamination from point source atmospheric As pollution in the world (Hocking et al., 1978; Houben et al., 2016; McMartin et al., 1999; Nriagu, 1983). The various environmental compartments are identified as pools on the landscape, which serve as sinks (reservoirs) where As can accumulate. These landscape pools can become sources (via flow transport, i.e. a flux) to lower landscape components depending on their connection to landscape hydrological processes and the proportion of As in the pool that is available for transport.

2.1 Arsenic speciation in soils, lake sediments and surface waters

The basic chemistry of As is important because this fundamentally controls its mobility. Arsenic occurs in four oxidation states (-III, 0, +III, and +V) and as both inorganic and organic

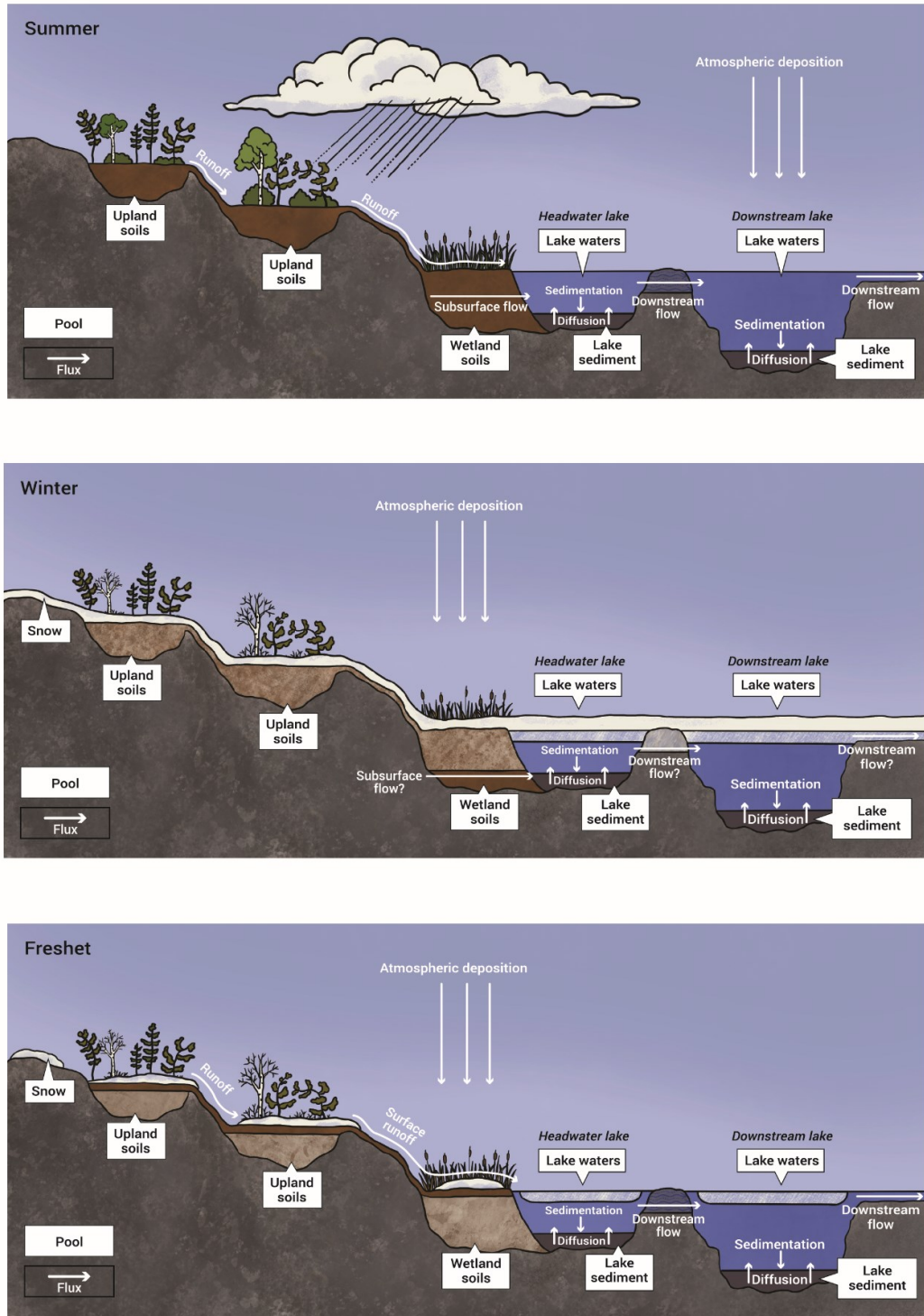


Figure 2.1: Conceptual diagram illustrating seasonal watershed pools and fluxes of As in a subarctic shield environment.

species (Wang and Mulligan, 2006). The inorganic species of As (arsenite [As(III)] and arsenate [As(V)]) are typically considered more toxic to biota than the major organic species (monomethylarsonic acid (MMAA), dimethylarsinic acid (DMAA), and arsenobetaine) (Chatterjee et al., 1995; Smedley and Kinniburgh, 2002). Of these inorganic species As(III) is generally considered more toxic than As(V) (Chatterjee et al., 1995; Smedley and Kinniburgh, 2002).

Inorganic As species dominate in abiotic freshwater environments and are usually present as oxyanions of As(V) and As(III). Arsenate is typically stable in oxidizing environments, such as well oxygenated surface waters and soils, while As(III) predominates in reducing environments, such as anoxic waters of the hypolimnion and porewater within lake sediments (Smedley and Kinniburgh, 2002). The proportion of MMAA and DMMA is low in most freshwater environments but increases where there is a possibility of biomethylation, such as warm nutrient and organic rich ponds (Wang and Mulligan, 2006). Arsenobetaine is relatively non-toxic and rarely found in soils and freshwaters, but is common in marine biota, where it is frequently referred to as “fish arsenic” because of its prevalence in seafood (Kaise and Fukui, 1992; Taylor et al., 2013).

In the solid phase, As is typically incorporated into the structure of minerals, adsorbed as a complexation, or co-precipitated with other elements such as iron (Fe) and sulfur (S) (Cullen and Reimer, 1989). Some of the most common As minerals and compounds are listed in Table 2.1 and include primary As minerals, derived from natural or anthropogenic processes, and secondary As minerals, which typically form as authigenic reprecipitation products from the dissolution of primary As minerals.

Table 2.1 List of common As-bearing minerals and compounds and their chemical formulae. A more complete list can be found in Table 2 from Drahotka and Fillipi (2009).

	Common primary As minerals/compounds	Common secondary As minerals
Geogenic origin	Arsenopyrite (FeAsS) Pyrite (FeS ₂) Enargite (Cu ₃ AsS ₄) Realgar (AsS) Orpiment (As ₂ S ₃) Tennantite ((Cu,Ag,Fe,Zn) ₁₂ As ₄ S ₁₃)	As adsorbed to metal (Fe, Mn, Al) (oxy)hydroxides Realgar (AsS) Orpiment (As ₂ S ₃) As-bearing framboidal pyrite (FeS ₂) Scorodite (FeAsO ₄ ·2H ₂ O)
Anthropogenic origin	Arsenic trioxide (As ₂ O ₃) Lead arsenate (PbHAsO ₄) Calcium arsenate (Ca ₃ (AsO ₄) ₂) Sodium arsenite (NaAsO ₂)	

Arsenic can also exist as arsine gas (AsH₃) but is highly unstable except under extremely reducing conditions (Cullen and Reimer, 1989). Recent advances in the remediation of As contaminated water have demonstrated the microbial conversion of dissolved As species to arsine gas, which is then released to the atmosphere at non-toxic levels, highlighting its potentially important role in environmental remediation in the future (Hayat et al., 2017).

The mobility of As in all media (i.e. soils, sediments, and water) is controlled by redox geochemistry, and precipitation-dissolution and adsorption-desorption reactions, which can be mediated by microbes (Cheng et al., 2009). Therefore, considering the co-existing physical, chemical, and biological conditions is critical in understanding the speciation and stability of As in both solid and dissolved phases. Since redox conditions in soils and sediments can be transient,

As can be repeatedly mobilized from the solid to aqueous phase and resequenced in new mineral forms with changes in the surrounding physical and chemical environment.

The mobility of As in the environment is largely coupled with the biogeochemical cycling of Fe, Mn, S, and dissolved organic matter (Bauer and Blodau, 2006; Couture et al., 2010; Kneebone et al., 2002). Under oxic conditions, Fe- and Mn-(oxy)hydroxide minerals are stable and are effective at scavenging As(V) from solution via adsorption (Bowell 1994; Smith et al. 1998; Drahota et al. 2012). Under neutral pH and well oxidized conditions As adsorption to Fe- and Mn-(oxy)hydroxides is an effective method of reducing As mobility in soils and sediments and has been used effectively as a remediation method to reduce aqueous concentrations of As in soil and sediment porewaters (Kneebone et al., 2002; Root et al., 2007). Under anoxic conditions and in the presence of an electron donor such as labile organic matter, the reductive dissolution of Fe (oxy)hydroxides releases As, as As(III), into the dissolved phase. If reducing conditions persist and the system moves along the redox cascade toward sulfate reduction, the coexistence of dissolved sulfides and As(III) can lead to the removal of As from solution through the precipitation of As–S mineral phases and/or Fe–S minerals that can adsorb or incorporate As into their structure (Bostick and Fendorf, 2003; O’Day et al., 2004; Zhang et al., 2014).

The mobility of As can also be influenced by competition between As and several other ions for sorption sites in soils and sediments. Arsenate is a phosphate (PO_4) analog, and PO_4 often outcompetes As(V) for sorption sites, thus facilitating desorption of As(V) when high concentrations of PO_4 are present (Bolan et al., 2013; Sørensen et al., 2012). High amounts of dissolved organic matter, such as fulvic acids, can also lead to increased As in solution by stimulating the desorption of As from metal oxides through enhanced competition for adsorption sites between organic anions and As(V) (Bauer and Blodau, 2006; Bowell, 1994). Recent field and laboratory

studies have provided evidence of As(III) and As(V) binding to natural dissolved organic matter, which alters the environmental mobility, fate, and toxicity of As (Buschmann et al., 2006; Hoffmann et al., 2014; Mikutta and Kretzschmar, 2011). Further, the formation of thiolated As in aquatic systems with elevated As has been noted, particularly in environments rich in OM and sulfur, and these complexes further complicate the prediction of As mobility (Couture et al., 2013; Kumar et al., 2020; ThomasArrigo et al., 2016).

2.2 Arsenic mobility and transport in terrestrial and aquatic environments

2.2.1 Catchment soils as a reservoir and source of arsenic

Catchment soils represent an important reservoir of metal(loid)s on the landscape since they contain the weathered products of nearby mineralized zones and are frequently the setting for the deposition of waste from industrial activities. Arsenic can accumulate rapidly in soils from anthropogenic sources if there is limited depletion through leaching, plant uptake and erosion (Smith et al., 1998). Soils can act as both a sink and a source of As on the landscape, their specific role influenced by both biogeochemical processes occurring in the soils and hydrological processes acting on the catchment.

Arsenic concentrations are typically low in uncontaminated soils (< 5 mg/kg) and vary with soil type depending on the nature of the parent material (Smith et al. 1998; Smedley & Kinniburgh 2002). Arsenic concentrations may be naturally elevated near mineralized zones, where As is often used as a pathfinder element in mineral exploration for metal sulfide deposits. In a review of the use of As as an indicator element for geochemical exploration, Boyle and Jonasson (1973) reported average concentrations of As in soils near metal sulfide deposits of 126 mg/kg, and as high as 8000 mg/kg. In the Yellowknife area, concentrations as high as 1910 mg/kg have been

reported in tills near mineral showings in the Yellowknife Greenstone Belt (Kerr, 2001). While concentrations in soils near mineralization sources may be substantially elevated due to the weathering of nearby parent material, these anomalies are typically highly localized (Boyle and Jonasson, 1973; Tanaka, 1988).

Arsenic emissions from mining activities, coal-fired power generation, and the broad application of As-bearing pesticides and herbicides (e.g. calcium arsenate, lead arsenate, sodium arsenite, arsenic trioxide) have resulted in the deposition of As across wide areas in many parts of the world. Common to these applications is the extensive dispersal of As on the landscape and the accumulation of As-bearing compounds at the soil surface upon deposition (e.g. Bromstad et al., 2017; Drahota et al., 2012). Arsenic concentrations can reach as high as several thousand mg/kg As in these areas (Bromstad et al., 2017; Drahota et al., 2012; McMartin et al., 1999; Smedley and Kinniburgh, 2002). The surface enrichment of As is a common characteristic of soil profiles in impacted areas, despite the theoretically high solubility rates of many anthropogenically derived As compounds (e.g. arsenic trioxide, lead arsenate, sodium arsenite) (Bromstad et al., 2017; Drahota et al., 2012; Smedley and Kinniburgh, 2002).

The mobility of arsenic in the soil environment is controlled by the mineralogy and solubility of the As hosting mineral and the physical, chemical, and biological conditions in the surrounding soil. In soils impacted by anthropogenic sources, examples exist across a spectrum of solubility, where As has been observed to dissolve rapidly from the host compound and reprecipitate as more environmentally stable secondary minerals (Cutler et al., 2013) or where dissolution can be slow and the original As hosting compound can persist on the landscape for decades (Bromstad et al., 2017). Consequently, it is critical to understand both the solid phase speciation of As in soils and the surrounding environmental conditions.

The wetting of soils can lead to reductive dissolution of As bound to Fe and Mn-oxyhydroxides through microbially-mediated redox changes. The most well documented examples are for paddy soils in southeast Asia, where elevated As in rice is a global health concern (Xu et al., 2017; Yuan et al., 2021). When paddy soils are flooded, reducing conditions develop in the soil profile and the release of redox sensitive elements, including As is often observed (Xu et al., 2017; Yuan et al., 2021). The release of As via reductive dissolution of Fe, Mn (oxy)hydroxides has also been demonstrated in industrially impacted soils and considerable efforts have been directed at developing a mechanistic understanding of the processes that release As bound to Fe, Mn (oxy)hydroxides (Cai et al., 2002; Chatain et al., 2005). The drying of soils that have experienced extended periods of reducing conditions through prolonged wetness, such as below the water table in wetland and peatland soils, can also lead to the mobility of As from soil minerals via oxidative dissolution, and this has been shown to drive increased As mobility in wetland soils during drought periods (Blodau et al., 2008; Drahota et al., 2021). Temperature also exerts a fundamental control on As mobility in soils through modification of microbial activity (Weber et al., 2010). Increased microbial activity under warmer temperatures can lead to enhanced microbial reduction of As hosting minerals and release to surrounding soil porewaters (Simmler et al., 2017; Weber et al., 2010).

The physical, chemical, and biological properties of soil are not static and are driven by long-term changes in climate, seasonal changes in moisture and temperature conditions, or on shorter time scales associated with high intensity rain events (or drought). Consequently, As mobility in soils is often transient and As pools on the landscape can oscillate between labile and recalcitrant sources (Figure 2.1). Understanding the coupling of As mobility and catchment transport processes is thus critical for modelling the fate of As in the soil environment.

In northern environments As may be tightly bound to soil minerals for much of the year due to low rainfall and long periods where soils are frozen. Identifying the timing and mechanics of As mobility in soils thus depends on seasonal processes in the soil environment. Despite acknowledgment that transient soil conditions have an important control on the mobility and translocation of As in soils, there has been limited research directed at understanding As mobility in subarctic soils, where soils are frozen for much of the year.

2.2.2 Terrestrial fluxes of As

Hydrological processes largely govern the timing and magnitude of the flux of particulate and dissolved materials, including metal(loid)s, across the landscape (Allan et al., 1993; Björkvald et al., 2008; Branfireun et al., 1996; Spence et al., 2015). However, metal(loid) fluxes can be source limited if metal(loid) pools are not available for transport during important hydrological events, such as during freshet when soils at depth are frozen (Figure 2.1). Consequently, understanding the seasonal variability in hydrological and soil processes, and the coupling of these processes, is critical to develop our understanding of terrestrial As fluxes and how these fluxes may be altered as hydrological processes in northern environments change. This section focuses on the seasonal processes that govern the terrestrial flux of metal(loid)s across the landscape, drawing on the As literature where available. The section concludes with a summary of several studies where terrestrial fluxes of As were estimated using a mass balance approach.

2.2.2.1 Metal(loid) catchment transport with snow melt

Snow melt typically represents the dominant hydrological event of the year in subarctic watersheds (Spence et al., 2011, 2009). During this period, soils remain frozen and snowmelt

runoff is restricted to the porous organic layer at the soil surface, which allows for rapid transport of meltwater from the catchment (Figure 2.1) (Carey, 2003). This period is important for the flux of DOC and metal(loid)s from hillslopes to streams (Björkvald et al., 2008; Carey, 2003; Huang and Matzner, 2007; Rember and Trefry, 2004). There has been more research directed at understanding DOC flux during snowmelt compared to the flux of As and other trace metal(loid)s. Since DOC and As (in atmospherically impacted areas) tend to be enriched in surface soils and since DOC is an important ligand for many trace metals, it is relevant to draw on the extensive literature related to DOC and snowmelt processes. An initial pulse of high DOC is typically observed in association with the ascending hydrograph limb of freshet and then a rapid decline once DOC stores in near-surface soils are depleted (Carey, 2003; Holmes et al., 2012; Rember and Trefry, 2004). Rember and Trefry (2004) measured a four-and-a-half-fold increase in DOC and between 3- and 25-fold increases in dissolved trace metals in association with peak freshet in the Kuparuk and Sagavanirktok rivers in Alaska. Further, more than 80% of the annual particulate trace metal budget was transported from the Kuparuk and Sagavanirktok rivers within a 12-day period during peak freshet. This clearly shows the importance of snowmelt on annual metal(oid) fluxes to rivers, however, gaps remain in understanding metal(loid) flux during snowmelt at the hillslope and catchment scale. This is particularly prescient for areas that have been impacted by atmospheric pollution where contaminant concentrations are typically enriched in near-surface soils that are hydrologically active during the snowmelt period.

Results from a study in a forested catchment in Europe, impacted by atmospheric industrial As emissions, showed amplification of As export during periods when flow pathways were restricted to upper soil layers (Huang and Matzner, 2007), suggesting As fluxes associated with snowmelt may be important for annual catchment budgets, however, specific investigations related

to As transport in snow melt runoff have yet to be undertaken. This points to a knowledge gap for northern regions where snow melt runoff may represent a substantial portion of annual catchment runoff (Spence and Woo, 2003). Beyond a basic understanding of the mass flux of As associated with snow melt, additional research gaps include: a) whether As is exported from catchments in the dissolved or particulate phase, which will address whether transport is via physical transport of soil materials or the dissolution of As hosting minerals; and b) the relationship between As and important ligands, such as DOC, since complexation between dissolved As and organic ligands may be an important mechanism for As mobilization and transport (Bauer and Blodau, 2006).

2.2.2.2 Metal(loid) catchment transport during the thawing season

During the period after freshet, hydrological storage capacity increases across the catchment due to deepening of the unfrozen layer in soils (Figure 2.1) (Spence et al., 2009). This has implications for the flux of trace metal(loid)s from the catchment in two ways. First, the generation of runoff requires storage capacity thresholds to be exceeded, and this is influenced by a variety of factors including: antecedent soil moisture conditions, rainfall intensity and duration, and the relative placement of landscape units along the hydrological cascade (Allan et al., 1993; Branfireun, 1999; Spence et al., 2009). Thus, runoff and solute transport later in the thaw season typically only occurs episodically when storage thresholds are exceeded. Second, runoff generation during this period will integrate a substantial subsurface component (Spence and Woo, 2003). In atmospherically impacted areas, soils at depth may have lower stores of As (Bromstad et al., 2017) and may act as a sink for As mobilized from more labile sources in surface soils (Huang and Matzner, 2007).

2.2.2.3 Metal(loid) fluxes during winter and the impact of climate change

Catchment fluxes of elements during winter have generally been ignored because soils are typically frozen and hydrological processes are limited, however, rapid warming at northern latitudes is extending the thawing season and delaying freezeback of unfrozen ground, which can lead to greater subsurface flow into winter (Walvoord and Kurylyk, 2016; Walvoord and Striegl, 2007). This has led to intensifying hydrologic cycles and strengthening land-water linkages (Vonk et al., 2019; Walvoord and Kurylyk, 2016). In areas of continuous permafrost, it has been inferred that the deepening of active layer conditions has increased groundwater flow in the subsurface and is responsible for observed increases in winter baseflow in some major arctic rivers (Déry et al., 2009). In the subarctic Precambrian shield, where less of the landscape is underlain by permafrost, increased winter streamflow has been attributed to changes in the timing and phase of fall precipitation, where more fall precipitation is arriving as rain rather than snow (Spence et al., 2015, 2011). In both environments, this has increased the wintertime loading of major ions, nutrient and trace metals to streams during a traditionally nascent period (Barker et al., 2014; Spence et al., 2015). To date, there have been no studies at the hillslope scale to explore As mobility and transport in soils during extended thaw seasons or winter.

2.2.2.4 Mass export of As from terrestrial catchments

Several mass balance studies measuring catchment transport of As have been undertaken and yield varying results regarding the export of As from terrestrial compartments on the landscape. A comparison of watershed retention efficiencies for trace meta(loid)s in a series of watersheds in Maryland showed lower watershed retention for As than other metals in the study (Hg, Cd, Se, Pb) (Lawson and Mason, 2001). In relatively unpolluted landscapes, several studies

have shown that terrestrial catchments can be net sinks for atmospherically derived As, because the retention capacity in soils is sufficient to immobilize much of the As coming from precipitation, litterfall, and throughfall (Landre et al., 2010). In contrast, in heavily polluted areas, such as the Black Triangle region in northern Czech Republic, the ability of catchment soils to retain As is often overwhelmed by the source, and catchments can be net exporters of As (Erbanova et al., 2008; Novak et al., 2011). Arsenic emissions have been greatly reduced in the Black Triangle region since the 1980's and ongoing monitoring of catchment fluxes allowed for a comparison between a period of high pollution and recent lower levels of pollution. The results from the two periods showed that during the high pollution period there was large export of As from the catchment, whereas a nearly net zero balance was reached in the contemporary period (Novak et al., 2011). These studies suggest rapid export of As when source contributions are high and once external loadings from the pollution source decrease, internal catchment processes controlled the attenuation of previously deposited As. A critical observation from Erbanova et al. (2008) was that during the period of emissions abatement, As export was correlated with water fluxes, rather than the size of the As pool in the study catchments. This points to the importance of understanding relationships between catchment hydrology, As mineralogy, and biogeochemical processes in the soils.

While much progress has been made in understanding and measuring processes that control the mobility and transport of As in terrestrial environments there is a need to expand the seasonal boundaries of investigation, particularly for northern regions. The overwhelming importance of snowmelt processes in annual metal(loid) budgets warrants additional studies related to As flux during snow melt. Further, the shift to wetter fall conditions in subarctic Canada, where more

precipitation is falling as rain rather than snow presents a potential mechanism for increased catchment output through activation of deeper soil layers.

2.2.3 Aquatic pools and fluxes

2.2.3.1 Lakes as reservoirs and sources of arsenic

Lakes have an important role in the transport of As across the landscape. They act as both integrators of upstream catchment processes and regulators of continued downstream transport (Figure 2.1) (Williamson et al., 2009). Catchment and atmospherically derived materials can accumulate in lake sediments, where they may undergo diagenesis and/or burial. Sedimentation processes can reduce metal remobilization and downstream export for conservative elements such as Pb and Hg, however, for redox sensitive species, such as As, the pH, Eh, and biogeochemical properties of lake water will influence the speciation and stability of As in both solid and aqueous phases. Figure 2.2 provides a conceptual model of the main biogeochemical processes controlling As cycling within lakes. The ability for lake sediments to both attenuate As from lake waters and to release As to overlying waters has been the focus of much study (e.g. Andrade et al., 2010; Deng et al., 2014; Martin and Pedersen, 2002; Wang and Mulligan, 2006).

Arsenic may enter a lake in both dissolved and particulate forms via stream water, catchment runoff, shoreline erosion, and atmospheric deposition through precipitation and dust. Arsenic trioxide is used as the deposition form in the example in Figure 2.2, since it is the primary arsenic source of concern in the study region, and is a common anthropogenic atmospheric pollutant. Further, As_2O_3 , is highly soluble and permits the demonstration of the various physical, chemical and biological processes involved in the aquatic cycling of As. Upon deposition, the solubility of the As compound is controlled by its mineral form, and the physical and chemical

properties of the lake water. Solid phase compounds that are added to the lake settle on the lake bottom as sediment or a portion of the compound may dissolve in the water column. In oxygenated environments with circumneutral pH, such as well mixed shallow lakes or the epilimnion of large lakes, dissolved As is typically stable as As(V) (Wang and Mulligan, 2006). Concentrations of As(III) and organic As species are typically low in oxygenated waters, but algal reduction and methylation of As(V) can result in measurable proportions of organic As and As(III) in waters with substantial primary production (Hasegawa et al., 2010; Hellweger et al., 2003) (Figure 2). In low oxygen environments, such as organic rich lake sediments or the hypolimnion of stratified lakes, As(III) can be the main As species in lake waters (Hollibaugh et al., 2005; Senn et al., 2007). The high particle reactivity of As(V) in oxic environments can lead to the adsorption of aqueous As(V) with particulate Fe, Mn (oxy)hydroxides and the subsequent removal of As from the water column (Aurilio et al., 1994; Root et al., 2007). Arsenic associated with Fe, Mn (oxy)hydroxides in lake sediments is typically stable under oxidizing conditions but can be released as As(III) to porewaters below the redox boundary in lake sediments via reductive dissolution or desorption of As bound to Fe, Mn (oxy)hydroxides (Andrade et al., 2010; Kneebone et al., 2002; Root et al., 2007; Schuh et al., 2018). Aqueous As(III) within sediment porewaters can diffuse upwards (and downwards) driven by concentration gradients in porewaters (Schuh et al., 2019, 2018). The sequestration of As from continued geochemical cycling can occur at depth in lake sediments when As(III) and reduced sulfur (S(II⁻)) are present in porewaters through the precipitation of As-sulfides and/or co-precipitation with Fe-sulfides (O'Day et al., 2004; Schuh et al., 2018; Smedley and Kinniburgh, 2002; Q. Sun et al., 2016). Bacteria play a central role in the cycling of As in surface waters and sediments through the microbial mediation of reduction and oxidation processes (e.g. Asta et al., 2012; Bright et al., 1994; Huang, 2014; J. Sun et al., 2016).

2.2.3.2 Fluxes of As across the sediment-water boundary

A typical geochemical stratigraphy in lake sediments includes a shallow peak in solid phase As when oxic conditions persist in the near surface sediments (Andrade et al., 2010; Schuh et al., 2018). This oxic layer reduces the diffusion of upward migrating porewater As across the sediment-water boundary, through oxidation of As(III) to As(V) and adsorption on Fe, Mn (oxy)hydroxides (Andrade et al., 2010; Root et al., 2007). The ability for As to be adsorbed requires the maintenance of oxic conditions within the surface sediment layer and presence of available adsorption sites on metal oxides. Processes and conditions that lead to thinning of the oxic layer in interfacial sediments in surface sediments can therefore lead to increased diffusion of As across the sediment-water boundary (Andrade et al., 2010; Bennett et al., 2012). The thinning or disintegration of the oxic layer in lake sediments can occur via several mechanisms, including increased accumulation of labile organic matter (via autochthonous or allochthonous sources) (Azizur Rahman and Hasegawa, 2012; Martin and Pedersen, 2004) or prolonged thermal stratification (Hollibaugh et al., 2005; Senn et al., 2007; Spliethoff et al., 1995).

Sediment redox processes are dynamic and the role of oscillating redox condition on the diffusion and retention of As across the sediment-water boundary has been the focus of substantial research (Arsic et al., 2018; Bennett et al., 2012; Johnston et al., 2020; Parsons et al., 2013; Phan et al., 2019). These studies have typically explored the mechanics of As mobility using laboratory experiments where oxygen conditions have been manipulated in soil or sediment incubations. The results generally show that As is coupled with Fe and Mn cycling, and under oxic conditions As is retained in interfacial sediments in association with Fe, Mn (oxy)hydroxides. Mechanical sparging or natural degradation of O₂ from overlying waters leads to the release of As into

overlying waters through the microbially mediated reductive dissolution of Fe and Mn (oxy)hydroxides and increased diffusion of As(III) across the sediment boundary (Arsic et al., 2018; Bennett et al., 2012). Repeated manipulations of oxic-anoxic conditions lead to corresponding oscillations in As flux, however, there is some evidence for decreased heterotrophic Fe reduction (and subsequent reduction in As flux) under conditions where labile stores of OM are

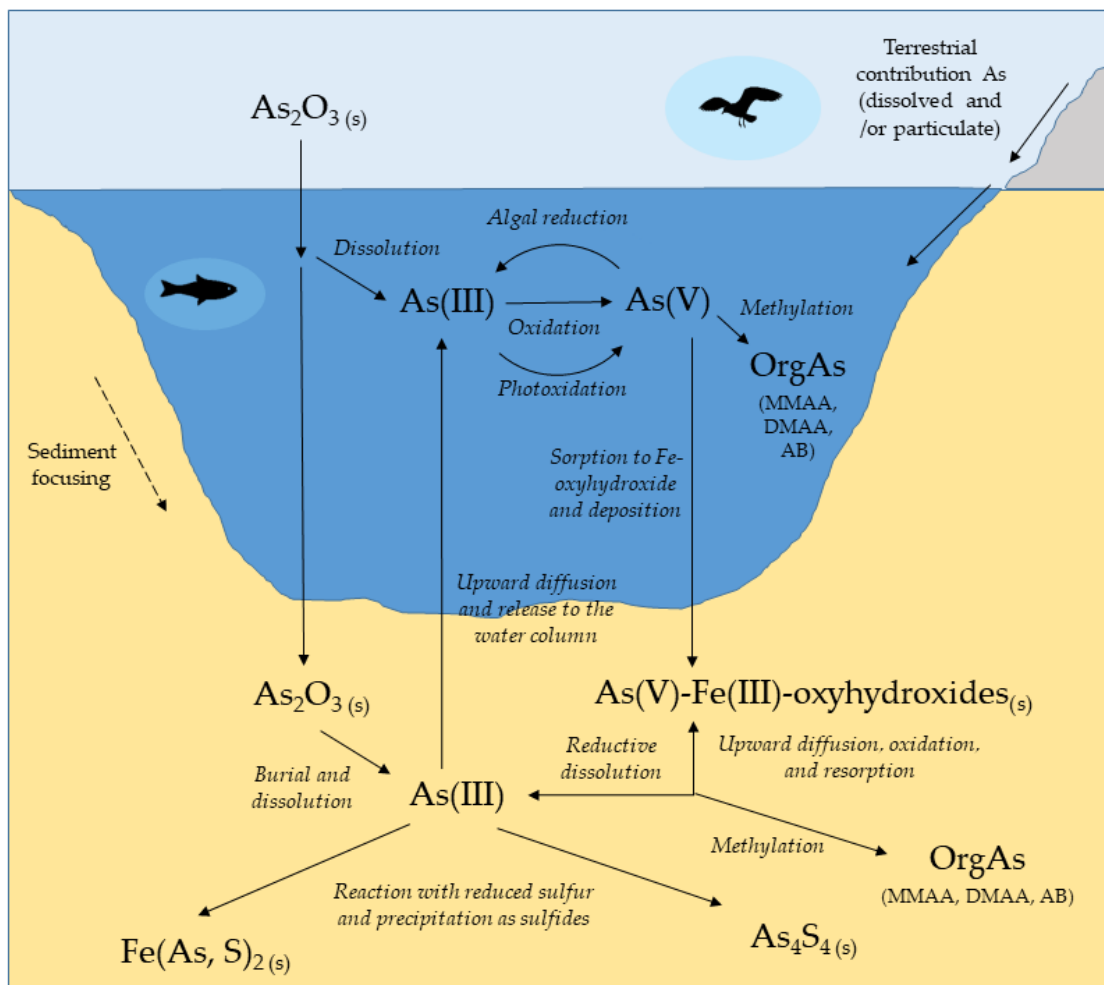


Figure 2.2: Conceptual diagram outlining the main biogeochemical processes controlling As cycling within lakes. The main hypothetical input is roaster-derived As_2O_3 . Aqueous and solid-phase As products are indicated in larger black font. Biogeochemical processes that influence the transformation of As products are indicated in italics. Figure modified from Schuh (2019).

depleted (Parsons et al., 2013). There is a paucity of field-based studies from northern environments that explore the influence of oscillations in redox conditions across the sediment-water boundary on As flux.

The flux of As across the sediment-water interface can lead to enrichment of overlying surface waters and has been the focus of several studies (Andrade et al., 2010; Deng et al., 2014; Martin and Pedersen, 2002). Arsenic enrichment of bottom waters is typically proportional to concentrations of As in surface sediments (Gawel et al., 2014), but is also influenced by other lake properties, including: lake morphometry and volume, water column stability, and sediment microbial activity (e.g. Barrett et al., 2019; Spliethoff et al., 1995). In shallow lakes with large reservoirs of labile As, particularly where a large surface area to lake water volume ratio exists, internal loading from lake sediments can result in sustained high lake water As concentrations years after external loading of As has ceased (Barrett et al., 2019; Martin and Pedersen, 2002).

2.2.3.3 Seasonal variation in lake water arsenic concentrations

The speciation and distribution of As in lakes is rarely in thermodynamic equilibrium and this is particularly evident in lakes that experience large differences in thermal structure and productivity related to seasonal processes (Hollibaugh et al., 2005; Spliethoff et al., 1995). Seasonality is a characteristic feature of northern environments and previous research related to seasonal influences on As mobility highlights several important ways in which seasonality influences the concentration and fate of As in lakes. In shallow lakes, warm summer sediment temperatures can lead to higher lake water As than during cooler months through increased microbial respiration and greater As flux into overlying waters (Barrett et al., 2019). In lakes that thermally stratify, significant As enrichment can occur if hypolimnetic anoxia develops (Hollibaugh et al., 2005;

Spliethoff et al., 1995). In dimictic lakes, turnover can lead to enrichment of the full water column and the duration of hypolimnetic anoxia has been shown to control the magnitude of As enrichment through the water column (Spliethoff et al., 1995). A trend towards increasing eutrophication in northern lakes has been observed in many parts of the world (Antoniades et al., 2011; Williamson et al., 2009) and eutrophication-induced anoxic events have been shown to increase As mobilization from the sediment to the water column (Bennett et al., 2012).

While there has been substantial research directed at understanding the influence of seasonality on As mobility in temperate and tropical regions (e.g. Hasegawa et al., 2010; Johnston et al., 2020; Martin and Pedersen, 2002), there has been relatively little attention paid to the influence of extended seasonal ice cover on As mobility. Specifically, there are several mechanisms worth investigation that could potentially lead to lake water enrichment of As under ice. Cryoconcentration, the process of excluding solutes from the forming ice cover, is more pronounced in subarctic lakes compared to temperate lakes, and can substantially increase solute concentrations under ice for a temporary period (Freitas et al., 1997; Schmidt et al., 1991; Willemse et al., 2004). In shallow lakes, where ice can represent a large proportion of lake volume, this could lead to considerable under ice As enrichment. The development of ice cover limits atmosphere-lake water interactions and can lead to development of anoxic conditions through the water column in shallow lakes (Mathias and Barica, 1980) or in the hypolimnion for lakes that inversely stratify (Joung et al., 2017). Previous research has shown that development of anoxic conditions under ice near the sediment boundary can lead to increased concentrations of reactive species of redox sensitive elements in bottom waters (Joung et al., 2017; Schroth et al., 2015), therefore new investigations directed at understanding the role of ice cover on As mobility are warranted.

2.3 Lake hydrology and chemical recovery of lake waters

Lake hydrology has a central influence on within lake contaminant dynamics and downstream export (Freitas et al., 1997; Semkin et al., 2005). The hydrologic connectivity between lakes ultimately controls the transport of As between waterbodies on the landscape (Figure 2.1). Since snowmelt is the principal contributor to streamflow in subarctic shield catchments, lakes in headwater catchments often experience the extreme situation where outflow terminates after the melt season (Mielko and Woo, 2006). Consequently, headwater lakes may only discharge stored constituents, including contaminants, episodically. If discharge is coincident with a period of enrichment due to the coupling of hydrologic and biogeochemical processes, it may result in a pulse of contaminant transport. This is in-line with the “hot moment” concept described by McClain et al. (2003), where disproportionately high fluxes occur intermittently compared to longer intervening time periods (McClain et al., 2003). The magnitude of this hot moment is a function of the morphology of the lake, internal biogeochemical processes and external hydrologic forces.

For lakes impacted by high atmospheric deposition of pollution, the flushing rate and amount of throughflow in the lake is an important determinant for recovery. In acid-stressed and metal impacted lakes around Sudbury, ON, the rate of chemical recovery was highest in hydrologically connected and rapid-flushing lakes (Mallory et al., 1998; Woodfine and Havas, 1995). There was a substantial climate component to recovery in Sudbury area lakes as well, where improvement in lake water quality was noted during drought conditions for non-redox sensitive pollutants, such as Cu, Ni, Zn, driven by an inferred decrease in loading of pollutants from the catchment and increased water residence time, which allowed for increased sedimentation of pollutants (Mallory et al., 1998). Since As is a redox sensitive element, and internal loading from sediments can lead

to substantial enrichment of lake water As (Martin and Pedersen, 2002), the trajectory of chemical recovery in response to changes in climate may be distinct from observations in the Sudbury region. Increased water residence time is an important driver of high P in lakes (Brett and Benjamin, 2008; Dillon, 1975; Dillon and Molot, 1996; Orihel et al., 2017), and chemical similarities between As and P, suggest that As recovery may be inhibited in low flow periods where longer lake water residence times may lead to high efflux of As from sediments. In the Yellowknife area, elevated As concentrations in lake waters persist more than 15 years after atmospheric As emissions from local mines ended and more than 50 years after the bulk of total As emissions were released (Houben et al., 2016; Palmer et al., 2015). Contemporary As concentrations in lakes adjacent to Giant Mine are highly variable, and the highest As concentrations were measured in small hydrologically disconnected lakes (Palmer et al., 2015). This suggests that the trajectory of chemical recovery of lake waters from As pollution is not consistent along a distance gradient from emission point sources and warrants research directed at identifying environmental processes that control lake recovery from As pollution.

2.4 Climate change and the fate of As in aquatic environments

Climate change has the potential to impact the fate of As in aquatic environments through a variety of mechanisms, including: a) influencing the long-term stability of As in lake sediments through changes in OM accumulation and thermal stability of lake waters; and b) altering watershed As transport through changing hydrological fluxes and pathways. Increased OM accumulation in lake sediments from autochthonous and allochthonous sources has been observed across northern environments (Adrian et al., 2009; Williamson et al., 2009). As noted previously in this chapter, this has the potential to destabilize reservoirs of As stored in interfacial sediments, as the addition of labile OM sources can lead to thinning of oxic boundaries in aquatic sediments

and an increase in the flux of As across the sediment boundary through the reductive dissolution of Fe (oxy)hydroxides (Macdonald et al., 2005; Martin and Pedersen, 2002). Long-term stratigraphic records have shown that late-Holocene warming led to increased As mobility in subarctic lake sediments, via increased fluxes of OM to lake sediments (Miller et al., 2020). Climate associated influences on regional hydrology also have the potential to influence the mobility of As via controlling the input of terrigenous As and OM (Miller et al., 2019). Under warmer and wetter conditions, enhanced weathering processes can increase terrigenous inputs of As and these changes have been recorded in lake sediment archives from the subarctic shield (Miller et al., 2019). Climate change is altering the thermal structure of lakes and shorter ice-covered seasons and warmer air temperatures are leading to warmer surface temperatures and prolonged periods of thermal stratification (Woolway et al., 2020). Changes in the thermal structure of lakes may influence As mobility via alterations in lake mixing processes and the duration of hypolimnetic anoxia (e.g. Barrett et al., 2019; Spliethoff et al., 1995), yet few studies exist from northern regions where lakes are ice-covered for much of the year.

Northern hydrological processes are changing rapidly because of climate change. One of the most widely cited observations is an increase in winter streamflow in northern rivers (Déry et al., 2009; McClelland et al., 2006; Peterson et al., 2002). In continuous permafrost regions, the increase in winter baseflow has been largely attributed to permafrost thaw and an increase in subsurface flow (e.g. Walvoord and Striegl, 2007). In shield terrain, where less of the landscape is underlain by permafrost, increased winter streamflow has been driven by a shift in the timing and phase of precipitation, where more fall precipitation is falling as rain, rather than snow, which can be devoted to winter streamflow generation (Spence et al., 2015, 2014). Shifting streamflow regimes have resulted in increased fluxes of nutrients and other solutes in northern rivers (e.g. Frey

and McClelland, 2009; Spence et al., 2015), yet little attention has been directed towards understanding how changing hydrological pathways and increased winter streamflow may alter contaminant mobility and transport in mining impacted areas.

2.5 Summary and connection with thesis objectives

Catchment soils can store large pools of legacy As in atmospherically contaminated landscapes and may represent a continued source of As to downstream aquatic environments. This review highlights that substantial research has been directed at understanding the distribution of As near point sources of As pollution and the biogeochemical processes that control the mobility and fate of As in the soil environment. It is clear that characterization of solid-phase As speciation contributes to a more complete understanding of the mobility and fate of As in terrestrial environments, yet has been rarely included in previous assessments of As distribution near pollution point sources. In Chapter 3, mineralogical tools are used in complement with geospatial and statistical methods to develop our understanding of the distribution and origin of As in soils in the Yellowknife area.

The importance of seasonality is often overlooked in field-based investigations of As mobility in contaminated northern landscapes, since the bulk of field work occurs in the open-water season and the winter period has typically been considered a period of watershed inactivity. As demonstrated in this chapter, seasonal variability in redox processes in terrestrial and aquatic environments, particularly under ice, and seasonal fluctuations in hydrologic processes may have a substantial influence on the cycling, transport, and fate of As in northern environments. This thesis addresses a major knowledge gap by characterizing As transport and cycling throughout the entire year and identifying seasonal influences on processes that control lake recovery from As pollution. Chapter 4 is devoted to a study that evaluates the seasonal variation of As and Sb in a

series of small shallow lakes near Giant Mine. Chapter 5 includes detailed geochemical characterization of lake waters, lake sediments and sediment porewaters to explore the cycling of As across seasons in two years with contrasting hydrological conditions. Finally, in Chapter 6, a watershed approach is used to explore the magnitude and relative influence of terrestrial and aquatic As fluxes to elucidate the importance and controls of the various watershed fluxes. These four chapters provide novel information on the mobility and fate of As in subarctic landscapes and advance our knowledge of the recovery of As impacted environments.

Chapter 3: Arsenic in soils of the Yellowknife area: Regional distribution, attribution of source, and estimation of geochemical background

Abstract

The estimation of geochemical background is complex in areas impacted by point sources of atmospheric emissions due to unknowns about pollutant dispersion, persistence of pollutants on the landscape, and natural concentrations of elements associated with parent material. This study combined mineralogical analysis with conventional statistical and geospatial methods to separate anthropogenically impacted soils from unimpacted soils in the Yellowknife area, Northwest Territories, Canada, a region that was exposed to 60 years of arsenic (As)-rich atmospheric mining emissions (1938-1999) and that hosts natural enrichments of As. High concentrations of As (up to 4700 mg kg⁻¹) were measured in publicly accessible soils near decommissioned roaster stacks in the region and strong relationships between As and distance from the main emission sources persisted in surface soils and soils at depth in the soil profile more than 60 years after the bulk of mining emissions were released. Mineralogical analysis provided unambiguous evidence regarding the source of As minerals and highlighted that most As in surface soils within 15 km of Yellowknife is hosted as anthropogenic arsenic trioxide (As₂O₃), produced by roaster stack emissions. Statistical protocols for the estimation of geochemical background were applied to an existing database of till geochemistry (N = 1490) after removing samples from mining impacted areas. Results suggested geochemical background for the region is 0.25 – 15 mg kg⁻¹ As, comparable to global averages, with upper thresholds elevated in volcanic units (30 mg kg⁻¹ As) that often host sulfide mineralization in greenstone belts in the region.

3.1 Introduction

The identification of geochemical background in soils is often sought during mineral exploration and environmental remediation activities (Reimann and Garrett, 2005). The assumption is that concentrations above (or below) a range of natural background conditions may reflect geochemical anomalies indicative of mineralization or pollution (Reimann et al., 2005). The quantification of background, however, can be ambiguous, because of the confounding effects of natural variability and past anthropogenic activities in a region (Matschullat et al., 2000; Reimann et al., 2005). The identification of background is also difficult because of inconsistency in terminology and methodological approaches (Matschullat et al., 2000; Parsons and Little, 2015; Reimann et al., 2005). Matschullat et al. (2000) aimed to clarify some of these issues and proposed that the term *geochemical background* reflect a relative measure to distinguish natural element concentrations from anthropogenically impacted concentrations. The term *geochemical baseline*, is often used interchangeably, yet is distinct and refers to ambient soil conditions in a region impacted by both geogenic processes and legacy anthropogenic impacts without distinguishing between the two (Parsons and Little, 2015). It is not realistic to consider geochemical background as a single value, since natural processes can lead to large ranges in element concentrations in unimpacted soils. Rather, geochemical background should be considered as a range of analyte concentrations in soils not impacted by anthropogenic activities (Reimann et al., 2005). An upper limit of the range of natural concentrations, defined with statistical reliability, is often sought to help identify soils impacted by anthropogenic pollution and to establish remediation criteria reflecting previously undisturbed conditions. The separation of anthropogenically-impacted soils from unimpacted soils is primarily important where samples with elevated analyte concentrations may present a risk

to human or ecological health or lead to a limitation of the usage potential of soils (Matschullat et al., 2000).

Previous reviews have highlighted numerous approaches for the estimation of geochemical background (e.g. Matschullat et al. 2000; Reimann and Filzmoser 2000; Reimann et al. 2005; Gałuszka 2007; Dung et al. 2013). Many of these approaches focused on statistical techniques to define a range of values or an upper threshold limit reflecting unimpacted soils. The application of statistical techniques requires careful consideration of the data distribution and since geochemical data are rarely normally or lognormally distributed many parametric methods (e.g. use of the mean and standard deviation) are typically not appropriate (Reimann et al., 2005; Reimann and Filzmoser, 2000; Reimann and Garrett, 2005). Estimates using non-parametric methods are much more robust against the influence of extreme outliers that are often present in geochemical datasets (Reimann and Filzmoser, 2000). For example, Reimann et al. (2005) reviewed several parametric and non-parametric methods for estimating geochemical background and highlight the use of the Tukey boxplot, median \pm 2 median absolute deviation ($Md \pm 2MAD$), and empirical cumulative distribution functions as well suited for the estimation of threshold values and ranges of background conditions. While statistical approaches yield thresholds and ranges with statistical reliability based on empirical distributions, it is widely acknowledged that a robust estimation of geochemical background benefits from the application of a variety of tools, including statistical, geospatial, and geochemical techniques (Matschullat et al., 2000; Reimann et al., 2005). Geographical displays allow for the geospatial visualization of datasets and facilitate the identification of hotspots or anomalies (Reimann et al., 2005). Geochemical methods, including mineralogical methods, provide indispensable information on how specific elements are hosted in mineral phases, which can yield important information on whether the mineral originated

from an anthropogenic or geogenic source (Bromstad et al., 2017). Realistic risk assessment should include careful study of the mineralogy of samples to determine how elements of concern are hosted and whether or not, and under what conditions, they are bioaccessible (Reimann and Garrett, 2005). The initiation of clean up activities solely because a statistical threshold has been reached may be unnecessary and could in fact worsen the environmental situation, if previously stable minerals are disturbed so that the solubility of minerals is enhanced via alteration of redox or weathering conditions (Reimann and Garrett, 2005). Mineralogical assessment can be time-consuming and expensive, therefore the power of mineralogical techniques is enhanced when used in combination with techniques that can be applied to larger sample populations (i.e. statistical and geospatial techniques). It should be acknowledged that different approaches will likely yield different estimates for geochemical background ranges and upper threshold limits. Undoubtedly, choices need to be made in the calculation of background estimates, therefore expert knowledge and clear articulation of method assumptions are required.

Regions impacted by point sources of pollution, such as smelters and refineries, present a complex environment for the determination of natural background, because of unknowns about the distribution and fate of pollutants in the environment and the natural presence of these elements in local soils and bedrock (Díez et al., 2007; Parsons and Little, 2015; Reimann et al., 2009, 2000). Arsenic (As) is a pollutant of global concern, because of its carcinogenic and toxic effects (Smedley and Kinniburgh 2002). An important contributor of As to the environment is the waste associated with the production of base metals and gold (e.g. McMartin et al. 1999; Jamieson 2014). The Yellowknife area in northern Canada presents a complicated environment to explore the concept of geochemical background since there is a 60-year legacy of As pollution in the region related to the mining and roasting of gold-bearing arsenopyrite and limited pre-mining

geochemical data from the area (Jamieson, 2014; Walker et al., 2015). The area also hosts natural enrichments of As associated in arsenopyrite-bearing gold ore bodies (Boyle, 1979; Kerr, 2006). Beyond the impact of past mining emissions on soils, the region is relatively pristine as there are few anthropogenic sources of pollution outside of the city proper, making this an opportune area to attempt to separate anthropogenic mining and geogenic sources of As in the soil environment. Previous estimates of geochemical background in soils in the Yellowknife region suggest As concentrations in soils are elevated relative to other jurisdictions due to natural processes associated with mineralization and bedrock enrichment (ESG, 2001; GNWT, 2003). Recent work has highlighted the persistence and widespread dispersion of As from historical mining and roasting emissions and suggests that elevated As in soils and lake sediments may be the result of widespread dispersion of As from past mining emissions rather than natural processes (Bromstad et al. 2017; Galloway et al. 2017; Jamieson et al. 2017; Schuh et al. 2018; Van Den Berghe et al. 2018; Cheney et al. 2020; Palmer et al. 2020; Sivarajah et al. 2020).

In this study we present a novel approach to differentiate between anthropogenic and natural sources of As at a regional scale by combining statistical and geospatial approaches for background estimation with solid-phase speciation analysis of As-hosting minerals in soils. The specific objectives of this study were to: 1) characterize the extent of influence of past mining emissions on soils in the region using data from surface and soil cores; and 2) estimate the range and upper threshold of geochemical background for soils overlying the predominant bedrock lithologies in the region. We explored whether mineralogical analysis would help to distinguish between natural and anthropogenic sources of As in soils close to mining point sources, so that geochemical background could be estimated using soils that were unequivocally representative of natural variability.

3.2 Background

3.2.1 Mining history and previous work on soils in the region

The Yellowknife Greenstone Belt was one of the most productive and profitable gold districts in Canadian history. The two largest mines in the region, Giant Mine (1949-2004) and Con Mine (1938-2003), produced more than 13 million ounces of gold over their operating periods (Bullen and Robb, 2006). Gold was hosted in arsenopyrite (FeAsS), that was roasted as part of the processing technique to make the ore more amenable to cyanidation. The roasting of As-bearing ore created emissions of sulfur dioxide (SO₂) and arsenic vapour, that condensed to arsenic trioxide (As₂O₃) dust when released to the atmosphere (Jamieson, 2014; Walker et al., 2015). Roasters were operational in the region for more than 60 years between the Giant (1949-1999) and Con mines (intermittently 1938-1970). During these operations more than 22 000 tonnes of As₂O₃ were released to the surrounding environment (Hocking et al., 1978; Wrye, 2008). Giant Mine was the largest emitter and released an estimated 20 000 tonnes of As₂O₃ over its mine life. The bulk of As₂O₃ emissions from Giant Mine (> 86%) were released prior to 1964 (Wrye, 2008). While there were high emissions in the early years of operations (pre-1958) at the two mines, in later years most of the As₂O₃ dust was captured. At Giant, > 90 % of the dust produced (~237 0000 tonnes) is currently stored in underground chambers, whereas at Con, the arsenic trioxide was treated on site, integrated with tailings, or sold commercially (Hauser et al. 2006).

The widespread distribution of As₂O₃ resulted in environmental impacts to soils (Hocking et al., 1978; Hutchinson et al., 1982; Jamieson et al., 2017), lake waters (Houben et al., 2016; Palmer et al., 2015), and lake sediments (Galloway et al. 2017; Schuh et al. 2018; Cheney et al. 2020; Palmer et al. 2020) across the region. Several studies since the 1970's have reported concentrations of As and antimony (Sb) (another roaster associated element) in near-surface soils

in the Yellowknife region (Bromstad et al., 2017; Hocking et al., 1978; Hutchinson et al., 1982; Jamieson et al., 2017; St. Onge, 2007). A detailed summary of existing soil research in the Yellowknife area is reported in Jamieson et al. (2017). Consistent among these studies spanning almost five decades is a clear inverse relationship between soil As concentrations and distance from the legacy point sources of pollution at Giant and Con Mines. It remains unclear, however, the extent to which geogenic sources of As, associated with sulfide mineralization near gold deposits, influence As concentrations in soils in the vicinity of legacy mining operations.

While previous work in the region has focused on estimating the distribution of total As in surface soils, there has been little attention directed at understanding the mineral form of As in surface soils across the region. Detailed mineralogical analyses of surface soils on the Giant Mine property demonstrated that the most common As hosts were As_2O_3 and roaster-generated iron-oxides (maghemite and hematite), both anthropogenic in origin from stack emissions (Bromstad et al., 2017; Walker et al., 2005). Bromstad et al. (2017) noted that most of the As_2O_3 observed in surface soils on the Giant Mine property was likely deposited prior to 1964. This indicates limited dissolution of As_2O_3 and suggests that legacy As_2O_3 is persisting on the landscape for decades, yet little information exists for soils beyond mine lease boundaries.

Several attempts have been made to estimate geochemical background As concentrations in soils in the Yellowknife region to support remediation and reclamation efforts. The Government of the Northwest Territories used an average natural background of 150 mg kg^{-1} As with a reasonable upper limit (90th percentile of available data) of 300 mg kg^{-1} for setting the site-specific soil quality guidelines for the Yellowknife area for residential (160 mg kg^{-1} As) and industrial (340 mg kg^{-1} As) soils (GNWT, 2003). This estimate of geochemical background was based on soil data from a variety of sources, but all within close proximity to Yellowknife (ESG, 2001). Based

on previous work, many of the soils used in this estimation were likely impacted by stack emissions in the region, even 50 cm below the surface, which may be influenced by dissolution and downward mobilization from surface soils (Hocking et al. 1978; Hutchinson et al. 1982; Kerr 2006; Jamieson et al. 2017). Kerr (2006) recognized the importance in removing sample data close to the historic roaster stacks in developing background As estimates. Data within 5 km of Giant Mine were not included in background estimates for granitoid (5 - 10 mg kg⁻¹) and volcanic lithologies (10 - 30 mg kg⁻¹), but no information is included on the methodology used to calculate geochemical background (Kerr 2006). Recent work has indicated that the impact of stack emissions in soils and lake sediments extends beyond 20 km from Yellowknife (Jamieson et al., 2017; Pelletier et al., 2020) and perhaps as far as 40 km (Cheney et al., 2020). Considering this information, an estimation of geochemical background should acknowledge these regional impacts and likely exclude soils near historical point sources of emissions, unless mineralogical evidence suggests that high As in soils near emissions point sources is associated with natural enrichment.

3.2.2 Study area

The study area includes much of the Slave Geological Province (172,500 km²), a late Archean craton extending from the north shore of Great Slave Lake, Northwest Territories to the Coronation Gulf in Nunavut. The treeline transition intersects the Slave craton and separates Taiga Shield, in the south, from Tundra Shield, in the north (Ecoregions Working Group, 1997). Underlying bedrock is composed of metavolcanic and metasedimentary rocks intruded by granitoid plutons (Helmstaedt, 2009). The Slave craton was glaciated in the late Wisconsinan and covered by the Laurentide Ice sheet until ~13,000 ka BP (Wolfe et al., 2017b). During deglaciation, the southern portion of the Slave craton, close to Great Slave Lake and below 280 MASL, was inundated by

Glacial Lake McConnell (13,000 to 9500 ka BP). Consequently, surficial materials in this region are dominated by glaciolacustrine and glaci-fluvial sediments (Wolfe et al., 2017b). Most of the study area was not covered by Glacial Lake McConnell and surficial materials are dominated by thin veneers of glacial till (Kerr 2006). Soils in the region are poorly developed because of the cold, dry climate, and relatively recent deglaciation (Wolfe et al., 2017a). In general, the region forms a gently undulating glaciated landscape characterized by thin covers of surficial materials and dominated by exposed bedrock outcrops (Wolfe et al., 2017a).

3.3 Material and methods:

This study relied on previously reported data from several soil and till geochemical surveys conducted in the Slave Geological Province (Table A1). Several of the studies employed distinct sampling and analytical techniques, which presented an issue of intercomparability between datasets. Therefore, data were not pooled for statistical analyses, and the two primary datasets (Jamieson et al. 2017; Kerr and Knight 2005) were used to address distinct and independent questions about: 1) the origin and distribution of As in soils close to emission point sources; and 2) estimating geochemical background of As in surficial materials across the Slave Geological Province.

3.3.1 Origin and distribution of As in soils near legacy point sources of mining emissions

The first part of this study was focused on understanding the distribution and mineralogy of As-hosting minerals in surface soils within a 30-km radius of Yellowknife (Figure 3.1) to elucidate the impact of past mining emissions on local soils. A central question for this part of the study was whether we could determine whether As measured in surface soils was of anthropogenic

or geogenic origin. Total As data presented were reported previously in Jamieson et al. (2017). Mineralogical data is from the MSc theses of Oliver (2018) and Maitland (2019), which relied on the same samples as collected in Jamieson et al (2017), using the same field collection and preparation methods.

3.3.1.1 Field collection

Four hundred and seventy-nine soil samples were collected during three summers (2015-2017) within a 30-km radius of Yellowknife using aluminum soil core tubes that were pushed or driven into the soil with a sledgehammer. All sampling targeted undisturbed locations free of municipal and industrial disturbance, including the Giant Mine and Con Mine properties. Soils were sampled from four distinct terrain units to assess the influence of terrain type on the variation of soil As across the region, including bedrock outcrop soils, bedrock outcrop soils with tree cover, forested soils, and peatlands. Bedrock outcrop soils were typically thin (< 30 cm) organic rich soil pockets within expansive bedrock outcrop areas. Bedrock outcrop soils with tree cover had similar soil conditions to bedrock outcrop soils, but with some trees, primarily jack pine (*Pinus banksiana*). Forested soils had thicker soils than the bedrock classes and were either characterized by: 1) a cover of black spruce (*Picea mariana*) with a thin organic layer overlying poorly developed soils or tills; or 2) a cover of white paper birch (*Betula papyrifera*) overlying thick deposits of fine-grained mineral soils, which are commonly underlain by permafrost in the region (Wolfe and Morse, 2016). Peatlands were thick organic deposits, typically overlying permafrost, with little to no tree cover. Cores were sealed in the aluminum tubes with laboratory wrapping film, frozen and shipped to Queen's University where they were kept frozen until analysis. Prior to analysis,

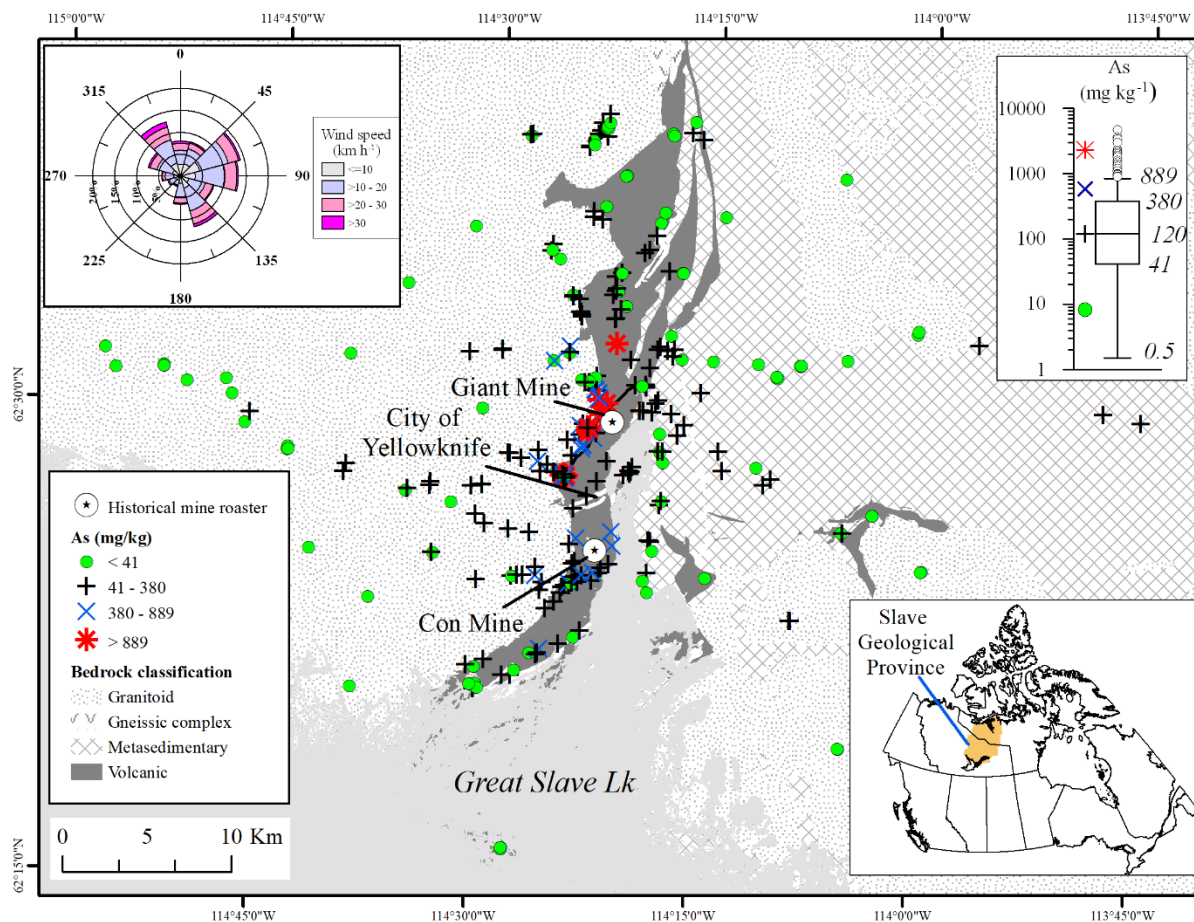


Figure 3.1: Arsenic concentrations in Public Health layer samples (0-5 cm) within a 30 km radius of Yellowknife (N = 407). Data are symbolized following the Tukey boxplot method (presented in upper right inset): less than 1st quartile (green circles), between 1st and 3rd quartile (black crosses), between 3rd quartile and upper fence (3rd quartile + 1.5*IQR) (blue X), and beyond the upper fence are considered outliers (red asterisk). Inset in upper left of figure shows mean wind speed and frequency for wind directions at Yellowknife (1953 – 1999) (Environment and Climate Change Canada, 2020).

core tubes were cut open with a table saw, separated with a ceramic knife and subsectioned into 5-cm intervals. In this study, samples were not sieved and only gently ground prior to analysis to preserve materials as they would be encountered in the field and to reduce the potential of screening out important As mineral hosts. Analytical efforts were focused on the samples from the upper 5-cm of the soil column (N = 407), referred to here as the Public Health layer after Parsons and Little (2015) and consistent with the surface layer of soil that contributes to incidental

human exposure (Health Canada, 2010). All surface materials were left in place during sampling, including leaf litter, mosses and surface vegetation, but large sticks and woody material were removed if present. Sixty samples were prepared for analysis from the 5-cm interval at the base of the core tube and are referred to as “downcore samples” to assess downward migration of As and the concentration-distance relationship at depth. The depth of these samples ranges from 10 - 38 cm below the soil surface and typically represent the base of the soil column at sampling locations. At eleven sites, soil cores were sectioned through the soil profile to explore chemical gradients in the soil column. The appendices in Jamieson et al. (2017) include descriptions of the groundcover and soil at each sampling site.

3.3.1.2 Total metal(loid) analyses

A portion of each subsectioned core was homogenized and submitted for near-total elemental analysis at the Analytical Services Unit (ASU) at Queen’s University. Samples were digested using *aqua regia* solution (HCl and HNO₃) and subsequently analysed for a suite of metal(loid)s via inductively coupled plasma-mass spectrometry (ICP-MS) (for Au and Sb) or inductively coupled plasma – optical emissions spectrometry (ICP-OES) (20 elements). Only the data for As (referred to here as total As) are discussed in this study, however, all analytical data are presented in the appendices of Jamieson et al. (2017). Sample homogeneity and analytical reproducibility were assessed using field duplicates (paired samples collected in close proximity in the field), split samples (samples from same depth interval prior to sample homogenization), and internal laboratory duplicates (samples from same depth interval after sample homogenization). These results are presented in Jamieson et al. (2017) and a summary of these results is presented in Appendix A.

3.3.1.3 Mineralogical analysis

A subset (N = 85) of the 479 Public Health layer samples were targeted for mineralogical analysis via Scanning Electron Microscopy (SEM) based automated mineralogy at Queen's University. Samples for detailed mineralogical analysis were selected to represent a range of total As concentrations (1.6 - 4700 mg kg⁻¹) and from spatially distributed locations across the region that integrated the distance gradient from point sources of mining emissions and proximity to ore bodies. Samples were air-dried, gently disaggregated in a mortar, and mounted in epoxy. Graphite powder (< 44µm) was added to minimize agglomeration. The epoxy was allowed to harden at room temperature and the pucks were ground and polished by hand, then carbon-coated. Details of sample puck preparation can be found in Oliver (2018) and Maitland (2019). Automated mineralogy was accomplished using methods similar to those described in Schuh et al. (2018). The method was optimised to find and identify As-bearing phases even in cases where only a few particles were present. Total particle counts ranged from hundreds to hundreds of thousands of grains per slide, and arsenic-hosting minerals comprise anywhere from less than ten grains to thousands of grains per thin section. The distribution of As amongst multiple As hosts in each samples was calculated based on the area occupied by that mineral and the mass of As present in that mineral (Schuh et al., 2018). Mineral Liberation Analysis - automated mineralogy (MLA-AM) was used to distinguish the number of particles and to calculate the area of each particular As-bearing phase in a thin section. The thickness of the phase in a thin section was assumed 1 µm. For arsenic trioxide, arsenopyrite, realgar, enargite, and scorodite the amount of As in each phase was determined using standard mineral formulae to calculate chemical compositions. For less well-defined minerals containing mixed spectra, approximate As weight % values were established based on previous work completed in the area (Table A2).

3.3.2 Estimation of natural background in the Slave Geological Province

The second part of this study was directed at developing an estimate of geochemical background for As in soils overlying the main bedrock lithologies of the Slave Geological Province and relied on data from till geochemical surveys conducted across the Slave craton (N = 1560) between 1992 and 2001 by the Geological Survey of Canada (Kerr and Knight 2005). Details on the field and laboratory analytical techniques are presented in Table A1. In brief, composite till samples were collected from hand dug pits 10-70 cm below the surface and were sieved prior to analysis to include silt and clay sized fractions ($< 63 \mu\text{m}$). Samples were analyzed for total As using instrumental neutron activation analysis (INAA), which is considered a total measurement of elements in a sample (Revel and Ayrault, 2000). The intention of the surveys was to compile geochemical information for mineral exploration, therefore, known areas of sulfide mineralization were often targeted, potentially skewing As measurements upwards. In this study, we provide new interpretation of these data to understand the range of geochemical background in different bedrock lithologies of the Slave Geological Province.

Finally, in order to enhance the geospatial visualization of data across the Slave craton, we included data from two additional till surveys (Kjarsgaard 2013; Normandeau 2020). Data from the three studies across the Slave craton were symbolized by quartiles using the Tukey boxplot method in figures, therefore differences in field, laboratory, or analytical methodologies were assumed to have little influence on grouping of data.

3.3.3 Data analysis

3.3.3.1 Spatial distribution of As and As mineralogy across the Yellowknife area

Spatial patterns in the distribution of As in Public Health layer soils in the Yellowknife area were displayed graphically in maps using boxplot classes, so that symbol classes transferred the data

structure into a spatial context (Reimann et al., 2005). We used concentration-distance plots to explore the relationship between soil As and distance from Giant Mine (the main emission source of As in the region). The effect of soil sample location in relation to Giant Mine and the prevailing wind direction axis, on soil As concentration, was also analyzed. Sites were classified according to terrain type and bedrock lithology to explore the influence of these two factors on the regional distribution of As in the region. Detailed sampling (N = 107) in two areas west of Giant Mine resulted in an uneven distribution of sampling points across the region, therefore these sampling plots were down sampled and the median concentration of As in each plot was used in subsequent analyses. Bedrock classes were based on the geospatial database of bedrock geological features in the Slave craton (Stubley and Irwin, 2019), and included granitoid, metasedimentary and volcanic lithology units. Direction relative to Giant Mine and the prevailing wind axis was determined by first calculating the angular direction (0-360°) relative to Giant Mine, then aligning the 0°/180° axis to the prevailing wind direction of 80° by subtracting this amount from the original angular direction and transforming to a scale of -1 to +1 by taking the cosine of the difference. Values of +1 indicate sites directly downwind of Giant Mine and values of -1 indicate sites directly upwind, in relation to the prevailing wind for this region. The influence of terrain type, bedrock lithology, and wind direction (grouped by cardinal direction) on the distribution of Public Health layer As concentrations was assessed using the non-parametric Kruskal Wallis test for significant differences between grouping variables. Post-hoc pairwise Wilcox tests were used to identify between which groups significant differences existed. The influence of distance relative to Giant Mine on soil As was assessed through bivariate linear regression. Log transformation were used where required to meet regression model assumptions.

A general linear model was subsequently formulated with two continuous variables (distance and normalized wind direction) and two factors (terrain type and bedrock lithology) to test for their individual effects on soil As concentrations, and any possible interactions among them. A reverse stepwise approach was used to sequentially remove non-significant independent variables ($p > 0.05$). The relative importance of any independent variable determined to be statistically significant was then calculated using the RELAIMPO package in R (Grömping, 2006). The independent R^2 metric was used to quantify relative importance of regressors. It is calculated by averaging sequential sums of squares over all orderings of regressors in the model. The sum of independent R^2 values yields the unadjusted R^2 for the full model. The independent R^2 for each regressor can be compared to determine its relative importance to observed variance in the dependent variable. In the context of our soil arsenic model, it represents the unique contribution of each independent variable to variance in soil As concentration across the study area. For partially correlated regressors, the independent R^2 is particularly useful because it summarizes only the independent contribution of each to the observed variance in the dependent variable.

We used the identification of As_2O_3 and the proportion of total As (from ICP-OES analysis) as As_2O_3 to fingerprint the extent and magnitude of anthropogenic impact in Public Health layer soils near Yellowknife. Although the minerals arsenolite and claudetite (both As_2O_5) can be found naturally, they are very rare, usually formed as oxidation products directly on arsenic sulfide precursor minerals. This association is not observed in the Yellowknife area and the particles of As_2O_3 in the regional soils, identified as arsenolite by microdiffraction (Bromstad et al. 2017) are discrete and resemble those observed in Giant Mine roaster dust from the underground chambers (Lum et al. 2020). Based on these features, and the known release of 22,000 tonnes of As, dominantly As_2O_3 , from Giant and Con roasters, we assumed that all As_2O_3 present in the soil

samples is anthropogenic. The roaster-derived maghemite and hematite are also anthropogenic, and can usually be distinguished from natural iron oxides by texture (Bromstad et al 2017), but the difficulty in doing that for hundreds of particles resulted in the decision to focus on As_2O_3 in this study. The concentration of As_2O_3 expressed in mg kg^{-1} was determined by multiplying total As (as measured by ICP-OES) for a sample by the proportion of As hosted as As_2O_3 using the SEM-automated mineralogy technique for the subsample slide mount.

3.3.3.2 Estimating geochemical background for the Slave Geological Province

The concept of estimating background can be problematic over large areas (e.g. continents) because of variability in geology, climate, vegetation, and soil forming processes (Reimann and Garrett, 2005). In this study, we developed an estimate of geochemical background for the four main lithologies of the Slave Geological Province, and justify its usefulness because the size of the study area ($\sim 172,500 \text{ km}^2$) is similar to previous studies (Chen et al., 2001; Reimann et al., 2009; Reimann and Garrett, 2005; Salminen and Tarvainen, 1997) and bedrock geology and surficial geomorphology are relatively consistent across the region. Climate and vegetation gradients in the region may influence some soil forming processes, but these differences were not expected to have a major influence on the distribution of As compared to anthropogenic sources or As-bearing mineralization.

Environmental data distributions are rarely normal or lognormal, because the data are spatially dependent and typically influenced by multiple processes that vary across space (Reimann and Filzmoser, 2000). This has consequences for statistical analyses that assume normal or log normal distribution. The quantification of geochemical background for the Slave Geological Province was based on 1564 till samples from Kerr and Knight (2005). Consistent with the graphical display

of Public Health layer samples in the Yellowknife area, As in tills from the Slave craton were displayed in maps using boxplot classes. Since there is a strong relationship between the concentration of soil As and distance from point sources of pollution in the region, we removed all data within 20 km of Yellowknife, based on the results from concentration-distance plots and mineralogical analyses. We tested normality of all remaining original and ln-transformed data (N = 1490) using histograms, quantile plots, boxplots, and the Shapiro –Wilks test of normality. Since neither the original nor ln-transformed distributions met assumptions of normality, several non-parametric methods were used for estimating the range and upper thresholds of geogenic background. These methods included the use of the median \pm 2 median absolute deviations (Md \pm 2MAD), Tukey boxplots, and calculation of the 90th, 95th, and 99th percentiles of the data. Outliers were identified as data beyond the third quartile plus 1.5 times the interquartile range (Q3 + (1.5 x IQR)) but were not excluded from the data so that natural geochemical anomalies were included, and because the data had already been screened for anthropogenic influence.

3.4 Results

3.4.1 Relationships between soil As and distance from legacy mining emission sources

The concentration of As in Public Health layer soils ranged from < 2 to 4700 mg kg⁻¹ (median = 120 mg kg⁻¹) within 30 km of Yellowknife (Figures 3.1 & 3.2A). In general, As concentrations were higher closer to Yellowknife and lower with increasing distance from the city and Giant Mine (Figs. 3.1 & 3.2A). Within 20 km of Yellowknife, 95% of Public Health layer samples exceeded the CCME guideline for residential soils (12 mg kg⁻¹), whereas only 49% of soils beyond 20 km exceeded this value (Figure 3.2A). No samples exceeded the Yellowknife specific guideline for

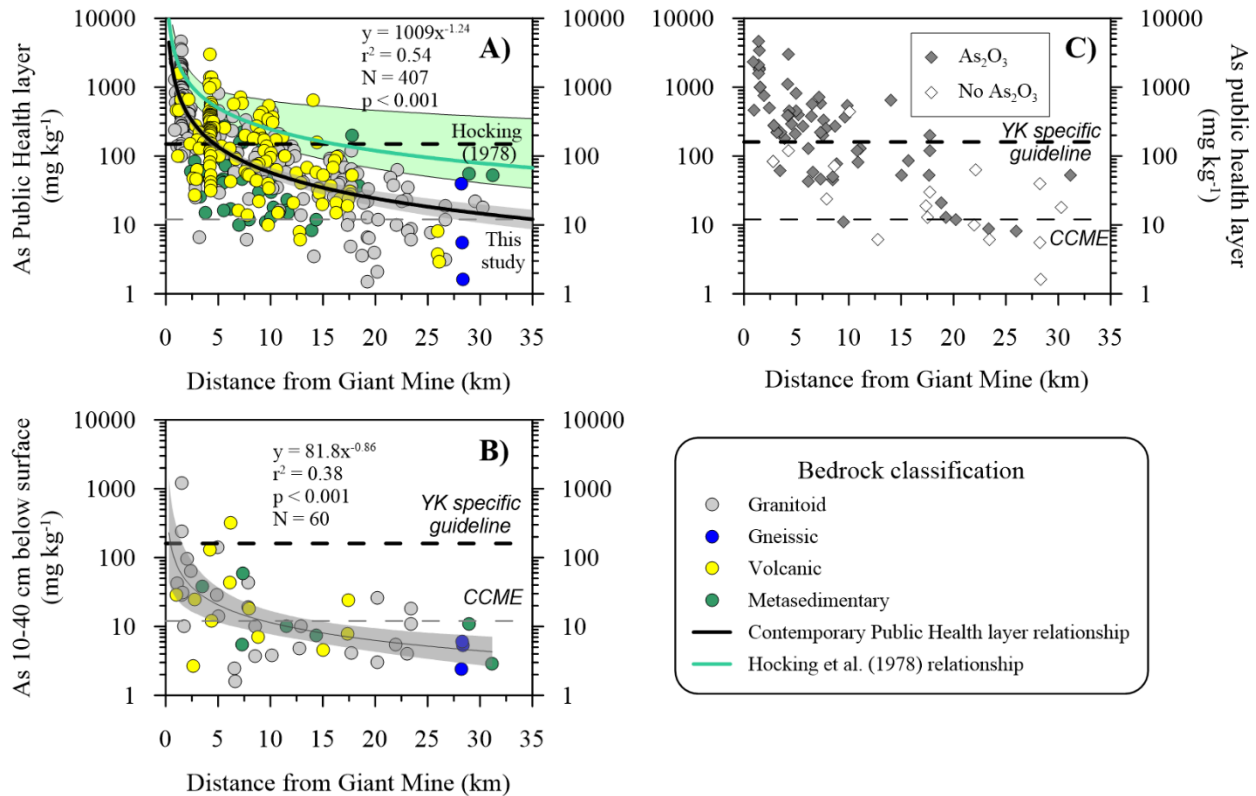


Figure 3.2: The concentration of arsenic in soils with distance from the historical Giant Mine roaster colour coded by underlying bedrock classification for: A) the Public Health layer (0-5 cm); and B) soils 10 – 40 cm below the soil surface. Panel C) The presence and absence of As₂O₃ in a subset of Public Health layer soils (N = 82) as determined by SEM. The CCME guideline for residential soils (12 mg kg⁻¹) (CCME 1997) and a Yellowknife specific remediation guideline for residential soils (160 mg kg⁻¹) (GNWT, 2003) are indicated as dashed lines. The 95% confidence interval of the regression lines in panels A and B are indicated by the shaded areas. The historical relationship between As in the A0 soil horizon and distance from Giant Mine from Hocking et al. (1978) is presented in panel A (95% confidence interval in green shade).

residential soils (160 mg kg⁻¹; GNWT 2003) beyond 17.5 km from Yellowknife, irrespective of underlying bedrock lithology. Figure 3.2A highlights that sampling likely did not extend far enough from Yellowknife to discern a distance at which concentrations no longer decreased since the slope of the relationship does not approach zero by the maximum sampling distance.

An inverse relationship between As concentration and distance from Giant Mine was also evident for samples collected at 10-40 cm depth in the soil profile (Figure 3.2B). The relationship

was significant ($p < 0.001$), however, the model fit was lower than observed for samples in Public Health layer soils (Figure 3.2B). Similar to the distribution of As in Public Health layer soils, there was substantial variation in the concentration of As in downcore samples (Figure 3.2B). Variation was higher for samples collected close to Giant Mine, where As ranged from 2.7 to 1200 mg kg⁻¹ within 5 km of the legacy roaster, compared to distances beyond 20 km where As ranged between 2 and 63 mg kg⁻¹ As. In downcore samples, most of the samples (85%) collected beyond 10 km from Giant Mine were below the CCME guideline for residential soils (12 mg kg⁻¹) (Fig 3.2B).

The results from chemical analyses through the soil profile demonstrate dampening of the As gradient in soil profiles with increasing distance from Yellowknife (Figure 3.3). Arsenic concentrations were highest in surface soils at all distances from Yellowknife and the chemical gradient was most pronounced in sites closest to Yellowknife, where mean As measured 795 mg kg⁻¹ in surficial soils (0 -5 cm) and 35 mg kg⁻¹ at depth (25 – 30 cm) (Figure 3.3). At sites beyond 15 km from Yellowknife mean As measured 27 mg kg⁻¹ and 5 mg kg⁻¹ in surficial soils and soils at depths > 20 cm from the surface, respectively (Figure 3.3). Soils at depth are often considered representative of conditions unimpacted by atmospheric emissions of contaminants (Kerr 2006) and for sites further than 10 km from Giant Mine, soil As > 20 cm below the surface ranged between 2-16 mg kg⁻¹ (Figure 3.3).

3.4.2 Variability in Public Health layer As by terrain type, wind direction, and underlying bedrock geology

While a significant decreasing trend in Public Health layer As concentrations was observed with increasing distance from Giant Mine, there was substantial variation in Public Health layer As concentrations throughout the region, including at sites proximal to legacy mine roasters (Fig 3.2).

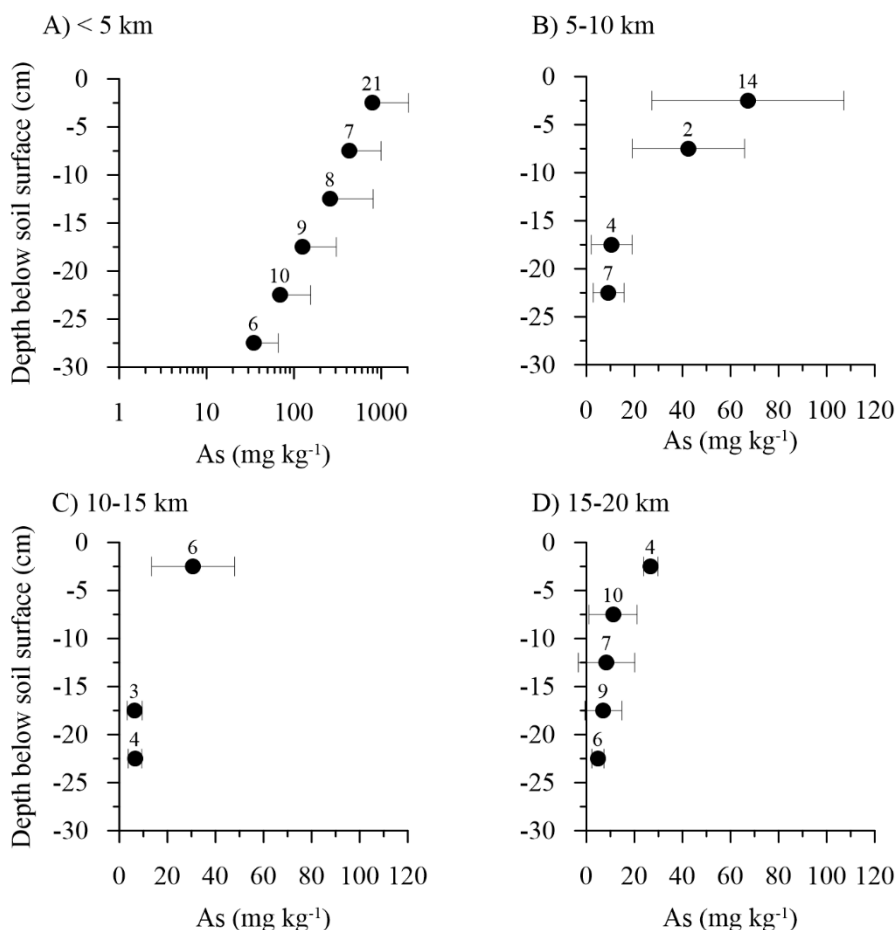


Figure 3.3: Soil core As profiles from sites along a distance gradient from Giant Mine in 5 km intervals: A) < 5 km; B) 5-10 km; C) 10-15 km; and D) 15-20 km. The black circles represent the mean concentration of As at each sampling interval. The horizontal lines represent the standard deviation of As measurements, and the numbers above the lines indicate the number of measurements included in the calculation of the summary statistics for each depth interval. Note, horizontal axis in panel A) is logarithmic scale and the standard deviation is only noted in the positive direction for clarity.

For example, within 5 km of the historic roaster stack at Giant Mine As concentrations ranged between 8 and 4700 mg kg⁻¹ (Figure 3.2A). The highest concentrations of As in soils were measured in areas adjacent to the legacy mine roasters at Giant and Con Mine and were highest in thin outcrop soils overlying granitoid bedrock immediately west of Giant Mine, consistent with predominant wind direction in the region from the east and not associated with areas of known sulfide mineralization (Figures 3.1 and 3.2A). We measured significant differences in the

distribution of As in Public Health layer soils for samples grouped by terrain unit (Kruskal-Wallis chi-squared = 19.96, df = 3, $p < 0.001$) and cardinal wind direction from the Giant Mine roaster stack (Kruskal-Wallis chi-squared = 19.49, df = 3, $p < 0.001$) (Figure 3.4). In the comparison between terrain units, median As concentration was lowest in samples collected from forested areas with thick soils. No significant differences were noted between the distributions of As collected on bedrock outcrops, whether they were tree covered or not, or in peatland terrain (Figure 3.4A). Comparison of soil As concentrations grouped by cardinal wind direction revealed significantly higher soil As to the south and west of Giant Mine than in areas to the north and east. Although significant differences in the distribution of As were measured in soils overlying different bedrock units, there was no significant difference between the distribution of As overlying granitoid and volcanic lithologies (Figure 3.4C). Soil As was lowest overlying metasedimentary units, which are predominately to the east of Yellowknife (Figure 3.1; Figure 3.4C).

A generalized linear model (GLM) with three statistically significant variables was identified for describing soil arsenic concentrations within 30 km of Yellowknife (adjusted $R^2=0.52$, $p < 0.0001$). The regressors included in this model were distance to Giant Mine, direction relative to Giant Mine (normalized to prevailing wind) and terrain type. Bedrock was removed from the model due to lack of significance between the two primary lithologies of interest (granitoid and volcanic). The model results are presented in Table A3 and show that distance from Giant Mine, wind direction and terrain type had a significant effect on ln-transformed As in the region. The relative importance analysis identified distance to be the single-most important predictor of soil arsenic in the context of the GLM model (independent $R^2 = 0.39$) followed by terrain type (independent $R^2=0.08$) and direction (independent $R^2=0.06$).

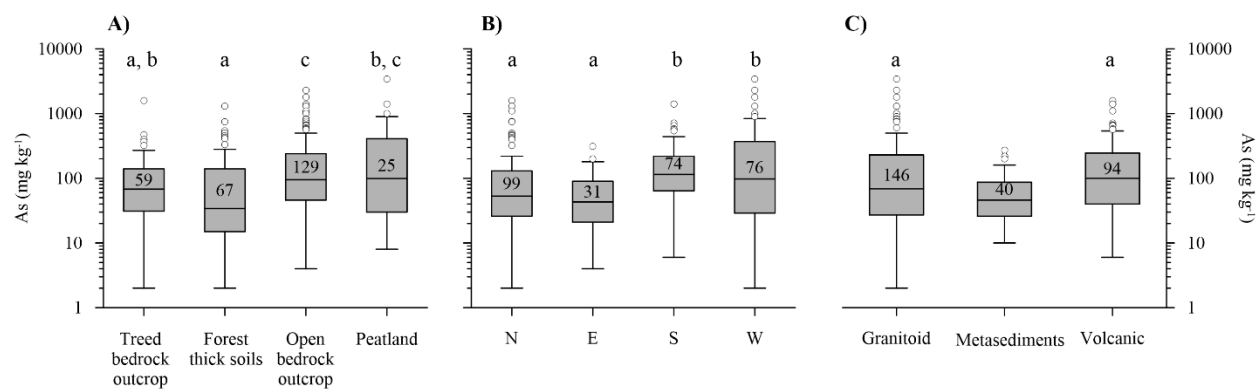


Figure 3.4: Arsenic concentrations in Public Health layer samples by terrain unit, wind direction, and bedrock lithology. Numbers within boxes represent the number of samples in each group. Letters above groups indicate between group comparisons with no significant difference using pairwise Wilcoxon rank sum test at $p < 0.05$.

3.4.3 Solid-phase As speciation in Public Health layer samples

Mineralogical results presented in Figs. 3.2C and 3.4 identify the extent to which legacy mining emissions were dispersed and continue to persist in surface soils. Arsenic trioxide was detected in 82% of the 85 Public Health layer samples that were investigated for As mineralogy, including several sites located more than 25 km from Giant Mine (Figure 3.2C). While Figure 3.2C highlights the presence or absence of As_2O_3 in samples, Figure 3.5 shows the relative proportion of As_2O_3 with respect to total As in each sample. In samples where As_2O_3 was detected it was the predominant As-hosting mineral but the relative proportion of total As as As_2O_3 differed along the distance gradient from Yellowknife and Giant Mine (Figure 3.5; Table A4). Specifically, for sites within 5km of Giant Mine, As_2O_3 accounted for more than 80% of total As measured in samples and at distances up to 20 km from Giant Mine more than 50% of total As (Figure 3.5). Arsenic trioxide was detected in 49 of 50 samples where total As was above the Yellowknife specific remediation guideline of 160 mg kg^{-1} (Figure 3.2C).

Several other As-hosting minerals were observed in samples from the region (see Table A4), including additional minerals inferred to derive from mining sources. Specifically, scorodite was

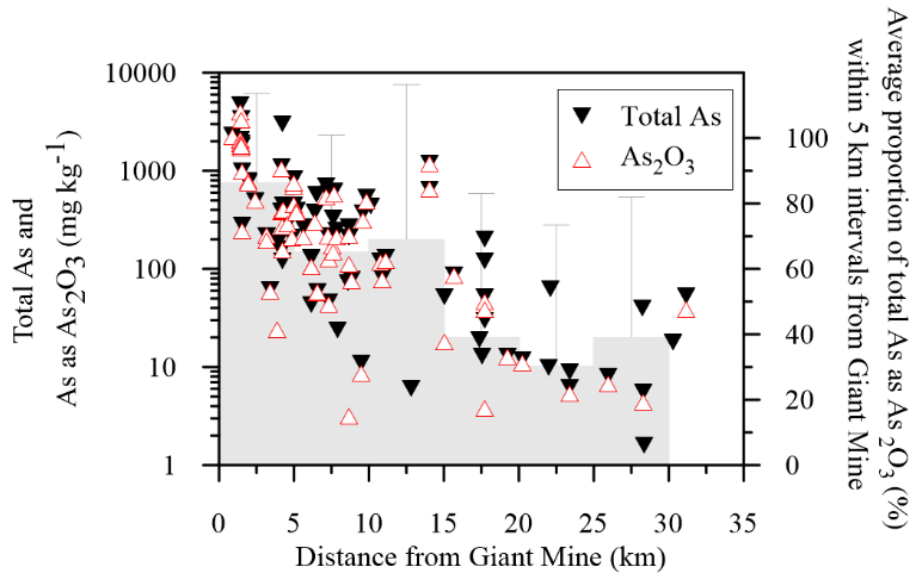


Figure 3.5: Total As and As₂O₃ (mg kg⁻¹) in Public Health layer samples (0-5 cm) with distance from the historic Giant Mine roaster. Total As (mg kg⁻¹) was measured by ICP-OES following an *aqua regia* digestion of the soils. The concentration of As₂O₃ (mg kg⁻¹) was determined by multiplying total As by the proportion of As hosted as As₂O₃ in each sample as determined by the SEM-automated mineralogy technique. The shaded bars represent the mean proportion of total As as As₂O₃ in samples from 5 km intervals with increasing distance from Giant Mine.

found in several samples near Con Mine and may be related to processing waste from pressure oxidation that was used later in mine life at Con Mine (Walker et al. 2015) and roaster-generated iron oxides, which were interpreted to be of anthropogenic origin based on texture, were widely observed near Giant Mine (Walker et al. 2005; Bromstad et al. 2017). However, as previously explained, distinction of these roaster-generated iron oxides from natural pedogenic Fe, Mn-oxides was not feasible for all samples. Consequently, the anthropogenic proportion of As in soils in the region was likely underestimated, since these other minerals were not considered in the proportion of total As as anthropogenic species (Figure 3.5). Arsenopyrite and As-bearing pyrite were expected to be the predominant As-hosting minerals associated with natural enrichments of As in the region, as these are the dominant As minerals in bedrock and mineralization. Arsenopyrite was observed in 24% of samples, but typically accounted for < 5% of As where it was detected

(Table A2). Where arsenopyrite measured > 10% of total As, total soil concentrations of As were less than the YK specific guideline of 160 mg kg⁻¹ (Table A2). Pyrite was observed more frequently than arsenopyrite (75% of samples), but the proportion of As in samples as pyrite was typically low and had a framboidal texture suggesting secondary precipitation.

3.4.4 Geochemical background in the Slave Geological Province

We used data from a geochemical survey that spans much of the Slave Geological Province, including relatively pristine areas beyond municipal and mining impacts, to better understand natural variability of As in surficial materials in the region and to provide context for soil As concentrations close to point sources of legacy mining emissions. The compilation presented in Figure 3.6A demonstrates substantial variation in the concentration of As in tills and soils across the Slave Geological Province (range: 0.25 – 1050 mg kg⁻¹). Arsenic concentrations measured < 22 mg kg⁻¹ in 95% of samples, yet there were distinct areas with clustering of outliers. The most obvious area dominated by outliers was observed near Yellowknife (Figures 3.6A & B), but smaller clusters were also observed in the Beaulieu River Belt and along the Northwest Territories – Nunavut border in the Courageous Lake and Indin Lake belts (Figure 6A) associated with known gold deposits in the region (GNWT, 2016).

Several statistical methods were applied to the till data presented in Kerr and Knight (2005) to estimate the range and upper threshold of geochemical background in the region. The data were screened to exclude samples collected within a 20 km radius of Yellowknife, since these data were expected to have been impacted by atmospheric emissions from legacy roasters in the region based on results from the concentration-distance plots (Figure 2) and mineralogical evidence (Figure 3.5) presented in sections 3.4.1 and 3.4.3. The distribution of the original and ln-transformed data

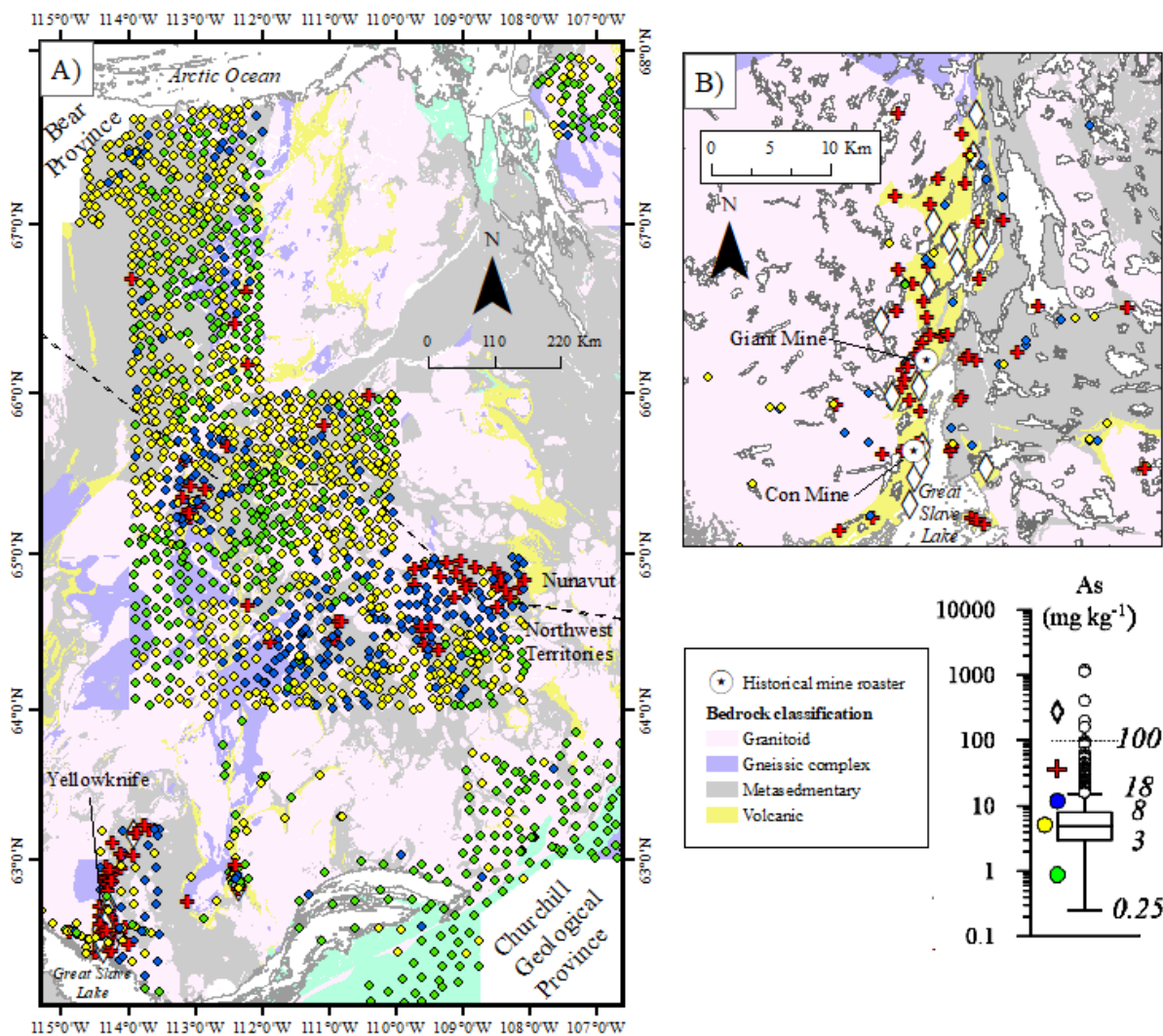


Figure 3.6: Distribution of As in soils and till in: A) the Slave Geological Province; and B) the Yellowknife area. All samples collected between 10 and 70 cm below the soil surface. Data presented in these maps represent a compilation of 4 geochemical soil surveys conducted between 1999 and 2016. See Methods for field and analytical methods for each of the studies in the compilation. Data are symbolized following the Tukey boxplot method, where data are presented as: less than 1st quartile (green circles), between 1st and 3rd quartile (yellow circles), between 3rd quartile and upper fence (3rd quartile + 1.5*IQR) (blue circles), and beyond the upper fence are considered outliers (red crosses) and far outliers (open diamonds).

differed significantly from an ideal Gaussian (normal) curve following results from the Shapiro-Wilk test for normality (Original data: $W = 0.08$, $p < 0.001$; ln-transformed data: $W = 0.95$, $p < 0.001$) (Figure A2). Multiple inflection points in the cumulative frequency diagram for the original

data indicated the presence of several subpopulations in the data and suggests the influence of multiple processes on the data distribution (Figure A2). The data were not screened further as we were interested in exploring subpopulations driven by differences in bedrock lithology and areas of mineralization. Since neither the original or ln-transformed data followed a normal distribution we excluded the use of parametric tools for the estimation of the range of geochemical background and focused on non-parametric methods, including the metrics provided by the Tukey boxplot. The lower and upper fences of the screened Kerr and Knight (2005) data suggests a geochemical background range in the Slave Geological Province between 0.25 and 15 mg kg⁻¹ As (Figure 3.6, Table 3.1). Several other statistical approaches were applied to the data to estimate the upper threshold of background As in tills in the region, since the definition of upper threshold is often the focus of efforts in environmental remediation work and the selection of which metric to use is often a point for discussion by decision-makers (Table 3.1). The Md±2MAD approach was the most conservative technique resulting in an upper threshold of 11 mg kg⁻¹. The use of the upper fence and the 90th percentile yielded slightly higher results of 15 and 14 mg kg⁻¹, respectively. The use of the 95th and 99th percentiles of the data distribution resulted in much higher estimates for the upper threshold of background and were within the portion of the data distribution identified as data outliers by the boxplot method ($> Q3 + 1.5 \times IQR$) (Figure 3.6, Table 3.1).

The large number of samples across bedrock lithologies in the Slave Province (N = 1490) allowed for the estimation of background As by bedrock unit and comparisons between units. Significant differences in the distribution of As in tills were noted between underlying bedrock types (Kruskal-Wallis test of differences: chi-squared = 58.66, df = 3, p < 0.001). The upper threshold of geochemical background As was highest in tills overlying volcanic bedrock units, but varied substantially depending on the metric used to define the upper threshold (Figure 3.7; Table

Table 3.1. Summary statistics for till As concentrations (mg kg^{-1}) from Kerr and Knight (2005) excluding samples within 20 km of Yellowknife, representing natural background in the region. Upper fence is calculated as the 3rd quartile + 1.5 x IQR (interquartile range).

	<i>N</i>	<i>Max</i>	<i>Min</i> ^a	<i>Median</i>	<i>MAD</i>	<i>Upper Threshold Estimates</i>				
						<i>Median + 2MAD</i>	<i>Upper fence</i>	<i>Percentile</i>		
							<i>90th</i>	<i>95th</i>	<i>99th</i>	
All samples	1490	1190	0.25	4.8	3.1	11	15	14	22	46
Volcanic	161	1190	0.25	5.6	4.7	15	30	39	65	282
Granitoid	570	36	0.25	4.5	3.1	11	15	12	14	27
Metasedimentary	613	1150	0.25	5.2	3.0	11	15	16	21	44
Gneissic complexes	146	26	0.25	3.4	3.1	9.6	13	9.8	11	19

^aNote, minimum detection limit for As in Kerr and Knight (2005) data was 0.25 mg kg^{-1} , therefore data reported at this level may represent values below the minimum detection limit of the instrument.

3.1). In tills overlying volcanic bedrock, upper thresholds of geochemical background ranged between 15 and 282 mg kg^{-1} for the $\text{Md} \pm 2\text{MAD}$ and 99th percentile approaches, respectively (Table 3.1). Upper thresholds for background As concentrations varied less between techniques in tills overlying lithologies other than volcanic bedrock (Table 3.1). Significant differences in the distribution of As in tills were noted between all bedrock lithology units except the volcanic and metasedimentary units (Figure 3.7).

3.5 Discussion

3.5.1 Impacts from legacy mining emissions persist in soils near Yellowknife

Impacts from mining emissions have been documented in Yellowknife area soils since Hocking et al. (1978). The data presented in this study demonstrate that soil As remains elevated in the Yellowknife region more than 60 years since the bulk of As_2O_3 was released from mining operations and more than 20 years since mining emissions ceased in the region. Strong relationships between the distance from the main emission point source (Giant Mine) and the concentration of As in Public Health layer soils and soils at depth persist in the region (Figures

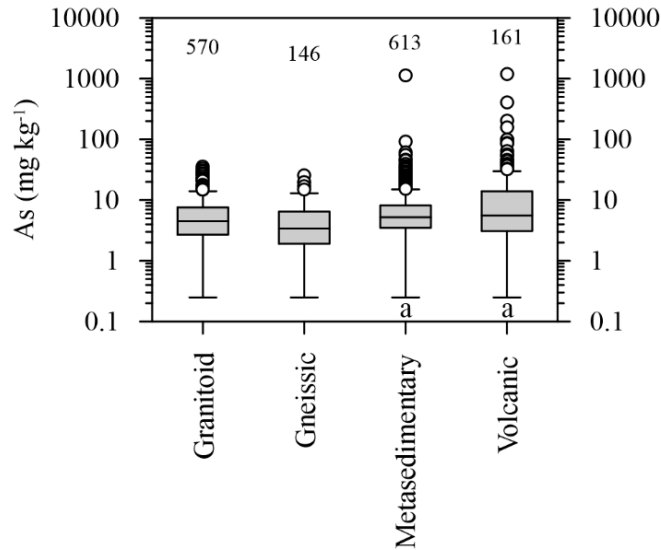


Figure 3.7: Tukey boxplots for As in silt and clay fraction of till (data > 20 km from YK) from the Kerr and Knight (2005) dataset. The horizontal line represents the median, the box limits represent the 1st and 3rd quartiles. Whisker limits indicate the upper (Q3 + 1.5*IQR) and lower (Q1 - 1.5*IQR) fences of the data distribution. Outliers represent values beyond the upper fences and are indicated by open circles. Numbers above the plots represent the number of samples for each bedrock type. Kruskal-Wallis test for differences between groups indicates that there are significant differences in the distributions between groups (chi-squared = 58.658, df = 3, p < 0.001). Letters below groups indicate As distributions that are not significantly different (p > 0.05) (Pairwise comparison between groups using Wilcoxon rank sum test). Note, the two highest As values in the volcanic group are associated with gossans near Discovery Mine (Kerr and Knight 2005).

3.2A & 3.2B). A comparison of the best fit lines for contemporary and historical relationships between soil As and distance from Giant Mine suggests that concentrations of soil As have decreased in the region since reported by Hocking et al. (1978) (Figure 3.2A). The comparison between the two datasets should be interpreted with caution, as the Hocking et al. (1978) data represent far fewer samples (N = 17) than reported in this study, were concentrated within 10 km of the historical roasters at Giant and Con mines, and employed different field and analytical methods. However, the distinct difference between the best fit lines, even within 10 km of Giant Mine, suggests the gradual recovery of soils in the region over the last 40 years.

The combination of statistical, geochemical and mineralogical methods applied in this study represent a novel approach to distinguishing between natural and anthropogenic enrichment of As in soils for areas impacted by legacy mining emissions. Multiple lines of evidence support the supposition that concentrations of As in Yellowknife area soils are elevated relative to other areas in Canada and the world because of the atmospheric deposition of As from legacy mining activities and not associated with natural enrichment from sulfide mineralization. First, the clear concentration-distance relationship between soil As and distance from contaminant point sources (Figure 3.2) are consistent with other regions that have been impacted by point sources of pollution (e.g. McMartin et al. 1999; Reimann et al. 2000) and suggest widespread As contamination of soils in the region, irrespective of proximity to sulfide mineralization. Second, sampling through the soil profile shows that As concentrations decrease substantially with sampling depth (Figure 3.3), consistent with an atmospheric source of As (Ukonmaanaho et al., 2004; Yang et al., 2014). The dampening of the As gradient in the soil profile with increasing distance from the contaminant point sources shows the far greater magnitude of impact in soils close to the legacy mine roasters. As such, As concentrations at depth, which are often used to represent atmospherically unimpacted conditions, should be interpreted with caution, as the continued dissolution and downward migration of As may result in reprecipitation of As minerals at depth that are ultimately derived from mining sources. Finally, mineralogical assessment of soil samples from the region provides unambiguous information on whether As found in soils is derived from anthropogenic or natural processes. The mineralogical evidence shows that As in Public Health layer soils is overwhelming associated with As_2O_3 in the region, as As_2O_3 accounts for more than 80% of total As for samples collected within 5 km of Giant Mine and more than 50% of total As at sites up to 20 km (Figure 3.5). Further, it should be acknowledged that while the remaining As identified in samples is not

associated with As_2O_3 , in many cases it may ultimately be derived from it, as secondary As-bearing minerals forming in-situ following the dissolution of As_2O_3 .

The abundance of As_2O_3 identified in Public Health layer soils was a surprising observation, since As_2O_3 is expected to be highly soluble under field conditions (Riveros et al., 2000). Typically, studies on the environmental fate of As_2O_3 have stressed the importance of understanding environmental conditions controlling the formation and stability of secondary As minerals, rather than assessing the factors that control As_2O_3 dissolution (Qi and Donahoe, 2008; Yang and Donahoe, 2007). Previous work in the Yellowknife region highlighted the persistence of As_2O_3 in soils on the mine property near the roaster at Giant Mine (Bromstad et al., 2017). Several reasons for the limited mobility of As_2O_3 in surface soils on site have been proposed, including the cold and dry climate of the Yellowknife area, slow dissolution kinetics, and the incorporation of Sb in the As_2O_3 structure, which may limit solubility (Bromstad et al., 2017; Dutrizac et al., 2000). This study builds on this previous work and shows that As_2O_3 is persisting in weathering environments throughout the region. Table A2 highlights that mineral phases that are likely geogenic in origin (arsenopyrite, pyrite, some of the Fe-oxides that formed as weathering products of those sulfide minerals) account for a small proportion of As-hosting minerals in the majority of samples in this study indicating that most of the As measured in surface soils in the region is attributable to legacy mining sources rather than natural enrichment associated with gold-bearing mineralization.

The extent of environmental impact from point sources of pollution is often sought for environmental management and remediation purposes. In this study, As concentration-distance relationships for Public Health layer soils (Figure 3.2A) and soils at depth (Figure 3.2B) suggest that impacts were relatively minor beyond 20 km from Giant Mine compared to areas close to

Giant Mine. Surface enrichments of As (Figure 3.3) and the identification of As_2O_3 (Figure 3.5) beyond 20 km indicates that while impacts are substantially less than in areas close to Yellowknife, soils beyond 20 km can be impacted by legacy mining emissions. This shows the important contribution of mineralogical analysis in regional background assessments for areas with legacy anthropogenic impacts. In general, the concentration-distance relationships, soil profile sampling and mineralogical assessment of samples indicated that sampling Public Health layer soils within a 30-km range was not far enough from Yellowknife to confidently determine a robust zone of influence from past mining emissions in soils in the region. Evidence from recent studies in lake sediments also suggests a wider impact from legacy pollution sources than previously reported and likely extend beyond 40 km from emission point sources (Cheney et al., 2020). Studies from Flin Flon, MB and Sudbury, ON estimate maximum impacts of As pollution up to 104 km from pollution sources (McMartin et al., 1999). We would expect the zone of influence to be smaller in the Yellowknife region, since the stacks for the roasters at Giant Mine were substantially shorter (max height approx. 70 m) (Silke, 2013) than at smelting facilities in Flin Flon and Sudbury (max height approx. 380 m) (Hutchinson and Whitby, 1977), which would reduce the atmospheric dispersion of pollutants. While we show that sampling of Public Health layer soils in this study did not extend to adequate distance from legacy mining emission sources, it is clear that soil As declines steeply with increasing distance from historical As emission sources so that As concentrations in most soils beyond 20 km are below Canadian guidelines for agricultural and residential soils (12 mg kg^{-1}) (Figures 3.2A & 3.2B).

3.5.2 Variability in Yellowknife area soil As driven by regional and local factors

The substantial variation in Public Health layer soil As in the Yellowknife area (Figure 3.1) highlights the importance of several regional and local factors beyond proximity to point sources of As emissions in controlling the distribution of As in soils in the region. The influence of dispersal of atmospheric pollutants along predominant wind axes is well established (Fritsch et al., 2010; McMartin et al., 1999; Reimann et al., 2009) and the data presented in this study show that soil As was significantly elevated at sites downwind to the west of Giant Mine irrespective of distance from the roaster (Figure 3.1; Table 3.1). Soil As was also elevated to the south of the Giant Mine roaster, that corresponds with the secondary wind axis in the region, but may be confounded by high As concentrations derived from emissions at Con Mine, that is located south of Giant Mine. The lowest concentrations of soil As were measured at sites east of Giant Mine and correspond with relatively rare westerly winds in the region (Figure 3.1). The distribution of soil As to the east of Giant Mine and Con Mine is also influenced by the lack of sampling within 2.5 km of the former roaster stacks because of the presence of Yellowknife Bay (Figure 3.1).

In smelter affected soils from temperate regions, soils from forested areas typically have higher metal(loid) burdens than in open areas, such as grasslands and crop fields, due to greater canopy interception and retention of atmospheric particles (Douay et al., 2009; Ettler et al., 2005). In this study we observe the inverse, where soil As was highest in open areas of bedrock outcrops. Much of the shield landscape is dominated by expansive bedrock outcrops with pockets of thin soils. Bromstad et al. (2017) highlight that these soil pockets act as sinks on the landscape, as atmospheric pollutants deposited on exposed bedrock areas are washed downslope and accumulate. In the relatively cold and dry climate there is little opportunity for these metal(loid)s in soils to be remobilized except during snowmelt or periods of high rainfall. At the local scale,

the distribution of As₂O₃ particles in individual samples may be an important factor driving As variability within localized areas, since As₂O₃ is extremely As-rich (76 wt % As). Consequently, bulk As concentration is highly dependant on the number of As₂O₃ particles found in a sample.

3.5.3 Estimation of geochemical background for the Slave Geological Province

The estimation of geochemical background in this study draws on a large number of till samples (N = 1490) collected over a wide area with consistent parent material that includes much of the Slave Geological Province. Our estimates for the upper threshold of geochemical background in the region were well below previous estimates for the area, including the estimate from ESG (2001) that was used to derive current residential (160 mg kg⁻¹) and industrial (340 mg kg⁻¹) environmental remediation guidelines in the region (GNWT, 2003) and were comparable to the Canadian Soil Quality Guideline for the Protection of Environmental and Human Health (12 mg kg⁻¹, CCME (2001)). The upper threshold limits estimated in this study (Table 3.1) were also in line with geochemical background estimates from other locations around the world. Reimann and Garrett (2005) summarized median As concentrations in soils from 14 studies across the world and highlighted As concentrations in undisturbed soils were typically < 30 mg kg⁻¹ As. The exception was soils in the Saualpe region in Austria where geochemical background As in soils was 101-115 mg kg⁻¹ and was attributed to natural As enrichment in parent material from the region.

We acknowledge that tills do not solely represent material weathered *in situ*, and may be derived from the erosion and entrainment of material from substantial distances up-ice. However, soil development in the Slave craton is limited, due to the cold dry climate, prevalence of exposed bedrock, and relatively recent deglaciation and recession of Glacial Lake McConnell and ancestral

Great Slave Lake. Consequently, tills represent the most common terrestrial unconsolidated material in the region and an appropriate medium to represent geochemical background in soils.

The estimation of upper thresholds of till As by underlying bedrock lithology suggests that underlying geology did have an effect on till As across the Slave Geological Province. The distribution of As was highest in tills overlying volcanic bedrock units (Figure 3.7). These are the units that typically host gold-bearing mineralization in greenstone belts throughout the region (Boyle, 1979; GNWT, 2016) and the world (Smedley and Kinniburgh, 2002; Tanaka, 1988). Boyle and Jonasson (1973), Tanaka (1988) and Smedley and Kinniburgh (2002) provide detailed summaries of As concentrations in various bedrock lithologies and soils from previous studies, including from the Yellowknife area. In general, concentrations of As in igneous source rocks are low ($0.1 - 12 \text{ mg kg}^{-1} \text{ As}$, $N = 411$) and less than in sedimentary units ($0.1 - 188 \text{ mg kg}^{-1} \text{ As}$, $N = 674$) because the adsorption and/or co-precipitation of As with Fe minerals during sedimentation processes can enrich As in sedimentary units. That being said, Boyle and Jonasson (1973) and Tanaka (1988) present a clear picture of substantial As enrichment in bedrock and soils near mineralized shear zones, which can host high concentrations of As associated with sulfide deposits. These As enrichments are typically localized and may only extend a few meters to a few hundred meters (Boyle and Jonasson, 1973; Smedley and Kinniburgh, 2002; Tanaka, 1988). For example, in a mineralized shear zone in a greenstone belt near Motapa Mine, Rhodesia (now Zimbabwe) very high concentrations ($> 1000 \text{ mg kg}^{-1} \text{ As}$) of As were measured in host rock and subsequently decreased to $\sim 1 \text{ mg kg}^{-1} \text{ As}$ within 100 m of the shear zone (Tanaka, 1988). In this study, clear As anomalies are noted in several areas across the Slave Province beyond Yellowknife, and these enrichments are highly localized and correspond with areas of known mineralization. We note that the highest concentrations of till As were measured overlying volcanics near the Discovery

gold deposit (Figure 6A) and were associated with sites where gossans, typical of weathered sulfide deposits, were identified by Kerr and Knight (2005). Regardless of high till As measured in some localized areas ($\text{As} > 100 \text{ mg kg}^{-1}$), the bulk of till data, as defined by the 95th percentile, was below $22 \text{ mg kg}^{-1} \text{ As}$ (Table 3.1).

3.6 Concluding remarks

Continued investigation and monitoring of soils are essential to the understanding of ecosystem recovery in areas that have been impacted by mining emissions. This study provides new information on the concentration and solid-phase speciation of As in soils in the Yellowknife region and presents a novel strategy for identifying and delineating anthropogenic impacts in soils. Mineralogical tools were critical in identifying the main mineral hosts of As in soils and allowed for the unambiguous attribution of most of the As in soils close to point sources of mining emissions to anthropogenic sources rather than natural As enrichment. The coupling of mineralogical results with broad geochemical surveys facilitated the delineation of impacted areas and estimation of the range of geochemical background. The large number of till samples collected across much of the Slave Geological Province as part of Geological Survey of Canada efforts (Kerr and Knight, 2005) was an immense resource and permitted the estimation of geochemical background conditions by underlying bedrock lithology, which showed that the upper threshold of geochemical background is likely slightly elevated in soils overlying volcanic bedrock units compared with other lithology units. Using more than a thousand soil measurements it can be concluded that natural arsenic enrichment may occur in areas of sulfide mineralization, but the influence is highly localized and cannot account for the broad enrichment of arsenic in soils by

mining emissions in the Yellowknife area, which are substantially elevated compared to geochemical background in the Slave Geological Province.

The fact that As was overwhelmingly associated with legacy mining emissions close to Yellowknife does not necessarily imply a risk to human or ecological health in interacting with these soils. Human health and ecological risk assessments have been conducted in the region (e.g. Canada North Environmental Services, 2018) and as new information is released these assessments should be revisited to ensure findings are up to date. The information from this study should be used to acknowledge that widespread As contamination persists in the region and will need to be considered in future land use management decisions. Ultimately, this study demonstrates the strength of using multiple methods in the estimation of geochemical background and will be useful for resource managers required to untangle anthropogenically impacted soils from those that may be naturally enriched in metal(loid)s.

Chapter 4: Seasonal variation of arsenic and antimony in surface waters of small subarctic lakes impacted by legacy mining pollution near Yellowknife, NT, Canada

Abstract

The seasonal variation in lake water arsenic (As) and antimony (Sb) concentrations was assessed in four small (< 1.5 km²) subarctic lakes impacted by As and Sb emissions from legacy mining activities near Yellowknife, Northwest Territories, Canada. Substantial variation in As concentrations were measured over the two-year period of study in all but the deepest lake (maximum depth 6.9 m), including a four-fold difference in As in the shallowest lake ([As]: 172-846 µg L⁻¹; maximum depth 0.8 m). Arsenic concentrations were enriched following ice cover development in the three shallowest lakes (50-110%) through a combination of physical and biogeochemical processes. Early winter increases in As were associated with the exclusion of solutes from the developing ice-cover; and large increases in As were measured once oxygen conditions were depleted to the point of anoxia by mid-winter. The onset of anoxic conditions within the water column was associated with large increases in the concentration of redox sensitive elements in lake waters (As, iron [Fe], and manganese [Mn]), suggesting coupling of As mobility with Fe and Mn cycling. In contrast, there was little difference in Sb concentrations under ice suggesting that Sb mobility was controlled by factors other than Fe and Mn associated redox processes. A survey of 30 lakes in the region during fall (open-water) and late-winter (under-ice) revealed large seasonal differences in surface water As were more common in lakes with a maximum depth < 4 m. This threshold highlights the importance of winter conditions and links between physical lake properties and biogeochemical processes in the chemical recovery of As-impacted subarctic landscapes. The findings indicate annual remobilization of As from

contaminated lake sediments may be inhibiting recovery in small shallow lakes that undergo seasonal transitions in redox state.

4.1 Introduction

Atmospheric metal(loid) pollution from industrial sources is a global concern (e.g. Matschullat, 2000) and the legacy of these activities can persist in aquatic environments decades after emissions are reduced or eliminated (Blais et al., 1999; Houben et al., 2016; Keller et al., 2007). Arsenic (As) and antimony (Sb) are metalloids of particular interest because of the associated human and ecological health risks (Bhattacharya et al., 2007; Filella et al., 2009), and are considered priority pollutants by the United States Environmental Protection Agency (EPA, 2014). High concentrations of these metalloids often exist together in mining waste streams due to the co-occurrence in hydrothermal mineral deposits (Fawcett et al., 2015; Serfor-Armah et al., 2006). Considerable research has been directed at understanding the biogeochemistry of As, because of its widespread occurrence in the environment and toxicity (Bhattacharya et al., 2007; Smedley and Kinniburgh, 2002). In contrast, processes that influence Sb mobility and sequestration remain relatively poorly understood, and there are fewer field studies directed at understanding Sb biogeochemical processes in aquatic systems (Filella et al., 2009).

The biological and chemical recovery of lakes from metalloid pollution is complex and is influenced by multiple factors, including the physical and hydrological properties of the lake and its basin, and the biogeochemical cycling of the pollutant (Belzile et al., 2004; Greenaway et al., 2012; Martin and Pedersen, 2002). Understanding recovery processes in small waterbodies is important because small lakes (<1 km²) dominate the global distribution of freshwaters and many aquatic processes are amplified in smaller lakes and ponds (Downing et al., 2006). The influence of benthic fluxes of metal(loid)s is magnified in small, shallow lakes due to the typically higher

ratio of sediment surface area to lake volume (Orihel et al., 2017). In lakes that have received inputs of As waste, recovery of surface waters may be delayed or confounded by the internal loading of As to the water column from As stored in the sediments (Martin and Pedersen, 2004, 2002). The seasonal and long-term fate of As is often coupled with the biogeochemical cycling of iron (Fe), and may vary throughout the year dependent on changes in redox conditions near the sediment boundary (Couture et al., 2008; Martin and Pedersen, 2002; Senn et al., 2007). Iron (oxy)hydroxides form under oxic conditions in near-surface lake sediments and can sequester As from the dissolved fraction through co-precipitation or adsorption (Dixit and Hering, 2003). The development of anoxia in sediments results in the reductive dissolution of Fe (oxy)hydroxides, releasing sorbed As to porewaters and the overlying water column (Arsic et al., 2018; Bennett et al., 2012). This process has been demonstrated for a variety of events that may induce anoxic conditions near the sediment boundary, including: lake eutrophication (Azizur Rahman and Hasegawa, 2012; Hasegawa et al., 2009) and the seasonal thermal stratification of the hypolimnion (Hollibaugh et al., 2005; Senn et al., 2007).

The biogeochemical cycling of Sb is less well understood than for As and conflicting examples exist regarding the mobility of Sb in oxidized surficial environments. Many field and laboratory-based studies demonstrate the importance of Fe (oxy)hydroxides in controlling Sb mobility in soils and lake sediments (e.g. Chen et al., 2003; Mitsunobu et al., 2010, 2006). In contrast, recent studies from contaminated environments have shown increased mobility of Sb under oxic conditions and suggest the competitive advantage of aqueous As(V) over Sb(V) for sorption sites on Fe (oxy)hydroxides (Fawcett et al., 2015) or Sb(III) oxidation and release of Sb(V) driven by the precipitation of Fe (oxy)hydroxides as a mechanism (Ren et al., 2019). In several studies, the limited mobility of Sb observed in anoxic environments has been attributed to

the precipitation of Sb(III) with reduced organic or inorganic sulfur to form solid phase species (Arsic et al., 2018; Bennett et al., 2017; Fawcett et al., 2015; Ren et al., 2019). Majzlan et al. (2016) discussed the apparent disagreement in the literature on whether Sb is mobile in the near-surface environment and suggested this was due to variable solubility of oxidation products of primary Sb minerals.

In light of this previous research there has been little consideration of how winter processes in subarctic environments may influence the mobility of As and Sb, because most field studies have been undertaken in temperate or tropical locations or restricted to the open-water season (e.g. Chen et al., 2003; Hollibaugh et al., 2005; Senn et al., 2007). Shallow subarctic lakes may be ice covered for more than half the year, which can strongly affect the physical and chemical properties of surface waters. The development of an ice cover may lead to the onset of seasonally anoxic conditions when the oxygen demand in the sediments exceeds the oxygen budget in the water column (Deshpande et al., 2015; Mathias and Barica, 1980) and the exclusion of dissolved solutes and gases from the ice matrix can increase solute concentrations in underlying waters (Bergmann and Welch, 1985; Hobbie, 1980; Pieters and Lawrence, 2009). Understanding the seasonality of water quality in small subarctic lakes is important because cryoconcentration and increased sediment efflux may increase As and Sb exposure to aquatic organisms or in some cases contribute to the delayed recovery of these systems.

This study examined the seasonal variation of As and Sb in four small subarctic lakes that were impacted by atmospheric deposition of contaminants from gold mining in the Yellowknife area. The primary elements of focus were As and Sb, because these metalloids were released in large quantities from historical ore roasting operations and often exhibit contrasting geochemical behavior in the environment (Arsic et al., 2018; Fawcett et al., 2015). The objective of this study

was to quantify the extent of seasonal variation in surface water quality of shallow subarctic lakes impacted by legacy mineral processing and to investigate the roles of physical (cryo- and evapo-concentration) and biogeochemical (sediment efflux) controls on surface water concentrations of As and Sb. We used a combination of frequent sampling at four lakes close to historical mining operations and a series of regional lake surveys to evaluate seasonality at the lake scale and a broader regional scale.

4.2 Materials and Methods

4.2.1 Environmental setting and background

The study area is located within the southern portion of the Slave Geological Province of the Canadian Shield (Figure 4.1). Small lakes are common in the region and remnant from the recession of Glacial Lake McConnell and ancestral Great Slave Lake within the last 10,000 years (Wolfe et al., 2017b). The climate of the region is continental subarctic and characterized by long, cold winters (-25.6°C January mean) and short, warm summers (17.0°C July mean) (Environment Canada, 2018). Temperatures typically drop below freezing in early October and remain below 0°C until mid-to-late April (Environment Canada, 2018). Consequently, small lakes such as those investigated in this study may be ice-covered for half of the year. Air temperatures during the study period were similar to climate normals (1980-2010) for Yellowknife, except for the winter of 2015-16 that was slightly warmer than average (Figure B1) (Environment Canada, 2018).

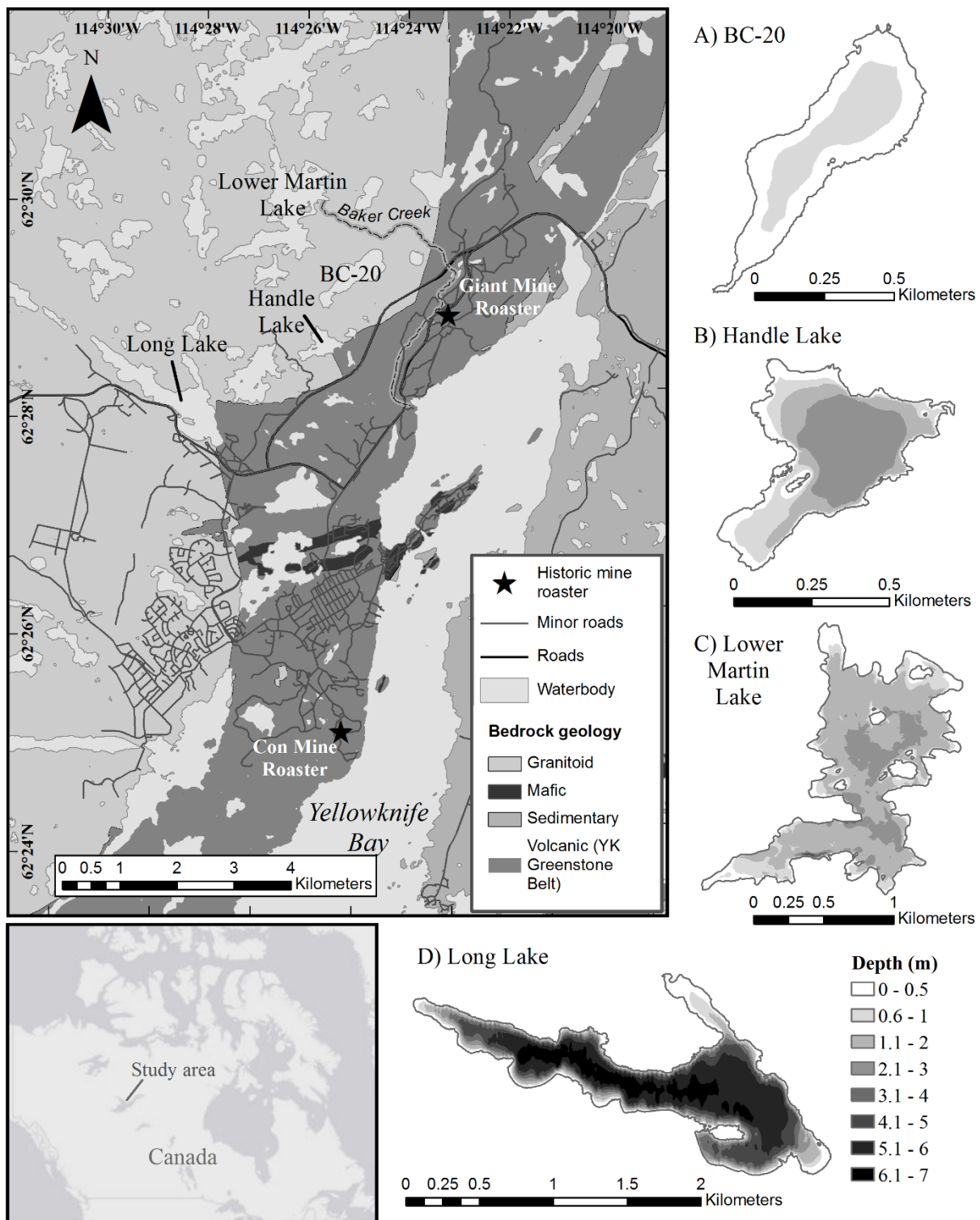


Figure 4.1: Study area (left panel) and bathymetry of the four study lakes: a) BC-20; b) Handle Lake; c) Lower Martin Lake; and d) Long Lake.

4.2.1.1 Arsenic and antimony pollution in the Yellowknife area, NT, Canada

The Yellowknife area was one of the most productive gold mining regions in Canada. More than 13.5 million ounces of gold were produced between 1938 and 2004, predominately from the two largest mines: Giant Mine (1949-2004) and Con Mine (1938-2003) (Moir et al., 2006). Roasting of gold-bearing arsenopyrite (FeAsS) resulted in emissions of a volatile gas phase of As ($\text{As}(\text{OH})_3$ or As_4O_6) that condensed to arsenic trioxide (As_2O_3) dust upon release from the roaster stacks and was subsequently distributed across the surrounding landscape (Hocking et al., 1978; Hutchinson et al., 1982; Walker et al., 2015). More than 20 000 tonnes of As_2O_3 were released during operations at Giant Mine, and most of these emissions (> 84%) occurred during the first 10 years of production prior to the installation of more efficient roasting technologies (Bromstad et al., 2017). The roasting of arsenopyrite was less extensive at Con Mine but was used as part of operations intermittently between 1942 and 1970, and an estimated 2500 tonnes of As_2O_3 were released to the atmosphere from the Con Mine roaster. Stibnite (Sb_2S_3) and antimony (Sb)-bearing sulphosalts were also present in the ore roasted at Giant Mine and the roasting of these minerals resulted in the production of a unknown gaseous phase of Sb that was incorporated into the structure of the As_2O_3 (Fawcett and Jamieson, 2011; Riveros et al., 2000). These large releases of As_2O_3 resulted in an enduring environmental legacy in the region, and concentrations of As and Sb remain elevated in regional lake waters (Houben et al., 2016; Palmer et al., 2015), lake sediments (Dushenko et al., 1995; Galloway et al., 2017; Schuh et al., 2018) and soils (Bromstad et al., 2017; Jamieson et al., 2017) more than 60 years after the bulk of these emissions were released.

4.2.1.2 Study lakes

Detailed field investigations were completed in four lakes within 5 km of the now decommissioned roaster at Giant Mine, Yellowknife, NT (Figure 4.1). All four lakes are natural waterbodies located beyond mine lease boundaries and downwind (prevailing easterly winds) from Giant Mine. The lakes are underlain by granitoid bedrock west of the Yellowknife Greenstone Belt that is composed of Archean metavolcanic rocks that hosted the Con and Giant mineral deposits (Moir et al., 2006). The study lakes were selected to investigate the influence of lake physical properties on seasonal changes in surface water quality, and thus lakes vary in surface area, volume, and hydrological characteristics (Table 4.1).

Table 4.1. Physical characteristics of the four study lakes

Study lake	Lake area (km ²)	Maximum depth (m)	Lake volume (m ³)	Sediment surface area: lake volume	End of winter ice thickness (m)	Distance to Giant Mine roaster (km)
BC-20	0.23	0.8	82,930	2.79	Frozen to bottom	1.8
Handle Lake	0.21	3.0	316,005	0.67	0.78 ^a , 0.59 ±0.01 ^c	2.5
Lower Martin Lake	1.21	2.9	1,693,859	0.80	0.84 ^a , 0.66 ±0.01 ^c	3.0
Long Lake	1.13	6.9	4,331,913	0.26	1.0 ^a , 0.65 ±0.03 ^b	4.9

^aEnd of April 2015, ^bEnd of April 2016 (mean and standard error of 5 measurements), ^cEnd of April 2016 (mean and standard error of 3 measurements).

All four study lakes are characterized by relatively simple basin morphology, including a single basin with relatively consistent depth across its extent (Figure 4.1). Long Lake (max. depth 6.9 m) (62.476 °N, 114.436 °W) and Lower Martin Lake (max. depth 2.9 m) (62.512 °N, 114.421°W) are fish-bearing, although fish are only present in Lower Martin Lake during the open-water season due to the onset of anoxic conditions in the water column in early winter, which forces the migration of fish from Lower Martin or results in winterkill. Long Lake has no discernable inflow or outflow and is surrounded by steep exposed bedrock outcrops on the northern

and eastern shores. Lower Martin Lake is part of the Baker Creek watershed that drains an area of approximately 155 km² and is the final lake in the Baker Creek system before flowing through the Giant Mine property and ultimately discharging into Yellowknife Bay in Great Slave Lake. Discharge from Lower Martin Lake has been monitored by the Water Survey of Canada since 1983 (station number 07SB013), and historical records indicate outflow from the lake typically occurs throughout the year, although average daily discharge is normally small (less than 0.2 m³/s) between late September and the start of freshet in early May. Discharge from Lower Martin was extremely low during the study period, driven by abnormally low water levels, and flow was non-existent except for a small period during freshet (Figure B1). Handle Lake (62.491 °N, 114.397°W) is a small bedrock bound lake (max. depth 3.0 m) with no channelized inflow or outflow located 2.5 km from the historic roaster at Giant Mine. BC-20 (unofficial name; 62.503 °N, 114.393 °W) is a small shallow (< 1.0 m) pond adjacent to the lower reaches of Baker Creek above the Giant Mine site. In both sampling years, BC-20 was frozen to bottom sediments by early January. The lake edge and the surrounding bedrock outcrops are buffered by wide expanses of peatlands (50-100m wide) and the presence of exposed and vegetated lake bottom sediments around the margin of the lake suggest the water level has receded in the recent past. No channelized flow exists between BC-20 and the surrounding watershed, however, ephemeral drainage to Baker Creek is expected during freshet and extremely wet periods through a series of wetlands at the north end of the lake.

4.2.2 Lake morphometry

Lake morphometry was determined for Long Lake, Handle Lake and BC-20 in June 2016 and Lower Martin Lake in September 2017 using a Garmin Fishfinder 250TM or Lowrance HDS5TM

depth sounder and chart plotter attached to a canoe. Bathymetric maps were constructed in ArcMap v.10.4 (ESRI, Redlands, California) for each of the study lakes using the individual point data (location and depth) collected during the surveys and converting to a raster. Lake volume estimates were calculated from the raster files using the surface volume tool in the 3D analyst extension in ArcMap v.10.4.

Changes in the volume of Handle Lake during the study period were estimated to support As and Sb mass balance models. Water level was recorded during summer on each site visit from a benchmark using a stadia rod and level. Lake volume on the open-water sampling dates was calculated by subtracting the difference in water level from the raster generated for the original bathymetric survey that was conducted on June 10 using the surface volume tool in the spatial analyst extension of ArcMap (v. 10.4). Winter water volume was estimated by removing the ice cover from the bathymetry raster using the same approach. The ice-cover thickness was adjusted by 9.05% to compensate for the increase in volume of ice over water due to phase change.

4.2.3 Water and sediment sampling

4.2.3.1 Frequent surface water sampling of the four study lakes

Lake water chemistry was sampled regularly at the four study lakes between July 2014 and September 2016. Samples were consistently collected at the same location in the center of the lakes. In the open-water season, surface water samples were collected from just below the surface (approx. 0.15 m) in acid-washed 250 mL polyethylene containers that had been rinsed three times with lake water. During winter, surface samples were collected 10-cm below the base of the ice cover through a 20-cm diameter hole drilled through the ice. Sampling at multiple intervals in the water column was conducted at Long Lake and Handle Lake in February, April, May/June and

July 2016 to assess the vertical profile of water quality during the ice-covered and ice-free seasons. No interval sampling was conducted in the two shallowest lakes (BC-20 and Lower Martin Lake) and no thermal stratification of the water column was observed at any of the lakes during the summer sampling periods (Figures B2 and B3). Water samples during winter and through the water column were collected using a peristaltic pump attached to Teflon™ line that was pre-washed with 5% HCl solution and rinsed with ultrapure water prior to each sampling trip. The lines were flushed with lake water from each sampling depth for 2 minutes prior to sample collection between sites and depth intervals. All metal(loid) data presented in this study refer to the filtered fraction ($< 0.45 \mu\text{m}$) of the sample, unless otherwise noted, and all samples were filtered immediately in the field and preserved with nitric acid (HNO_3) to 2% (v/v). Following collection, water samples were stored in a cooler with ice packs and delivered the same day to an accredited government laboratory (Taiga Laboratory, Yellowknife, NT).

Water samples were analyzed for general chemistry (including major ions, dissolved organic carbon and nutrients), and 25 total and dissolved metal(loid)s. Dissolved organic carbon was measured by high temperature combustion on a total carbon analyzer (SM5310) (APHA, 1992). Concentrations of major cations and anions were determined by ion chromatography (SM4110) (APHA, 1992). Phosphorous was measured colorimetrically (SM4500P) (APHA, 1992). Total (unfiltered) and dissolved (filtered $< 0.45 \mu\text{m}$) metal(loid) concentrations were determined by inductively coupled plasma mass spectrometry (ICP-MS) following EPA method 200.8 (Creed et al., 1994). In addition to ICP-MS metal(loid) analyses, a subset of water samples were analyzed for total inorganic arsenic and arsenite [As(III)] via hydride generation quartz furnace atomic absorption spectrometry (HG-AAS) at ALS Laboratories in Kelso, WA, according to EPA method 1632. Arsenate [As(V)] was estimated by difference between total inorganic As

and As(III). The minimum reporting limit for As(III) and total inorganic As was $0.02 \mu\text{g L}^{-1}$. Water for As speciation was filtered to less than $0.45 \mu\text{m}$ and preserved with hydrochloric acid in the field (McCleskey et al., 2004). Water chemistry results from individual sites are presented in the supplementary information (Tables B2-B5). Field blanks and field duplicates were collected as part of quality assurance and quality control measures in the study. All samples collected as field blanks ($N = 12$) reported values below method detection limits (MDL) of 0.2 and $0.1 \mu\text{g L}^{-1}$ for As and Sb, respectively. The mean relative percent difference (RPD) between field duplicates ($N = 13$) was 4% (st. dev. = 3.9%) and 2% (st. dev. = 2.7%) for As and Sb, respectively.

4.2.3.2 Regional lake water and sediment surveys

In addition to the detailed investigation of seasonal variation in 4 lakes, surface water from 31 lakes was sampled in March 2015. These lakes were part of a group of 86 lakes within 30 km of Yellowknife that were originally sampled in September 2012 and September 2014 as part of a broad survey of surface water and near-surface sediment quality that was conducted to assess the distribution of legacy pollutants in the region (Palmer et al., 2015; Galloway et al., 2017). The resampling reported in this paper was designed to capture late-winter water chemistry in the region and to explore the influence of lake physical properties on seasonal differences in surface water concentrations of As and Sb. Lakes represented a range of size (i.e. surface area and depth) and distance from legacy point sources of pollutants. Sample collection methods and analytical methods are similar to those reported in Palmer et al. (2015) and used in the repeated sampling of the four lakes in this study (see Appendix B). Relationships between surface waters and near-surface sediment conditions were explored to examine potential influences of sediment properties on lake water chemistry. In brief, and as described in Galloway et al. (2017), near-surface

sediments were collected with an Ekman grab sampler and the top 2-5 cm were retained for analyses. Sediments were analyzed for element concentrations by ICP-MS following aqua regia digestion. Total organic carbon (TOC%) was determined by Rock-Eval 6 pyrolysis as the sum of S1, S2, S3, and residual carbon fractions (Lafargue et al., 1998). These data are reported in Galloway et al. (2017).

4.2.4 Water column oxygen depletion

On each sampling date, *in-situ* measurements of dissolved oxygen, pH, and temperature were made with a YSI 6920 multiprobe sonde (Yellow Springs Inc., Yellow Springs, Ohio) calibrated with certified reference solutions within 24 hours of field sampling. The rate and timing of oxygen depletion in Handle Lake and Lower Martin Lake was measured with MiniDOT® dissolved oxygen loggers (Precision Measurement Engineering Inc., Vista, California) during the 2015-16 ice-covered and ice-free seasons. The loggers were installed 1-m above the sediment surface to record water column oxygen levels and temperature at 10-minute intervals. This information was compiled into daily mean conditions and data presented in the figures represent these daily mean levels. The temperature range of the sensors is 0 to 35°C with an accuracy of +/- 0.1°C. In this study water column measurements of < 0.5 mg L⁻¹ O₂ are considered to represent anoxic conditions following Zogorski et al. (2006).

4.2.5 Measuring solute exclusion from lake ice

Lake ice thickness was recorded on each winter sampling date using a calibrated hooked rod through a hole drilled in the ice. Results from late April 2015 and 2016 are presented in Table 4.1. The extent of solute exclusion from the lake ice cover was assessed by collecting ice chips from

augered holes in each of the lakes. The lake ice at two of the sites consisted of a thin layer of white ice overlying a thick layer of black ice. No melting of the snow cover was observed prior to the April sampling periods, therefore it is assumed that white ice represents water that was redistributed to the ice surface through cracks or near the shoreline and subsequently mixed with the snow cover prior to freezing (i.e. overflow), whereas black ice represents lake water frozen *in-situ*. Ice samples were collected from both ice types in Ziploc™ bags, melted, and stored in high density polyethylene bottles prior to general chemical analyses and metal(loid) analyses at Taiga Laboratories in Yellowknife, NT.

4.2.6 Data analysis

Seasonal enrichment factors were calculated for each of the study lakes to evaluate the change in water chemistry during the period of ice cover and during the open-water season, and to test the hypothesis that elemental concentrations in shallow lakes increase over winter as a result of solute exclusion and increased sediment efflux of redox sensitive elements. Water chemistry data from the end of the winter season (April) were divided by results from the last sampling period prior to freeze-up (typically October) to yield a winter enrichment factor. The summer enrichment factor was calculated by dividing results from end of summer (September) by early open-water season conditions (June). It was assumed that changes in redox state near the sediment boundary would have little effect on the flux of the cations and anions Ca^{2+} , K^+ , Mg^{2+} , and Cl^- across the sediment boundary, therefore winter enrichment in the sum of these major ions (Σ major ions) was expected to primarily represent cryoconcentration and was used to compare with changes in the redox sensitive elements of interest (Fe, Mn, As, and Sb) that were expected to respond to cryoconcentration and changes in sediment efflux.

For the regional lake water surveys, the percent difference between late-winter and open-water surface water elemental concentrations was used to assess whether there were identifiable physical thresholds that controlled the difference in surface water chemistry between seasons, following:

$$\left(\frac{[Late\ winter] - [Fall]}{[Fall]} \right) \times 100\% \quad (\text{Equation 4.1})$$

Where [Late winter] and [Fall] represent the concentration of elements from the regional water quality surveys in March and September, respectively. It was expected that, at a regional scale, larger seasonal differences in surface water concentrations would be observed for shallow lakes, where the surface area to lake volume ratio was large, in contrast with deep lakes, where the influence of solute exclusion and sediment diffusive fluxes would be dampened by large water volumes.

4.2.6.1 Assessing the relative influence of summer and winter processes in Handle Lake

The relative influence of physical (cryo- and evapoconcentration) and biogeochemical (sediment efflux) processes on As and Sb concentrations across seasons were assessed in Handle Lake using water column profile sampling and a mass balance approach. It was assumed that differences in the mass of As and Sb in Handle Lake between sampling periods would be the net result of sedimentation and sediment efflux processes, whereas changes in concentration without any corresponding changes in mass were the result of cryo- or evapoconcentration. This approach assumed no input or output of elements via groundwater or from the surrounding catchment. Concentrations of As, Sb, Fe and Mn were measured at 3-4 depth intervals through the water column on February 16, April 14, May 9, and July 27, 2016 and the depth-weighted mean concentration was calculated to obtain a lake-wide estimate of As and Sb concentrations for these

dates. The depth-weighted mean concentration was combined with the lake volume estimate (see section 2.2) for the sampling dates to generate an estimate of As and Sb mass.

The influence of cryo- and evapoconcentration on water concentrations of As and Sb were modelled for the under-ice and open-water seasons using the data generated in the mass balance estimates. The expected concentrations of As and Sb due to cryoconcentration were modelled as the mass of the elements prior to freeze-up (September) divided by the changing lake volume over the winter period. The influence of evapoconcentration on lake water concentrations of As and Sb was modelled using a similar approach, and the mass of As and Sb calculated for early June was divided by the adjusted volume for late July to yield an estimated concentration due to evapoconcentration.

The statistical analyses were conducted using the software program R v.3.4.1 (R core team, 2017) and results of statistical tests were deemed significant at $p < 0.05$.

4.3 Results

Concentrations of dissolved As (filtered fraction $< 0.45\mu\text{m}$) were above Canadian and World Health Organization guidelines of $10\ \mu\text{g L}^{-1}$ for the maximum allowable concentration for drinking water in all study lakes during all sampling periods (Health Canada, 2017; WHO, 2011) (Figure 4.2). Dissolved Sb concentrations were below the $20\ \mu\text{g L}^{-1}$ WHO guideline for drinking water quality in all lakes during the entire study (WHO, 2011) (Figure 4.3). Dissolved As and Sb concentrations were highest in BC-20 (max As: $846\ \mu\text{g/L}$; max Sb: $10.1\ \mu\text{g/L}$), followed by Handle Lake (max As: $236\ \mu\text{g/L}$; max Sb: $7.5\ \mu\text{g/L}$), Lower Martin Lake (max As: $94.2\ \mu\text{g L}^{-1}$; max Sb: $2.1\ \mu\text{g L}^{-1}$), and Long Lake (max As: $39.9\ \mu\text{g L}^{-1}$; max Sb: $2.1\ \mu\text{g L}^{-1}$), respectively (Table 4.2). Arsenic and Sb in surface waters from the study lakes were predominately in the dissolved fraction (Table 4.2).

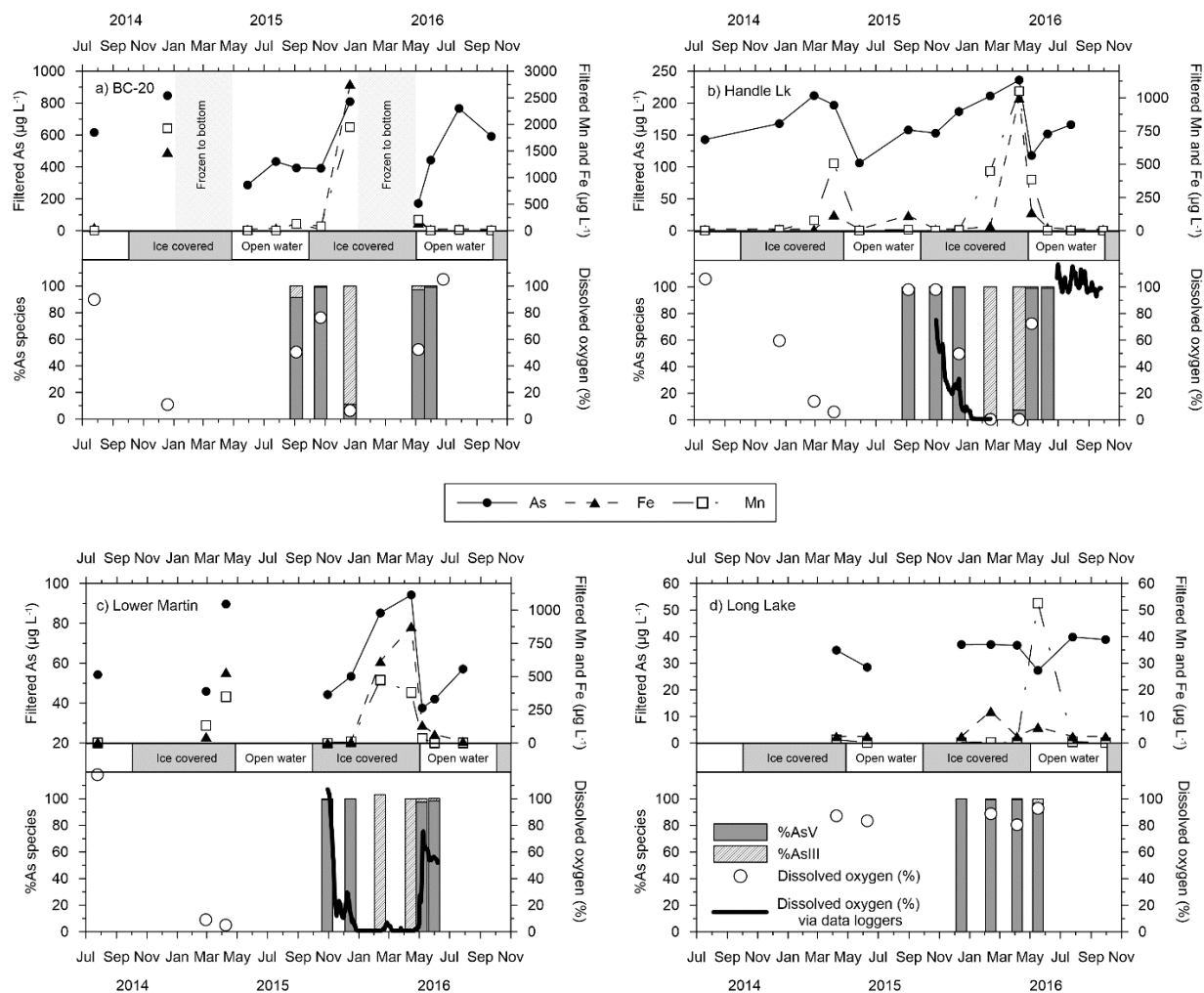


Figure 4.2: The seasonal variation in As, Fe, Mn, and dissolved oxygen (saturation %) and the proportion of inorganic arsenic species in surface waters of the four study lakes, July 2014 to September 30, 2016. The top panel of each plot represents the concentration of As, Fe, and Mn in the filtered fraction ($< 0.45\mu\text{g/L}$) of surface waters of the four detailed study lakes, including: a) BC-20; b) Handle Lake; c) Lower Martin Lake; and d) Long Lake. The lower panels in each plot show the proportion of each of the inorganic species of arsenic (As(III) and As(V)) present in the filtered fraction ($< 0.45\mu\text{m}$) of surface waters at different sampling periods and the amount of dissolved oxygen (saturation %) measured in situ. **Note difference in scale amongst the figures.**

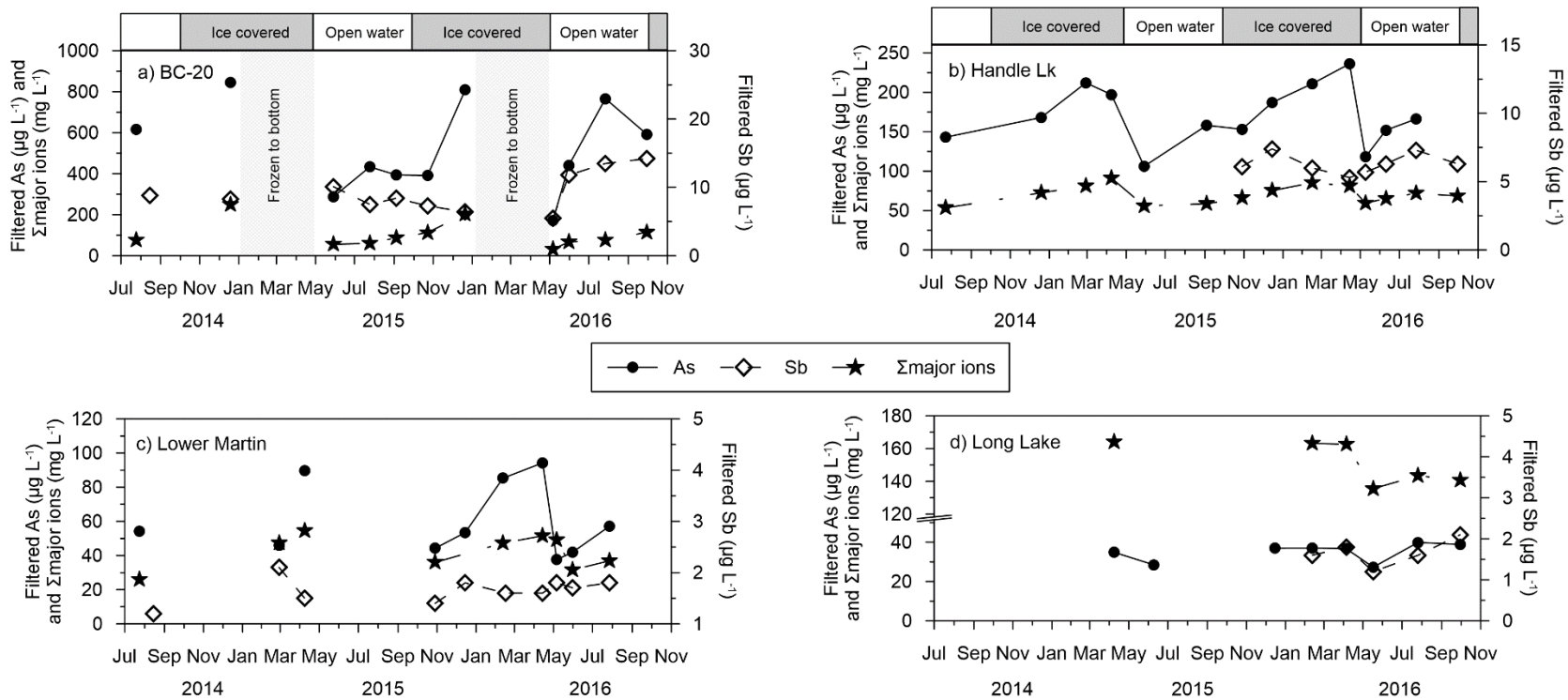


Figure 4.3: Concentrations of As, Sb and the sum of major ions in the filtered fraction ($< 0.45 \mu\text{m}$) of surface waters for each of the study sites, July 2014 to November 2016.

Table 4.2. Summary statistics for select elements and water quality parameters at the four detailed study sites. The total metal(loid) concentration in the dissolved fraction (< 0.45 µm) represents the mean from all sampling periods and the standard deviation is reported in parentheses. The winter enrichment factor represents the increase in surface water concentration during the ice-covered season (October to April) and the open-water season (June to September). For sites with more than one year of data, the enrichment factor represents the year with the greatest increase in concentration.

Site	Surface water concentration (filtered < 0.45 µm)				Proportion of total metal(loid) in dissolved fraction (stdev)	Maximum winter enrichment factor	Maximum summer enrichment factor
	Mean	Maximum	Minimum	N			
As (µg L⁻¹)							
BC-20	522	846	172	11	0.99 (0.15)	2.1	1.3
Handle Lk	170	236	106	14	0.99 (0.05)	1.5	1.1
Lower Martin Lk	60	94	38	10	0.88 (0.18)	2.1	-
Long Lk	35	40	27	8	0.96 (0.04)	1.0	-
Sb (µg L⁻¹)							
BC-20	9.3	14	5.5	11	0.98 (0.12)	0.9	1.2
Handle Lk	6.3	7.5	5.3	13	0.96 (0.08)	0.9	1.1
Lower Martin Lk	1.7	2.1	1.2	10	0.93 (0.11)	1.1	-
Long Lk	1.7	2.1	1.2	5	0.99 (0.05)	0.9	-
Fe (µg L⁻¹)							
BC-20	433	2760	23	11	0.44 (0.26)	95	0.9
Handle Lk	23	208	<5.0	14	0.18 (0.23)	83	0.5
Lower Martin Lk	231	876	<5.0	10	0.48 (0.38)	350	-
Long Lk	4.1	12	<5.0	8	0.25 (0.18)	1.0	-
Mn (µg L⁻¹)							
BC-20	396	1950	4.2	11	0.59 (0.37)	23	1.2
Handle Lk	178	1050	0.5	14	0.32 (0.42)	2100	0.2
Lower Martin Lk	138	473	0.4	10	0.53 (0.51)	950	-
Long Lk	7.0	53	<0.2	8	0.08 (0.16)	0.5	-
Σ Major ions (mg L⁻¹)							
BC-20	103	249	31	11	-	1.8	1.7
Handle Lk	70	91	53	14	-	1.2	1.1
Lower Martin Lk	42	54	26	9	-	1.4	-
Long Lk	-	-	-	-	-	NA	-
Specific conductivity (µs cm⁻¹)							
BC-20	470	1090	166	11	-	1.7	1.7
Handle Lk	314	423	242	14	-	1.3	1.2
Lower Martin Lk	185	244	131	10	-	1.4	-
Long Lk	431	475	384	7	-	1.1	-

4.3.1 Seasonal changes in water column dissolved oxygen

BC-20, Handle Lake, and Lower Martin Lake all experienced periods of winter anoxia in the water column (Figure 4.2). In both study years, the water column in these three lakes was typically oxygen depleted (< 0.5 mg L⁻¹ O₂) by early January, although interannual variation between sites

and years was noted (Figure 4.2). The rate of oxygen depletion was greater in Lower Martin Lake than Handle Lake, and oxygen levels were below 0.5 mg L^{-1} by December 25, 2015 at Lower Martin Lake and January 8, 2016 at Handle Lake (Figure 4.2). Dissolved oxygen was not measured continuously at BC-20, but dissolved oxygen levels were below 5% during sampling on December 21, 2015. Surface waters at Long Lake remained well oxygenated throughout the entire study (Figure 4.2). Oxygen levels decreased at depth ($> 3 \text{ m}$) during winter sampling in February and April but did not reach anoxic conditions at the sediment boundary (Figure B2).

4.3.2 The concentration of arsenic and major ions in lake ice

Water chemistry of black ice samples indicated that almost all ($> 95\%$) major ions and total unfiltered As and Sb were excluded during black ice development (Table B1). Conversely, concentrations of total unfiltered As and Sb were comparable or higher in white ice than in lake waters collected prior to freeze-up at Lower Martin Lake and BC-20, respectively (Table B1). This difference likely reflects the source and mechanism of white ice development, since white ice forms from the freezing of lake waters that have been redistributed to the ice surface. If white ice forms after substantial ice development, the sourced water represents lake waters that may have been elementally enriched by solute exclusion.

4.3.3 Seasonal changes in surface water chemistry

Seasonal differences in concentrations of As, Sb, Fe, Mn, and Σ major ions were observed in surface waters of all four study lakes (Figures 4.2 & 4.3), although the pattern of change in Long Lake was different than the other three lakes. In the three shallow lakes (BC-20, Handle Lake and Lower Martin Lake) concentrations of these elements typically increased under ice and were

highest during late winter. The winter enrichment factor was greatest for the redox sensitive elements Fe and Mn, except in Long Lake, where no increase in elemental concentrations of Fe and Mn was observed over winter (Table 4.2). A large decrease in element concentrations was observed in BC-20, Handle Lake and Lower Martin Lake in association with spring snowmelt and the loss of the ice cover in early May (Figures 4.2 & 4.3).

The variation in elemental concentrations of surface waters was low in Long Lake, the deepest and largest volume lake in the study, which did not experience anoxia in the water column. There was no evidence of under ice enrichment in concentrations of As, Sb, Fe, Mn, or Σ major ions (Figures 4.2 & 4.3; Table 4.2). Similar to the other three sites, concentrations of As, Sb, and Σ major ions decreased at Long Lake during freshet (Figures 4.2 & 4.3). In contrast to the three shallow sites, a large increase in surface water Mn was measured in Long Lake during freshet sampling.

Seasonal changes in surface water As concentrations were greatest in the shallowest and lowest volume lake in the study (BC-20), and surface water As varied more than 4-fold over the entire study period (172-846 $\mu\text{g L}^{-1}$). Large winter increases in surface water As in the three shallowest lakes were associated with the depletion of oxygen from the water column and large increases in Fe and Mn (Figure 4.2). When data from all four study lakes were included, the winter enrichment factor was more strongly correlated with the surface area to lake volume ratio (Spearman rank order correlation, $r_s = 0.95$; $p = 0.051$) than lake volume alone ($r_s = -0.63$; $p = 0.367$). Increases in surface water As concentrations were also measured during the open-water season at BC-20, Handle Lake, and Lower Martin Lake; however, concentrations of Fe and Mn remained low. In these three shallow lakes, the concentrations of As in surface waters were lowest in May post-snowmelt and gradually increased over the course of the open-water season, although

to a lesser extent than during the ice-covered season (Table 4.2). Conditions during the summer of 2016 at BC-20 were the exception, when the surface water As concentration measured in July was $766 \mu\text{g L}^{-1}$, a value comparable to late winter concentrations measured in the lake (Figure 4.2).

Data presented in Figure 4.4 highlight the relationship between elemental concentrations of surface waters and dissolved oxygen levels during the development of the ice cover. In the three shallow lakes, concentrations of As, Fe, and Mn were highest under anoxic conditions and the relationship is best described by a logarithmic or exponential model. In contrast, the relationship between concentrations of major ions and dissolved oxygen in the water column is best represented by a linear model, and lacks a large increase in major ions in association with the development of anoxia.

Compared to large changes in As, Fe, and Mn in the three shallowest lakes, there was less variation in surface water Sb concentrations over the study period and no large increases in Sb were associated with the onset of anoxia in the water column (Figure 4.3). Although somewhat limited by the frequency of sampling in the study, the data in Figure 4.3 suggest that the concentration of Sb in surface waters at Handle and Lower Martin Lake increased between the two early-winter sampling periods (November – December), and subsequently decreased later in the winter after the onset of anoxia in the water column (Figure 4.3).

4.3.4 Seasonal As and Sb mass loading in Handle Lake

Water column profiling during winter in Handle Lake revealed a depth gradient in As, Sb, Fe, and Mn concentrations, with concentrations of all elements increasing closer to the sediment boundary (Figure B4). No water column gradient was observed for As, Sb, Fe, or Mn during open-water sampling in May and July (Figure B4).

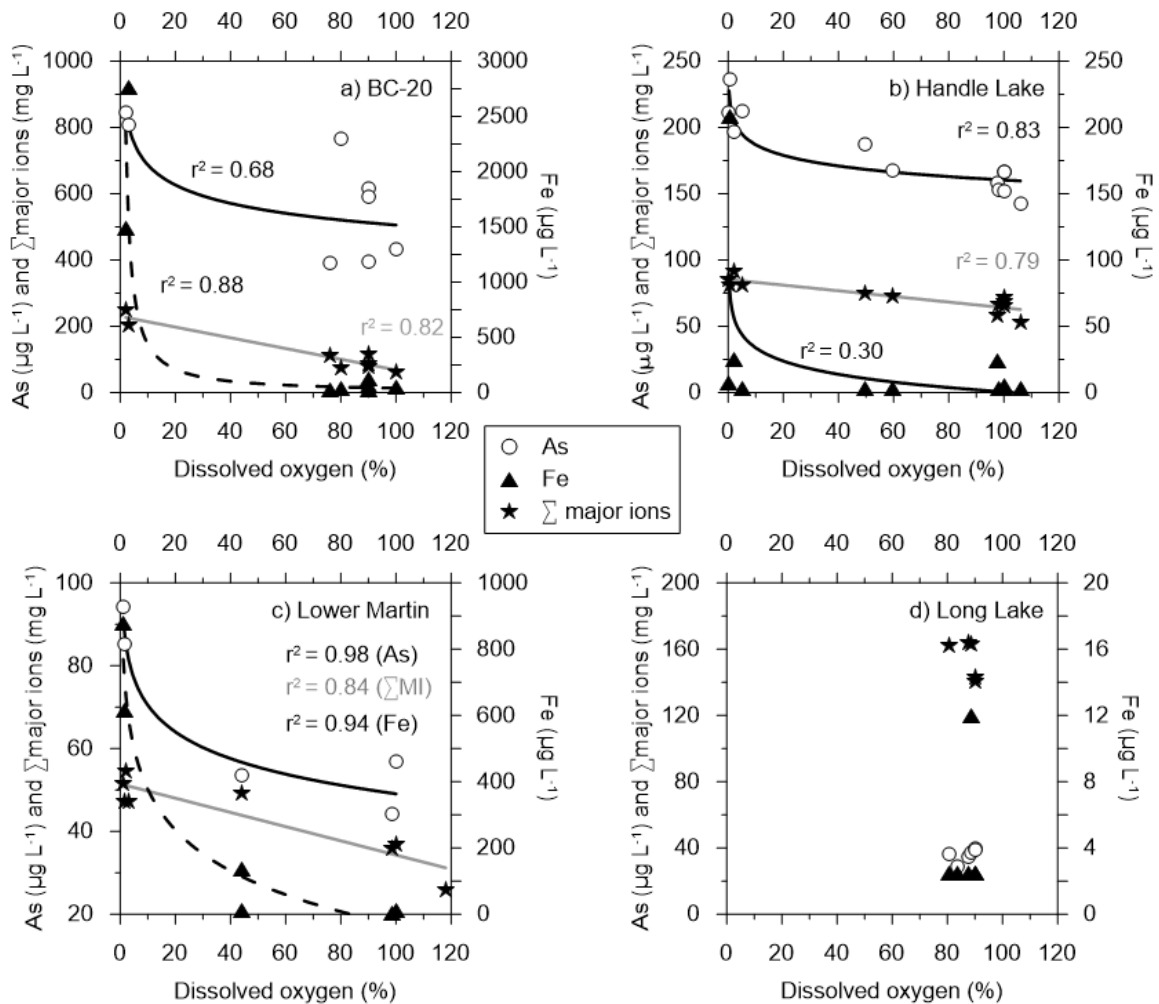


Figure 4.4: Relationships between selected elements (As, Fe, and the sum of major ions) and dissolved oxygen in surface waters for: a) BC-20; b) Handle Lake; c) Lower Martin Lake; and d) Long Lake. Reported data are from sampling periods between July and the end of April. Data collected during snowmelt period are excluded. The coefficients of determination (r^2) presented in figures represent linear and logarithmic regression models with $p < 0.001$. Note the different concentration scales between panels. All metal(loid) and ion data refer to the filtered fraction ($< 0.45 \mu\text{m}$) in surface waters.

Lake volume decreased 19% over the winter period with the development of an ice-cover and there was a subsequent 42% increase in the estimated lake wide mean concentration of As (Table 4.3). Model estimates for cryoconcentration influence on water column As concentrations were similar to measured values in early winter (December), but underestimated concentrations of

As in February and April by approximately 12% (Table 4.3). Water column mass of As was also relatively similar between the end of the open-water season and early winter, but increased approximately 15% between December and February with the onset of water column anoxia. The mass increase in As between December and April represented an estimated sediment efflux of $273 \mu\text{g m}^{-2} \text{ day}^{-1}$ over that period (Table 4.3). In contrast with As, no sediment efflux of Sb was observed in Handle Lake in winter. Water column concentrations of Sb decreased less than 10% over the ice-cover period and did not correspond with expected concentrations from the cryconcentration model (Table 4.3). The total Sb load in the Handle Lake water column also decreased over the ice-cover period by approximately 25%, corresponding to an estimated flux of $18 \mu\text{g m}^{-2} \text{ day}^{-1}$ Sb from the water column to lake sediments between December and April 2016 (Table 4.3).

Lake volume decreased in Handle Lake over the open water season (approximately 8%) and concentrations of As were similar to model estimates for evapoconcentration. Lake-wide mass of As was consistent between the two summer sampling periods and the estimated sediment-water efflux of As was low ($7.8 \mu\text{g m}^{-2} \text{ day}^{-1}$). The concentration and mass of Sb in the water column increased over the open-water season, but the increase was small compared to changes observed for As over winter and suggested a low rate of Sb release from lake sediments during summer ($< 3 \mu\text{g m}^{-2} \text{ day}^{-1}$) (Table 4.3).

Table 4.3. Mass balance and sediment-water flux estimates in Handle Lake for As and Sb.

				Arsenic			Antimony			
	Sampling date	Ice thickness (m)	Lake volume (m ³)	Concentration (µg L ⁻¹) ^a	Calculated concentration (µg L ⁻¹)	Mass (kg)	Concentration (µg L ⁻¹) ^a	Calculated concentration (µg L ⁻¹)	Mass (mg)	
Winter	September 4, 2015	-	292,012	158	-	46.1	7.5	-	2190	
	December 15, 2015	0.30	241,017	187	191	45.1	7.4	9.1	1784	
	February 16, 2016	0.51	208,082	253	222	52.6	5.8	10.5	1207	
	April 14, 2016	0.59	196,284	265	235	52.0	6.8	11.2	1335	
	<i>Percent change (Dec. - April)</i>			-18.6%	41.7%	23.0%	15.4%	-8.1%	23.1%	-25.2%
<i>Sediment - water flux (µg m⁻² day⁻¹) (Dec. - April)</i>						273.3			-17.7	
Summer	June 10, 2016	-	316,005	152	-	48.0	6.3	-	1991	
	July 27, 2016	-	292,012	166	164	48.5	7.3	6.8	2132	
	<i>Percent change</i>			-7.6%	9.2%	7.9%	0.9%	15.9%	7.9%	7.1%
	<i>Sediment - water flux (µg m⁻² day⁻¹)</i>						7.8			2.5

4.3.5 Seasonal changes in inorganic arsenic speciation of surface waters

In all four lakes, the proportion of inorganic As species was dominated by arsenate [As(V)] (> 90%) during the open-water season and early in the ice-cover season when surface water conditions remained well oxygenated (Figure 4.2). During the ice-covered season of 2015-16 the relative proportion of arsenite [As(III)] increased in the three shallowest lakes in association with the depletion of oxygen from surface waters. In these three lakes there was a rapid return to As(V) as the dominant inorganic species following snowmelt and the erosion of the ice cover (Figure 4.2). In Long Lake, As(V) accounted for more than 96% of the total inorganic As in all sampling periods.

4.3.6 Potential influence of snowmelt on surface water As concentrations and speciation

Sampling of Lower Martin Lake on 6 May, 2016, three days prior to the loss of lake ice, provided an opportunity to evaluate the influence of snowmelt on the concentration and speciation of As in surface waters in a shallow lake in the region. On that day, most of the snow cover had melted from the surrounding catchment and a small area of open water was present between the lake shore and floating ice cover ($[As] = 26.5 \mu\text{g L}^{-1}$). Surface waters collected from below the ice cover reflect snowmelt input to the lake, were oxygenated (> 40% DO saturation) and represented the lowest concentrations of As measured in Lower Martin Lake during the study ($[As] = 37.6 \mu\text{g L}^{-1}$). As(V) accounted for 98% of inorganic As species in surface waters in contrast to three weeks earlier when As(III) was the predominant species under anoxic water column conditions (Figure 4.2).

4.3.7 Seasonal differences in As, Sb, Fe, and major ions in the regional lake surveys

A steep decrease in surface water As concentration was observed with greater distance from the historic Giant Mine roaster in the open-water and under-ice sampling periods (Figure B5), consistent with previous studies in the region (Houben et al., 2016; Palmer et al., 2015). Seasonal differences in surface water As between the two sampling periods were not correlated with distance from the mine roaster (Spearman rank order correlation: $r_s = 0.02$; $p = 0.44$; $n = 32$). Therefore, distance was not integrated as a covariate in subsequent analyses related to the influence of physical lake properties on seasonal differences in surface water As.

Late-winter element concentrations were typically higher than during the open-water sampling period and lake depth had an important influence on these seasonal differences. The largest changes in As and Fe between the late-winter and open-water seasons were typically in lakes with a maximum depth less than 4 m (Figure 4.5). Measured differences were as high as $125 \mu\text{g L}^{-1}$ As and $5757 \mu\text{g L}^{-1}$ Fe within a lake. Large seasonal differences in Sb were only measured in lakes shallower than 2 m and, in contrast with As and Fe, surface water Sb was higher in the open water season for 33% of the lakes (Figure 4.5c).

4.3.8 Relationship between surface water and near-surface sediment chemistry

Surface water and sediment concentrations of As were positively correlated during the open-water sampling period (Figure B6a). Furthermore, the highest concentrations of surface water As were measured in lakes with high sediment TOC (Figure B6b).

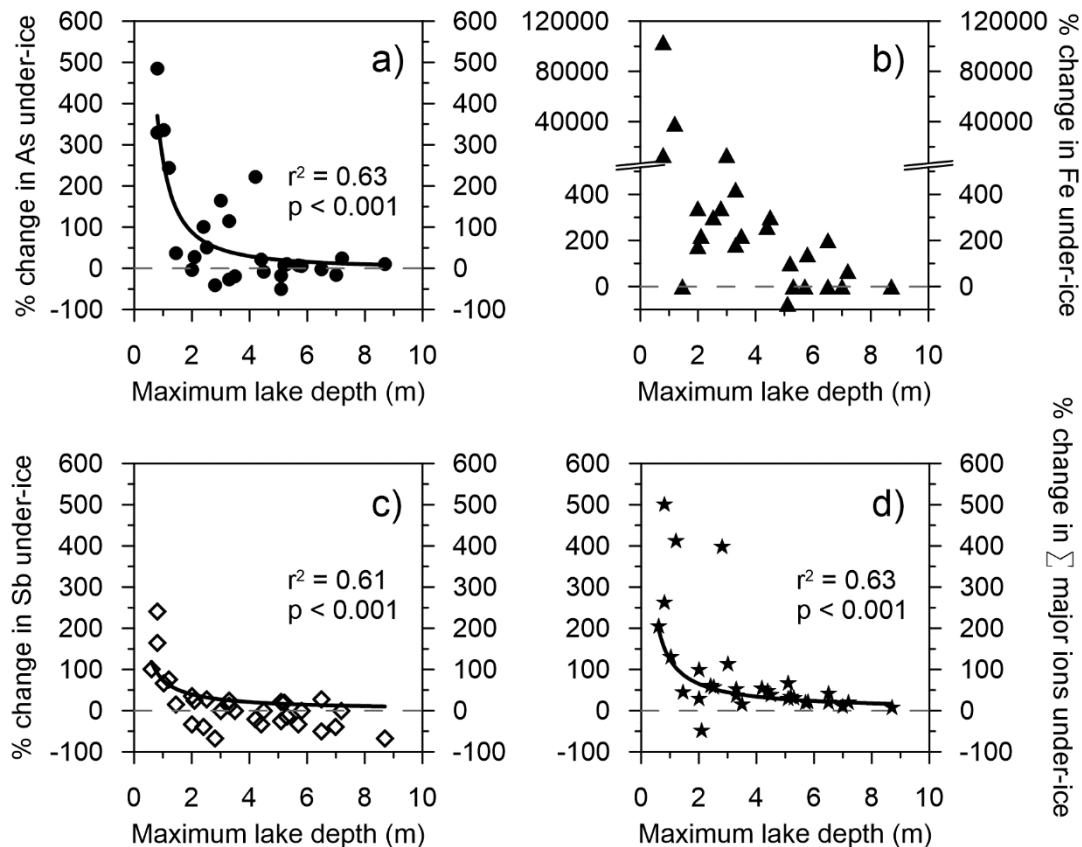


Figure 4.5: Relationships between seasonal change in surface water concentrations of elements (as the percent change in water chemistry between fall and late winter) and maximum lake depth in 31 lakes within 30 km of Yellowknife, including: a) As; b) Fe; c) Sb; and d) sum of major ions. Only lakes with maximum depth < 10 m were included. All metal(loid) and ion data refer to the filtered fraction (< 0.45 μm) in surface waters.

4.4 Discussion

Concentrations of As and Sb remain elevated in surface waters of small lakes near the historic roaster at Giant Mine 50 years after the bulk of roaster emissions were deposited across the landscape. High concentrations of As and Sb in regional surface waters have been previously reported in the literature over the last 40 years (Houben et al., 2016; Palmer et al., 2015; Wagemann et al., 1978). These studies present surface water results collected during the open-water season and were primarily developed to assess the magnitude and regional distribution of legacy pollutants in surface waters. In this study we build on this previous work by demonstrating that concentrations of surface water As can vary more than 5-fold between open-water and ice-covered

seasons and are greatest for lakes with a maximum depth < 4 m (Figure 4.5). We also found evidence that seasonal variation in under-ice water chemistry is likely driven by a combination of solute exclusion during ice formation and lake bottom biogeochemical processes.

4.4.1 Seasonal changes in surface water As influenced by a combination of physical and biogeochemical processes

Regular sampling of four lakes near the historic Giant Mine roaster and seasonal sampling of 31 lakes across the region highlight substantial variation in surface water quality of shallow lakes in the region. Seasonal differences varied in magnitude, and increased or decreased dependent on the element of interest, which underlines the complex interactions that influence the seasonal variability of legacy pollutants in lakes in the region. The development of ice-cover strongly enriched surface water concentrations of As, Fe, Mn, and major ions of the three shallowest lakes (Figures 4.2 & 4.3). The measurement of low elemental concentrations in lake ice (Table B1) indicated that the development of the ice cover was effective in excluding solutes during its development and early winter increases in surface water As and major ions, likely reflect the influence of cryoconcentration. The similarity in modelled and measured concentrations of As during early winter in Handle Lake support the suggestion that early season concentration increases are due to solute exclusion and cryoconcentration (Table 4.3).

Large increases in surface water As, Fe, and Mn in association with the onset of anoxia in the water column in the three shallowest lakes indicated an increase in the sediment efflux of these elements due to seasonal oxic-anoxic transitions (Figures 4.2 and 4.4). Results from under ice water column sampling and As mass balance estimates for Handle Lake indicated: 1) an increase in concentrations of As, Fe, and Mn towards the sediment boundary (Figure B4), consistent with

sediment efflux of these elements; and 2) an increase in mass of As in the water column coinciding with the onset of anoxic conditions in the water column (Table 4.3).

In BC-20, Handle Lake, and Lower Martin Lake, rapid oxygen depletion from the water column was facilitated by the relatively high ratio of sediment surface area to lake volume (> 0.6) and the high sediment oxygen demand of the organic-rich bottom sediments (BC-20: 17% TOC; Handle: 28% TOC; Lower Martin: 25% TOC) (Table 4.1; Figure 4.2). Previous solid phase speciation of As in sediments in the study lakes has shown that near-surface Fe (oxy)hydroxides may host a substantial amount of As (3-4 wt %) (Schuh et al., 2018; Van Den Berghe et al., 2018). Therefore, late-winter increases in surface water As were likely due to seasonal desorption/dissolution from Fe (oxy)hydroxides following the removal of the oxic boundary in near-surface sediments. While the aerobic zone in near-surface sediments may be quite thin (< 2 cm), this layer can be an effective barrier to diffusion of As across the sediment-water boundary for much of the year (Andrade et al., 2010; Bennett et al., 2012; Martin and Pedersen, 2004). Lakes close to historic roasting operations in the Yellowknife region contain large reservoirs of As stored in lake sediments at depths between 10 and 30 cm (Schuh et al., 2019, 2018; Thienpont et al., 2016; Van Den Berghe et al., 2018). The continued dissolution of As at depth that is primarily derived from legacy As_2O_3 , results in steep porewater gradients that drive the upward diffusion of As(III) towards the sediment surface (Schuh et al., 2018; Van Den Berghe et al., 2018). High porewater concentrations of As just below the sediment Fe(III) redoxcline under oxic conditions are an additional source of aqueous As available for release to overlying waters with the onset of anoxia at the sediment boundary during prolonged ice cover. The data presented here suggest that increased sediment efflux of As with change in redox state at the sediment boundary is likely an important mechanism in controlling seasonal changes in the surface water quality of shallow lakes.

Further, the positive correlation between surface water and sediment As concentrations supports the hypothesis that elevated surface water As is sustained by the continued internal loading from contaminated sediments (Figure B6a).

In contrast to large changes measured in the three shallowest lakes, changes in lake water chemistry were small over winter in the deepest lake (Long Lake) (Figure 4.2). Similarly, we found that differences in As between the two regional surface water surveys were low for lakes with a maximum depth > 4 m (Figure 4.5). This threshold is similar to the findings of Leppi et al. (2016) from a series of lakes in northern Alaska that showed minimal oxygen depletion in lakes with a maximum depth > 4 m. Considerable variation in late winter dissolved oxygen conditions has been noted in shallow arctic and subarctic lakes, which has been attributed to differences in landscape (lake surface area, littoral area) and limnological (trophic status) properties (Leppi et al., 2016; Mathias and Barica, 1980) that may contribute to the extent of seasonal change in surface water As concentrations for lakes less than 4 m deep (Figure 4.5). As pointed out by Mathias and Barica (1980) the empirical relationship between oxygen depletion rate and lake depth primarily reflects differences in the sediment surface area to lake volume ratio with changing lake depth.

Temporal changes in surface water concentrations of As were also measured over the open-water season in the three shallowest lakes although differences in As were typically small and not associated with increases in Fe and Mn or low oxygen conditions (Figure 4.2). The diffusion of As across the sediment-water boundary during the open-water season has been estimated in Long Lake and for a littoral area in Lower Martin Lake by applying Fick's First Law of diffusion to sediment porewater information (Schuh et al., 2019; Van Den Berghe et al., 2018). These studies suggest internal loading of As from lake sediments occurs during the open-water season. Across the study region, surface water As was highest in lakes with organic-rich surficial sediments

highlighting a potential link between internal As loading and organic matter accumulation (Figure B6b). Organic matter accumulation at the sediment boundary alters the position of the Fe(III) redoxcline in lake sediments by increasing sediment oxygen demand and microbial respiration rates. The thinning of the aerobic zone in near-surface sediments limits the area where upwardly mobile As may be scavenged by adsorption on Fe oxy(hydroxides), thus leading to higher rates of sediment efflux (Martin and Pedersen, 2004). Sediment temperature has also been shown to influence sediment efflux rates of As through increased microbial respiration rates, thinning of the oxic layer and reductive dissolution of Fe-oxyhydroxides (Barrett et al., 2019). A temperature effect may explain why large increases in summer concentrations of surface water As were noted in BC-20, the shallowest and warmest study lake (Figure 4.2). Daily mean sediment temperatures in BC-20 were well above 20°C for much of July 2016 (Figure B7).

Hydrological processes may also have an important influence on surface water As during the open-water season. In particular, evaporative fluxes are high in the region during summer and lakes typically have a negative water balance during this period when evaporative fluxes can greatly exceed precipitation (Gibson et al., 1998; Spence, 2006). Although there is limited understanding of the water balance of the study lakes, the large surface area to volume ratio in BC-20, Handle and Lower Martin suggests evapoconcentration of solutes may also contribute to summer enrichment of As concentrations in these lakes that is supported by similar summer enrichment factors for Σ major ions and specific conductivity (Table 4.2).

4.4.1.1 The relative influence of biogeochemical processes vs cryo- and evapoconcentration in controlling As concentration and loading in Handle Lake

The arsenic mass balance estimates for Handle Lake were used to elucidate the relative influence of winter and summer processes on the flux and concentration of As in shallow lakes in the region. These data suggest that increases in surface water concentrations of As during summer were predominately attributed to a decrease in lake volume driven by evaporative processes, since there was little change in As mass between the two sampling periods and 86% of the summer increase in As concentration can be attributed to the evapoconcentration estimate (Table 4.3). These data also suggest that winter processes have a greater influence on water column concentrations (42% increase in [As]) and loading of As (+ 7 kg As) compared to open water processes and were driven by a combination of cryoconcentration and sediment As release with the onset of anoxia in the water column (Figure B4; Table 4.3). The influence of these two processes on lake water concentrations of As was relatively equal, since the cryoconcentration estimate accounted for approximately 56% of the increase in surface water As concentration between December and April (Table 4.3). While the results from Handle Lake are instructive for a general understanding of the partitioning of summer and winter processes driving water column As concentrations and mass balance, it is difficult to generalize the results across the wider region, since variation in lake biophysical properties, such as depth and surface area to volume ratio, sediment organic content, and sediment temperature will alter the relative influence of these processes.

4.4.2. Periods of seasonal anoxia alter the oxidation state of surface water arsenic.

In freshwaters, As typically exists as inorganic oxyanions of arsenate [As(V)] and arsenite [As(III)]. (Smedley and Kinniburgh, 2002; Wang and Mulligan, 2006). Arsenate tends to

dominate in oxidizing environments, whereas As(III) is more stable under reducing conditions (Smedley and Kinniburgh, 2002). Results from this study follow this expected pattern. Inorganic As was measured predominately as As(V) in all study periods when the lakes were well oxygenated, whereas As(III) was the dominant inorganic As species after lake waters were depleted of oxygen (Figure 4.2). In the winter of 2015-16, the measurement of As(III) as the dominant species in the water column corresponded with the onset of anoxic conditions and is likely the result of both the reduction of lake water As(V) to As(III) and the mobilization of As(III) from sediment porewaters to overlying lake waters. The oxidation of As(III) to As(V) occurred rapidly in spring upon removal of the ice cover. In Lower Martin Lake, this transition occurred in association with snowmelt inputs to the lake from the landscape prior to the loss of ice cover (Figure 4.2). The mechanisms controlling the rapid oxidation of As(III) under-ice warrant additional attention, since abiotic oxidation of As(III) under circumneutral conditions is expected to be slow compared to microbially and photochemically mediated As(III) oxidation with intense sunlight (Asta et al., 2012; Hug et al., 2001), as would be expected in subarctic locations in early May.

4.4.3 Changes in surface water Sb concentrations across seasonal redox transitions

In the four lakes studied in detail, the seasonal enrichment factors showed that concentrations of Sb were relatively unchanged over the duration of winter and increased in the open water season, contrary to the patterns of seasonal enrichment factors for As, Fe, and Mn (Figures 4.2 & 4.3; Table 4.2). In the regional dataset, surface water Sb concentration changed little between open-water and under-ice seasons. Antimony concentrations were frequently lower under ice except for the shallowest lakes (< 2 m) (Figure 4.5). Further, Sb mass balance estimates in Handle Lake

indicated a 25% decrease in lake wide mass of Sb over the duration of winter, and a slight increase in mass of Sb in the water column between the two summer sampling periods (Table 4.3). These data suggest that Sb mobility does not increase in association with the transition from oxic-anoxic conditions in the lakes, a finding that is consistent with several recent studies that have highlighted the contrasting mobility of As and Sb in contaminated lake sediments (Arsic et al., 2018; Fawcett et al., 2015). Water column sampling under-ice at Handle Lake, however, presented conflicting results, as Sb concentrations increased with proximity to the sediment boundary in association with increases in concentrations of Fe and Mn (Figure B4), suggesting that Sb may be released from lake sediments with the removal of the oxic boundary. The use of surface water chemistry to explore questions pertaining to biogeochemical processing within lake sediments has limitations. Whether the water column profile data indicate contrasting geochemical behaviour, settling of colloidal fractions ($< 0.45 \mu\text{m}$) of Sb from the water column, or are simply a limitation of attempting to use changes in low concentrations of trace metalloids in surface waters to understand biogeochemical processes occurring within lake sediments remains unresolved. Detailed porewater and mineralogical analyses are warranted to help elucidate the processes controlling Sb retention and release from sediments to inform the long-term fate of this element.

4.5 Conclusions and directions for future research

Concentrations of surface water As remain high in lakes close to point sources of legacy mining emissions, because sediments are a persistent source of As to overlying waters that are seasonally re-cycled. Observed seasonal changes were greatest for lakes with a maximum depth $< 4\text{m}$ and were driven by a combination of physical and biogeochemical processes. Lake depth control was apparent in the regional study lakes distal from the point source of contamination, suggesting that

this physical parameter is an important control in lakes with a seasonal ice cover regardless of contamination.

Knowledge gaps persist regarding the long-term fate of As and Sb in lakes in the region and important directions for future research include:

- a) Further work to clarify the biogeochemical processes controlling Sb mobility, including detailed porewater analyses and solid-phase speciation of near surface sediments;
- b) Exploring the role of repeated redox oscillations at the sediment-water boundary on the biogeochemical cycling of As and Sb to determine the long-term net gain or loss of these elements from the water column. The influence of oscillating redox conditions on As-bearing floodplain soils has been explored experimentally using laboratory bioreactors (Parsons et al., 2013), and a similar approach may help to explain long-term (i.e. decadal) changes in shallow lakes that experience seasonal redox oscillations in contaminated lake sediments;
- c) Detailed studies directed at understanding the role of snowmelt processes on As cycling in subarctic lakes. Results from this study suggest that large winter additions of As to the water column may be offset by the rapid oxidation of aqueous As(III) and the precipitation and sedimentation of As-bearing minerals.
- d) Experimental work to investigate the influence of temperature in controlling sediment-water fluxes of metal(loid)s. This is important for gaining a better understanding of how summer sediment diffusive fluxes may vary temporally in shallow lakes where sediment and water temperatures can change quickly and spatially between lakes with different physical and biological characteristics. Temperature investigations are also

important in light of expected lake warming associated with climate change (Williamson et al., 2009).

Finally, this study highlights the importance of winter processes for understanding the chemical and biological recovery in shallow subarctic lakes from metalloid pollution. The interpretation of surface water and sediment geochemistry in areas with transient redox conditions requires investigations across the spectrum of redox conditions. Clearly, sampling in the open-water season, when most environmental research takes place in the subarctic, does not account for a critical period in the annual cycling of As and Sb.

Chapter 5: Hydrologic control on winter dissolved oxygen mediates arsenic cycling in a small subarctic lake

Abstract

The seasonal development of an ice cover is a characteristic feature of subarctic lakes, yet the biogeochemical cycling of redox elements under ice, including arsenic (As), are poorly understood. We conducted comprehensive geochemical characterization of lake waters, sediment porewaters and lake sediments over two consecutive years to develop a conceptual model of As, iron (Fe), and sulfur (S) dynamics under ice in a shallow subarctic lake (mean depth 2.0 m) impacted by more than 60 years of arsenic pollution from local gold mining emissions. Lake sediments were a source of As to overlying waters during both winters when oxygen was depleted from interfacial sediments through the reductive dissolution of As-bearing Fe (oxy)hydroxides, but the influence on lake water chemistry was distinctly different between years and dependent on winter hydrology of the lake. When the lake was hydrologically disconnected from the upstream watershed, anoxia developed through the entire water column and high concentrations of As ($> 100 \mu\text{g L}^{-1}$) and Fe ($> 1000 \mu\text{g L}^{-1}$) were measured in lake water. During the second winter, open-water flow persisted at the lake inlet, which replenished dissolved oxygen in the under-ice water column, suppressed the upward migration of the Fe and SO_4 redox boundaries, and limited sediment As efflux. These findings demonstrate how changing hydrology, specifically ice cover duration and hydrological connectivity, can influence the winter cycling of As, Fe, and S in shallow subarctic lakes.

5.1 Introduction

The mobility of arsenic (As) in aquatic systems is largely controlled by the biogeochemical cycling of iron (Fe), sulfur (S) and organic matter (OM) (Bauer and Blodau, 2006; Couture et al., 2010; Kneebone et al., 2002; Root et al., 2007). The influence of biogeochemical processes on lake water As can vary seasonally due to changes in lake physical properties, such as sediment temperature (Barrett et al., 2019), thermal stratification of the water column (Hollibaugh et al., 2005; Senn et al., 2007), and in cold regions, development of an ice cover (Joung et al., 2017; Palmer et al., 2019; Schroth et al., 2015), leading to complex trajectories of recovery for As impacted systems. Despite recognition of the seasonality in As mobility, there has been little investigation of As cycling in cold regions, where the development of an ice cover can strongly affect oxygen and temperature conditions in lakes. Recent work has highlighted the importance of under ice investigations of CO₂ and CH₄ processes in understanding annual C budgets (e.g. Denfeld et al. 2018). Many of the under ice physical dynamics relevant to carbon cycling are also relevant to As cycling, such as inverse temperature stratification, limited atmospheric gas exchange, heterotrophic sediment respiration and development of anaerobic conditions in the water column, and this knowledge can guide investigations related to As cycling. These processes are particularly important for shallow lakes, which are globally abundant and are hot spots on the landscape of biogeochemical processing (Deshpande et al., 2015; Downing, 2010).

Shallow subarctic lakes are ice-covered for much of the year and experience large seasonal changes in temperature, light, and biological activity (Bertilsson et al., 2013) that can alter fluxes, speciation, and bioavailability of As. At the landscape scale, within-lake processes are influenced by changes in climate and hydrology that may alter connectivity and flow between individual waterbodies, and ultimately the transport and fate of contaminants (Freitas et al., 1997; Semkin et

al., 2005). One of the most widely observed recent changes in northern hydrology has been a shift to increased winter streamflow (e.g. McClelland et al. 2006; Déry et al. 2009; Spence et al. 2014), which has altered water chemistry in rivers and streams across a range of scale from small watersheds ($< 150 \text{ km}^2$) (e.g. Spence et al. 2015) to continental-sized watersheds ($> 1.5 \text{ M km}^2$) (Holmes et al., 2012; Tank et al., 2016). While changes in stream chemistry have largely been attributed to processes happening on land, such as thawing permafrost, alteration of hydrologic flow paths, and changes in vegetation, changes in stream flow can also influence within-lake biogeochemical processing of nutrients, metal(loid)s, and carbon by mediating the delivery of organic matter and oxygen, which have important controls on the redox state of waterbodies.

Redox processes have a fundamental control on the speciation of inorganic As and its interactions with Fe and S. Under oxic conditions in lakes, ferric iron (Fe(III)) dominates and forms insoluble Fe (oxy)hydroxides which have a high affinity for arsenate (As(V)) and can remove aqueous As through sorption and co-precipitation reactions (Kneebone et al., 2002; Root et al., 2007). Under anoxic conditions and in the presence of an electron donor such as labile organic matter, the reductive dissolution of Fe (oxy)hydroxides releases As, as As(III), into the dissolved phase. If reducing conditions persist and the system moves along the redox cascade towards sulfate reduction, the co-existence of dissolved sulfides and As(III) can lead to the removal of As from solution through the precipitation of As-S mineral phases and/or Fe-S minerals that can adsorb or incorporate As into their structure (Bostick and Fendorf, 2003; O'Day et al., 2004; Tang et al., 2019). These processes apply to environments near redox boundaries in sediments (Martin and Pedersen, 2002; Schuh et al., 2019), but also in lakes where the redox boundary may migrate into the water column due to stratification and prolonged anoxia in the hypolimnion (Ford et al., 2006; Hollibaugh et al., 2005; Senn et al., 2007).

We conducted a two-year investigation of As, Fe and S biogeochemical cycling in surface water and sediment under contrasting winter streamflow and oxygen conditions in a small subarctic lake impacted by 60 years of As pollution. High-frequency sampling allowed for a detailed characterization of under-ice enrichment of lake water As, which is common in shallow subarctic lakes (< 4 m deep) associated with winter anoxia (Palmer et al., 2019). Further, we explored As dynamics in lake water through the transition from anoxic to oxic conditions associated with spring snowmelt and ice-off, an area of study that has received increased recent attention in limnology (Block et al., 2019; Denfeld et al., 2018), yet remains understudied with respect to As cycling. We used a combination of water column profiling, sediment porewater analyses, bulk sediment chemistry and solid-phase speciation of As in near-surface sediments to characterize As dynamics between the water column and sediment under differing winter conditions in this rapidly changing subarctic environment.

5.2 Materials and methods

5.2.1 Site description

Atmospheric emissions from historical gold mining operations distributed large amounts of pollutants across the Yellowknife, NT region between 1938 and 1999. Arsenic was the main contaminant of concern and the primary source of arsenic pollution was the roasting of gold-bearing arsenopyrite at the two largest mines in the area, Giant Mine (1948-2004) and Con Mine (1938-2003). Over the operating life of these mines, > 20,000 tonnes of arsenic trioxide (As_2O_3) was released to the atmosphere and 84% of these emissions were released prior to 1958 (Hocking et al., 1978; Wrye, 2008). As a result, a legacy of arsenic contamination persists in soils and lakes in the region (Galloway et al., 2017; Houben et al., 2016; Jamieson et al., 2017; Palmer et al., 2019, 2015). Details of the mining history, production methods, and characterization of mine waste from

operations near Yellowknife have been reported previously (Fawcett et al., 2015; Jamieson, 2014; Moir et al., 2006; Walker et al., 2015).

This study focused on Lower Martin Lake, a small (1.2 km²) and shallow (mean depth 2.0 m) lake located approximately 3 km from the historic roaster stack at Giant Mine (Figure 5.1). The large sediment surface area to water volume ratio (0.8) magnifies the influence of benthic processes on lake water conditions (Palmer et al., 2019). Lower Martin Lake is the final lake in the Baker Creek watershed (121 km²) prior to Baker Creek passing through the Giant Mine site and ultimately discharging into Yellowknife Bay of Great Slave Lake (Figure 5.1). Regionally, Lower Martin Lake is important in controlling the flux of legacy atmospheric mining pollutants to Great Slave Lake (a relatively pristine and large subarctic lake) because the Baker Creek watershed was highly exposed to deposition from Giant Mine roaster emissions (Jamieson et al., 2017; Palmer et al., 2019). The inflow to Lower Martin Lake is a shallow wetland connected to Martin Lake upstream. During the first winter of this study (2017-18) the stream channel through the wetland was frozen to the bottom by late November, and Lower Martin Lake was hydrologically disconnected from lakes further upstream in the Baker Creek watershed. High rainfall in the following summer (June and July 2018) raised water levels in the watershed and open-water flow persisted in the wetland stream connecting Martin and Lower Martin Lake during the second winter of the study (2018-19). The Water Survey of Canada maintains a hydrometric gauge at the outlet of Lower Martin Lake (station ID: 07SB013) and has been recording discharge continuously since 1983 (ECCC, 2019). Spence et al. (2015) highlighted a recent shift towards increased winter baseflow in the region, due to an increase in September precipitation falling as rain rather than snow. This allows seasonal storage deficits built up over the summer to be overcome and runoff

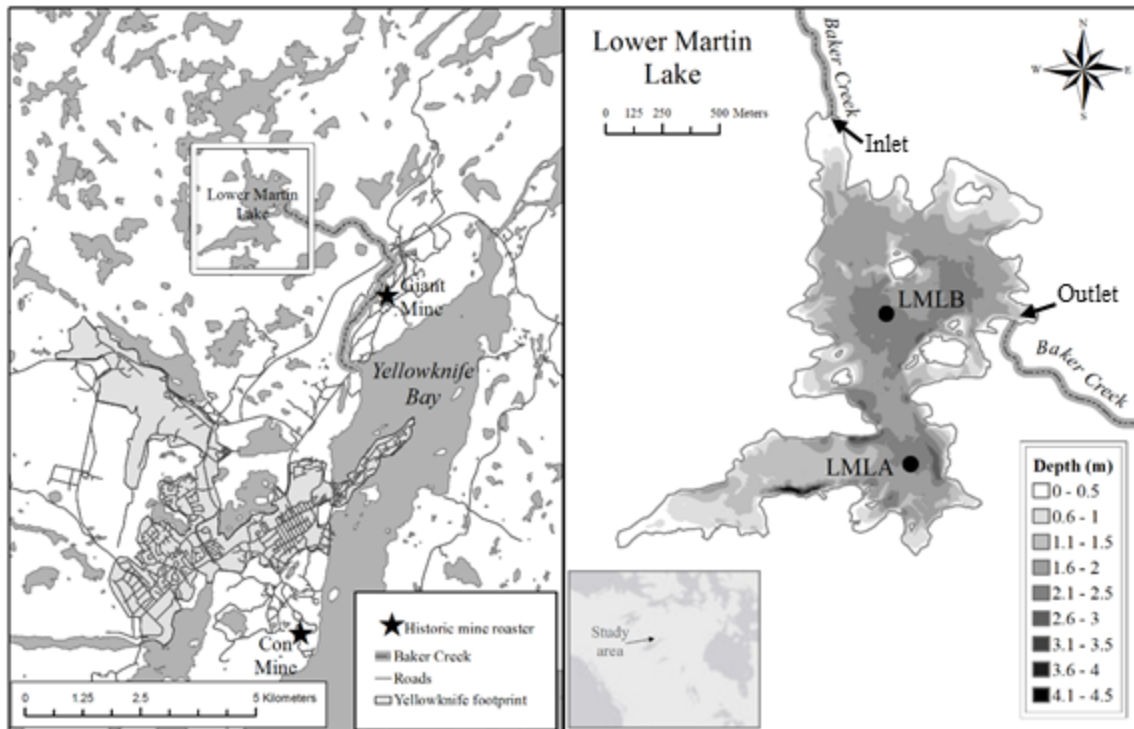


Figure 5.1: Map of study area and sampling locations. LMLA and LMLB are locations of sediment coring, sediment porewater sampling and lake-water chemistry profiles.

generation thresholds to be more frequently exceeded (Spence et al., 2015). Between 1972 and 1996 the winter months of October to April accounted for 8% of the Baker Creek annual yield, whereas during the recent period between 1997 and 2014 winter streamflow accounted for 20% of annual yield. While the Baker Creek basin exhibits substantial interannual variability in streamflow ($\sigma = 0.17 \text{ m}^3 \text{ s}^{-1}$), the two years of this study provide an exceptional opportunity to examine how changing winter streamflow conditions impact element cycling in shallow lakes within the basin.

5.2.2 Instrumentation

Time series measurements of temperature, specific conductivity, and dissolved oxygen were recorded on moored installations deployed at two locations in Lower Martin Lake (LMLA and

LMLB) between September 2017 and October 2019 to evaluate changing lake water properties over the study period. All sensors were installed 1.0 m above the lake bottom (approximately mid-depth in the water column). Open-water installations were suspended from a buoy anchored to the lake bottom and winter sensors were deployed below a PVC pipe anchored in the lake ice in late October or early November. Additional sensors were installed within 0.3 m of the lake bottom in March 2018 to measure dissolved oxygen levels at 15 min intervals to test the hypothesis that benthic oxygen production during increased sunlight conditions in spring would lead to oxidizing conditions near the sediment boundary. Temperature and specific conductivity were measured with Onset U24-001 loggers with a resolution of $\pm 0.01^{\circ}\text{C}$ and $\pm 1 \mu\text{S cm}^{-1}$, respectively. The rate and timing of oxygen depletion was measured with MiniDOTTM dissolved oxygen loggers (Precision Measurement Engineering, Vista, California) (accuracy: $\pm 0.3 \text{ mg L}^{-1}$; resolution: $\pm 0.01 \text{ mg L}^{-1}$) and factory calibration of the instruments was verified in May 2018.

5.2.3 Sample collection

5.2.3.1 Water column samples

Water column profiles of conductivity, temperature, pH, and dissolved oxygen were obtained at LMLA and LMLB at least once per month using a multi-parameter probe (YSI 6920, Yellow Springs Inc., Yellow Springs, Ohio) that was calibrated with certified reference solutions prior to field sampling. Water samples were collected through the water column on each site visit using a peristaltic pump and TeflonTM line that had been pre-washed with 5% HCl solution and rinsed with ultrapure water. The lines were flushed with lake water for 2 minutes at each sampling interval prior to sample collection. Open-water samples were collected at depths of 0.5, 1.3, 1.8, and 1.95 m below the water surface. Samples were collected under ice at the same intervals, except the

uppermost water column sample was collected below the base of the ice surface when the thickness of the ice exceeded 0.5 m. Samples were filtered in the field using a high capacity groundwater filter (Versapor® membrane; maximum pore size of 0.45 µm) attached to the Teflon™ line. Additional unfiltered samples were collected from the upper water column to assess the seasonal variation in the proportion of metal(loid)s in particulate (> 0.45 µm) and dissolved (< 0.45 µm) fractions.

Mean water column concentrations of As and Fe were calculated from each sampling visit using a depth-weighted approach at LMLA and LMLB for samples collected between the water surface and 1.8 m below the surface to aid visualization of the chemical time series. Data collected close to the sediment boundary were not included in the depth-weighted calculation because vertical sampling accuracy was limited and the steep chemical gradient near the sediment boundary in winter had the potential to artificially skew the calculation depending on where the measurement was made. The timing of ice-on and ice-off from Lower Martin Lake was estimated from frequent visits to the field site and confirmed using remotely sensed imagery available for the area (Sentinel-Hub, 2020).

5.2.3.2 Sediment porewaters

Sediment porewaters were collected during open-water (June-October), early-winter (November-December), and late-winter (February-April) conditions in both study years to investigate seasonal and interannual changes in porewater chemical gradients near the sediment-water boundary. Two different methods for porewater collection were used during the study: high-resolution dialysis arrays (peepers) and Rhizon CSS samplers (Rhizosphere Research Products, Wangeningen, Netherlands).

Peepers were deployed in late-winter (March 2018 and February 2019) by attaching them to a plastic pipe, lowering them into the sediment, and fixing the pipe to the ice surface to prevent the peepers from sinking in the unconsolidated sediments during deployment. Duplicate peepers were installed back to back approximately 20 cm apart with sampling cells above and below the sediment-water interface, and the location of the sediment boundary was visually referenced using an underwater camera at the time of deployment and retrieval. Prior to installation, peepers were soaked in 0.5% HNO₃ solution for 24-hrs and rinsed three times with ultrapure water. The peeper cells (5 mL volume at 1-cm spacing) were filled with ultrapure water, covered with a permeable polyethersulfone filter membrane (0.22 µm; Sterlitech Corp.) and submerged in ultrapure water in airtight cases. The peeper cases were deoxygenated over a three-week period by bubbling high-purity N₂ gas through the cases, initially for a 24 hour period, followed by twice a day for 20 minutes. Peepers were deployed in the lake sediments for 14 days to allow for equilibration of sample cells with surrounding porewaters and surface waters (Carignan et al., 1994). Upon retrieval, peepers were returned to the peeper cases, purged with N₂ gas, and transported to the laboratory where water samples were extracted in an oxygen-free glovebox that had been purged with high-purity N₂ gas.

It was not possible to use peepers in the open-water season because the high water content of the sediments in Lower Martin Lake (> 95% in the upper 30 cm) could not support the peepers during the two-week deployment without them sinking further into the sediments. Therefore, all open-water and early winter porewater sampling was conducted using Rhizon samplers. Porewaters were extracted with Rhizons from sediment cores in the field to prevent disturbance of the sediment during transport. The collection of sediment porewaters using Rhizons followed methods outlined in the literature (e.g. Seeberg-Elverfeldt et al. 2005; Shotbolt 2010). In brief,

sediments were collected in 7-cm diameter core tubes with a gravity corer. Holes were predrilled in the core tubes at 1-cm intervals to allow for the insertion of Rhizon porewater samplers. All Rhizon samplers (5-cm porous section and 0.15 μm mean pore size) were pre-washed with 30 mL of 1% HCl solution and 30 mL of ultrapure water. Porewater samples (3-5 mL) were extracted through Rhizons and into 12 mL acid-washed syringes using vacuum pressure created by the syringe. Dissolved oxygen levels were measured through the porewater sampling ports across the sediment-water interface with a PreSens Microx 4TM fibre optic oxygen meter attached to PSt7 sensors (PreSens Precision Sensing GmbH, Regensburg, Germany). Sediment porewater sampling in late winter 2018 using peepers and Rhizons demonstrated the comparability of the two methods (see Appendix A).

5.2.3.3 Sediment cores

Duplicate sediment cores were collected from Lower Martin Lake in September 2017 and April 2018 to examine differences in sediment geochemistry under oxic and anoxic surface water conditions. Sediment cores were collected at LMLA and LMLB (Figure 5.1) using an 8.8 cm internal diameter gravity corer (Uwitec, Mondsee, Austria). Sediments were extruded in the field in an oxygen-free atmosphere to preserve solid-phase As hosting minerals. This was done by sealing the sediment core and extruder in a glovebag and purging the glove bag of oxygen with N₂ gas. The top 30 cm of each core was sectioned into 0.5 cm (0-10 cm) or 1 cm (10-30 cm) intervals and placed in Whirl-PakTM bags and immediately frozen until they were freeze-dried in a vacuum atmosphere to prevent oxidation of reduced As-hosting solid phases. Water content (% water) was determined for all section intervals using the initial mass of wet sediment and the mass of the final freeze-dried sediment. Bulk density (g cm^{-3}) was calculated for the same core sections using the

mass of the freeze-dried sediment and the diameter of the core tube. Organic content of the lake sediments was estimated by loss on ignition (LOI).

5.2.4 Lake water and sediment porewater analyses

All lake water and porewater samples for total metal(loid) analyses were preserved with nitric acid (HNO₃) to 1% (v/v) and analyzed by inductively coupled plasma mass spectrometry (ICP-MS) following EPA method 200.8 (Creed et al., 1994) at Taiga Environmental Laboratory (Yellowknife, NT). Samples for the analyses of total inorganic As and arsenite (As(III)) were preserved with 0.125M ethylenediaminetetraacetic acid (EDTA) and glacial acetic acid, and analyzed by the laboratory of the Canada Research Chair in Global Change Ecotoxicology at Université de Montréal via hydride generation atomic fluorescence spectrometry (HG-AFS). Concentrations of arsenate (As(V)) were calculated as the difference between total inorganic As and As(III). EDTA was added to all sample vials or syringes prior to sample collection to immediately preserve As species. During winter 2018-19, lake water samples were collected to determine dissolved sulfide (S(-II)) and ferrous iron (Fe(II)) concentrations through the water column. All samples were analyzed immediately in the field using a Hach DR1900 spectrophotometer. Ferrous iron was determined using the 1,10-phenanthroline method according to Standard Methods for Water and Wastewater (American Public Health Association, 1999), with a method detection limit of 20 µg/L. Dissolved sulfide concentrations were determined using the methylene blue method (American Public Health Association, 1999) with a method detection limit of 5 µg/L. Low volume (1-2 mL) sediment porewater samples were analysed for hydrogen sulfide ($\Sigma\text{H}_2\text{S}$) and sulfate (SO_4^{2-}) concentrations in September 2018 and February 2019 to investigate the vertical migration of the sulfate reduction boundary. Samples were preserved with 0.5% zinc

acetate (v/v) and immediately frozen until analysis. $\Sigma\text{H}_2\text{S}$ was determined spectrophotometrically following methods outlined by Cline (1969) with a typical limit of detection less than 0.3 $\mu\text{g/L}$ and a precision of approximately 5% RSD. Sulfate concentrations were determined by ion chromatography with a typical limit of detection of 0.05 mg L^{-1} and a precision of 2% RSD.

5.2.5 Sediment geochemistry and As mineralogy

Metal(loid) concentrations in sediment core intervals were determined at the Analytical Services Unit, Queen's University via ICP-MS following *aqua regia* digestion of the freeze-dried sediments. Analytical accuracy was assessed using certified reference material MESS-4 (N=8) and all reference results were within laboratory control limits. Analytical precision was assessed through the analysis of duplicate samples (N=3) and relative percent differences in duplicate sample results of element concentrations were less than 20%. Results for laboratory blanks (N=5) were all below method detection limits, including for As (< 0.1 $\mu\text{g g}^{-1}$), Sb (< 0.02 $\mu\text{g g}^{-1}$), Fe (< 10 $\mu\text{g g}^{-1}$), Mn (< 1 $\mu\text{g g}^{-1}$), and S (< 20 $\mu\text{g g}^{-1}$).

Seasonal differences in the relative proportions of As-hosting solid phases in the surface layer (0-2 cm) of sediment cores collected in September 2017 and April 2018 were identified using a scanning electron microscopy (SEM)-based automated mineralogy technique. Dried sediment was mounted in epoxy on glass slides and polished in kerosene to 30 μm thickness following procedures described in Schuh et al. (2018, 2019). Automated mineralogy was performed using a FEI™ Quanta 650 Field Emission Gun Environmental SEM and Mineral Liberation Analyzer (MLA) software. Operating conditions, backscatter electron image standardization and resolution, and X-ray acquisition modes are the same as in Schuh et al. (2018, 2019). The relative contribution

of each As-hosting phase to the total mass of As in a sample was calculated using the following equation from Schuh et al. (2018):

$$As_{\%}^{h_x} = \frac{V^{h_x} \delta^{h_x} C_{As}^{h_x}}{\sum_{h=1}^n m_{As}^h} * 100 \quad (\text{Equation 5.1})$$

where $As_{\%}^{h_x}$ is the relative contribution of a particular host phase (h_x) to the total As in a sample (by mass), V^{h_x} is the volume of the host phase in μm^3 (assuming a sample thickness of 1 μm), δ^{h_x} is the density of the As-hosting phase, $C_{As}^{h_x}$ is the concentration of As associated with the host phase, and $\sum_{h=1}^n m_{As}^h$ is the total mass of As in all As-hosting phases. The mineral densities used in each calculation are from the Mineralogical Society of America (2000). Arsenolite, realgar, and goethite ($\alpha\text{-FeOOH}$) were used as model compounds for As_2O_3 , As-sulphide, and Fe-oxyhydroxide, respectively.

5.3 Results

5.3.1 Contrasting winter streamflow between 2017-18 and 2018-19

Lower Martin Lake was hydrologically disconnected from the upper and lower portions of the Baker Creek watershed during fall and winter 2017-18 until streamflow resumed May 9, 2018 in association with freshet (Figure 5.2). Total rainfall in summer 2018 (256 mm) was substantially higher than the 30-year climate normal for summer precipitation (155 mm) (ECCC, 2018), which increased water levels throughout the region and resulted in sustained baseflow during the following winter (2018-19). Open-water flow persisted at the inlet of Lower Martin Lake during winter 2018-19 and dissolved oxygen levels measured at the lake inlet were consistently $> 5 \text{ mg L}^{-1}$ (Figure 5.2).

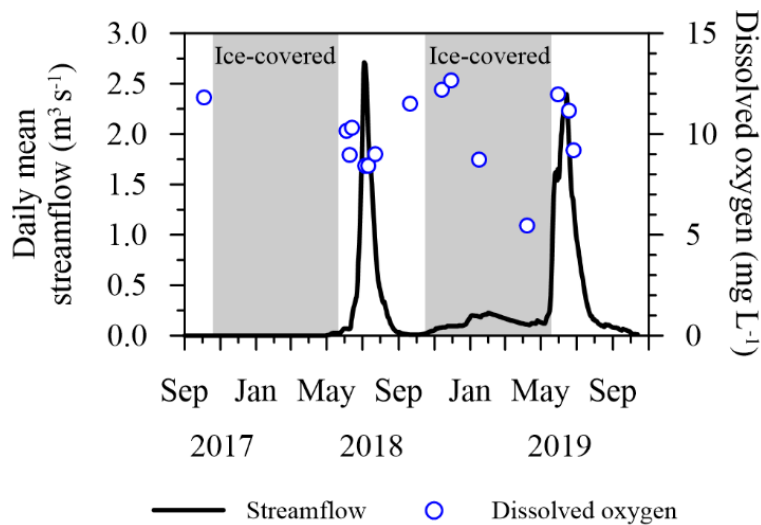


Figure 5.2: Daily mean streamflow ($\text{m}^3 \text{s}^{-1}$) at the outlet of Lower Martin Lake (ECCC, 2019; station 07SB013) and dissolved oxygen levels (mg L^{-1}) measured at the lake inlet, September 2017 to October 2019.

5.3.2 Dissolved oxygen

Water column concentrations of dissolved oxygen decreased rapidly in Lower Martin Lake with the development of an ice-cover during both study years (Figure 5.3). The full water column was depleted of oxygen to the point of anoxia ($< 0.5 \text{ mg L}^{-1} \text{ O}_2$) for greater than three months during winter 2017-2018 but did not reach anoxic conditions in 2018-19, remaining $> 1 \text{ mg L}^{-1}$ for the duration of winter (Figure 5.3). The timing and duration of water column anoxia in 2017-18 varied between sampling locations, indicating low lateral mixing of the water column under ice when the lake was hydrologically disconnected from the surrounding watershed. Oxygen was depleted from the water column at site LMLB 26 days earlier than at LMLA (Figure 5.3). The timing of reoxygenation of the water column was relatively similar in spring 2018 at LMLA (May 5) and LMLB (April 29), and because of the lag in onset of anoxic conditions between the locations the duration of anoxia was 20 days longer at LMLB (116 d) than at LMLA (96 d).

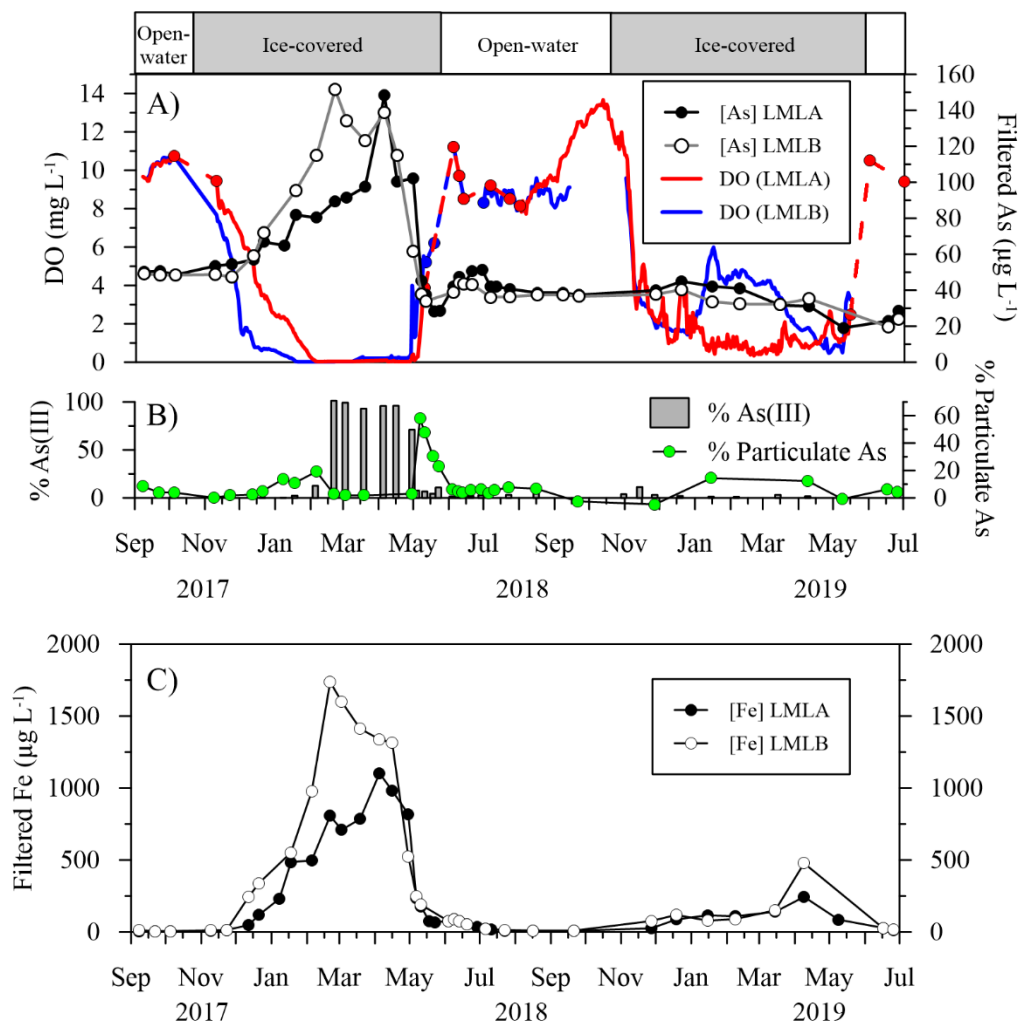


Figure 5.3: Time-series of A) total filtered As and dissolved oxygen; and C) total filtered Fe at two locations in Lower Martin Lake, September 2017 to July 2019. Water concentrations represent the depth-integrated mean of 3-4 sampling intervals within the water column. Dissolved oxygen was measured continuously 1m above the sediment boundary, except for the periods represented by red and blue circles connected with dashed lines, which indicate discrete measurements and interpolated DO levels between measurements. The middle panel B) represents the proportion of total inorganic As as As(III) at the mid-water column sampling depth and the proportion of total As in the particulate fraction at LMLA. Results of full water column As speciation analyses are presented in Figure 5.4.

5.3.3 Depth-weighted mean concentrations of As and Fe

Mean water column concentrations of filtered As and Fe were relatively similar during the open-water and early winter seasons in both years, and there was little difference in concentrations of

As and Fe between the two sampling locations during these periods (Figure 5.3). Large increases in filtered As and Fe were measured during winter 2017-18 in association with the onset of anoxia through the water column (Figure 5.3), and As increased 179% (from 53 to 148 $\mu\text{g L}^{-1}$) and 202% (from 49 to 148 $\mu\text{g L}^{-1}$) between ice-on and maximum concentrations in mid-winter at LMLA and LMLB, respectively. Peak As and Fe concentrations were measured 43 days earlier at LMLB (February 21) than at LMLA (April 5), consistent with the higher oxygen depletion rate at LMLB (Figure 5.3). Anoxic conditions persisted in the water column at both sites well into spring 2018, and mean water column concentrations of As and Fe decreased from mid-winter peak concentrations at both locations prior to snowmelt and ice-off.

Mean water column concentrations of filtered As and Fe during winter 2018-19 contrasted sharply with the previous winter (Figure 5.3). Mean As decreased approximately 20% (40 – 32 $\mu\text{g L}^{-1}$) from ice-on to mid winter (November 27 – March 15), and there was little difference in As between sampling locations. An increase in filtered Fe concentrations was measured over winter 2018-19 (LMLA: 25 to 243 $\mu\text{g L}^{-1}$; LMLB: 76 to 477 $\mu\text{g L}^{-1}$), but concentrations were almost an order of magnitude lower than the previous winter and there was little difference between sampling locations.

Arsenic was predominately measured in the filtered ($< 0.45 \mu\text{m}$) fraction during the open-water season during both study years ($< 10\%$ particulate As) (Figure 5.3). The proportion of total As in the particulate fraction was highest in May 2018 (up to 58%), during the anoxic to oxic transition of the water column. Higher proportions of particulate As (10-15% of total As) were also measured under ice in 2017-18 prior to anoxia developing throughout the water column and throughout winter 2018-19.

5.3.4 Water column profiles of As, Fe, and S

Chemical profile sampling during the two contrasting years revealed important differences in the vertical distribution of filtered Fe, As, and inorganic As species between seasons and study years (Figure 5.4). In all open-water sampling periods, concentrations of filtered As and Fe were similar with depth and As(V) accounted for more than 95% of total inorganic As in the water column (Figures 5.3 & 5.4). Distinct chemical gradients appeared in both sampling years with ice-on, after which concentrations of filtered As and Fe were higher near the sediment boundary, suggesting sediment efflux of these elements, although concentrations of As and Fe were lower and chemical gradients were less pronounced in winter 2018-19 than in 2017-18 (Figure 5.4). Prolonged anoxia in the water column during winter 2018 led to a reversal in the As chemical gradient by March 2018 with lower concentrations of As developing near the sediment boundary than in the upper portion of the water column (Figure 5.4). In contrast, Fe concentrations were higher near the sediment boundary throughout the ice-cover season.

Development of anoxia in the water column in winter 2017-18 also resulted in changes in inorganic As speciation in the water column. As(III) represented more than 70% of total inorganic arsenic through the water column by late February (Figures 5.3 & 5.4). During winter 2018-19, As(V) was the principal inorganic As species through the water column during all sampling events, except for samples adjacent to the sediment boundary at LMLB (Figures 5.4 & 5.5). Vertical sampling in March 2019 revealed that elevated concentrations of total filtered As and Fe near the sediment boundary (Figure 5.4) corresponded with the presence of high concentrations of ferrous iron ($\text{Fe(II)} > 2000 \mu\text{g L}^{-1}$), dissolved sulfide ($\text{S(-II)} > 400 \mu\text{g L}^{-1}$), and As(III) ($> 200 \mu\text{g L}^{-1}$) (Figure 5.5).

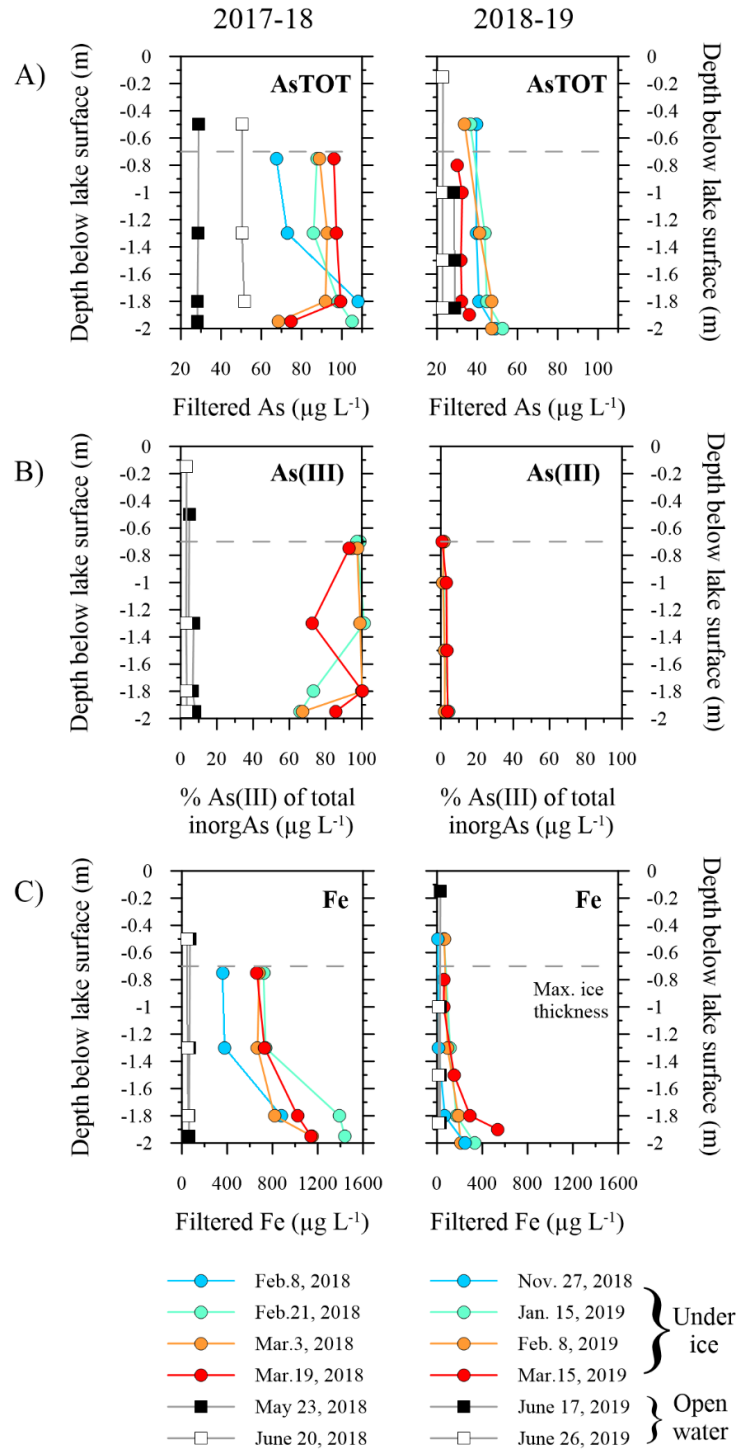


Figure 5.4: Water column profiles of: A) filtered As, B) inorganic As speciation, and C) filtered Fe during consecutive years at LMLA. Note the horizontal dashed line represents the extent of maximum ice thickness in the lake, and water sampled above that line was below the lake ice earlier in the season when the ice was thinner. Symbols identify measurements taken in winter under ice (coloured circles) and during the open-water season (black and white squares).

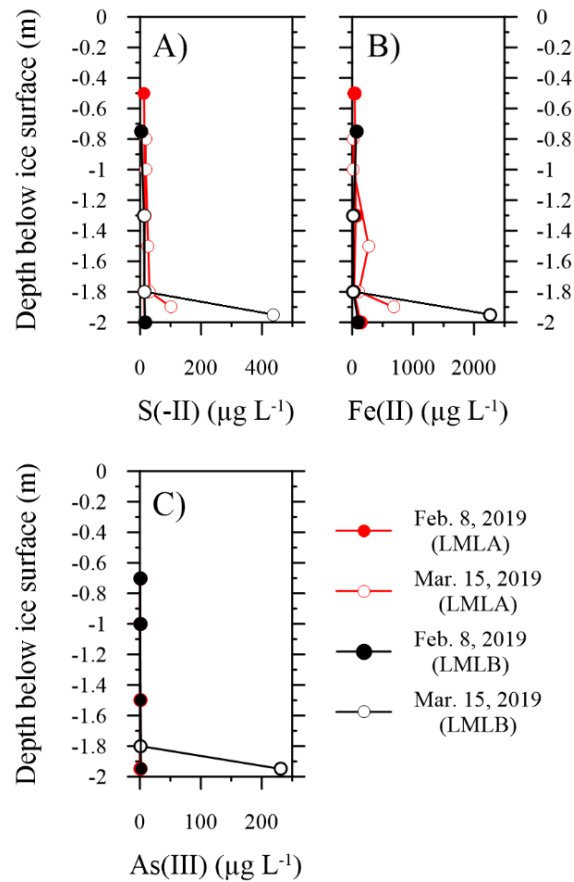


Figure 5.5: Water column concentrations of filtered: A) S(-II); B) Fe(II); and C) As(III) during winter 2019 at LMLA and LMLB. Note the water column did not fully reach anoxia in 2019.

5.3.5 Water column As during the anoxic to oxic lake water transition in spring 2018

Depth-integrated water column concentrations of filtered As decreased abruptly from mid-April to early May 2018 at LMLA (100 to 37 $\mu\text{g L}^{-1}$) and LMLB (115 to 34 $\mu\text{g L}^{-1}$) as the lake transitioned from anoxic to oxic water column conditions (Figure 5.3). Mean spring 2018 lake water As concentrations were approximately 20% lower than the preceding fall, prior to ice-on (Figure 5.3). The anoxic to oxic transition also corresponded with a decrease in the proportion of dissolved inorganic As as As(III) and an increase in the particulate fraction of As in surface waters (up to 58%) (Figure 5.3).

The oxygenation of the water column occurred while the lake was ice covered and was initiated near the sediment boundary well before snow started melting in the catchment. By early April, dissolved oxygen levels near the sediment boundary fluctuated diurnally ($0.2\text{-}1.4\text{mg L}^{-1}\text{ O}_2$) (Figure 5.6a) but overlying waters remained anoxic (Figure 5.6b), suggesting a benthic source of oxygen. The benthic production of oxygen initiated the oxidation of As(III) to As(V) near the sediment boundary by mid-April (Figure 5.6b), while As(III) continued to dominate in overlying waters.

Minimum hourly air temperatures crossed the 0°C threshold in late-April (Figure C4) and resulted in rapid snowmelt from the ice surface and surrounding landscape. The influx of snowmelt water to the lake on April 27, as inferred by the sharp decrease in specific conductivity of lake water (Figure 5.6a), led to the further oxygenation of the water column. The full water column was oxygenated by April 30th (Figure 5.6a), more than two weeks before the complete loss of ice cover on the lake (approx. May 18, 2018). Water chemistry profile sampling over the anoxic to oxic transition indicated that the proportion of total inorganic As as As(III) was $> 90\%$ through the water column at the end of winter in early April. As the entire water column was progressively oxygenated from the influx of snowmelt and benthic oxygen production, the concentration of filtered As and the proportion of inorganic As as As(III) decreased until the water column was relatively isochemical (40 ug L^{-1}) and dominated by As(V) by May 7 (Figure 5.6b).

5.3.6 Porewater profiles across seasons

The vertical distribution of filtered As and Fe in sediment porewaters showed large seasonal differences in profile shape but little difference between years (Figure 5.7). During the open-water season, sharp peaks in porewater As concentrations ($120\text{ - }160\text{ }\mu\text{g L}^{-1}$) were measured

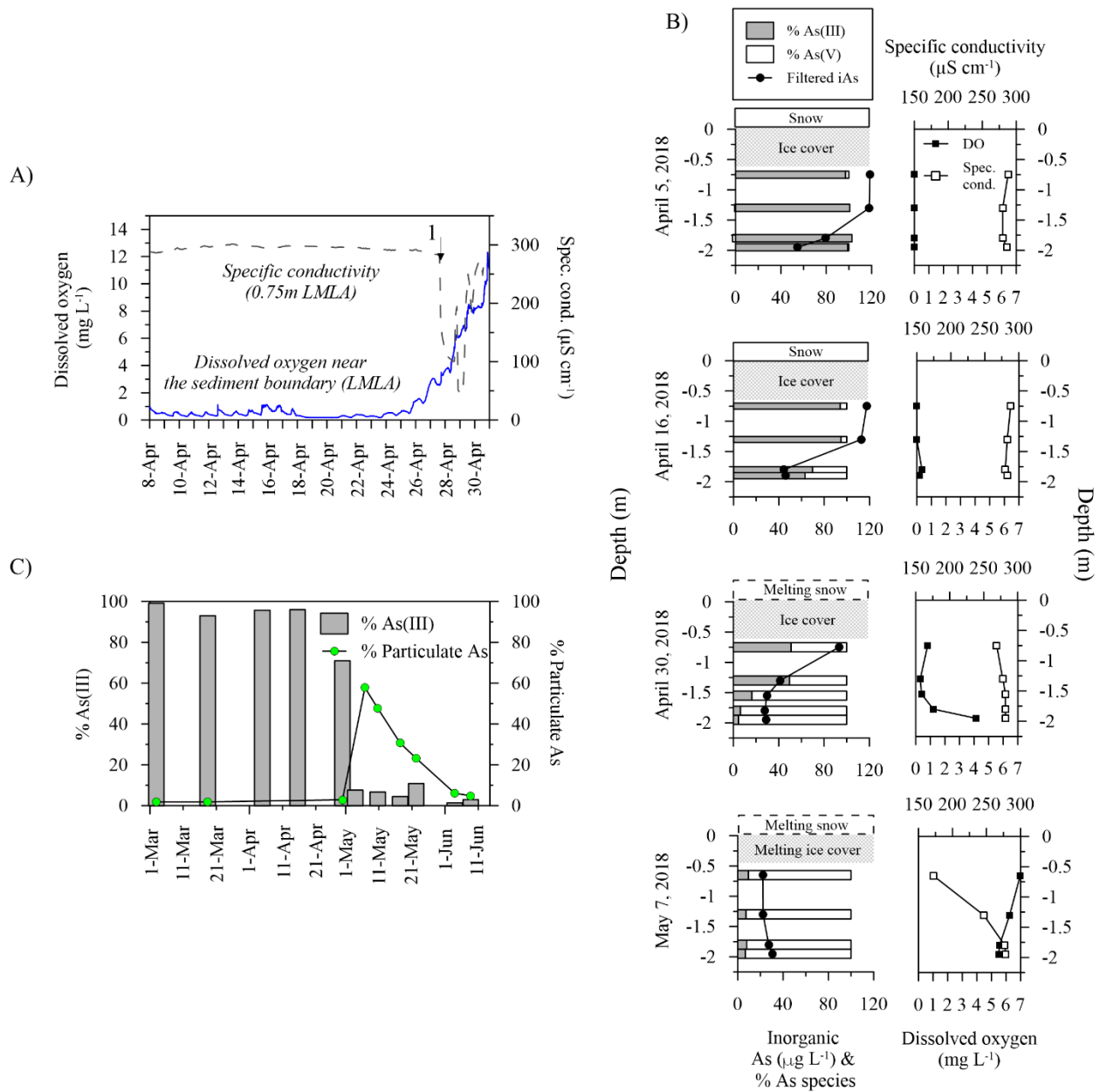


Figure 5.6: A) Dissolved oxygen measured 30 cm above the sediment boundary and the specific conductivity of surface waters. The number 1 in the plot indicates timing of snowmelt water entering the lake. B) Water column measurements of filtered As, the proportion of inorganic As species, dissolved oxygen and specific conductivity at LMLB during the snowmelt period. C) The proportion of total inorganic As as As(III) and the particulate fraction of total As during the snowmelt period at LMLA.

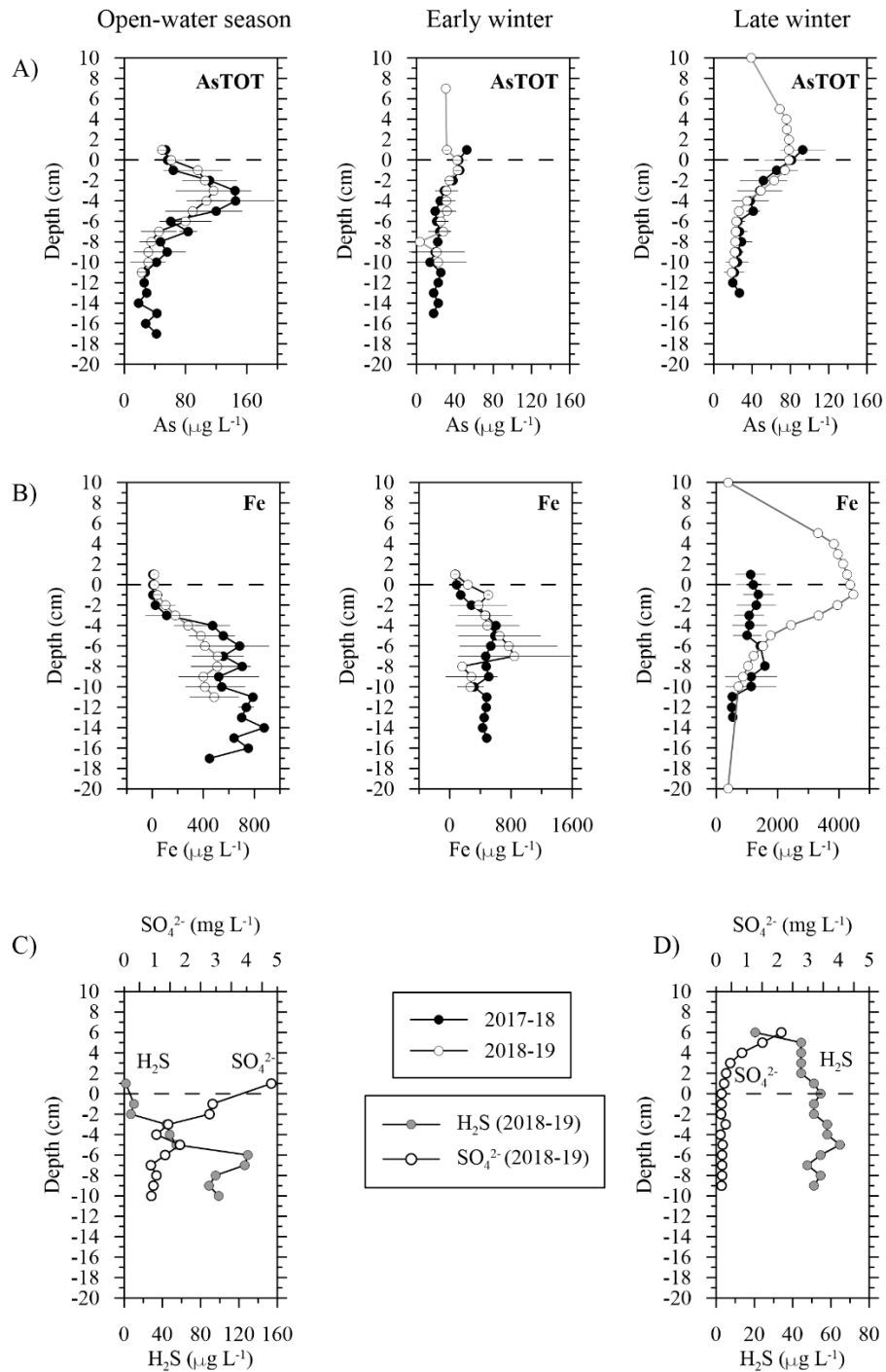


Figure 5.7: Mean and standard deviation of porewater concentrations of: A) filtered As; and B) filtered Fe in the open-water season (2017: N = 4; 2018: N = 6), early winter (2017: N = 2; 2018: N = 3), and late winter (2018: N = 4; 2019: N = 2). Bottom panels represent: C) open-water; and D) late-winter SO₄ and $\Sigma\text{H}_2\text{S}$ concentrations in porewaters during the second year of the study (2018-19). Open-water and early season porewaters were collected with Rhizon samplers and late winter porewaters were collected using peepers (see methods for details and Appendix C for comparison of sampling methods).

approximately 3 cm below the sediment surface and decreased upwards towards the sediment boundary and overlying water. Sediment porewater profiles from early winter indicated a gradual increase in As concentrations ($\sim 20 - 40 \mu\text{g L}^{-1}$) from depths below 10 cm to overlying waters near the sediment boundary (Figure 5.7a). Late-winter porewater concentrations of As similarly increased from low concentrations at depth to much higher concentrations across the sediment-water boundary but the chemical gradient was slightly steeper in sediments within 5 cm of the sediment-water interface ($\sim 40 - 100 \mu\text{g L}^{-1}$) (Figure 5.7a).

Sediment porewater concentrations of $\Sigma\text{H}_2\text{S}$ and SO_4^{2-} measured in August 2018 when bottom waters and interfacial sediments were oxic showed that concentrations of $\Sigma\text{H}_2\text{S}$ were close to the method detection limit in overlying water and the upper 2 cm of sediment but increased sharply below 2 cm ($> 80 \mu\text{g L}^{-1}$) (Figure 5.7c). Changes in SO_4^{2-} were inversely related to changes in $\Sigma\text{H}_2\text{S}$, with maximum concentrations ($160 \mu\text{g L}^{-1}$) measured in overlying waters (Figure 5.7c). Porewater samples from February 2019, when bottom waters just above the sediment boundary were anoxic, showed the upward migration of the sulfate reduction front into the overlying water column as elevated concentrations of $\Sigma\text{H}_2\text{S}$ ($\sim 40 \mu\text{g L}^{-1}$) persisted approximately 5 cm above the sediment-water interface (Figure 5.7c).

5.3.7 Solid-phase bulk chemistry and changes in As mineralogy at the sediment-water boundary

Lake sediments in Lower Martin Lake were predominately composed of organic material (LOI% $> 70\%$) and had a very high water content through the upper 30 cm ($> 97\%$) (Table C1). Sediment As concentrations were highest ($2000-2500 \text{ mg kg}^{-1}$) at 12-15 cm below the sediment surface in

both summer and winter cores (Figure 5.8a). In surficial sediments (0-1 cm), arsenic concentrations were an order of magnitude lower (250-490 mg kg⁻¹) than at the peak, but were

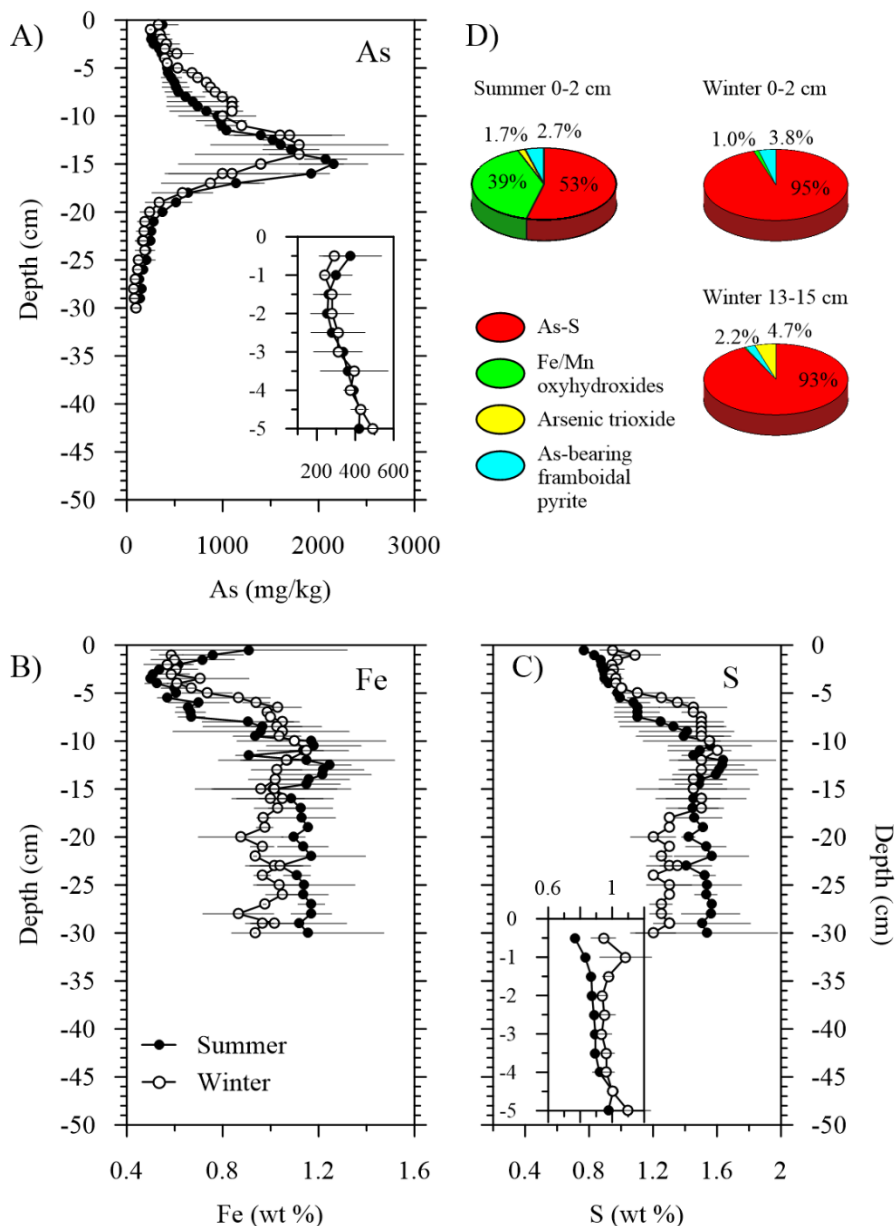


Figure 5.8: Solid-phase chemistry of duplicate sediment cores (LMLA and LMLB) during the open-water season (September 2017) and under ice (April 2018), including A) As; B) Fe; and C) S. Error bars represent the standard deviation of concentrations at discrete intervals from duplicate cores. Inset panels highlight near surface (0-5cm) concentrations of elements. D) The mass distribution of As in solid-phase host minerals in surface sediments collected in September 2017 and April 2018 and at the As maxima for April 2018. See Supporting Information (Table S2) for assumptions in derivation of As mass distribution.

enriched compared to depths > 25 cm in the sediment profile (22-97 mg kg⁻¹). Sedimentary Fe and S concentrations were highest 6-10 cm below the sediment-water interface and remained relatively consistent with depth in the lower portions of the sediment profiles (Fe: 1.0 - 1.2 wt%; S: 1.2 - 1.6 wt%) (Figure 5.8b,c). Substantial surficial enrichment in Fe was measured in the cores collected under oxic bottom water conditions (up to 1.2 wt%), but not during winter when anoxic conditions were present through the water column. In contrast, slight surficial enrichments in S (\bar{x} = 0.95 wt. % S) were measured in the cores collected under anoxic water column conditions in winter compared to the open-water season (\bar{x} = 0.77 wt. % S) (Figure 5.8). There was little difference in sediment As concentration in surficial sediments between the open-water and winter sampling seasons (Figure 5.8a).

Solid-phase speciation of As hosting phases by SEM and automated mineralogy in surficial sediments (0-2 cm) revealed distinct differences in the mass distribution of As in host minerals between seasons (Figure 5.8; Table C2). Under oxic surface water conditions, As was hosted primarily in Fe-oxyhydroxide (39%) and As-S (53%) mineral phases. In contrast, under anoxic bottom water conditions, Fe (oxy)hydroxides were absent and more than 95% of As was hosted in As-S mineral phases. In samples from both sampling periods, As-bearing framboidal pyrite was prevalent, indicating secondary sulfide precipitation, but the low concentration of As in framboidal pyrite (Table C2; Schuh et al. 2018) resulted in pyrite accounting for < 5% of total As in the samples by mass. At peak sediment As concentrations 13-15 cm below the sediment surface, As was predominately hosted in As-S minerals (> 92%), but was also present in smaller proportions associated with As₂O₃ and As-bearing framboidal pyrite (Figure 5.8d).

5.4 Discussion

This study provides new insights on the seasonal cycling of As, Fe, and S in shallow ice-covered lakes through comprehensive geochemical characterization of the aquatic system in Lower Martin Lake, including surface waters, sediments, and sediment porewaters. We showed that lake sediments were a source of As (and other redox sensitive elements) to overlying waters during winter, through within-lake biogeochemical processing, and the magnitude of As efflux and its impact on water column inventories and speciation was strongly driven by interannual variability in streamflow. Further, we used frequent geochemical sampling through the water column during the spring transition from anoxic to oxic lake water conditions to provide new information on the reoxygenation of the water column after winter anoxia in shallow subarctic lakes and demonstrate the role of biological and physical processes in this important, yet understudied, seasonal transition.

5.4.1 Seasonal As cycling coupled with biogeochemical cycling of Fe and S

Seasonal variability in the concentration and mobility of As in near-surface sediments, sediment porewaters and overlying surface waters was driven by the transient redox conditions within these zones and was associated with the biogeochemical cycling of Fe and S. In the open-water season, the decrease in aqueous As and Fe in sediment porewaters towards the sediment-water interface indicated that the upward diffusion of dissolved As and Fe was attenuated within the thin oxic layer (Figure 5.7). In the solid-phase bulk geochemical profiles, high Fe concentrations in the upper sediments and the identification of Fe (oxy)hydroxides as an important As hosting mineral in this zone (Figs. 5.8b,d) suggests that the mobilization of As across the sediment-water boundary was limited by precipitation and/or adsorption with Fe (oxy)hydroxide minerals. This is consistent

with previous studies during open-water conditions in the region (Schuh et al., 2019, 2018; Van Den Berghe et al., 2018) and in the wider literature, where the mechanism of As sequestration by Fe-oxyhydroxide precipitation under oxic conditions has been widely acknowledged (e.g. Martin and Pedersen 2002; Root et al. 2007; Couture et al. 2010). The oxic boundary within interfacial sediments was absent by early winter in both study years (Figure C2), as the ice cover limited oxygen entrainment in the lake and microbial respiration depleted oxygen within the sediments. Consequently, the Fe(III) redoxcline migrated upwards (Figure 5.7b) releasing As and Fe to overlying waters (Figure 5.4a,c). The absence of Fe (oxy)hydroxide minerals in near surface sediments in late-winter sediments suggests reductive dissolution of these minerals as the mechanism controlling release of As and Fe to overlying waters.

The prolonged period of water column anoxia that developed in winter 2018 had an important influence on water column As. The duration of anoxia and the presence of abundant organic matter in the sediments likely led to the development of sulfate reducing conditions in the water column. Dissolved sulfide measurements were not made in the water column during winter 2017-18 but late winter field observations of malodourous water under ice and the presence of high concentrations of dissolved sulfide in bottom waters in the following winter (2018-19) (Figures 5.5 & 5.7d) suggests that the sulfate reduction boundary migrated upwards into the water column. There was a noticeable decrease in mean As (Figure 5.3) and the inversion of the As gradient in the water column (Figure 5.4a) in late winter 2018, which may be due to the removal of As and Fe from solution by the formation of Fe-sulfide and As-sulfide mineral phases. This is supported by the abundance of framboidal pyrite (Fe(II)-S₂) and As(III)-S minerals observed in surficial sediments collected in winter 2018 (Figure 5.8d) and the co-existence of aqueous As(III), Fe(II), and S(-II) in late-winter bottom waters (Figure 5.5). Removal of As from solution under

sulfate reducing conditions has been observed previously in lake sediments in the region (Schuh et al., 2018) and also in the hypolimnion of meromictic lakes (Hollibaugh et al., 2005). The data presented here highlight the importance of sulfide mineral precipitation at shorter time scales (i.e. seasonal) than previously observed and again signifies the importance of understanding interactions with both Fe and S in the seasonal cycling of As in shallow subarctic lakes. This builds our conceptual understanding of under-ice redox dynamics and adds to previous work that has focused on the anoxic release of As via reductive dissolution of Fe and Mn (oxy)hydroxides followed by As sequestration by reprecipitation of Fe (oxy)hydroxide minerals once oxic conditions are restored (Barrett et al., 2019; Joung et al., 2017; Palmer et al., 2019; Schroth et al., 2015). This study also highlights the spatial variability of under-ice redox processes, when there is limited under-ice circulation, as the timing of As removal from the water column varied substantially between locations in the lake. Peak water column As and Fe concentrations were measured 43 days earlier at LMLB than LMLA in winter 2017-18, corresponding with a higher dissolved oxygen depletion rate than at LMLA, and earlier removal of As via the likely precipitation of reduced As- and Fe-sulfide mineral phases (Figure 5.3).

In contrast to oscillating redox conditions observed in the upper sediments, reducing conditions persisted at depths below 5 cm in the sediments throughout the study period and provide insight into long-term behaviour of As under reducing conditions and interactions with reduced Fe and S. Two important mechanisms controlling As mobility are apparent at depth in the sediments. First, the detection of solid-phase As_2O_3 (Figure 5.8d) and the presence of high concentrations of dissolved As in sediment porewaters (Figure 5.7a) suggests the continued dissolution of legacy As_2O_3 buried in lake sediments and its upward migration along chemical gradients. Second, the identification of As-S minerals as the predominant host of As at depth suggests that the labile

fraction of As in sediments is eventually sequestered by secondary As-sulfide precipitation. This has been highlighted in other studies from the region (Schuh et al., 2019, 2018; Van Den Berghe et al., 2018) and suggests that the legacy source of labile As at depth in the sediments (As_2O_3) is finite and will slowly be exhausted through sulfide mineral precipitation, thus limiting aqueous As available for upward diffusion towards the sediment boundary. While this suggests that contaminated lake sediments are moving along a trajectory towards recovery, the rate of As removal by sulfide sequestration will likely be very slow (i.e., decades) and site-specific and dependent on several factors, including: inventories and dissolution kinetics of legacy As_2O_3 , and the physical (e.g. redox state and temperature) and biological (e.g. microbial activity) characteristics of the sediment.

5.4.2 The magnitude of winter increase in lake water As is controlled by the position of redox boundaries within the water column

Our results demonstrate that the mobilization of As from lake sediments occurred during both winters. The influence of remobilization on lake water chemistry, however, was substantially different between years due to interannual differences in watershed hydrology, which controlled the position of redox boundaries within the water column. During winter 2017-18 when oxygen inputs to the lake were limited, the chemocline migrated upwards and reducing conditions were present through the entire water column, as indicated by dissolved oxygen levels $< 0.5 \text{ mg L}^{-1}$ and the presence of As(III) as the predominant inorganic As species in the water column (Figure 5.3). Full water column anoxia and the subsequent removal of the Fe redox boundary did not allow for precipitation of Fe(III) mineral phases in the water column and resulted in the continued mobilization of Fe and As from lake sediments to the overlying water column causing large

increases in water column concentrations of Fe and As (filtered Fe > 1000 $\mu\text{g L}^{-1}$; filtered As > 100 $\mu\text{g L}^{-1}$) (Figure 5.3).

The continued influx of oxygenated water through the lake inlet during the following winter (2018-19) maintained mid-water column levels of dissolved oxygen above 2 mg L^{-1} at both LMLA and LMLB for much of the winter (Figure 5.3), which suppressed the upward migration of the Fe(III) and sulfate reduction fronts (Figure 5.5b,c & 5.7b,c,d). Thus, cycling of As and Fe likely continued within the lower water column, where precipitation and settling of As and Fe mineral phases near the Fe(III) redoxcline limited the vertical migration of As and Fe in the water column (Figure 5.9). During early winter 2017 and throughout winter 2018-19 when the Fe(III) redoxcline was positioned within the water column, there was a noticeable increase in the proportion of total As in the particulate fraction compared to the open-water season (Figure 5.3) supporting the mechanism of As adsorption to the precipitation and settling of Fe(III) minerals (Figure 5.9).

The data from this study provide new information on the under-ice biogeochemical cycling of redox sensitive elements, for which there is currently a paucity of studies. Previous work in shallow temperate lakes has shown that reactive pools of dissolved Fe and Mn may form under ice in bottom waters from the reductive dissolution of Fe/Mn (oxy)hydroxides, and the vertical migration of these zones is a function of the severity and duration of cold conditions (Joung et al., 2017; Schroth et al., 2015). Here, we highlight the importance of hydrological connectivity and delivery of O_2 from beyond the lake basin in controlling the upward migration of redox boundaries and fluxes of redox sensitive elements into the water column. In this specific study, the concentration of As in inlet water was much lower than in Lower Martin Lake (typically < 20 $\mu\text{g L}^{-1}$), therefore, in addition to supplying oxygenated water through winter, the inlet also served as

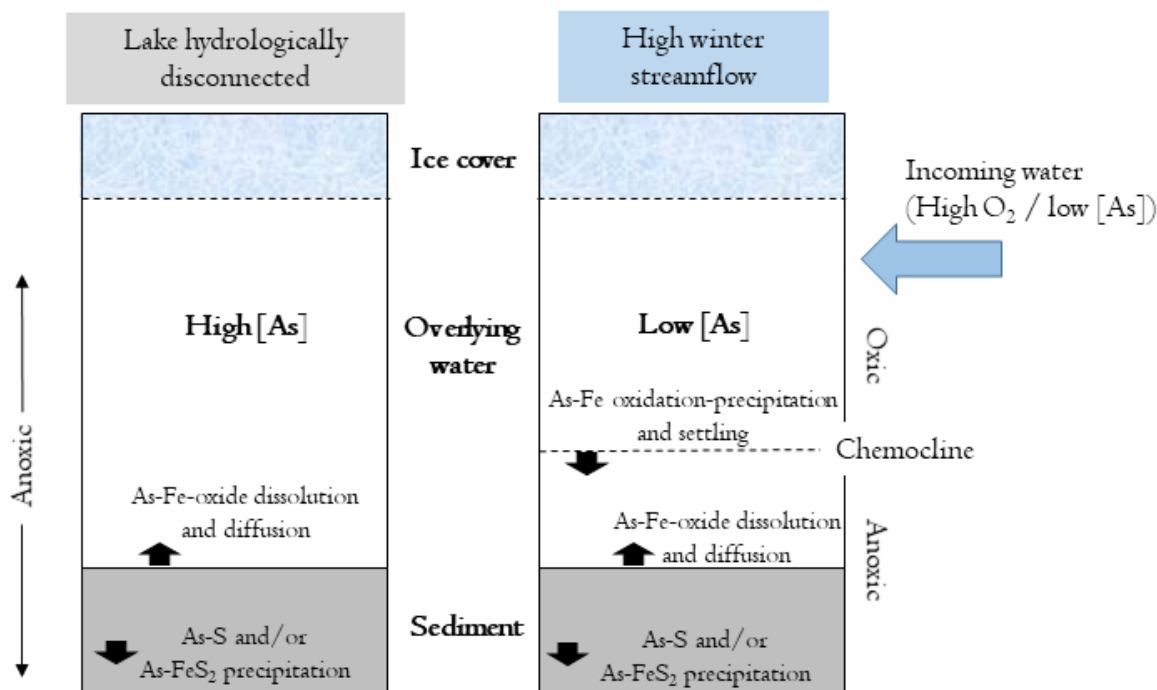


Figure 5.9: Conceptual model of the geochemical cycling of As in Lower Martin Lake and the influence of contrasting winter hydrological conditions. The model represents mid-winter conditions prior to As-S precipitation in the water column, which occurred under prolonged water column anoxia in the hydrologically disconnected lake scenario.

a source of lower As water that could “flush” Lower Martin Lake. A mass balance approach was beyond the scope of this paper, but future modelling will help to weigh the relative contributions of lake flushing and suppression of the upward migration of redox sensitive elements from lake sediments on winter lake water quality and recovery from As pollution. A rough estimate using the lake volume of Lower Martin Lake (Palmer et al., 2019) and assuming discharge volume over winter measured at the lake outlet (ECCC, 2019) is equal to inflow volume indicates that the full lake volume is displaced at minimum 1.5 times between November and May. A full mass balance of lake inputs, snowmelt contributions from the catchment and sediment fluxes will help to elucidate the relative importance of the various transport processes on the recovery of shallow lakes in subarctic environments.

5.4.3 Oxidation of the water column during the spring transition from anoxic to oxic lake water conditions

Reoxygenation of the water column after winter anoxia was initiated near the sediment boundary and began more than a month before the start of snowmelt and the loss of ice cover in spring 2018 (Figure 5.6). Diurnal variation in dissolved oxygen levels adjacent to the sediment boundary in early April (Figure 5.6a) likely reflected benthic production of oxygen from photosynthesis in lake sediments as the availability of light increased with longer daylight hours. Observations from under water photography of the sediment surface suggested that much of the lake bottom was covered by microbial mats. In high latitude environments, benthic oxygen production from microbial mats is an important source of O₂ to overlying waters under ice during spring sunlight conditions (Baehr and Degrandpre, 2002; Vopel and Hawes, 2006). This has important implications for the biogeochemical cycling of redox sensitive elements and the data presented here highlight this, with the oxidation of As(III) to As(V) occurring in water overlying sediment almost two weeks earlier than in the upper water column (Figure 5.6b). Further, benthic oxygen production in early spring implies the reestablishment of an oxic layer in lake sediments prior to overlying water, thus limiting sediment efflux of As and other redox sensitive elements, which is an important consideration for annual mass flux estimates. In contrast with previous focus on the role of snowmelt water to initiate spring changes to the under-ice water column chemistry of Arctic lakes (Bergmann and Welch, 1985; Vincent et al., 2008), this study demonstrates that benthic processes may have an important influence initiating water column reoxygenation and redox cycling in shallow productive lakes.

In contrast with other elements, such as mercury (e.g. Douglas et al. 2017), the delivery of snowmelt to the lake did not result in an increase in water column concentrations of As. Rather, water column As decreased abruptly during the snowmelt period, including by more than 50% in the one-week period between April 30 and May 7th (Figure 5.3a). The rapid decrease in As was likely due to the delivery of oxygenated snowmelt water to the lake and subsequent removal of As and Fe from solution via (co)precipitation of As and Fe (oxy)hydroxide minerals. The increase in particulate As in the water column during the spring transition (Figure 5.3b) is consistent with particle adsorption of As with Fe (oxy)hydroxide minerals, since As(V) has a high affinity for adsorption with Fe (oxy)hydroxides (Belzile and Tessier, 1990; Root et al., 2007). The detailed sampling in this study highlights the influence of landscape (i.e. snowmelt) and within-lake biological processes (i.e. benthic photosynthesis) in controlling the biogeochemical cycling of elements during this important spring transition from anoxic to oxic conditions in shallow lakes.

5.5 Conclusions and implications for climate change

This study highlights the coupling of hydrological and biogeochemical processes on element cycling during winter, an understudied part of the year, but one that is gaining recent attention in the literature because of its importance in contributing to annual lake and stream processes (Block et al., 2019; Denfeld et al., 2018; Spence et al., 2015; Tank et al., 2016). The two contrasting hydrological years investigated in this paper demonstrate the influence of different streamflow conditions on biogeochemical processing within lakes in the Baker Creek system. Greater winter hydrological connectivity between water bodies altered As cycling by mediating the delivery of oxygenated water and suppressed the upward migration of the Fe(III) redoxcline in the water column (Figure 5.5b; Figure 5.9). Based on the results from this study we developed a conceptual model of contrasting winter cycling of As under different winter streamflow scenarios, which

points to the coupling of seasonality and hydrological connectivity on the biogeochemical cycling of As (and other redox sensitive elements) (Figure 5.9).

Increased winter streamflow has been one of the clearest hydrological shifts observed across the circumpolar north in association with recent warming (Spence et al., 2015, 2014; Walvoord and Striegl, 2007). Spence et al. (2011) highlighted a substantial increase in winter streamflow in the Baker Creek watershed after 1997 due to increased fall precipitation arriving as rain, rather than snow, which raised water levels, supporting winter streamflow generation. Using the historical streamflow record for the outlet of Lower Martin Lake and assuming water column anoxia developed when there was no winter flow at the lake outlet, we estimate that winter water column anoxia has become less frequent since 1997 in association with increased winter streamflow (64% anoxia between 1983 and 1996 vs. 27% anoxia between 1997 and 2018) (Appendix C: Figure C5). Future research using a mass balance approach will provide insights into the implications of less frequent winter anoxia on the long-term transport and storage of As in contaminated subarctic watersheds.

Chapter 6: Terrestrial and aquatic fluxes of arsenic in a subarctic landscape during years with contrasting hydrological conditions

Abstract

Climate change is altering the timing and magnitude of hydrological processes across northern landscapes. This will influence the transport and fate of pollutants, such as arsenic (As), in areas impacted by legacy mining pollution. A holistic understanding of the chemical recovery of lakes from As pollution requires consideration of within-lake biogeochemical cycling of As and processes occurring in the surrounding catchment. This study used a watershed mass balance approach to assess seasonal and interannual fluxes of As in a subarctic watershed impacted by more than 60 years of atmospheric mining emissions, spanning a transition from drought conditions to high streamflow between September 2017 and September 2019. We complemented sediment flux estimates from the mass balance approach with experimental incubations of lake sediments under field conditions and diffusive flux modelling of sediment porewaters to explore seasonal As dynamics at the sediment-water interface under changing redox and temperature conditions. Total annual fluxes of As were dominated by transport of As at the lake inlet and outlet. There was a net loss of As from the lake in both years, suggesting the gradual recovery of the lake more than 20 years after atmospheric As emissions ended in the region. Inlet concentrations of As were consistently lower than outlet concentrations highlighting that As contributions from the local catchment and lake sediments continue to influence lake water quality. Results from the mass balance showed that lake sediments continue to supply As to overlying waters on an annual basis, but seasonal differences in the magnitude and direction of this flux had important implications for the mass budget. Field incubations of lake sediment under different oxygen and temperature conditions corroborated seasonal patterns of sediment As flux and flux estimates were within an order of magnitude between the field incubations and the mass balance

calculations. High concentrations of As ($71 - 218 \text{ ug L}^{-1}$) were measured in snowmelt runoff from the local catchment in both years, and through runoff generation in the wet summer of 2018. Catchment runoff was an important source of As to the lake and corresponded with 280 and $82 \text{ g As ha}^{-1} \text{ yr}^{-1}$ for 2017-18 and 2018-19, respectively. Evaluation of an 11-year record of streamflow at the outlet of the lake revealed important interactions between climate and the chemical recovery of lakes from As pollution. Shorter lake water retention time, associated with high streamflow, facilitated the downstream transport of As, whereas longer lake water residence time delayed recovery and yielded higher within lake concentrations of As due to increased influence of internal loading of As from contaminated sediments. Results from this study show that the trajectory of recovery for As impacted lakes is fundamentally controlled by climate interactions with hydrology, catchment transport, and within lake biogeochemical processes.

6.1 Introduction

The chemical recovery of lakes impacted by mining pollution is influenced by processes happening across scales from within the lake itself (e.g. sediment-water interactions), to the local catchment (e.g. hillslope transport), and in the entire watershed (e.g. connectivity of stream networks). These processes vary in spatial scale but are all fundamentally influenced by climate. The alteration of hydrological processes by climate change has led to widespread changes in the magnitude and timing of streamflow across the circumpolar north (McClelland et al., 2006; Spence et al., 2015; Walvoord and Striegl, 2007). An increase in winter streamflow has been one of the most common observations associated with climate change and has been attributed to increased subsurface flow paths due to permafrost thaw (Jacques and Sauchyn, 2009) and changes in timing, magnitude and phase of precipitation patterns (Spence et al., 2011). As a consequence, there has been increased interest in exploring how changing hydrological conditions will influence streamwater chemistry (Holmes et al., 2012; Spence et al., 2015; Tank et al., 2016). Much of this work has focused on how changing flows paths and streamflow alter nutrient and carbon loading in large rivers. Despite this growing body of literature, there has been limited recognition of how changing hydrology may impact the chemical recovery of mining impacted lakes, which can be numerous in areas near mining operations and are often near urban centres, thus are valued recreational and subsistence areas.

Arsenic (As) is a contaminant of global concern because of its toxicity and carcinogenic effects at low concentrations (Smedley and Kinniburgh, 2002; Wang and Mulligan, 2006). Arsenic contamination of soils and waterbodies can be associated with legacy gold mining operations, since gold is often hosted in As-bearing sulfide mineral deposits. For redox sensitive contaminants, such as arsenic (As), the chemical recovery of lake waters can be confounded by

within lake processing and internal loading from contaminated lake sediments. To date, studies on As mobility in the environment have typically focused on specific terrestrial and aquatic compartments. For example, the mobility of As within lake sediments and across the lake sediment-lake water interface has been a focus of much interest (Couture et al., 2010; Martin and Pedersen, 2002; Schuh et al., 2018). There has also been substantial work dedicated to understanding the solubility of As minerals in soils and export from terrestrial catchments (Drahota et al., 2006; Drahota and Pertold, 2005; Huang and Matzner, 2007; Novak et al., 2011). There have been limited investigations that integrate As fluxes across entire watersheds and these types of studies are needed to develop a landscape scale understanding of lake recovery, particularly under changing climate conditions.

The Yellowknife region is an opportune area to study watershed fluxes of As since the area was impacted by 50 years of atmospheric mining emissions associated with gold mine production and large stores of As persist in soils and lakes. Two historical gold mines operated in the region and ore roasting at the mines were responsible for the release of more than 20,000 tonnes of As-bearing emissions to the atmosphere between 1949 and 1999. Most of the As in stack emissions (>86%) were released during the early years (1949-1958) of operations at Giant Mine, prior to implementation of environmental and operational controls (Bromstad et al., 2017; Hocking et al., 1978; Jamieson, 2014). Atmospheric As emissions released over the life of Con Mine were lower (2500 tonnes between 1948 and 1970) due to changes in ore processing techniques. A detailed summary of mining operations at Giant Mine is provided by Jamieson (2014). Previous studies have focused on the extent of As contamination in soils and lakes in the region (Cheney et al., 2020; Hocking et al., 1978; Houben et al., 2016; Hutchinson et al., 1982; Jasiak et al., 2021; Palmer et al., 2021, 2015), the mobility of As in aquatic environments (Andrade et al., 2010; Leclerc et

al., 2021; Palmer et al., 2020a; Schuh et al., 2018), and biological impacts and recovery in aquatic environments (Dushenko et al., 1995; Sivarajah et al., 2020, 2019; Thienpont et al., 2016).

In this study we used a watershed mass balance approach to explore the magnitude and partitioning of As fluxes in two consecutive years with contrasting hydrological conditions. There has been increased acknowledgement of the importance of winter and spring biogeochemical processes on carbon and arsenic cycling in northern environments (Denfeld et al., 2018; Palmer et al., 2020), and this study integrates detailed measurements during these important periods. The specific objectives of this study were: 1) to measure the dominant terrestrial and aquatic As fluxes for two consecutive years; 2) to compare and contrast the magnitude and timing of these fluxes under different hydrological conditions; and 3) to explore long-term patterns in As export from the watershed to elucidate how changing hydrological conditions may influence the recovery of As impacted watersheds. Here, we present the first study to date that integrates a watershed approach to measuring fluxes across the contaminated landscape. The results from this study will help to inform resource management decisions in the region that require an understanding of how climate change may alter recovery processes in the region, but are also broadly applicable to understanding the recovery of other As impacted landscapes.

6.2 Materials and Methods

6.2.1 Site description

Lower Martin Lake is a small (1.2 km²) and shallow (mean depth 2.0 m; max depth 4.5 m) lake located approximately 3 km from historical gold ore roasting operations at Giant Mine. Lower Martin Lake is the final lake in the Baker Creek watershed (121 km²) prior to Baker Creek passing through the Giant Mine site and entering Yellowknife Bay of Great Slave Lake (Figure 6.1). As such, the lake plays an important role in controlling the delivery of water and legacy mining

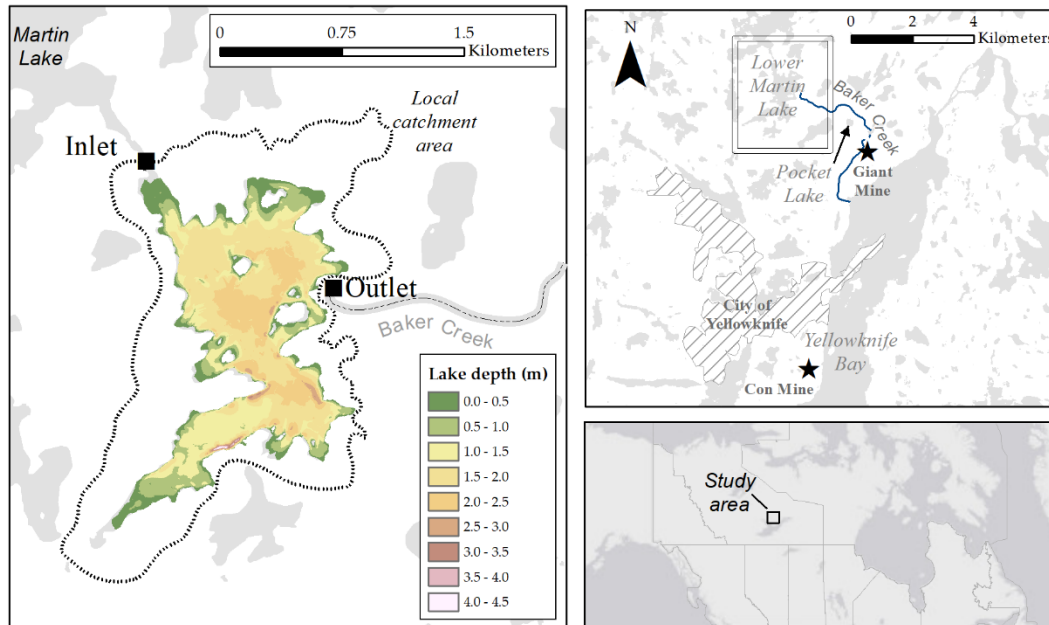


Figure 6.1: Maps of the study area. The left panel includes bathymetric data for Lower Martin Lake, the perimeter of the local catchment area, and the location of the lake inlet and outlet. The top right panel shows the location of Lower Martin Lake in relation to Yellowknife, Pocket Lake, Great Slave Lake, and the historical mine roasters at Giant and Con mines.

pollutants to Great Slave Lake. Inflow is primarily via a wetland at the north end of the lake that connects Martin Lake to Lower Martin Lake (Figure 6.1). The outlet is through a narrow rocky channel on the east side of the lake and Water Survey of Canada has been recording streamflow and water level at this location since 1983 and 2002, respectively (Station ID: 07SB013).

Surface runoff from the local catchment is predominately delivered during the snowmelt period and is typically low during summer and fall due to the high storage capacity of soils in the region and low rainfall (Spence, 2006; Spence et al., 2009). Streamflow is intermittent in the Baker Creek basin and driven by the “fill-and-spill” nature of hydrological processes in the subarctic shield, where small post-freshet runoff events are often attenuated along the lake chain through losses to lake storage and evaporation (Spence, 2006; Spence et al., 2014).

6.2.2 Field methods

6.2.2.1 Lake and stream water measurements

Water column samples were collected approximately biweekly at two locations (approximately 2 m depth) in Lower Martin Lake (LMLA and LMLB) during the study period (September 2017 to October 2019) to evaluate seasonal As dynamics. Detailed methodological information is outlined in Palmer et al. (2020). Briefly, water samples were collected through the water column (0.5, 1.3, 1.8, 1.95 m below the surface) using a peristaltic pump and TeflonTM lines that were pre-washed with 5% HCl solution and rinsed with ultrapure water. Samples were filtered inline with a high capacity groundwater filter (VersaporTM membrane; maximum poresize of 0.45 μm). Several unfiltered samples were collected to assess the proportion of As in particulate ($> 0.45 \mu\text{m}$) and dissolved ($< 0.45 \mu\text{m}$) fractions in the water column. Results from Palmer et al. (2020) showed that As was predominately present in the dissolved fraction except during the spring snowmelt period and at the base of the water column in winter 2019 due to suspected As adsorption to Fe-oxyhydroxides precipitating in the water column. The mass balance approach in this study required total unfiltered concentrations of As for the various watershed fluxes, so it was assumed that filtered As represented total unfiltered As when no total As data was available.

Water samples at the lake inlet and outlet were collected approximately bi-weekly to assess changes in streamwater chemistry through the study period. Filtered and unfiltered samples were collected for metal(loid) analysis in trace metal free vials and preserved with nitric acid (HNO_3) (1% v/v). Filtered samples were passed through a 0.45 μm syringe tip filter immediately after collection in the field.

6.2.2.2 Catchment runoff

The Pocket Lake subcatchment has been the focus of hydrological investigations of Taiga shield terrain since the 1970s (Landals and Gill, 1972; Spence and Woo, 2006). We reinstrumented the outlet of the Pocket Lake subcatchment with a V-notch weir and water level logger (HOBO U20-001-01; Onset Computer Corporation, Massachusetts) in a screened groundwater well strapped to the upslope side of the weir. Water level was recorded every 15 minutes with a precision and resolution of ± 0.5 cm and ± 0.21 cm, respectively. Discharge at the catchment outlet weir was calculated using a standard v-notch equation calibrated with spot measurements throughout the runoff period.

Daily surface runoff samples were collected whenever runoff was present, which was typically during snowmelt and high rainfall events in summer 2018. Filtered and unfiltered samples were collected above the weir in trace metal free vials. Samples for the dissolved fraction of metal(loid)s were filtered on site through 0.45 μm syringe tip filters.

Soil As concentrations in the Pocket Lake subcatchment were expected to be substantially higher than in the local catchment for Lower Martin Lake since Pocket Lake is approximately 2 km closer to the historical roaster at Giant Mine and a strong relationship between soil As and distance to Giant Mine is present in the region (Bromstad et al., 2017; Jamieson et al., 2017; Palmer et al., 2021). Bromstad et al. (2017) report soil As concentrations > 2000 mg kg^{-1} As in the drainage basin for Pocket Lake. To compensate for the influence of the difference in location we collected surface runoff samples from the local catchment of Lower Martin Lake in spring 2018 and 2019 ($n = 14$) and prorated the longer surface runoff chemistry record at Pocket Lake ($N = 28$) from the runoff chemistry relationship between the two locations for use in the mass balance estimation of watershed fluxes. Runoff As at Lower Martin Lake was $2.7 (\pm 0.7 \text{ stdev})$ times lower

than at Pocket Lake and this factor was used for pro-rating runoff chemistry at Lower Martin Lake (see Appendix D: Figure D3 for details).

6.2.2.3 Sediment fluxes

Contaminated lake sediments are an important source of remobilized As to overlying waters in the region (Andrade et al., 2010; Palmer et al., 2019; Schuh et al., 2018). The flux of As between sediments and overlying water varies seasonally since alterations to temperature and redox conditions can influence As flux (Arsic et al., 2018; Bennett et al., 2012; Palmer et al., 2020, 2019). To explore the relative contribution of sediment As fluxes within the watershed As mass balance and to quantify the seasonality of these fluxes we used both direct measurements of sediment As flux, via a series of sediment microcosm incubations, and theoretical estimates of sediment flux using sediment porewater chemistry and Fick's first law of diffusion.

6.2.2.3.1 Mesocosm experiments

Field incubations of sediment were conducted under three scenarios representing the seasonality of conditions in the overlying water column of Lower Martin Lake, including steady-state oxic conditions (representing open-water conditions), the transition from anoxic to oxic conditions (representing reoxygenation of the water column after winter anoxia), and the transition from oxic to anoxic conditions (representing the development of anoxia in bottom waters during winter).

Sediment cores for field incubations were collected using an 8.8 cm diameter Uwitec gravity corer. All core collection targeted approximately 40 cm of sediment and 20 cm (1.2L) of overlying water. After collection, cores were sealed and incubated on the lake bottom under field

conditions of light and temperature in a modified “sediment core lander” for a series of treatments (Orihel and Rooney, 2012). Dissolved oxygen levels were measured in the overlying water of all cores on dates when water was extracted using a PreSens Microx 4TM fiber optic oxygen meter attached to PSt7 sensors (PreSens Precision Sensing GmbH, Regensburg, Germany). Overlying water in the core treatments were extracted for chemical analysis through Rhizon CSS samplers (Rhizosphere Research Products, Wageningen, Netherlands; 5-cm porous section and 0.15 μm mean pore size) using 12 mL acid washed syringes. All Rhizons were pre-washed with 30 mL of 1% HCl solution and 30 mL of ultrapure water.

Cores were collected in September 2017 (N = 4; mean sediment temperature 10.2°C) and July 2018 (N = 4; mean sediment temperature 19.4°C) to represent well-oxygenated open water conditions under different temperature treatments. Dissolved oxygen levels in overlying water were maintained > 30 % O₂ saturation through the experiment by removing the caps during sampling of overlying water. Overlying water in the cores were sampled on days 0, 1, 3, 6, and 8 of the experiments.

To explore As fluxes through the transition from anoxic-oxic-anoxic conditions that is often observed under ice during winter in shallow lakes in the region, sediment cores were collected in March 2018 (N = 2; mean sediment temperature 3.0°C) and oxygen levels in the overlying water were manipulated over a 21 day treatment. Overlying waters in cores were naturally depleted of dissolved oxygen (< 0.5 mg L⁻¹) upon collection. The cores were reoxygenated on Day 0 of the experiment by removing caps and allowing interaction with the atmosphere. Dissolved oxygen levels remained > 30% from Day 0 to Day 14 of the experiment. On Day 14 the caps were sealed and high purity nitrogen (N₂) gas was bubbled gently into the water overlying sediment with care not to disturb sediments. Once dissolved oxygen levels were

depleted to $< 0.5 \text{ mg L}^{-1}$ the cores were sealed and incubated on the lake bottom. Overlying water was sampled on Day 14, 17, and 20 via Rhizon samplers inserted in pre-drilled sampling ports. Overlying water was bubbled with high-purity N_2 gas through the sampling ports after each sample collection to preserve anoxic conditions in the overlying water of the cores.

6.2.2.3.2 Sediment porewater analysis and Fick's First Law of Diffusion

Sediment porewater As concentrations from the open-water season were used to explore diffusive fluxes of As between sediments and overlying water. The sediment porewater data used in this study were previously reported in Palmer et al. (2020). Briefly, sediment porewaters were extracted from sediment cores using Rhizon CSS samplers inserted through pre-drilled ports in the core tubes following methods outlined in the literature (Seeberg-Elverfeldt et al., 2005; Shotbolt, 2010). Rhizons were pre-washed with 30 mL of 1% HCl and rinsed with 30 mL ultrapure water. Porewater samples were extracted at 1 cm intervals (starting 1 cm above the sediment-water interface) using 12 mL syringes under vacuum pressure.

6.2.3 Lake water, stream water, catchment runoff and sediment porewaters analysis

All water samples collected in this study (lake water, stream water, catchment runoff, sediment porewater, microcosm water) were preserved with nitric acid (HNO_3) to 1% (v.v) and stored below 4°C prior to analysis by inductively coupled plasma - mass spectrometry (ICP-MS) for a suite of 22 metal(loid)s, including As, at an accredited government laboratory (Taiga Environmental Lab, Yellowknife, NT).

6.2.4 Lower Martin Lake water budget

A daily water budget for Lower Martin Lake was developed for the study period (September 1, 2017 to November 1, 2019) to support the As mass balance calculations. All main

hydrological inputs and outputs to the lake were measured in the field, except for lake inflow, since the wetland was difficult to instrument for streamflow measurements (Q_{IN}), therefore we solved the following for Q_{IN} :

$$\Delta S = Q_{IN} + Q_{RO} + P - E - Q_{OUT} \quad (\text{Equation 6.1})$$

Where ΔS is daily change in whole lake storage, Q_{RO} is daily runoff from the local catchment, P is daily precipitation to the lake surface, E is daily evaporation from the lake surface, and Q_{OUT} is daily discharge through the lake outlet.

We quantified ΔS (m^3) using an initial lake volume estimate from a bathymetric survey conducted in September 2017 (Palmer et al., 2019) and daily stage measurements from Water Survey of Canada (Station ID: 07SB013) (ECCC, 2020). Initial lake volume was generated using the bathymetry raster files and the surface volume tool in the 3D analyst extension in ArcMap (v.10.4). Daily changes in lake volume represented daily changes in water level. Calculated differences in lake volume assumed no change in surface area of the lake, so differences in lake volume were calculated as lake area (1.21 km^2) multiplied by the change in stage (m). The volume of water associated with ice cover was removed from the winter lake volume estimate because lake ice development effectively excludes solutes such as As (Palmer et al., 2019; Pieters and Lawrence, 2009). The volume of water associated with the ice cover was estimated using ice thickness measured during each sampling period and was adjusted by 9.05% to accommodate the increase in lake ice volume due to phase change. Ice thickness measurements between sampling dates were estimated via cubic spline interpolation (Figure D7).

Daily runoff from the local catchment of Lower Martin Lake (Q_{RO}) (m^3) was estimated by scaling daily discharge for the contributing area for the Pocket Lake outlet weir ($51\,728 \text{ m}^2$) to the local catchment of Lower Martin Lake ($1\,978\,404 \text{ m}^2$) (Figure 6.1). Contributing areas for the

outlet of the Pocket Lake subcatchment and the outlet of Lower Martin Lake were calculated using the *Upslope Area* tool in SAGA (v7.9.1) applied on a LIDAR-derived 1 m resolution DEM.

The precipitation (P) (mm day^{-1}) term included contributions from rainfall and snowmelt directly to the lake surface. Rainfall (mm day^{-1}) was measured using a Texas Instrument TE525M tipping bucket at a meteorological tower at Landing Lake, approximately 5 km north of Lower Martin Lake. The snowmelt contribution represents the mean snow water equivalent (SWE) (mm) of the snow pack measured across the lake at the end of winter in 2018 and 2019. A minimum of 10 snow depth and 3 snow density measurements were used to calculate SWE. Mean end of winter SWE was added to the water budget over a 10-day period starting on the day that catchment runoff was first observed at Pocket Lake. This approach likely overestimates the amount of water entering the lake via direct snowmelt since sublimation of the snowpack is ignored.

Evaporation from the lake surface (E) (mm day^{-1}) was estimated using an eddy covariance system at Landing Lake. Climate conditions were assumed to be comparable at Landing Lake and Lower Martin Lake because the lakes are relatively close to each other (approximately 5 km) and have similar surface area and depth, thus water temperatures, air temperatures, and wind speeds are expected to be similar.

Daily streamflow at the outlet of Lower Martin Lake outlet (Q_{OUT}) (m^3) was obtained through the Water Survey of Canada hydrometric gauge (Station ID 07SB013).

6.2.5 Data analysis

6.2.5.1 Mass balance estimation

The daily water balance components for Lower Martin Lake were integrated with measured and interpolated daily concentrations of As for the various flux terms to create a daily As mass balance for Lower Martin Lake, following:

$$\Delta S (As_L) = Q_{IN} (As_{IN}) + Q_{RO} (As_{RO}) - Q_{OUT} (As_{OUT}) + As_{IP} \quad (\text{Equation 6.2})$$

The precipitation and evaporation terms were not included because concentrations of As in snowpack and rainfall were all below analytical detection limits (see supporting information Table S1). We quantified whole lake As storage by integrating the depth-weighted mean concentration of As from the two sampling locations (As_L) with lake volume on each sampling day. A record of daily mean lake water As concentration was generated for the entire study period via cubic spline interpolation between sampling dates. A daily record of inputs and exports of As to/from Lower Martin Lake were determined by integrating daily streamflow and catchment runoff measurements with concentrations of As measured in those compartments. Daily As concentrations were estimated in streamflow and runoff components using cubic spline interpolation for gaps between sampling dates. Internal processing of As (As_{IP}) included both sediment efflux and sedimentation processes and was estimated as the residual of equation 2.

6.2.5.2 Calculation of sediment As fluxes from field incubations and sediment porewater gradients

In addition to estimating internal processing of As at the lake scale using the residual of the mass balance in Equation 6.2, we used sediment mesocosms and porewater gradients to further explore seasonal As dynamics at the sediment-water interface and to validate the residual term estimates.

Sediment As fluxes in the mesocosm experiments were estimated by fitting a least squares regression line to the cumulative change in As concentration of overlying water during each core treatment (Lavery et al., 2001). The slope of the relationship divided by the surface area of sediment in the core was taken as the As flux ($\mu\text{g m}^{-2} \text{day}^{-1}$).

Sediment porewater concentrations of As were used to estimate the flux of As across the sediment-water boundary (F_{As}) following Fick's First Law of Diffusion:

$$F_{As} = -\phi D_{As} \frac{\Delta C_{As}}{\Delta z} \quad (\text{Equation 6.3})$$

Where ϕ is sediment porosity, D_{As} is the temperature-corrected diffusion coefficient for arsenite (AsIII), ΔC_{As} is the linear As concentration gradient between the porewater maxima and overlying water, and Δz is the vertical distance between the porewater maxima and overlying water. Details on specific parameters used in the diffusive flux modelling are included in Table 6.3.

6.3 Results

6.3.1 Rainfall and streamflow generation

Streamflow at the inlet and outlet of Lower Martin Lake was non-existent during the first 9 months of this study (September 2017 to May 2018) (Figure 6.2a), and the lake was hydrologically disconnected from the upper and lower portions of the watershed. Higher than normal (climate normal 1981-2010) rainfall in June (114 mm) and July 2018 (86 mm) (Figure D1) raised lake water levels and resulted in streamflow generation throughout the Baker Creek watershed, including at the lake inlet and outlet (Figure 6.2a). Peak streamflow at the lake outlet in 2018 was higher than the 39-year mean and was observed in July, delayed from typical peak flow that occurs in association with snowmelt in late May (Figure 6.2a). Streamflow at the lake inlet and outlet receded in late summer 2018, but sustained winter baseflow above the 39-year mean persisted at the inlet and outlet during the second winter of the study (2018-19), maintaining hydrologic connectivity over winter. The timing of peak flow in June and July 2019 was more representative of mean streamflow conditions at the outlet and receded in late summer-fall 2019.

6.3.2 Stream chemistry and arsenic loading via lake inlet and outlet

Substantial variation in stream water As was observed over the period of study at the lake inlet and outlet, with As concentrations varying 7-fold and 3-fold at the inlet and outlet, respectively. Arsenic concentrations were consistently higher from May 2018 to January 2019 at the lake outlet compared to the lake inlet, but noticeably started to converge through winter and summer 2019 (Figure 6.2a). Highest As concentrations were measured at the lake inlet ($88 \mu\text{g L}^{-1}$) and outlet ($69 \mu\text{g L}^{-1}$) in spring 2018 in association with streamflow generation after a sustained period with no flow. Arsenic concentrations subsequently decreased at both locations with an increase in streamflow. There was also a noticeable increase in As concentration at the outflow between June and August 2018 and in June at the lake inlet. As concentrations decreased at both locations after summer 2018, except for a small rise in inlet and outlet As during early winter 2018-2019.

Differences in As concentration over the two contrasting streamflow years yielded differences in As loading into and out of Lower Martin Lake. Substantially more water was discharged from Lower Martin Lake in 2018-19 than 2017-18 (38% increase), but there was only an 8% increase in total As export (240 vs 260 kg), because of higher outlet As concentrations in the first year of the study (Figure 6.2c). Similarly at the lake inflow, 38% more water entered the lake in 2018-19 than 2017-18 but only 18% more As.

6.3.3 As inputs from terrestrial catchments

Snowmelt runoff was associated with high concentrations of As at the Pocket Lake subcatchment in both study years (Figure 6.3a and 6.3b) with concentrations exceeding $500 \mu\text{g L}^{-1}$ during peak snowmelt. High As concentrations in snowmelt runoff were due to interactions with soils, because As concentrations in the snowpack were below analytical detection limits (Table D1). Clear

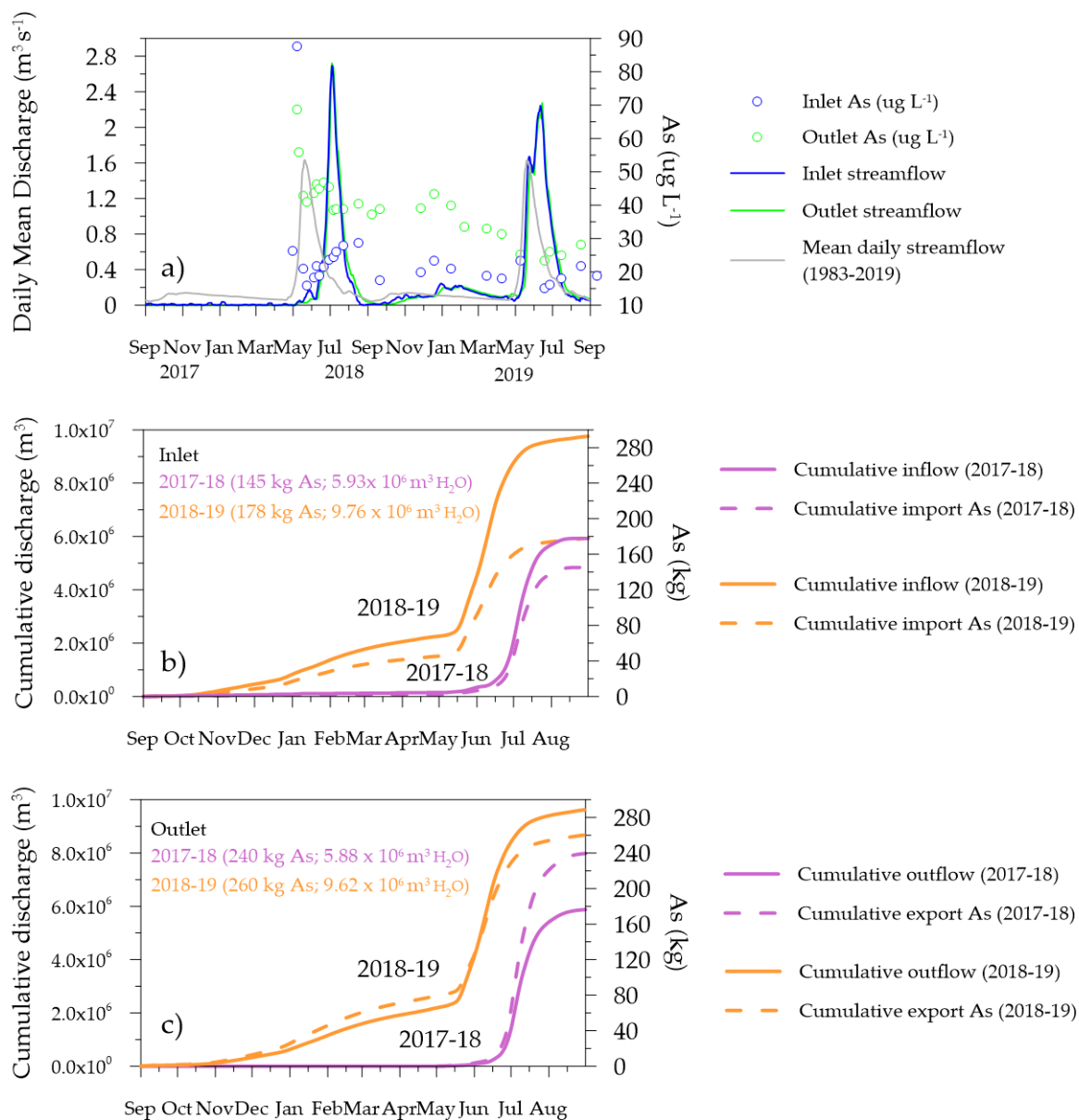


Figure 6.2: A) Mean daily streamflow and approximately bi-weekly measurements of total As in surface waters at the inlet and outlet of Lower Martin Lake, September 2017 to September 2019; B) annual cumulative inflow and As mass at the inlet of Lower Martin Lake for September 2017-18 and September 2018-19; annual cumulative discharge and As mass at the outflow of Lower Martin Lake, September 2017-18 and September 2018-19.

seasonal trends emerged between the two snowmelt years, as As concentrations were highest close to the initiation of the main snowmelt period and declined as snowmelt progressed in both years.

High rainfall in 2018 resulted in the generation of surface runoff in mid-summer. During the mid-

summer 2018 runoff period, As concentrations were lowest in early June, but increased to concentrations comparable with snowmelt runoff in late summer in association with sustained discharge at the outlet of the Pocket Lake subcatchment. The wet summer of 2018 yielded a basin discharge 3-fold larger than in 2019 and differences in As loading from the catchment reflected these differences in discharge, with 2.5 kg As ($483 \text{ g ha}^{-1} \text{ yr}^{-1}$) export in 2018 compared to 0.75 kg ($144 \text{ g ha}^{-1} \text{ yr}^{-1}$) export in 2019. Scaling As export from the Pocket Lake subcatchment to the full

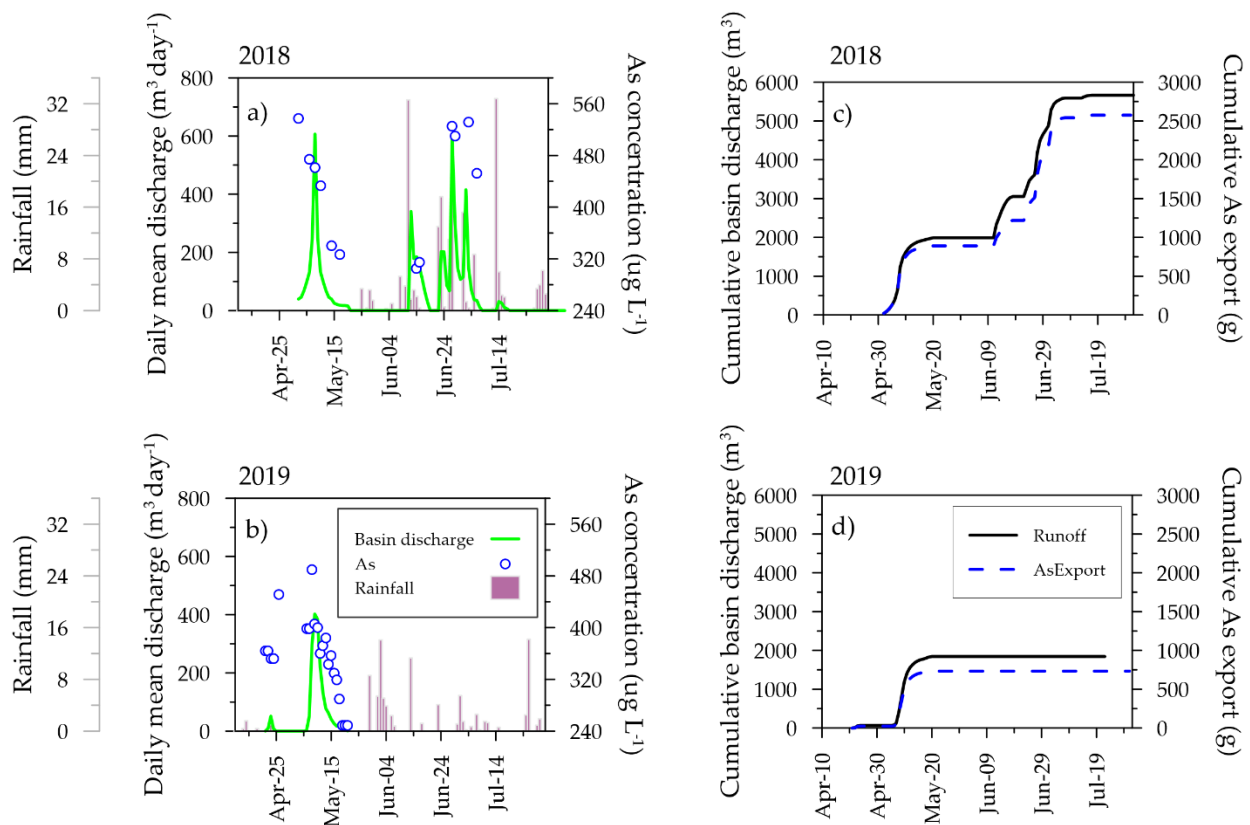


Figure 6.3: The hydrology and runoff chemistry from the Pocket Lake subcatchment. Panels a) and b) represent basin discharge, rainfall, and runoff As concentrations for 2018 and 2019, respectively. Panels c) and d) represent the cumulative basin discharge and cumulative As export from the subcatchment in the same years.

local catchment of Lower Martin Lake, using the prorated concentrations from section 6.2.2.2, yielded a basin discharge of 55.3 kg As ($280 \text{ g ha}^{-1} \text{ yr}^{-1}$) in 2018 and 16.3 kg As ($82 \text{ g ha}^{-1} \text{ yr}^{-1}$) in 2019.

6.3.4 Changes in lake storage

Lake volume varied approximately 5% during the study period, and clear increases in lake volume were noted during spring and summer, associated with increased runoff generation from the catchment and streamflow in the upper watershed (Figure 6.4). In contrast, lake water mass of As varied more than 600% over the period of study (Figure 6.4). The mass of As in the lake increased substantially through winter 2017-18, associated with a period of full water column anoxia that persisted from February to late-April, as the lake was hydrologically disconnected from the surrounding watershed (Palmer et al., 2020). Peak As storage (233 kg As) was reached in April 2018 after anoxia persisted through the water column for more than 3 months. Conversely, the water column remained oxygenated throughout winter 2018-19 and no substantial increase in lake storage of As was observed (Figure 6.4). A decline in the mass of As in the water column was observed during spring (April-May) in both study years. The decline was more pronounced in May 2018, as the water column transitioned from anoxic-oxic conditions. During the six-week period between April 5 and May 17, 2018, 163 kg As was removed from the water column, with most of the decline (100 kg As) occurring before the onset of snowmelt in the catchment on May 2, 2018 and the increase in streamflow at the lake inlet (Figures. 6.2a & 6.4). In contrast, during the same six-week period in 2019, 21 kg As was removed from the water column and all of this occurred prior to the onset of the main snowmelt period on May 6, 2019. Throughout the study, storage of As in Lower Martin Lake was closely associated with As concentrations in the water

column, rather than the volume of water in the lake, as demonstrated by the minimal change in lake mass of As during peak flows in spring and summer (Figures. 6.2a & 6.4). Over the entire study period, the mass of As declined almost two-fold between September 2017 (84 kg As) and September 2019 (43 kg As).

6.3.5 Sediment As fluxes

Clear seasonal patterns in the flux of As between lake sediments and overlying waters were observed through the study period (Figure 6.5; Table 6.1). Lake sediments were a substantial source of As to overlying waters during summer in both study years, adding 59 kg As ($507 \mu\text{g m}^{-2} \text{ day}^{-1}$) and 62 kg As ($532 \mu\text{g m}^{-2} \text{ day}^{-1}$) to the water column between June and September, in 2018 and 2019, respectively (Table 6.1). Lake sediments were also a source of As to the water

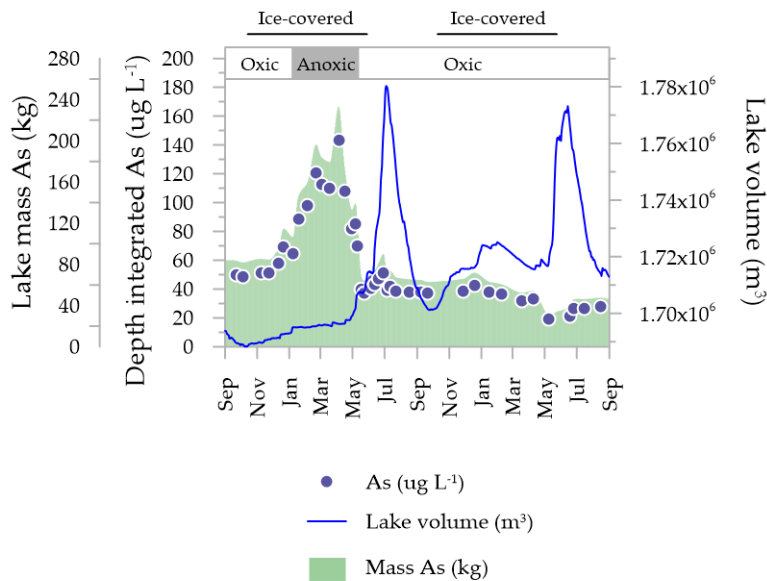


Figure 6.4: Lake volume (m^3), depth-integrated lake water As concentration ($\mu\text{g L}^{-1}$) and the mass of As (kg) stored in the water column of Lower Martin Lake September 2017 to September 2019. Periods of ice-cover and full water column anoxia ($<0.5 \text{ mg/L O}_2$) are indicated across the top of the figure.

column during winter in both years, but the contribution was much higher during winter 2017-18 (145 kg As; 747 $\mu\text{g m}^{-2} \text{day}^{-1}$) than winter 2018-19 (20 kg As; 103 $\mu\text{g m}^{-2} \text{day}^{-1}$) in association with full water column anoxia. The spring interval between April and June represented a period of As removal from the water column, and in both years the mass of As removed from the water column exceeded the mass of As associated with sediment efflux during winter (Table 6.1). Arsenic fluxes between the sediments and overlying water were lowest during fall and suggested minimal efflux of As from sediments during this period.

We explored the mechanisms controlling sediment-water As interactions through the manipulation of dissolved oxygen conditions in the overlying water of sediment mesocosms incubated on the lake bottom under representative field conditions (light and temperature). The various mesocosm treatments yielded results consistent with the time series fluxes derived from

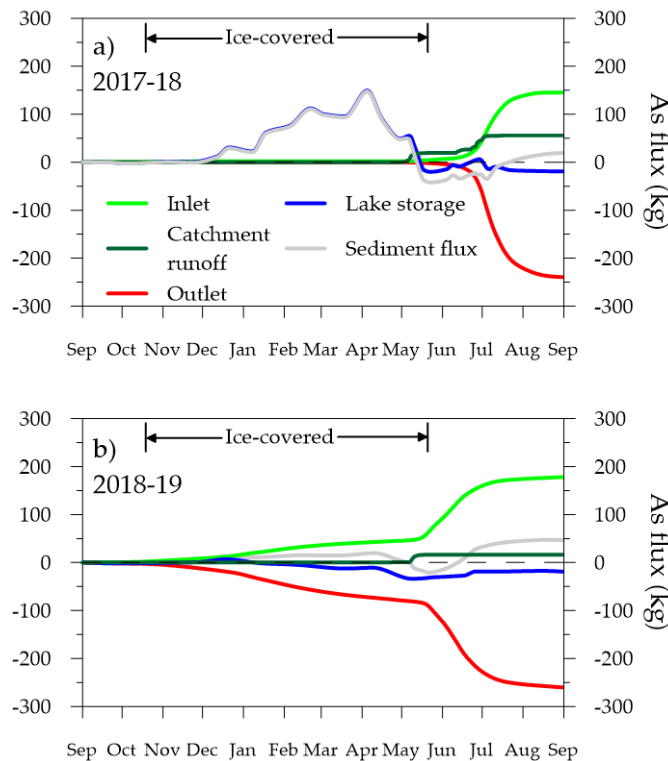


Figure 6.5: Cumulative mass fluxes in Lower Martin Lake for the two consecutive study years.

the watershed As mass balance model (Tables 6.1 and 6.2). Under warm sediment conditions (~20 °C) and well-oxygenated water conditions, lake sediments were a source of As to overlying water and released approximately $290 \pm 288 \mu\text{g As m}^{-2} \text{ day}^{-1}$ (Table 6.2). In contrast, the mean flux of As was lower ($-21 \mu\text{g} \pm 124 \text{ As m}^{-2} \text{ day}^{-1}$) under cooler sediment conditions (~ 10°C) representing fall conditions and the direction of the flux was not consistent between cores. Sparging of O₂ from overlying water in the sediment mesocosms under winter conditions resulted in the release of As to overlying water with a measured mean flux of $595 \pm 123 \mu\text{g As m}^{-2} \text{ day}^{-1}$ (Table 6.2). The reoxygenation of the mesocosms removed As from the water column at a mean rate of $-643 \pm 145 \mu\text{g As m}^{-2} \text{ day}^{-1}$.

Table 6.1. Seasonal mass fluxes of As (kg) in the Lower Martin Lake watershed partitioned into the following seasons: fall (Sep. 1 – Oct. 31), winter (Nov. 1 – Mar. 31), spring (Apr. 1 – May 31), and summer (June 1 – Aug. 31). Annual values in parentheses refer to the percentage of individual annual fluxes of the total input or output of As in the watershed.

	<i>Inlet</i>		<i>Catchment</i>		<i>Outlet</i>		<i>Sediment flux</i>		<i>Lake storage</i>	
	2017-18	2018-19	2017-18	2018-19	2017-18	2018-19	2017-18	2018-19	2017-18	2018-19
<i>Sep-Nov</i>	0.8	3.6	0.0	0.0	0.0	-4.4	0.1	-0.3	0.9	-1.1
<i>Nov-Apr</i>	0.9	37.7	0.0	0.0	0.0	-66.5	136	18.3	137	-10.4
<i>April</i>	0.0	4.0	0.0	0.5	0.1	-7.9	-89.0	-13.9	-89.1	-17.3
<i>May</i>	4.8	44.4	19.3	15.8	-3.4	-41.6	-86.9	-19.8	-66.2	-1.2
<i>Jun-Sep</i>	139	88.4	36.5	0.0	-236	-140	58.8	62.5	-1.9	11.0
TOTAL	145 (66%)	178 (74%)	56 (25%)	16 (7%)	-240 (93%)	-260 (93%)	19.4 (9%)	46.8 (21%)	-19.1 (7%)	-19.0 (7%)

Table 6.2. Measured fluxes for select elements during experimental sediment incubations. Treatments include exposure to different temperature and redox conditions. See supplemental information for plots for each element during each treatment.

Treatment	Date	Treatment days	# cores	Temp °C	As $\mu\text{g/m}^2/\text{day}$
Oxic	Sep. 19 -27, 2017	8	4	10.2 +/- 1.2	-21 +/- 124
Oxic	July 18 - 26, 2018	8	2	19.4 +/- 1.1	290 +/- 288
Anoxic-oxic transition	Mar. 8 - 22, 2018	15	2	3.0 +/- 0.08	-643 +/- 145
Oxic-anoxic transition	Mar. 22 - 28, 2018	7	2	3.0 +/- 0.08	595 +/- 123

Estimates of sediment As fluxes using sediment porewater As measurements and Fick's Law also demonstrated that sediments were a source of As to overlying waters under oxygenated surface water conditions (Table 6.3). A weak positive relationship between As flux and sediment temperature was observed but was not statistically significant ($r^2 = 0.21$; $p = 0.04$; $N = 20$) (Figure D5). Modelling As fluxes with Fick's Law did not capture the lower flux rates that were measured under cooler sediment conditions in fall in the sediment incubations and observed in the time-series data. Further, we were unable to model winter fluxes under anoxic conditions using sediment porewater chemistry because the chemical gradient was inverted and fluxes were likely dominated by chemical processes (e.g. reductive dissolution and desorption) rather than diffusive processes.

Table 6.3. Theoretical sediment fluxes calculated using porewater As measurements and Fick's Law. As fluxes represent the mean flux \pm 1 standard deviation.

Date	# cores	Temp °C	Temp corrected D_{As} $cm^2 s^{-1}$	Porosity	As flux $\mu g/m^2/day$
September 2017	4	8.6	7.22	0.94	123 +/- 34
June 2018	2	14	8.53	0.94	154 +/- 124
August 2018	2	13	8.28	0.94	113 +/- 42
September 2018	4	5	6.42	0.94	86 +/- 61

6.3.6 Long-term patterns in As fluxes

The 11-year streamflow and water chemistry dataset collected at the outlet of Lower Martin Lake allowed for the exploration of longer-term patterns in As flux and concentration in the watershed. Lake water retention time and streamflow proved to have an important influence on both the concentration and flux of As leaving the lake (Figure 6.6b and 6.6c). Higher lake water retention times were associated with higher concentrations of As, suggesting that the influence of internal

loading of As from contaminated sediments on lake waters is enhanced in periods of low streamflow.

The significant positive relationship between As export and annual discharge demonstrates that As export at the lake outlet is primarily controlled by streamflow rather than concentration. Further, the 11-year record shows that the magnitude of As loading is largely dependent on whether

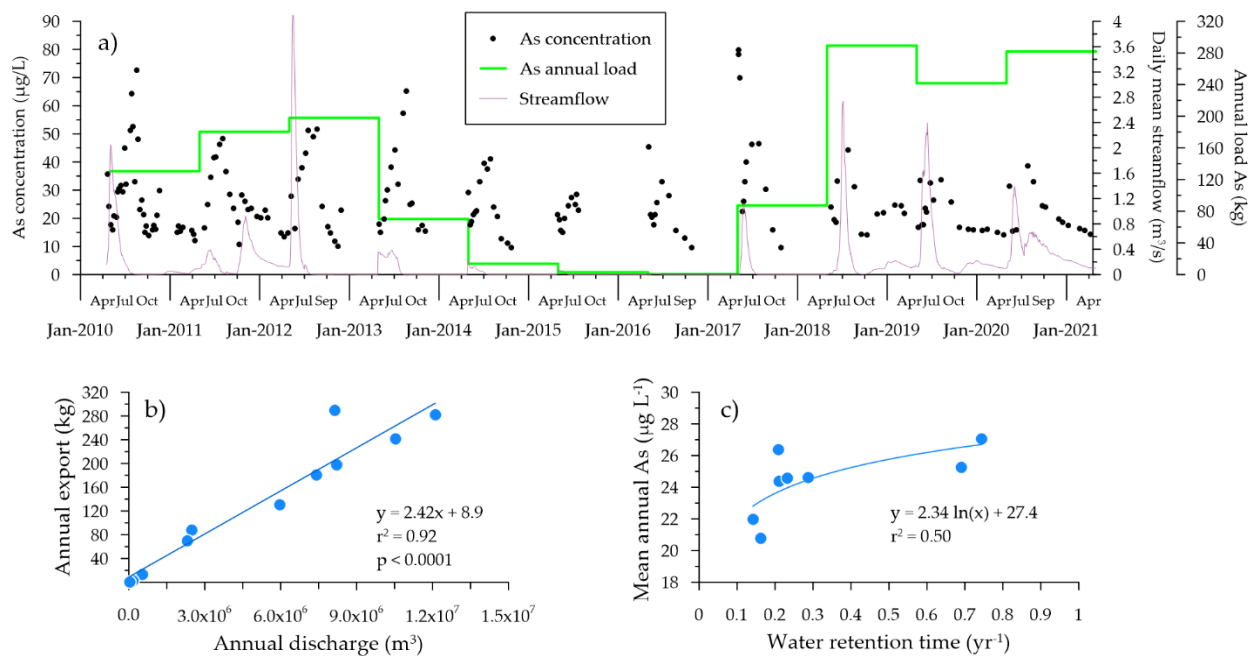


Figure 6.6: a) Hydrograph, As concentration, and annual As loading in Baker Creek, near the outlet of Lower Martin Lake, May 2010 to May 2021. Annual As loads were calculated from interpolated daily As concentration and daily mean streamflow measurements from May 1- April 30; b) Relationship between annual As export and total annual discharge in Baker Creek (near the outlet of Lower Martin Lake); and c) Relationship between mean annual As concentration in Baker Creek and WRT in Lower Martin Lake. Data in c) presented for WRT < 1 yr because assumed that for longer residence times the water at Baker Creek sampling location represented the contributing area below the outlet of Lower Martin Lake. Water retention time calculated as ratio of total annual discharge and mean lake volume.

there was substantial winter baseflow or not. Previous studies have highlighted a shift towards increased winter streamflow in the region and proposed that this will alter streamwater fluxes of nutrients and major ions (Spence et al., 2015). Here we show that this shift in winter hydrology will also influence the cycling and recovery of As impacted watersheds. Years where winter streamflow was present had higher annual As export than years without winter baseflow, irrespective of the size of the spring freshet peak. Two contrasting years, 2011-12 and 2012-13, provide a clear example of the importance of winter streamflow (Figure 6.6a). Spring freshet in 2011 was small relative to the other years during the study period, yet substantial winter streamflow led to annual As export that was comparable to the following year where most of annual stream discharge was associated with a large spring freshet. This shows that export is not only driven by spring freshet patterns, but also by changing winter hydrology, where little change in spring freshet but increased winter flow will lead to higher annual export of As.

These observations are in contrast to the behavior of other contaminants, such as mercury and organochlorines where water retention time has been shown to be inversely related to concentration (Diamond et al., 2005; Richardson et al., 2021; Semkin et al., 2005). Our data show that these concentration-retention time relationships are dependent on the biogeochemical behavior of the contaminant. Specifically, in the case of redox sensitive elements, such as As, longer lake water residence time can lead to greater internal loading of As from contaminated lake sediments, thus confounding the chemical recovery of lake waters.

6.4 Discussion

This study used a full watershed mass balance approach spanning two years of high frequency measurements to elucidate the relative importance of individual fluxes of As in the Lower Martin Lake watershed at annual and seasonal scales. We show that catchment runoff and internal

recycling are significant fluxes of As to the lake, but the relative importance of these fluxes on the watershed mass budget is mediated by changes in hydrology. In dry periods, sediment As fluxes dominate the mass budget, whereas, in wet years, the local catchment is activated and can deliver large amounts of terrestrially derived As to the lake.

6.4.1 Annual fluxes dominated by regional stream hydrology

The study period spanned two years representing distinct differences in regional hydrology. The study began at the end of an approximately 4-year drought period, characterized by low streamflow (primarily isolated to spring freshet) in Baker Creek, and covered the transition to high streamflow (including substantial winter streamflow) in the latter part of the study (Figure 6.2). Irrespective of differences in regional hydrology, the total amount of As entering and leaving Lower Martin Lake was dominated by transport at the lake inlet and lake outlet in both study years (Figure 6.5; Table 6.1). Annual As export exceeded input approximately 1.5-fold and there was a net loss of As from the water column in both study years, indicating that Lower Martin Lake acted as a conduit for As transport in the watershed and did not retain watershed As. Annual As export from Lower Martin Lake was comparable in the two years of the study, even though 61% more water left the lake in the second year of the study (Figure 6.2). Much of the difference in As export from the lake was attributed to higher concentration of As in the water column in the first year of the study (Figures 6.2 & 6.4). This higher As was likely derived from internal sediment loading that had built up in the lake during a low flow period where there had been little input from the upper watershed since 2014 and indicated the flushing of internally derived As following this period of low flow.

Previous studies in the region have inferred the continued loading of As to lakes from contaminated soils in the catchment through interpretation of lake sediment records (Jasiak et al., 2021; Schuh et al., 2019; Thienpont et al., 2016). Here we provide the first estimates of terrestrial contributions of As to lakes in the region and confirm the ongoing loading of As to lakes from contaminated soils more than 50 years after the bulk of mining emissions were released and 20 years after atmospheric mining emissions in the region ended. The terrestrial loading estimates from this study are considerably higher than estimates reported from other parts of the world. Specifically, terrestrial As loading during the wet summer of 2018 ($280 \text{ g As ha}^{-1} \text{ yr}^{-1}$) was 74 times higher than reported for a remote forested catchment impacted by atmospheric As emissions in the Czech Republic ($3.8 \text{ g As ha}^{-1} \text{ yr}^{-1}$) (Huang and Matzner, 2007) and 22 times higher during the drier summer of 2019, when catchment runoff was isolated to the spring melt period. The higher loading rates observed in this study are likely largely due to the higher concentrations of As in near-surface soils measured near Pocket Lake and Lower Martin Lake than in the study by Huang and Matzner (2007), but may also reflect differences in how As is hosted in the soils. Our data show that As is primarily being delivered through surface runoff in the dissolved fraction (Appendix D: Figure D3), suggesting that the dissolution of As hosting minerals in soils is an important mechanism in the ongoing delivery of As to local lakes, rather than via erosive processes and particulate associated transport. Arsenic trioxide is the predominant mineral host of As in surface soils close to Giant Mine (Bromstad et al., 2017; Palmer et al., 2021) and is expected to be soluble under conditions present during snowmelt and surface runoff generation. There is a steep gradient in As concentrations in soil profiles close to mining point sources in the region and soil As is typically highest in the top 5 cm of soils (Jamieson et al., 2017; Palmer et al., 2021). The observation that As concentrations in surface runoff were highest associated with the early phases

of snowmelt is consistent with runoff pathways being restricted to the uppermost soils in early spring when limited penetration of the thaw front has occurred. On an annual basis, loading from the local catchment represented a substantial source of As to Lower Martin Lake in wet years (2017-18: 25% of annual input), when high summer rainfall led to substantial catchment runoff in June and July (Table 6.1). Previous hydrological investigations in the Pocket Lake catchment have shown that catchment runoff is typically restricted to the snowmelt period due to the arid climate and high storage capacity of catchment soils in the region (Spence and Woo, 2003). Catchment runoff in 2018-19 was closer to typical conditions in the region, with catchment runoff associated with snowmelt predominately occurring over a two-week period in May (Figure 3). Under these typical conditions catchment loading of As represented a small portion of total As entering the lake over the year (7% of annual input) (Table 6.1).

In both study years, lake sediments were a net source of arsenic to the water column suggesting that contaminated stores of As in lake sediments continue to supply As to the water column for downstream transport or within-lake cycling. While the mass budget of winter 2017-18 was dominated by internal As loading from sediments, there was less sediment derived As exported from Lower Martin Lake in 2017-18 than the following year because winter sediment derived As was returned to sediments in spring 2018 before streamflow began at the lake outlet (Table 6.1). This shows the importance of increased winter streamflow in facilitating the flushing of internally derived As from Lower Martin Lake and flow through of water from the upper watershed.

6.4.2 Seasonality of watershed As fluxes

6.4.2.1 Autumn as a period of watershed quiescence?

Arsenic transport within the Lower Martin Lake watershed was relatively low during autumn in both study years, representing less than 2% of annual As fluxes (Table 6.1). The low transport of As across the watershed suggests a period of watershed transport quiescence in subarctic shield environments. Low internal loading of As from contaminated lake sediments estimated in the mass balance calculations were corroborated by the results from experimental sediment incubations. While sediment and lake water oxygen conditions were relatively similar between autumn and summer sampling, lower sediment As fluxes measured in the autumn incubations suggested a temperature influence on sediment-water As flux. No significant positive flux-temperature relationship was observed when pooling all the data from the diffusive flux calculations and sediment incubations (Figure D5). The lack of clarity around the influence of temperature suggests that future laboratory controlled studies related specifically to temperature influences on As mobility across the sediment-water interface are warranted, since previous field and laboratory studies have noted a positive influence of temperature on sediment As efflux and attributed the increase in As flux to an increase in microbially mediated dissimilatory iron reduction and subsequent release of As adsorbed onto Fe-oxyhydroxide minerals (Barrett et al., 2019; Johnston et al., 2020).

Although no terrestrial inputs of As were recorded during autumn over the period of study, substantial autumn runoff events are common when rainfall amounts exceed the storage capacity of soils in the region (Spence and Woo, 2006). The relative contribution of individual autumn runoff events in the annual mass flux of As is likely small since individual runoff events associated with high rainfall in summer and autumn typically account for less than half the contribution from

the snowmelt period (Spence and Woo, 2006, 2003). A shift in autumn precipitation phase has been observed in the region, with more autumn precipitation arriving as rain rather than snow (Spence et al., 2011), which could lead to higher terrestrial inputs of As to local lakes if these conditions become more common and surface and subsurface storage thresholds are exceeded.

6.4.2.2 Contrasting winter hydrology drives major differences in watershed fluxes of As

Contrasting winter hydrology between the two study years resulted in distinct differences in the cycling and transport of As in the Lower Martin Lake watershed. The lake was hydrologically disconnected from the surrounding Baker Creek watershed through the first winter, and anoxic conditions developed through the water column as sediment oxygen demand exceeded the oxygen budget in the lake (Palmer et al., 2020). During this period, lake inputs and outputs of As were negligible, but internal loading of As was substantial, and at peak loads in April 2018 were comparable to the cumulative As inputs at the lake inflow for the entire 2017-18 study year (Figure 6.5). Yet, the influence of high over-winter internal loading of As on As export from the lake was dampened by the net loss of As from the water column in early spring, as As was returned to sediments prior to streamflow generation at the lake outlet (Figure 6.5; Table 6.1).

In contrast to 2017-18, winter fluxes of As were an important component of annual exports and imports of As in 2018-19 (Figure 6.5; Table 6.1). The magnitude of winter sediment As flux was lower than in 2017-18 but still accounted for 34% of total lake input in winter 2018-19. Further, because the lake was hydrologically connected to the surrounding watershed, 30% of lake output over winter was derived from the lake sediments (Table 6.1), indicating that increased winter connectivity in the watershed augments As removal from lakes.

6.4.2.3 Spring as a period of major watershed flux of As

Spring represented the most dynamic period of As mobilization and transport during the study period. Snowmelt led to activation of the local catchment and mobilization of As from terrestrial stores, and the increase in streamflow delivered low As water to the lake from the upper watershed. At the same time, several external and internal forcings influenced within lake biogeochemical processes that alter the cycling of As between lake sediments and overlying waters, thus altering the amount of As that was available for export from the lake during this typically high flow period.

The partitioning of watershed fluxes by season showed that catchment runoff, primarily driven by snowmelt, was an important source of As to the lake in May and June of both years, delivering 19.3 and 16.3 kg As to the lake in spring 2018 and 2019, respectively (Table 6.1). The relative contribution of catchment runoff to total As inputs to the lake, however, varied between years and was dependent on differences in regional hydrology. During the first year of the study, streamflow was low through spring as snowmelt generated during freshet was likely dedicated to overcoming storage deficits in lakes that had accumulated in the region over the preceding drought period. Consequently, catchment derived As was the dominant As input into the lake over this period and accounted for 80% of total incoming As in spring 2018 (Table 6.1). Sustained winter baseflow leading into the second year of the study resulted in higher streamflow at the lake inlet during spring and reduced the relative influence of catchment runoff on total As inputs during spring 2019 (25%; Table 6.1).

While spring snowmelt led to activation and transport of As from the local catchment and upper watershed, there were important processes occurring under ice that influenced the transport of As from the watershed. In both years, May and June represented a period of As removal from the water column. Previous research in Lower Martin Lake attributed the removal of As from the

water column to water column reoxygenation from benthic oxygen production in late winter and snowmelt intrusion in spring (Palmer et al., 2020). The reoxygenation of the water column led to the precipitation and settling of Fe-oxyhydroxides in the water column, which removes As (as AsV) from the water column through adsorption and co-precipitation with Fe-oxyhydroxides. In both years, the removal of As from the water column occurred before peak streamflow, therefore the influence of overwinter loading of As to the water column is dampened.

6.4.2.4 Summer fluxes dominated by streamflow and internal loading from contaminated sediments

The two summers included in this study were characterized by high streamflow, thus As fluxes at the lake inlet and outlet dominated the mass balance. In both summers, contributions from the upper watershed accounted for 59% of total incoming As, highlighting the continued loading of As from upstream sources. Despite the dominant influence of regional streamflow, there were distinct difference between years in the relative partitioning of individual watershed fluxes during summer. In the wet summer of 2018, a greater proportion of As entering the lake was derived from the local catchment (16%) than in 2019, indicating that while internal loading from sediments was fairly consistent between years, increased rainfall that leads to surface runoff generation can result in substantial additional loading of As. This suggests that the cumulative influence of high rainfall, which leads to enhanced streamflow and surface runoff from the catchment, will lead to an increase in the magnitude and diversity of sources for incoming As.

6.5 Implications for recovery of impacted lakes

The observed reduction of As in the water column of Lower Martin Lake through the study period and the gradual convergence of As concentrations at the lake inlet and outlet in the second

year of the study (Figure 6.2a) suggests that increased hydrological connectivity in the Baker Creek basin leads lake chemistry to reflect conditions along the stream network. In contrast, when Lower Martin Lake was hydrologically disconnected from the upper watershed lake chemistry reflected conditions within the local catchment and was influenced heavily by internal loading of As. Since sediment efflux was observed in summer and winter, we suggest that subarctic lakes act as “pipes” under wet conditions where hydrological connectivity is high and water retention times are limited, thus increasing the influence of water arriving from the upper watershed and limiting the influence of internal sediment loading on lake waters. Under high connectivity conditions surface water delivered from the upper watershed dominates and As concentrations are lower than in years when hydrological connectivity is low. The cumulative lake water renewal rate shows that Lower Martin Lake gradually shifted from acting as an isolated “bucket”, with little influence from the upper watershed in 2017-18 (renewal rate: 3.4), to more of a “pipe” in 2018-19 (renewal rate: 5.6) (Appendix D: Figure D6). This is consistent with studies related to carbon cycling that showed that in lake retention of DOC declined with an increase in discharge and lower water residence time (de Wit et al., 2018). Although the biogeochemical cycling of C and As are distinct, the parallels suggest that increased precipitation and stream discharge in subarctic environments will lead to enhanced flushing of contaminated waters from the watershed.

Chapter 7: Conclusions and directions for future research

7.1 Key findings and contributions

The research presented in this thesis was designed to achieve the broad goal of increasing our understanding of the environmental processes that control the chemical recovery of northern landscapes impacted by atmospheric As pollution. A regional survey of soil As concentrations, and mineralogical analysis to identify the main As-host minerals, provided new information on the current distribution, source, and solid-phase speciation of As in soils across the study area (presented in Chapter 3). The following three studies (Chapters 4 through 6) were focused on exploring within-lake and watershed processes that influence seasonal and long-term changes in lake water As concentrations. Chapters 4 through 6 provided new insights on linkages between climate, hydrology and the aquatic biogeochemical cycling of As. The findings from the four research chapters directly addressed the specific thesis objectives outlined in Chapter 1 (section 1.2) and are highlighted below.

Objective 1: Describe the distribution and mineralogy of As in near-surface soils in the

Yellowknife area to determine the geogenic and mining associated contributions of As to soils

More than 450 near-surface soil samples were collected within a 30 km radius of the decommissioned Giant Mine roaster to explore the distribution of As in Yellowknife area soils more than 20 years after stack emissions ended. The results from Chapter 3 show that a strong relationship between soil As concentrations and distance to point sources of As emissions persists in near-surface soils in the region. Mineralogical analysis on 82 of the samples collected indicated that As_2O_3 is the predominant mineral host of As at sites within 15 km of the legacy mine roasters. This evidence demonstrates that high concentrations of As in near-surface soils

near Yellowknife are the result of past mining emissions and not natural enrichment associated with As-bearing sulfide mineralization. The results from Chapter 3 inform subsequent studies in the thesis, by determining that terrestrial soils are a large reservoir of As that may continue to release As to local lakes via catchment runoff processes.

Objective 2: Develop new approaches to estimate the range of geochemical background for As in areas impacted by legacy As emissions

One of the main purposes in defining geochemical background in environmental chemistry is to distinguish between natural geogenic concentrations of elements and anthropogenic contamination (Reimann and de Caritat, 2017). The estimation of geochemical background often relies on statistical and geospatial techniques, which can be powerful, but do not provide unambiguous evidence of element source. In Chapter 3, mineralogical tools (scanning electron microscopy with an automated mineralogy software) were combined with statistical and geospatial tools to highlight a new approach for estimating geochemical background of As in surficial materials. The removal of samples (based on identification of As_2O_3) within 20 km of Yellowknife from geochemical survey data from the Geological Survey of Canada allowed for the exploration of the range of geochemical background As in surficial materials across the entire Slave Geological Province. This area is composed of diverse bedrock lithology and significant areas of gold mineralization, which provided context for the Yellowknife Greenstone Belt, an area where high As in soils has been attributed to natural mineralization. The results from Chapter 3 show that As enrichment near areas of mineralization are present but anomalous and do not reflect conditions across the entire Slave Geological Province. Chapter 3 suggests that the range of geochemical background for As in surficial materials of the Slave Geological Province

is 0.25 – 15 mg kg⁻¹ As, with an upper threshold in material overlying volcanic bedrock units of 30 mg kg⁻¹ As. This is much lower than the current upper threshold for geochemical background used by the Government of the Northwest Territories (150 mg kg⁻¹ As) (GNWT, 2003) and should be considered by resource managers when updating soil remediation guidelines for the area.

Objective 3: Contrast the seasonal variation of two roaster derived pollutants (As and Sb) in surface waters of shallow lakes near Yellowknife, NT

Subarctic lakes are ice-covered for much of the year and the presence of ice limits lake-atmosphere interactions, which can lead to depletion of dissolved oxygen from the water column if the O₂ budget in the water column is exceeded by biological demand in the water and sediments. Consequently, seasonal changes in redox conditions may occur, particularly under ice in shallow lakes. In Chapter 4, surface waters were collected regularly over 2 years to explore the seasonal variation of As and Sb in surface waters. Arsenic and Sb are elements associated with stack emissions in the Yellowknife area, but often exhibit contrasting geochemical behaviour. The results in Chapter 4 showed substantial under-ice enrichment of As and other redox sensitive elements (Fe and Mn) suggesting that seasonal variation in lake water As is associated with Fe and Mn redox cycling. A regional survey of 30 lakes in the open-water season and under ice in late winter revealed substantial As enrichment under ice for lakes < 4m, corroborating the results from the four detailed study lakes and indicating that under ice As enrichment is widespread in shallow lakes across the region. In contrast, there was little difference in Sb concentrations under ice from the four detailed study lakes or in the regional survey, suggesting that surface water Sb concentrations are not coupled with Fe and Mn redox

processes. The findings presented in Chapter 4 highlight the importance of understanding seasonal redox processes when evaluating the trajectory of recovery for As impacted lakes in cold regions.

Objective 4: Investigate seasonal controls on the geochemical cycling of As in shallow subarctic lakes

Objective 5: Investigate the influence of winter hydrology on the geochemical cycling of As in shallow lakes

Chapter 5 built on the concept of seasonality that was described in Chapter 4 and explored the geochemical and hydrological processes that influence seasonal and interannual differences in surface water As for a shallow lake near Giant Mine. Geochemical characterization of surface waters, sediments, and sediment porewaters across seasons in two consecutive years highlighted the coupling of As mobility with the cycling of Fe and S. Lake sediments were a source of As to overlying water in both study years, but the position of the redox boundary within the overlying water, controlled by differences in winter hydrology, mediated under ice enrichment of As.

During the first winter, the lake was hydrologically disconnected from the surrounding watershed and anoxic conditions developed through the water column, persisting for more than 2 months, and leading to high As under ice ($> 100 \mu\text{g L}^{-1}$). In contrast, during the second winter, oxygenated stream water continued to be supplied to the lake and suppressed the redox boundary, thus limiting under ice enrichment of As. These results addressed thesis objectives 4 and 5 and provided new insights on linkages between hydrology and the geochemical cycling of As in shallow lakes in the region.

Objective 6: Compare the magnitude and timing of terrestrial and aquatic As fluxes to a lake under different hydrological conditions

Objective 7: Describe long-term patterns in As export from a contaminated watershed to elucidate how changing hydrological conditions associated with climate change may influence the recovery of As impacted watersheds

Chapters 4 and 5 focused on within-lake processes that influenced the seasonality of surface water As in shallow lakes. Chapters 6 built on these results and integrated processes across the watershed of Lower Martin Lake, including local catchment contributions, internal recycling, and lake inflows and outflows, to assess the relative partitioning of these watershed processes across seasons. Results from Chapter 6 addressed thesis objectives 6 and 7 and highlight the fundamental control of climate and hydrological connectivity to the trajectory of recovery for lakes in the region. In dry periods, the study lake was hydrologically disconnected from the surrounding watershed and there was little input or export of As associated with streamflow. Internal loading from contaminated sediments and local catchment derived As led to high concentrations and mass of As within the lake, suggesting that local contributions of As, via surface runoff and sediment inputs, delay recovery of shallow lakes in dry periods. In wet periods, substantial contributions were delivered from the local catchment via surface runoff, comparable to sediment derived loads in summer. However, total As fluxes during wet periods were dominated by transport at the lake inlet and outlet, and total export of As exceeded inputs by nearly 10%, suggesting that wet periods facilitate lake recovery in the region. The evaluation of an 11-year record of streamflow and As concentrations further supported the results from the watershed mass balance through demonstrating that shorter lake water retention time, associated with high streamflow, led to higher export of As, and by extension, the recovery of lake waters.

Conversely, longer lake water retention time led to higher concentrations of As in lake waters, lower export of As, and thus, overall, delayed chemical recovery in the lake.

7.2 Future research directions

The work presented in this thesis highlights the importance of year-round investigations, including during the winter and spring-melt periods, for assessing the chemical recovery of shallow northern aquatic systems from As pollution. The results are also applicable to other regions impacted by As pollution, and for the geochemical cycling of other redox sensitive elements. In developing and interpreting the results from this thesis new research questions have emerged that warrant consideration for future study. Suggestions for future research, based on the advancement of knowledge in this thesis, are outlined in the section below.

1) Mobility of As within the soil pool

The results from this thesis showed that the landscape surrounding lakes in the Yellowknife region is a reservoir of legacy As (Chapter 3), and contaminated soils continue to contribute arsenic to lakes over time (Chapter 6). The primary pathway for terrestrial materials to enter lakes in the subarctic shield terrain around Yellowknife is through snowmelt runoff, but changing precipitation conditions associated with climate change may be altering this pattern (Spence et al., 2015). Changes in the magnitude and timing of rainfall events will alter flow paths and the amount of water running off the landscape, thus influencing the amount of arsenic transported to lakes. From a catchment perspective, investigations related to comparing As fluxes from different landscape units are warranted. The results from Chapter 6 treat terrestrial catchments as a homogeneous unit or “black box”, however, subarctic shield catchments are comprised of a mosaic of exposed bedrock, shallow soil pockets, thicker soil filled valleys, and expansive peatlands. The contribution of As from each of these catchment units will differ,

likely in association with hydrological storage processes and flow pathways. New investigations are warranted to directly assess the mobility and transport of As from the various catchment units in shield terrain to identify important catchment sources and sinks for As.

The mobility of As within individual catchment units ultimately determines its potential for transport. New research dedicated to exploring the biogeochemical controls on As mobility in contaminated soils within different landscape units would strengthen our understanding of the factors that enhance and reduce As mobility on the landscape. For example, the results from this thesis highlight that As_2O_3 has persisted in surface soils for decades, and high concentrations of As are present in catchment runoff. Further research is required to assess controls on the solubility of As_2O_3 and other As-bearing minerals present in soils, and the mechanisms that drive reprecipitation in the soil environment. The role of dissolved organic matter (DOM) in regulating As mobility in the soil environment is a particular area in need of investigation, as increases in terrestrial derived DOM inputs to aquatic environments have been documented across the north (e.g. Tank et al., 2016; Wauthy et al., 2018), but there is a paucity of field investigations related to how this may affect As transport.

2) *Landscape controls on surface water As*

This thesis generated detailed information on the geochemical cycling of As between surface waters, sediments and sediment porewaters across seasons in shallow lakes near the decommissioned mine roaster at Giant Mine. These data provided novel insights on seasonal controls on As cycling in subarctic environments. New investigations across broader scale are now needed to explore landscape level factors that drive As variation and recovery in subarctic lakes. Surface water As generally declines in lakes with increasing distance from legacy mine

roasters in the region, but substantial variation in surface water As can occur between lakes within close proximity (Houben et al., 2016; Palmer et al., 2015). This suggests that impacts from atmospheric mining emissions, and the subsequent recovery of lakes, are not consistent across the region. Lake water surveys that integrate differences in lake morphometry, lake connectivity, hydrological position, catchment landcover types, and catchment to lake area ratios will help to identify vulnerable lake types and to highlight lake properties that facilitate or delay lake recovery. Hydrogeomorphic approaches have been used successfully for classifying lakes along water chemistry variables (Martin et al., 2011; Martin and Soranno, 2006) and should be considered for the Yellowknife region.

3) Role of wetlands in storage and release of legacy mining contaminants

Wetlands cover large areas of the subarctic shield and are important landscape features for the storage and transmission of water, nutrients, and pollutants along terrestrial-aquatic pathways. The fluctuation of water levels in wetlands alters the position of redox boundaries within wetland soils, which will have important control on the mobility of redox sensitive elements, such as As. Since wetlands often occupy the space between upland terrain and aquatic habitats, new investigations related to As mobility in wetland environments would be worthwhile. Research from the Sudbury, ON region has highlighted that wetlands continue to be a major source of smelting associated metals decades after smelter emissions were reduced in the region (Szkokan-Emilson et al., 2014). New investigations related to the role of wetlands in controlling As mobility and transport would build our understanding of the role that wetlands play in the recovery of the landscape and how those conditions may change in the future.

4) *Climate change impacts on As mobility in lakes and long-term trajectories of change*

Climate change is causing widespread impacts on the physical properties of lakes, including loss of ice cover, changes in evaporation and water budgets, warming surface water temperatures, and alterations in mixing regimes (Maberly et al., 2020; Woolway et al., 2020). These changes will likely have an important impact on the mobility and fate of As in lakes impacted by mining pollution, and future studies should aim to address this important gap. Specifically, new studies are needed to evaluate how shorter ice-cover periods and alteration of lake mixing regimes will impact As cycling in lakes. Chapter 6 in this thesis highlighted the important role that climate and lake hydrology play in the cycling and transport of As, but additional modelling-based studies would be valuable to explore future scenarios with intermittent drought and wet periods, and changes in lake thermal properties.

5) *Contrasting As and Sb geochemistry*

The bulk of this thesis was focused on processes that control the mobility, transport, and fate of As in subarctic environments, but results from Chapter 4 highlighted an interesting contrast in seasonal As and Sb mobility under fluctuating redox conditions. Previous studies have highlighted the contrasting geochemistry of As and Sb (Arsic et al., 2018; Fawcett et al., 2015; Warnken et al., 2017), and the Yellowknife area presents a model environment where the biogeochemical processes influencing As and Sb mobility could be studied further under field and experimental conditions. For the Yellowknife area, there remains uncertainty about the solid-phase hosts of Sb in contaminated lake sediments, and future studies should include detailed geochemical characterization of lake waters, sediments, and sediment porewaters. This thesis used experimental sediment incubations from a lake with organic rich sediments (LOI >

75% in surficial sediments) to explore As mobility through changes in redox and temperature. While the manipulation of dissolved oxygen conditions within the incubations showed a clear response in As flux, the influence of temperature manipulations on Sb flux were less conclusive. Future dedicated incubation studies using sediments with different sediment characteristics (e.g. OM, water content) would be worthwhile to explore contrasting As and Sb mobility under different temperature and redox conditions.

7.3 Concluding statement

The results presented in this thesis provide new insights into the mobility, transport, and fate of As in an environment that was impacted by more than 50 years of atmospheric As emissions. Seasonality is a defining characteristic of northern environments, which alters the speciation, mobility, and environmental fate of As. The observation of spring “redox shock” in shallow lakes associated with the incursion of snowmelt water into lakes and its subsequent impact on As speciation and mobility is a key insight into the speed and magnitude that seasonal processes can influence As mobility in the environment. Future work is warranted to elucidate the cascade of biogeochemical processes and reactions occurring during this dynamic period.

The enduring legacy of As contamination on the landscape is clear and future work remains to understand the trajectory of recovery for lakes and landscapes. While there have been longstanding concerns about the human health and environmental impacts of past mining emissions on the Yellowknife region, there has been considerable research interest in tackling critical questions related to population health effects (e.g. Cheung et al., 2020), levels of mining associated contaminants in country foods (e.g. Chételat et al., 2019), and risks associated with eating country foods (e.g. Tanamal et al., 2020). It is my hope that territorial, federal, and Indigenous governments recognize the value of this research and work towards new economic

and educational opportunities that capitalize on the remediation of the landscape and reconciliation with the Yellowknives Dene First Nation and Métis who's lives were affected by mining activities.

References

- Acosta, J.A., Martínez-Martínez, S., Faz, A., Arocena, J., 2011. Accumulations of major and trace elements in particle size fractions of soils on eight different parent materials. *Geoderma* 161, 30–42. <https://doi.org/10.1016/j.geoderma.2010.12.001>
- Adrian, R., O'Reilly, C.M., Zagarese, H., Baines, S.B., Hessen, D.O., Keller, W., Livingstone, D.M., Sommaruga, R., Straile, D., Van Donk, E., Weyhenmeyer, G.A., Winder, M., 2009. Lakes as sentinels of climate change. *Limnol. Oceanogr.* 54, 2283–2297. https://doi.org/10.4319/lo.2009.54.6_part_2.2283
- Ahmed, K.M., Bhattacharya, P., Hasan, M.A., Akhter, S.H., Alam, S.M.M., Bhuyian, M.A.H., Imam, M.B., Khan, A.A., Sracek, O., 2004. Arsenic enrichment in groundwater of the alluvial aquifers in Bangladesh: An overview. *Appl. Geochemistry* 19, 181–200. <https://doi.org/10.1016/j.apgeochem.2003.09.006>
- Allan, C.J., Roulet, N.T., Hill, A.R., 1993. The biogeochemistry of pristine, headwater Precambrian shield watersheds: an analysis of material transport within a heterogeneous landscape. *Biogeochemistry* 22, 37–79. <https://doi.org/10.1007/BF00002756>
- American Public Health Association, 1999. *Standard Methods for the Examination of Water and Wastewater*, American Water Works Association. Washington, DC.
- Andrade, C.F., Jamieson, H.E., Kyser, T.K., Praharaj, T., Fortin, D., 2010. Biogeochemical redox cycling of arsenic in mine-impacted lake sediments and co-existing pore waters near Giant Mine, Yellowknife Bay, Canada. *Appl. Geochemistry* 25, 199–211. <https://doi.org/10.1016/j.apgeochem.2009.11.005>
- Antoniades, D., Michelutti, N., Quinlan, R., Blais, J.M., Bonilla, S., Douglas, M.S. V., Pienitz, R., Smol, J.P., Vincent, W.F., 2011. Cultural eutrophication, anoxia, and ecosystem recovery in Meretta Lake, High Arctic Canada. *Limnol. Oceanogr.* 56, 639–650. <https://doi.org/10.4319/lo.2011.56.2.0639>
- Arsic, M., Teasdale, P.R., Welsh, D.T., Johnston, S.G., Burton, E.D., Hockmann, K., Bennett, W.W., 2018. Diffusive gradients in thin films (DGT) reveals antimony and arsenic mobility differs in a contaminated wetland sediment during an oxic-anoxic transition. *Environ. Sci. Technol.* 52, 1118–1127. <https://doi.org/10.1021/acs.est.7b03882>
- Asta, M.P., Kirk Nordstrom, D., Blaine McCleskey, R., 2012. Simultaneous oxidation of arsenic and antimony at low and circumneutral pH, with and without microbial catalysis. *Appl. Geochemistry* 27, 281–291. <https://doi.org/10.1016/j.apgeochem.2011.09.002>
- Aurilio, A.C., Mason, R.P., Hemond, H.F., 1994. Speciation and Fate of Arsenic in Three Lakes of the Aberjona Watershed. *Environ. Sci. Technol.* 28, 577–585. <https://doi.org/10.1021/es00053a008>
- Azizur Rahman, M., Hasegawa, H., 2012. Arsenic in freshwater systems: Influence of eutrophication on occurrence, distribution, speciation, and bioaccumulation. *Appl. Geochemistry* 27, 304–314. <https://doi.org/10.1016/j.apgeochem.2011.09.020>

- Baehr, M.M., Degrandpre, M.D., 2002. Under-ice CO₂ and O₂ variability in a freshwater lake. *Biogeochemistry* 61, 95–133. <https://doi.org/10.1023/A:1020265315833>
- Barker, A.J., Douglas, T.A., Jacobson, A.D., McClelland, J.W., Ilgen, A.G., Khosh, M.S., Lehn, G.O., Trainor, T.P., 2014. Late season mobilization of trace metals in two small Alaskan arctic watersheds as a proxy for landscape scale permafrost active layer dynamics. *Chem. Geol.* 381, 180–193. <https://doi.org/10.1016/j.chemgeo.2014.05.012>
- Barrett, P.M., Hull, E.A., Burkart, K., Hargrave, O., McLean, J., Taylor, V.F., Jackson, B.P., Gawel, J.E., Neumann, R.B., 2019. Contrasting arsenic cycling in strongly and weakly stratified contaminated lakes: Evidence for temperature control on sediment-water arsenic fluxes. *Limnol. Oceanogr.* 64, 1333–1346. <https://doi.org/10.1002/lno.11119>
- Bauer, M., Blodau, C., 2006. Mobilization of arsenic by dissolved organic matter from iron oxides, soils and sediments. *Sci. Total Environ.* 354, 179–190. <https://doi.org/10.1016/j.scitotenv.2005.01.027>
- Belzile, N., Chen, Y.W., Gunn, J.M., Dixit, S.S., 2004. Sediment trace metal profiles in lakes of Killarney Park, Canada: From regional to continental influence. *Environ. Pollut.* 130, 239–248. <https://doi.org/10.1016/j.envpol.2003.12.003>
- Belzile, N., Tessier, A., 1990. Interactions between arsenic and iron oxyhydroxides in lacustrine sediments. *Geochim. Cosmochim. Acta* 54, 103–109. [https://doi.org/10.1016/0016-7037\(90\)90198-T](https://doi.org/10.1016/0016-7037(90)90198-T)
- Bennett, W.W., Hockmann, K., Johnston, S.G., Burton, E.D., 2017. Synchrotron X-ray absorption spectroscopy reveals antimony sequestration by reduced sulfur in a freshwater wetland sediment. *Environ. Chem.* 14, 345–349. <https://doi.org/10.1071/en16198>
- Bennett, W.W.W., Teasdale, P.P.R., Panther, J.J.G., Welsh, D.T.D., Zhao, H.H., Jolley, D.D.F., 2012. Investigating arsenic speciation and mobilization in sediments with DGT and DET: A mesocosm evaluation of oxic-anoxic transitions. *Environ. Sci. Technol.* 46, 3981–3989. <https://doi.org/10.1021/es204484k>
- Bergmann, M.A., Welch, H.E., 1985. Spring meltwater mixing in small arctic lakes. *Can. J. Fish. Aquat. Sci.* 42, 1789–1798. <https://doi.org/10.1139/f85-224>
- Bertilsson, S., Burgin, A., Carey, C.C., Fey, S.B., Grossart, H.P., Grubisic, L.M., Jones, I.D., Kirillin, G., Lennon, J.T., Shade, A., Smyth, R.L., 2013. The under-ice microbiome of seasonally frozen lakes. *Limnol. Oceanogr.* 58, 1998–2012. <https://doi.org/10.4319/lo.2013.58.6.1998>
- Bhattacharya, P., Welch, A.H., Stollenwerk, K.G., McLaughlin, M.J., Bundschuh, J., Panaullah, G., 2007. Arsenic in the environment: Biology and Chemistry. *Sci. Total Environ.* 379, 109–120. <https://doi.org/10.1016/j.scitotenv.2007.02.037>
- Björkvald, L., Buffam, I., Laudon, H., Mörtz, C.M., 2008. Hydrogeochemistry of Fe and Mn in small boreal streams: The role of seasonality, landscape type and scale. *Geochim. Cosmochim. Acta* 72, 2789–2804. <https://doi.org/10.1016/j.gca.2008.03.024>
- Blais, J.M., Duff, K.E., Laing, T.E., Smol, J.P., 1999. Regional contamination in lakes from the Noril'sk region in Siberia, Russia. *Water. Air. Soil Pollut.* 110, 389–404.

- Block, B.D., Denfeld, B.A., Stockwell, J.D., Flaim, G., Grossart, H.P.F., Knoll, L.B., Maier, D.B., North, R.L., Rautio, M., Rusak, J.A., Sadro, S., Weyhenmeyer, G.A., Bramburger, A.J., Branstrator, D.K., Salonen, K., Hampton, S.E., 2019. The unique methodological challenges of winter limnology. *Limnol. Oceanogr. Methods* 17, 42–57. <https://doi.org/10.1002/lom3.10295>
- Blodau, C., Fulda, B., Bauer, M., Knorr, K.H., 2008. Arsenic speciation and turnover in intact organic soil mesocosms during experimental drought and rewetting. *Geochim. Cosmochim. Acta* 72, 3991–4007. <https://doi.org/10.1016/j.gca.2008.04.040>
- Bolan, N., Mahimairaja, S., Kunhikrishnan, A., Choppala, G., 2013. Phosphorus-arsenic interactions in variable-charge soils in relation to arsenic mobility and bioavailability. *Sci. Total Environ.* 463–464, 1154–1162. <https://doi.org/10.1016/j.scitotenv.2013.04.016>
- Bostick, B.C., Fendorf, S., 2003. Arsenite sorption on troilite (FeS) and pyrite (FeS₂). *Geochim. Cosmochim. Acta* 67, 909–921. [https://doi.org/10.1016/S0016-7037\(02\)01170-5](https://doi.org/10.1016/S0016-7037(02)01170-5)
- Bowell, R.J., 1994. Sorption of arsenic by iron-oxides and oxyhydroxides in soils. *Appl. Geochemistry* 9, 279–286. [https://doi.org/10.1016/0883-2927\(94\)90038-8](https://doi.org/10.1016/0883-2927(94)90038-8)
- Boyle, R.W., 1979. The geochemistry of gold and its deposits (No. Bulletin 280). Ottawa, ON.
- Boyle, R.W., Jonasson, I.R., 1973. The geochemistry of arsenic and its use as an indicator element in geochemical prospecting. *J. Geochemical Explor.* 2, 251–296. [https://doi.org/10.1016/0375-6742\(73\)90003-4](https://doi.org/10.1016/0375-6742(73)90003-4)
- Branfireun, B.A., 1999. Catchment-scale hydrology and methylmercury biogeochemistry in the Low Boreal Forest zone of the Precambrian Shield. McGill University.
- Branfireun, B.A., Heyes, A., Roulet, N.T., 1996. The hydrology and methylmercury dynamics of a Precambrian Shield headwater peatland. *Water Resour. Res.* 32, 1785–1794.
- Brett, M.T., Benjamin, M.M., 2008. A review and reassessment of lake phosphorus retention and the nutrient loading concept. *Freshw. Biol.* 53, 194–211. <https://doi.org/10.1111/j.1365-2427.2007.01862.x>
- Bright, D.A., Brock, S., Reimer, K.J., Cullen, W.R., Hewitt, G.M., Jafaar, J., 1994. Methylation of arsenic by anaerobic microbial consortia isolated from lake sediment. *Appl. Organomet. Chem.* 8, 415–422. <https://doi.org/10.1002/aoc.590080416>
- Bromstad, M.J., Wrye, L.A., Jamieson, H.E., 2017. The characterization, mobility, and persistence of roaster-derived arsenic in soils at Giant Mine, NWT. *Appl. Geochemistry* 82, 102–118. <https://doi.org/10.1016/j.apgeochem.2017.04.004>
- Bullen, W., Robb, M., 2006. Economic contribution of gold mining in the Yellowknife mining district, in: Anglin, C.D., Falck, H., Wright, D.F., Ambrose, E.J. (Eds.), *Gold in the Yellowknife Greenstone Belt, Northwest Territories: Results of the EXTECH III Multidisciplinary Research Project*. Geological Association of Canada, Mineral Deposits Division, pp. 38–49.
- Buschmann, J., Kappeler, A., Lindauer, U., Kistler, D., Berg, M., Sigg, L., 2006. Arsenite and arsenate binding to dissolved humic acids: Influence of pH, type of humic acid, and

- aluminum. *Environ. Sci. Technol.* 40, 6015–6020. <https://doi.org/10.1021/es061057+>
- Cai, Y., Cabrera, J.C., Georgiadis, M., Jayachandran, K., 2002. Assessment of arsenic mobility in the soils of some golf courses in South Florida. *Sci. Total Environ.* 291, 123–134. [https://doi.org/10.1016/S0048-9697\(01\)01081-6](https://doi.org/10.1016/S0048-9697(01)01081-6)
- Canada North Environmental Services, 2018. Giant Mine Human Health and Ecological Risk Assessment. Edmonton, AB.
- Carey, S.K., 2003. Dissolved organic carbon fluxes in a discontinuous permafrost subarctic alpine catchment. *Permafr. Periglac. Process.* 14, 161–171. <https://doi.org/10.1002/ppp.444>
- Carignan, R., St-Pierre, S., Gachter, R., 1994. Use of diffusion samplers in oligotrophic lake sediments: Effects of free oxygen in sampler material. *Limnol. Oceanogr.* 39, 468–474. <https://doi.org/10.4319/lo.1994.39.2.0468>
- Chatain, V., Sanchez, F., Bayard, R., Moszkowicz, P., Gourdon, R., 2005. Effect of experimentally induced reducing conditions on the mobility of arsenic from a mining soil. *J. Hazard. Mater.* 122, 119–128. <https://doi.org/10.1016/j.jhazmat.2005.03.026>
- Chatterjee, A., Das, D., Mandal, B.K., Chowdhury, T.R., Samanta, G., 1995. Arsenic in groundwater in six districts of West Bengal, India: the biggest arsenic calamity in the world. Part I. Arsenic species in drinking water and urine of the affected people. *Analyst* 120, 643–650.
- Chen, M., Ma, L.Q., Hoogeweg, C.G., Harris, W.G., 2001. Arsenic background concentrations in florida, u.s.a. surface soils: Determination and interpretation. *Environ. Forensics* 2, 117–126. <https://doi.org/10.1006/enfo.2001.0050>
- Chen, Y.W., Deng, T.L., Filella, M., Belzile, N., 2003. Distribution and early diagenesis of antimony species in sediments and porewaters of freshwater lakes. *Environ. Sci. Technol.* 37, 1163–1168. <https://doi.org/10.1021/es025931k>
- Cheney, C.L., Eccles, K.M., Kimpe, L.E., Thienpont, J.R., Korosi, J.B., Blais, J.M., 2020. Determining the effects of past gold mining using a sediment palaeotoxicity model. *Sci. Total Environ.* 718, 137308. <https://doi.org/10.1016/j.scitotenv.2020.137308>
- Cheng, H., Hu, Y., Luo, J., Xu, B., Zhao, J., 2009. Geochemical processes controlling fate and transport of arsenic in acid mine drainage (AMD) and natural systems. *J. Hazard. Mater.* 165, 13–26. <https://doi.org/10.1016/j.jhazmat.2008.10.070>
- Chételat, J., Cott, P.A., Rosabal, M., Houben, A., McClelland, C., Rose, E.B., Amyot, M., 2019. Arsenic bioaccumulation in subarctic fishes of a mine-impacted bay on Great Slave Lake, Northwest Territories, Canada. *PLoS One* 14, 1–23. <https://doi.org/10.1371/journal.pone.0221361>
- Cheung, J.S.J., Hu, X.F., Parajuli, R.P., Rosol, R., Torng, A., Mohapatra, A., Lye, E., Chan, H.M., 2020. Health risk assessment of arsenic exposure among the residents in Ndilo, Dettah, and Yellowknife, Northwest Territories, Canada. *Int. J. Hyg. Environ. Health* 230, 113623. <https://doi.org/10.1016/j.ijheh.2020.113623>
- Couture, R.M., Gobeil, C., Tessier, A., 2010. Arsenic, iron and sulfur co-diagenesis in lake

- sediments. *Geochim. Cosmochim. Acta* 74, 1238–1255.
<https://doi.org/10.1016/j.gca.2009.11.028>
- Couture, R.M., Gobeil, C., Tessier, A., 2008. Chronology of atmospheric deposition of arsenic inferred from reconstructed sedimentary records. *Environ. Sci. Technol.* 42, 6508–6513.
<https://doi.org/10.1021/es800818j>
- Couture, R.M., Rose, J., Kumar, N., Mitchell, K., Wallschläger, D., Van Cappellen, P., 2013. Sorption of arsenite, arsenate, and thioarsenates to iron oxides and iron sulfides: A kinetic and spectroscopic investigation. *Environ. Sci. Technol.* 47, 5652–5659.
<https://doi.org/10.1021/es3049724>
- Creed, J.T., Brockhoff, C.A., Martin, T.D., 1994. Method 200.8: Determination of trace elements by inductively coupled plasma – mass spectrometry, rev. 5.4. Cincinnati, Ohio.
- Cullen, W.R., Reimer, K.J., 1989. Arsenic speciation in the environment. *Chem. Rev.* 89, 713–764. <https://doi.org/10.1021/cr00094a002>
- Cutler, W.G., Brewer, R.C., El-Kadi, A., Hue, N. V., Niemeyer, P.G., Peard, J., Ray, C., 2013. Bioaccessible arsenic in soils of former sugar cane plantations, Island of Hawaii. *Sci. Total Environ.* 442, 177–188. <https://doi.org/10.1016/j.scitotenv.2012.09.081>
- de Wit, H.A., Couture, R.-M., Jackson-Blake, L., Futter, M.N., Valinia, S., Austnes, K., Guerrero, J.-L., Lin, Y., 2018. Pipes or chimneys? For carbon cycling in small boreal lakes, precipitation matters most. *Limnol. Oceanogr. Lett.* <https://doi.org/10.1002/lo2.10077>
- Denfeld, B.A., Baulch, H.M., del Giorgio, P.A., Hampton, S.E., Karlsson, J., 2018. A synthesis of carbon dioxide and methane dynamics during the ice-covered period of northern lakes. *Limnol. Oceanogr. Lett.* 3, 117–131. <https://doi.org/10.1002/lo2.10079>
- Deng, T., Wu, Y., Yu, X., Guo, Y., Chen, Y.W., Belzile, N., 2014. Seasonal variations of arsenic at the sediment-water interface of Poyang Lake, China. *Appl. Geochemistry* 47, 170–176.
<https://doi.org/10.1016/j.apgeochem.2014.06.002>
- Déry, S.J., Hernández-Henríquez, M.A., Burford, J.E., Wood, E.F., 2009. Observational evidence of an intensifying hydrological cycle in northern Canada. *Geophys. Res. Lett.* 36, 1–5. <https://doi.org/10.1029/2009GL038852>
- Deshpande, B.N., Macintyre, S., Matveev, A., Vincent, W.F., 2015. Oxygen dynamics in permafrost thaw lakes: Anaerobic bioreactors in the Canadian subarctic. *Limnol. Oceanogr.* 60, 1656–1670. <https://doi.org/10.1002/lno.10126>
- Diamond, M.L., Bhavsar, S.P., Helm, P.A., Stern, G.A., Alae, M., 2005. Fate of organochlorine contaminants in arctic and subarctic lakes estimated by mass balance modelling. *Sci. Total Environ.* 342, 245–259. <https://doi.org/10.1016/j.scitotenv.2004.12.045>
- Díez, M., Simón, M., Dorronsoro, C., García, I., Martín, F., 2007. Background arsenic concentrations in Southeastern Spanish soils. *Sci. Total Environ.* 378, 5–12.
<https://doi.org/10.1016/j.scitotenv.2007.01.013>
- Dillon, P.J., 1975. The phosphorus budget of Cameron Lake, Ontario: The importance of flushing rate to the degree of eutrophy of lakes. *Limnol. Oceanogr.* 20, 28–39.

<https://doi.org/10.4319/lo.1975.20.1.0028>

- Dillon, P.J., Molot, L.A., 1996. Long-term phosphorus budgets and an examination of a steady-state mass balance model for central Ontario lakes. *Water Res.* 30, 2273–2280.
- Dixit, S., Hering, J.G., 2003. Comparison of arsenic(V) and arsenic(III) sorption onto iron oxide minerals: Implications for arsenic mobility. *Environ. Sci. Technol.* 37, 4182–4189. <https://doi.org/10.1021/es030309t>
- Douay, F., Pruvot, C., Waterlot, C., Fritsch, C., Fourrier, H., Loriette, A., Bidar, G., Grand, C., de Vaufléury, A., Scheifler, R., 2009. Contamination of woody habitat soils around a former lead smelter in the North of France. *Sci. Total Environ.* 407, 5564–5577. <https://doi.org/10.1016/j.scitotenv.2009.06.015>
- Douglas, T.A., Sturm, M., Blum, J.D., Polashenski, C., Stuefer, S., Hiemstra, C., Steffen, A., Filhol, S., Prevost, R., 2017. A Pulse of Mercury and Major Ions in Snowmelt Runoff from a Small Arctic Alaska Watershed. *Environ. Sci. Technol.* 51, 11145–11155. <https://doi.org/10.1021/acs.est.7b03683>
- Downing, J.A., 2010. Emerging global role of small lakes and ponds : little things mean a lot. *Limnetica* 29.
- Downing, J.A., Prairie, Y.T., Cole, J.J., Duarte, C.M., Tranvik, L.J., Striegl, R.G., McDowell, W.H., Kortelainen, P., Caraco, N.F., Melack, J.M., Middelburg, J.J., 2006. The global abundance and size distribution of lakes, ponds, and impoundments. *Limnol. Oceanogr.* 51, 2388–2397. <https://doi.org/http://dx.doi.org/10.1016/B978-012370626-3.00025-9>
- Drahota, P., Filippi, M., Ettler, V., Rohovec, J., Mihaljevič, M., Šebek, O., 2012. Natural attenuation of arsenic in soils near a highly contaminated historical mine waste dump. *Sci. Total Environ.* 414, 546–555. <https://doi.org/10.1016/j.scitotenv.2011.11.003>
- Drahota, P., Paces, T., Pertold, Z., Mihaljevic, M., Skrivan, P., 2006. Weathering and erosion fluxes of arsenic in watershed mass budgets. *Sci. Total Environ.* 372, 306–316. <https://doi.org/10.1016/j.scitotenv.2006.09.002>
- Drahota, P., Peřestá, M., Trubač, J., Mihaljevič, M., Vaněk, A., 2021. Arsenic fractionation and mobility in sulfidic wetland soils during experimental drying. *Chemosphere* 277. <https://doi.org/10.1016/j.chemosphere.2021.130306>
- Drahota, P., Pertold, Z., 2005. Fluxes of arsenic in soil-water system in the Celina-Mokrsko gold district, Bohemian Massif. *Miner. Depos. Res. Meet. Glob. Chall.* 927–930. https://doi.org/10.1007/3-540-27946-6_236
- Dung, T.T.T., Cappuyns, V., Swennen, R., Phung, N.K., 2013. From geochemical background determination to pollution assessment of heavy metals in sediments and soils. *Rev. Environ. Sci. Biotechnol.* 12, 335–353. <https://doi.org/10.1007/s11157-013-9315-1>
- Dushenko, W.T., Bright, D.A., Reimer, K.J., 1995. Arsenic bioaccumulation and toxicity in aquatic macrophytes exposed to gold mine effluent: relationships with environmental partitioning, metal uptake, and nutrients. *Aquat. Bot.* 50, 141–158.
- Dutrizac, J.E., Riveros, P.A., Chen, T.T., 2000. Recovery and Purification of Arsenic Oxide –

- Giant Mine (No. Project No. 601903). Ottawa, ON.
- Environment Canada, 2018. Historical Canadian daily climate data [WWW Document]. Environ. Canada. URL http://climate.weather.gc.ca/historical_data/search_historic_data_e.html (accessed 1.10.18).
- EPA, 2014. Priority pollutant list [WWW Document]. United States Environ. Prot. Agency. URL <https://www.epa.gov/sites/production/files/2015-09/documents/priority-pollutant-list-epa.pdf> (accessed 1.10.19).
- Erbanova, L., Novak, M., Fottova, D., Dousova, B., 2008. Export of arsenic from forested catchments under easing atmospheric pollution. *Environ. Sci. Technol.* 42, 7187–7192. <https://doi.org/10.1021/es800467j>
- ESG, 2001. Arsenic levels in the Yellowknife area: Distinguishing between natural and anthropogenic inputs. Kingston, ON.
- Ettler, V., Vaněk, A., Mihaljevič, M., Bezdička, P., 2005. Contrasting lead speciation in forest and tilled soils heavily polluted by lead metallurgy. *Chemosphere* 58, 1449–1459. <https://doi.org/10.1016/j.chemosphere.2004.09.084>
- Fawcett, S.E., Jamieson, H.E., 2011. The distinction between ore processing and post-depositional transformation on the speciation of arsenic and antimony in mine waste and sediment. *Chem. Geol.* 283, 109–118. <https://doi.org/10.1016/j.chemgeo.2010.02.019>
- Fawcett, S.E., Jamieson, H.E., Nordstrom, D.K., McCleskey, R.B., 2015. Arsenic and antimony geochemistry of mine wastes, associated waters and sediments at the Giant Mine, Yellowknife, Northwest Territories, Canada. *Appl. Geochemistry* 62, 3–17. <https://doi.org/10.1016/j.apgeochem.2014.12.012>
- Filella, M., Williams, P.A., Belzile, N., 2009. Antimony in the environment: Knowns and unknowns. *Environ. Chem.* 6, 95–105. <https://doi.org/10.1071/EN09007>
- Ford, R.G., Wilkin, R.T., Hernandez, G., 2006. Arsenic cycling within the water column of a small lake receiving contaminated ground-water discharge. *Chem. Geol.* 228, 137–155. <https://doi.org/10.1016/j.chemgeo.2005.11.021>
- Freitas, H., Diamond, M., Semkin, R., Gregor, D., 1997. Contaminant fate in high arctic lakes : development and application of a mass balance model. *Sci. Total Environ.* 201, 171–187.
- Frey, K.E., McClelland, J.W., 2009. Impacts of permafrost degradation on arctic river biogeochemistry. *Hydrol. Process.* 23, 169–182. <https://doi.org/10.1002/hyp.7196>
- Fritsch, C., Giraudoux, P., Cœurassier, M., Douay, F., Raoul, F., Pruvot, C., Waterlot, C., Vaufleury, A. de, Scheifler, R., 2010. Spatial distribution of metals in smelter-impacted soils of woody habitats: Influence of landscape and soil properties, and risk for wildlife. *Chemosphere* 81, 141–155. <https://doi.org/10.1016/j.chemosphere.2010.06.075>
- Galloway, J.M., Swindles, G.T., Jamieson, H.E., Palmer, M.J., Parsons, M.B., Sanei, H., Macumber, A.L., Patterson, R.T., Falck, H., 2017. Organic matter control on the distribution of arsenic in lake sediments impacted by ~ 65 years of gold ore processing in subarctic Canada. *Sci. Total Environ.* <https://doi.org/10.1016/j.scitotenv.2017.10.048>

- Gałaszka, A., 2007. A review of geochemical background concepts and an example using data from Poland. *Environ. Geol.* 52, 861–870. <https://doi.org/10.1007/s00254-006-0528-2>
- Gawel, J.E., Asplund, J.A., Burdick, S., Miller, M., Peterson, S.M., Tollefson, A., Ziegler, K., 2014. Arsenic and lead distribution and mobility in lake sediments in the south-central Puget Sound watershed: The long-term impact of a metal smelter in Ruston, Washington, USA. *Sci. Total Environ.* 472, 530–537. <https://doi.org/10.1016/j.scitotenv.2013.11.004>
- Gibson, J.J., Reid, R., Spence, C., 1998. A six-year isotopic record of lake evaporation at a mine site in the Canadian subarctic: results and validation. *Hydrol. Process.* 12, 1779–1792. [https://doi.org/10.1002/\(SICI\)1099-1085\(199808/09\)12:10/11<1779::AID-HYP694>3.0.CO;2-7](https://doi.org/10.1002/(SICI)1099-1085(199808/09)12:10/11<1779::AID-HYP694>3.0.CO;2-7)
- GNWT, 2016. A guide to mineral deposits, Northwest Territories. Yellowknife, NT.
- GNWT, 2003. Environmental Guideline for Contaminated Site Remediation. Yellowknife, NT. <https://doi.org/10.1519/JSC.0b013e318242d2ec>
- Greenaway, C.M., Paterson, A.M., Keller, W., Smol, J.P., 2012. Dramatic diatom species assemblage responses in lakes recovering from acidification and metal contamination near Wawa, Ontario, Canada: a paleolimnological perspective. *Can. J. Fish. Aquat. Sci.* 69, 656–669. <https://doi.org/10.1139/f2012-003>
- Grömping, U., 2006. Relative importance for linear regression in R: the package relaimpo. *J. Stat. Softw.* 17, 1–27.
- Hasegawa, H., Rahman, M.A., Kitahara, K., Itaya, Y., Maki, T., Ueda, K., 2010. Seasonal changes of arsenic speciation in lake waters in relation to eutrophication. *Sci. Total Environ.* 408, 1684–1690. <https://doi.org/10.1016/j.scitotenv.2009.11.062>
- Hasegawa, H., Rahman, M.A., Matsuda, T., Kitahara, T., Maki, T., Ueda, K., 2009. Effect of eutrophication on the distribution of arsenic species in eutrophic and mesotrophic lakes. *Sci. Total Environ.* 407, 1418–1425. <https://doi.org/10.1016/j.scitotenv.2008.10.024>
- Hayat, K., Menhas, S., Bundschuh, J., Chaudhary, H.J., 2017. Microbial biotechnology as an emerging industrial wastewater treatment process for arsenic mitigation: A critical review. *J. Clean. Prod.* 151, 427–438. <https://doi.org/10.1016/j.jclepro.2017.03.084>
- Health Canada, 2017. Guidelines for Canadian drinking water quality - Summary Table. Ottawa, ON.
- Hellweger, F.L., Farley, K.J., Lall, U., Toro, D.M. Di, 2003. Greedy Algae Reduce Arsenate. *Limnol. Oceanogr.* 48, 2275–2288. <https://doi.org/10.2307/3597829>
- Helmstaedt, H., 2009. Crust-mantle coupling revisited: The Archean Slave craton, NWT, Canada. *Lithos* 112, 1055–1068. <https://doi.org/10.1016/j.lithos.2009.04.046>
- Hemond, H.F., 1995. Movement and distribution of arsenic in the Aberjona watershed. *Environ. Health Perspect.* 103, 35–40.
- Hobbie, J.E., 1980. Limnology of tundra ponds, US/IBP Syn. ed, US/IBP Synthesis series. Dowden, Hutchinson, and Ross Inc. https://doi.org/10.1007/SpringerReference_30406

- Hocking, D., Kuchar, P., Plambeck, J.A., Smith, R.A., 1978. The Impact of Gold Smelter Emissions on Vegetation and Soils of a Sub-Arctic Forest-Tundra Transition Ecosystem. *J. Air Pollut. Control Assoc.* 28, 133–137. <https://doi.org/10.1080/00022470.1978.10470580>
- Hoffmann, M., Mikutta, C., Kretzschmar, R., 2014. Arsenite binding to sulfhydryl groups in the absence and presence of ferrihydrite: A model study. *Environ. Sci. Technol.* 48, 3822–3831. <https://doi.org/10.1021/es405221z>
- Hollibaugh, J.T., Carini, S., Gürleyük, H., Jellison, R., Joye, S.B., LeCleir, G., Meile, C., Vasquez, L., Wallschläger, D., 2005. Arsenic speciation in Mono Lake, California: Response to seasonal stratification and anoxia. *Geochim. Cosmochim. Acta* 69, 1925–1937. <https://doi.org/10.1016/j.gca.2004.10.011>
- Holmes, R.M., McClelland, J.W., Peterson, B.J., Tank, S.E., Bulygina, E., Eglinton, T.I., Gordeev, V. V., Gurtovaya, T.Y., Raymond, P.A., Repeta, D.J., Staples, R., Striegl, R.G., Zhulidov, A. V., Zimov, S.A., 2012. Seasonal and Annual Fluxes of Nutrients and Organic Matter from Large Rivers to the Arctic Ocean and Surrounding Seas. *Estuaries and Coasts* 35, 369–382. <https://doi.org/10.1007/s12237-011-9386-6>
- Houben, A.J., D’Onofrio, R., Kokelj, S. V., Blais, J.M., 2016. Factors affecting elevated arsenic and methyl mercury concentrations in small shield lakes surrounding gold mines near the Yellowknife, NT, (Canada) region. *PLoS One* 11, 1–16. <https://doi.org/10.1371/journal.pone.0150960>
- Huang, J.H., 2014. Impact of microorganisms on arsenic biogeochemistry: A review. *Water. Air. Soil Pollut.* <https://doi.org/10.1007/s11270-013-1848-y>
- Huang, J.H., Matzner, E., 2007. Biogeochemistry of organic and inorganic arsenic species in a forested catchment in Germany. *Environ. Sci. Technol.* 41, 1564–1569. <https://doi.org/10.1021/es061586d>
- Hug, S.J., Canonica, L., Wegelin, M., Gechter, D., Von Gunten, U., 2001. Solar oxidation and removal of arsenic at circumneutral pH in iron containing waters. *Environ. Sci. Technol.* 35, 2114–2121. <https://doi.org/10.1021/es001551s>
- Hutchinson, T.C., Aufreiter, S., Hancock, R.G. V, 1982. Arsenic pollution in the Yellowknife Area from gold smelter activities. *J. Radioanal. Chem.* 71, 59–73. <https://doi.org/10.1007/BF02516141>
- Hutchinson, T.C., Whitby, L.M., 1977. The effects of acid rainfall and heavy metal particulates on a boreal Forest ecosystem near the sudbury smelting region of Canada. *Water. Air. Soil Pollut.* 7, 421–438. <https://doi.org/10.1007/BF00285542>
- Jacques, J.M.S., Sauchyn, D.J., 2009. Increasing winter baseflow and mean annual streamflow from possible permafrost thawing in the Northwest Territories, Canada. *Geophys. Res. Lett.* 36, 1–6. <https://doi.org/10.1029/2008GL035822>
- Jamieson, H.E., 2014. The legacy of arsenic contamination from mining and processing refractory gold ore at Giant Mine, Yellowknife, Northwest Territories, Canada. *Rev. Mineral. geochemistry* 79, 533–551.
- Jamieson, H.E., Maitland, K.M., Oliver, J.T., Palmer, M.J., 2017. Regional distribution of

- arsenic in near-surface soils in the Yellowknife area. Northwest Territories Geological Survey, NWT Open File 2017-03. Yellowknife, NT.
- Jasiak, I., Wiklund, J.A., Leclerc, E., Telford, J.V., Couture, R.M., Venkiteswaran, J.J., Hall, R.I., Wolfe, B.B., 2021. Evaluating spatiotemporal patterns of arsenic, antimony, and lead deposition from legacy gold mine emissions using lake sediment records. *Appl. Geochemistry* 134, 105053. <https://doi.org/10.1016/j.apgeochem.2021.105053>
- Johnston, S.G., Karimian, N., Burton, E.D., 2020. Seasonal Temperature Oscillations Drive Contrasting Arsenic and Antimony Mobilization in a Mining-Impacted River System. *Water Resour. Res.* 56, 1–20. <https://doi.org/10.1029/2020WR028196>
- Joung, D.J., Leduc, M., Ramcharitar, B., Xu, Y., Isles, P.D.F., Stockwell, J.D., Druschel, G.K., Manley, T., Schroth, A.W., 2017. Winter weather and lake-watershed physical configuration drive phosphorus, iron, and manganese dynamics in water and sediment of ice-covered lakes. *Limnol. Oceanogr.* 62, 1620–1635. <https://doi.org/10.1002/lno.10521>
- Kaise, T., Fukui, S., 1992. The chemical form and acute toxicity of arsenic compounds in marine organisms. *Appl. Organomet. Chem.* 6, 155–160. <https://doi.org/10.1002/aoc.590060208>
- Keller, W., Yan, N.D., Gunn, J.M., Heneberry, J., 2007. Recovery of Acidified Lakes : Lessons From Sudbury , Ontario , Canada. *Water, Air, Soil Pollut. Focus* 7, 317–322. <https://doi.org/10.1007/s11267-006-9061-2>
- Kerr, D., 2006. Quaternary Geology and Exploration Geochemistry (No. Special Publication Number 3), Gold in the Yellowknife Greenstone Belt, Northwest Territories: Results of the EXTECH III Multidisciplinary Research Project. Ottawa, ON.
- Kerr, D.E., Knight, R.D., 2005. Till geochemistry, Slave Province, Northwest Territories and Nunavut. Geological Survey of Canada, Open File 5015.
- Kneebone, P.E., O’Day, P.A., Jones, N., Hering, J.G., 2002. Deposition and fate of arsenic in iron- and arsenic-enriched reservoir sediments. *Environ. Sci. Technol.* 36, 381–386. <https://doi.org/10.1021/es010922h>
- Kumar, N., Noël, V., Planer-Friedrich, B., Besold, J., Lezama-Pacheco, J., Bargar, J.R., Brown, G.E., Fendorf, S., Boye, K., 2020. Redox Heterogeneities Promote Thioarsenate Formation and Release into Groundwater from Low Arsenic Sediments. *Environ. Sci. Technol.* 54, 3237–3244. <https://doi.org/10.1021/acs.est.9b06502>
- Lafargue, E., Marquis, F., Pillot, D., 1998. Rock-Eval 6 Applications in Hydrocarbon Exploration, Production, and Soil Contamination Studies. *Rev. l’Institut Français du Pétrole* 53, 421–437. <https://doi.org/10.2516/ogst:1998036>
- Landre, A.L., Watmough, S.A., Dillon, P.J., 2010. Metal pools, fluxes, and budgets in an acidified forested catchment on the precambrian shield, central Ontario, Canada. *Water. Air. Soil Pollut.* 209, 209–228. <https://doi.org/10.1007/s11270-009-0193-7>
- Lavery, P.S., Oldham, C.E., Ghisalberti, M., 2001. The use of Fick’s first law for predicting porewater nutrient fluxes under diffusive conditions. *Hydrol. Process.* 15, 2435–2451. <https://doi.org/10.1002/hyp.297>

- Lawson, N.M., Mason, R.P., 2001. Concentration of mercury, methylmercury, cadmium, lead, arsenic, and selenium in the rain and stream water of two contrasting watersheds in western Maryland. *Water Res.* 35, 4039–4052. [https://doi.org/10.1016/S0043-1354\(01\)00140-3](https://doi.org/10.1016/S0043-1354(01)00140-3)
- Leclerc, É., Venkiteswaran, J.J., Jasiak, I., Telford, J. V., Schultz, M.D.J., Wolfe, B.B., Hall, R.I., Couture, R.M., 2021. Quantifying arsenic post-depositional mobility in lake sediments impacted by gold ore roasting in sub-arctic Canada using inverse diagenetic modelling. *Environ. Pollut.* 288. <https://doi.org/10.1016/j.envpol.2021.117723>
- Leppi, J.C., Arp, C.D., Whitman, M.S., 2016. Predicting Late Winter Dissolved Oxygen Levels in Arctic Lakes Using Morphology and Landscape Metrics. *Environ. Manage.* 57, 463–473. <https://doi.org/10.1007/s00267-015-0622-x>
- Maberly, S.C., O'Donnell, R.A., Woolway, R.I., Cutler, M.E.J., Gong, M., Jones, I.D., Merchant, C.J., Miller, C.A., Politi, E., Scott, E.M., Thackeray, S.J., Tyler, A.N., 2020. Global lake thermal regions shift under climate change. *Nat. Commun.* 11, 1–9. <https://doi.org/10.1038/s41467-020-15108-z>
- Macdonald, R.W., Harner, T., Fyfe, J., 2005. Recent climate change in the Arctic and its impact on contaminant pathways and interpretation of temporal trend data. *Sci. Total Environ.* 342, 5–86. <https://doi.org/10.1016/j.scitotenv.2004.12.059>
- Mallory, M.L., McNicol, D.K., Cluis, D. a, Laberge, C., 1998. Chemical trends and status of small lakes near Sudbury, Ontario, 1983-1995: evidence of continued chemical recovery. *Can. J. Fish. Aquat. Sci.* 55, 63–75. <https://doi.org/10.1139/f97-213>
- Martin, A.J., Pedersen, T.F., 2004. Alteration to lake trophic status as a means to control arsenic mobility in a mine-impacted lake. *Water Res.* 38, 4415–4423. <https://doi.org/10.1016/j.watres.2004.08.025>
- Martin, A.J., Pedersen, T.F., 2002. Seasonal and Interannual Mobility of Arsenic in a Lake Impacted by Metal Mining. *Environ. Sci. Technol.* 36, 1516–1523.
- Martin, S.L., Soranno, P.A., 2006. Lake landscape position: Relationships to hydrologic connectivity and landscape features. *Limnol. Oceanogr.* 51, 801–814. <https://doi.org/10.4319/lo.2006.51.2.0801>
- Martin, S.L., Soranno, P.A., Bremigan, M.T., Cheruvilil, K.S., 2011. Comparing hydrogeomorphic approaches to lake classification. *Environ. Manage.* 48, 957–974. <https://doi.org/10.1007/s00267-011-9740-2>
- Mathias, J.A., Barica, J., 1980. Factors Controlling Oxygen Depletion in Ice-Covered Lakes. *Can. J. Fish. Aquat. Sci.* 37, 185–194. <https://doi.org/10.1139/F80-024>
- Matschullat, J., 2000. Arsenic in the geosphere - A review. *Sci. Total Environ.* 249, 297–312. [https://doi.org/10.1016/S0048-9697\(99\)00524-0](https://doi.org/10.1016/S0048-9697(99)00524-0)
- Matschullat, J., Ottenstein, R., Reimann, C., 2000. Geochemical background - Can we calculate it? *Environ. Geol.* 39, 990–1000. <https://doi.org/10.1007/s002549900084>
- McClain, M.E., Boyer, E.W., Dent, C.L., Gergel, S.E., Grimm, N.B., Groffman, P.M., Hart, S.C., Harvey, J.W., Johnston, C.A., Mayorga, E., McDowell, W.H., Pinay, G., 2003.

- Biogeochemical Hot Spots and Hot Moments at the Interface of Terrestrial and Aquatic Ecosystems. *Ecosystems* 6, 301–312. <https://doi.org/10.1007/s10021-003-0161-9>
- McClelland, J.W., Déry, S.J., Peterson, B.J., Holmes, R.M., Wood, E.F., 2006. A pan-arctic evaluation of changes in river discharge during the latter half of the 20th century. *Geophys. Res. Lett.* 33, 2–5. <https://doi.org/10.1029/2006GL025753>
- McCleskey, R.B., Nordstrom, D.K., Maest, A.S., 2004. Preservation of water samples for arsenic(III/V) determinations: An evaluation of the literature and new analytical results. *Appl. Geochemistry* 19, 995–1009. <https://doi.org/10.1016/j.apgeochem.2004.01.003>
- McKenzie, J., Kurylyk, B., Walvoord, M., Bense, V., Fortier, D., Spence, C., Grenier, C., 2020. Invited Perspective: What Lies Beneath a Changing Arctic? *Cryosph. Discuss.* 1–10. <https://doi.org/10.5194/tc-2020-132>
- McMartin, I., Henderson, P.J., Nielsen, E., 1999. Impact of a base metal smelter on the geochemistry of soils of the Flin Flon region, Manitoba and Saskatchewan 1, 1. <https://doi.org/10.1139/cjes-36-2-141>
- Mielko, C., Woo, M.K., 2006. Snowmelt runoff processes in a headwater lake and its catchment, subarctic Canadian Shield. *Hydrol. Process.* 20, 987–1000. <https://doi.org/10.1002/hyp.6117>
- Mikutta, C., Kretzschmar, R., 2011. Spectroscopic evidence for ternary complex formation between arsenate and ferric iron complexes of humic substances. *Environ. Sci. Technol.* 45, 9550–9557. <https://doi.org/10.1021/es202300w>
- Miller, C., Parsons, M.B., Jamieson, H.E., Swindles, G.T., Nasser, N.A., Galloway, J.M., 2019. Lake-specific controls on the long-term stability of mining-related, legacy arsenic contamination and geochemical baselines in a changing northern environment, Tundra Mine, Northwest Territories, Canada. *Appl. Geochemistry* 109. <https://doi.org/https://doi.org/10.1016/j.apgeochem.2019.104403>.
- Miller, C.B., Parsons, M.B., Jamieson, H.E., Ardakani, O.H., Gregory, B.R.B., Galloway, J.M., 2020. Influence of late-Holocene climate change on the solid-phase speciation and long-term stability of arsenic in sub-Arctic lake sediments. *Sci. Total Environ.* 709, 136115. <https://doi.org/10.1016/j.scitotenv.2019.136115>
- Mitsunobu, S., Harada, T., Takahashi, Y., 2006. Comparison of antimony behavior with that of arsenic under various soil redox conditions. *Environ. Sci. Technol.* 40, 7270–7276. <https://doi.org/10.1021/es060694x>
- Mitsunobu, S., Takahashi, Y., Terada, Y., Sakata, M., 2010. Antimony(V) incorporation into synthetic ferrihydrite, goethite, and natural iron oxyhydroxides. *Environ. Sci. Technol.* 44, 3712–3718. <https://doi.org/10.1021/es903901e>
- Moir, I., Falck, H., Hauser, R.L., Robb, M., 2006. The history of mining and its impact on the development of Yellowknife; in *Gold in the Yellowknife Greenstone Belt, Northwest Territories*, in: Anglin, C.D., Falck, H., Wright, D.F., Ambrose, E.J. (Eds.), *Results of the EXTECH III Multidisciplinary Research Project*. Geological Association of Canada, Mineral Deposits Division, Special Publication No. 3., pp. 11–28.

- Novak, M., Erbanova, L., Fottova, D., Cudlin, P., Kubena, A., 2011. Behaviour of arsenic in forested catchments following a high-pollution period. *Environ. Pollut.* 159, 204–211. <https://doi.org/10.1016/j.envpol.2010.09.002>
- Nriagu, J.O., 1983. Arsenic enrichment in lakes near the smelters at Sudbury, Ontario. *Geochim. Cosmochim. Acta* 47, 1523–1526. [https://doi.org/10.1016/0016-7037\(83\)90311-3](https://doi.org/10.1016/0016-7037(83)90311-3)
- O'Day, P.A., Vlassopoulos, D., Root, R., Rivera, N., 2004. The influence of sulfur and iron on dissolved arsenic concentrations in the shallow subsurface under changing redox conditions. *Proc. Natl. Acad. Sci.* 101, 13703–13708. <https://doi.org/10.1073/pnas.0402775101>
- Orihel, D.M., Baulch, H.M., Casson, N.J., North, R.L., Parsons, C.T., Seckar, D.C.M., Venkiteswaran, J.J., 2017. Internal phosphorus loading in Canadian fresh waters: a critical review and data analysis. *Can. J. Fish. Aquat. Sci.* 2029, 1–25. <https://doi.org/10.1139/cjfas-2016-0500>
- Orihel, D.M., Rooney, R.C., 2012. A field-based technique for sediment incubation experiments. *J. Limnol.* 71, 233–235. <https://doi.org/10.3274/JL12-71-1-N1>
- Palmer, M.J., Chételat, J., Jamieson, H.E., Richardson, M.C., Amyot, M., 2020. Hydrologic control on winter dissolved oxygen mediates arsenic cycling in a small subarctic lake. *Limnol. Oceanogr.* 1–17. <https://doi.org/10.1002/lno.11556>
- Palmer, M.J., Chételat, J., Richardson, M., Jamieson, H.E., Galloway, J.M., 2019. Seasonal variation of arsenic and antimony in surface waters of small subarctic lakes impacted by legacy mining pollution near Yellowknife, NT, Canada. *Sci. Total Environ.* 684, 326–339. <https://doi.org/10.1016/j.scitotenv.2019.05.258>
- Palmer, M.J., Galloway, J.M., Jamieson, H.E., Patterson, R.T., Falck, H., Kokelj, S. V., 2015. The concentration of arsenic in lake waters of the Yellowknife area, NWT Open File 2015-06.
- Palmer, M.J., Jamieson, H.E., Borčinová Radková, A., Maitland, K., Oliver, J., Falck, H., Richardson, M., 2021. Mineralogical, geospatial, and statistical methods combined to estimate geochemical background of arsenic in soils for an area impacted by legacy mining pollution. *Sci. Total Environ.* 776, 145926. <https://doi.org/10.1016/j.scitotenv.2021.145926>
- Parsons, C.T., Couture, R.M., Omeregic, E.O., Bardelli, F., Greneche, J.M., Roman-Ross, G., Charlet, L., 2013. The impact of oscillating redox conditions: Arsenic immobilisation in contaminated calcareous floodplain soils. *Environ. Pollut.* 178, 254–263. <https://doi.org/10.1016/j.envpol.2013.02.028>
- Parsons, M.B., Little, M.E., 2015. Establishing geochemical baselines in forest soils for environmental risk assessment in the montague and goldenville gold districts, Nova Scotia, Canada. *Atl. Geol.* 51, 364–386. <https://doi.org/10.4138/atlgeol.2015.017>
- Pelletier, N., Chételat, J., Cousens, B., Zhang, S., Stepner, D., Muir, D.C.G., Vermaire, J.C., 2020. Lead contamination from gold mining in Yellowknife Bay (Northwest Territories), reconstructed using stable lead isotopes. *Environ. Pollut.* 259. <https://doi.org/10.1016/j.envpol.2019.113888>
- Peryea, F.J., Creger, T.L., 1994. Vertical distribution of lead and arsenic in soils contaminated

- with lead arsenate pesticide residues. *Water. Air. Soil Pollut.* 78, 297–306.
<https://doi.org/10.1007/BF00483038>
- Peterson, B.J., Holmes, R.M., McClelland, J.W., Vörösmarty, C.J., Lammers, R.B., Shiklomanov, A.I., Shiklomanov, I.A., Rahmstorf, S., 2002. Increasing river discharge to the Arctic Ocean. *Science* (80-.). 298, 2171–2173. <https://doi.org/10.1126/science.1077445>
- Phan, V.T.H., Bernier-Latmani, R., Tisserand, D., Bardelli, F., Le Pape, P., Frutschi, M., Gehin, A., Couture, R.M., Charlet, L., 2019. As release under the microbial sulfate reduction during redox oscillations in the upper Mekong delta aquifers, Vietnam: A mechanistic study. *Sci. Total Environ.* 663, 718–730. <https://doi.org/10.1016/j.scitotenv.2019.01.219>
- Pieters, R., Lawrence, G.A., 2009. Effect of salt exclusion from lake ice on seasonal circulation. *Limnol. Oceanogr.* 54, 401–412. <https://doi.org/10.4319/lo.2009.54.2.0401>
- Qi, Y., Donahoe, R.J., 2008. The environmental fate of arsenic in surface soil contaminated by historical herbicide application. *Sci. Total Environ.* 405, 246–254.
<https://doi.org/10.1016/j.scitotenv.2008.06.043>
- Reimann, C., Banks, D., De Caritat, P., 2000. Impacts of airborne contamination on regional soil and water quality: The Kola Peninsula, Russia. *Environ. Sci. Technol.* 34, 2727–2732.
<https://doi.org/10.1021/es9912933>
- Reimann, C., de Caritat, P., 2017. Establishing geochemical background variation and threshold values for 59 elements in Australian surface soil. *Sci. Total Environ.* 578, 633–648.
<https://doi.org/10.1016/j.scitotenv.2016.11.010>
- Reimann, C., De Caritat, P., 2005. Distinguishing between natural and anthropogenic sources for elements in the environment: Regional geochemical surveys versus enrichment factors. *Sci. Total Environ.* 337, 91–107. <https://doi.org/10.1016/j.scitotenv.2004.06.011>
- Reimann, C., Filzmoser, P., 2000. Normal and lognormal data distribution in geochemistry: Death of a myth. Consequences for the statistical treatment of geochemical and environmental data. *Environ. Geol.* 39, 1001–1014. <https://doi.org/10.1007/s002549900081>
- Reimann, C., Filzmoser, P., Garrett, R.G., 2005. Background and threshold: Critical comparison of methods of determination. *Sci. Total Environ.* 346, 1–16. https://doi.org/10.1007/978-3-642-35470-0_54
- Reimann, C., Garrett, R.G., 2005. Geochemical background - Concept and reality. *Sci. Total Environ.* 350, 12–27. <https://doi.org/10.1016/j.scitotenv.2005.01.047>
- Reimann, C., Matschullat, J., Birke, M., Salminen, R., 2009. Arsenic distribution in the environment: The effects of scale. *Appl. Geochemistry* 24, 1147–1167.
<https://doi.org/10.1016/j.apgeochem.2009.03.013>
- Rember, R.D., Trefry, J.H., 2004. Increased concentrations of dissolved trace metals and organic carbon during snowmelt in rivers of the alaskan arctic. *Geochim. Cosmochim. Acta* 68, 477–489. [https://doi.org/10.1016/S0016-7037\(03\)00458-7](https://doi.org/10.1016/S0016-7037(03)00458-7)
- Ren, M., Ding, S., Fu, Z., Yang, L., Tang, W., Tsang, D.C.W., Wang, D., Wang, Y., 2019. Seasonal antimony pollution caused by high mobility of antimony in sediments: In situ

- evidence and mechanical interpretation. *J. Hazard. Mater.* 367, 427–436.
<https://doi.org/10.1016/j.jhazmat.2018.12.101>
- Revel, G., Ayrault, S., 2000. Comparative use of INAA and ICP-MS methods for environmental studies. *J. Radioanal. Nucl. Chem.* 244, 73–80.
- Richardson, M., Chételat, J., MacMillan, G.A., Amyot, M., 2021. Mercury concentrations and associations with dissolved organic matter are modified by water residence time in eastern Canadian lakes along a 30° latitudinal gradient. *Limnol. Oceanogr.* 66, S64–S80.
<https://doi.org/10.1002/lno.11580>
- Riveros, P.A., Dutrizac, J.E., Chem, T.T., 2000. Recovery of marketable arsenic trioxide from arsenic-rich roaster dust, in: *Proceedings of the V International Conference on Clean Technologies for the Mining Industry*. pp. 135–149.
- Root, R.A., Dixit, S., Campbell, K.M., Jew, A.D., Hering, J.G., O'Day, P.A., 2007. Arsenic sequestration by sorption processes in high-iron sediments. *Geochim. Cosmochim. Acta* 71, 5782–5803. <https://doi.org/10.1016/j.gca.2007.04.038>
- Salminen, R., Tarvainen, T., 1997. The problem of defining geochemical baselines. A case study of selected elements and geological materials in Finland. *J. Geochemical Explor.* 60, 91–98.
- Schmidt, S.K., Moskal, W., De Mora, S.J., Howard-Williams, C., Vincent, W.F., 1991. Limnological properties of Antarctic ponds during winter freezing. *Antarct. Sci.* 3, 379–388. <https://doi.org/10.1017/S0954102091000482>
- Schroth, A.W., Giles, C.D., Isles, P.D.F., Xu, Y., Perzan, Z., Druschel, G.K., 2015. Dynamic Coupling of Iron, Manganese, and Phosphorus Behavior in Water and Sediment of Shallow Ice-Covered Eutrophic Lakes. *Environ. Sci. Technol.* 49, 9758–9767.
<https://doi.org/10.1021/acs.est.5b02057>
- Schuh, C.E., Jamieson, H.E., Palmer, M.J., Martin, A.J., 2018. Solid-phase speciation and post-depositional mobility of arsenic in lake sediments impacted by ore roasting at legacy gold mines in the Yellowknife area, Northwest Territories, Canada. *Appl. Geochemistry* 91, 208–220. <https://doi.org/10.1016/j.apgeochem.2017.10.025>
- Schuh, C.E., Jamieson, H.E., Palmer, M.J., Martin, A.J., Blais, J.M., 2019. Controls governing the spatial distribution of sediment arsenic concentrations and solid-phase speciation in a lake impacted by legacy mining pollution. *Sci. Total Environ.* 654, 563–575.
<https://doi.org/10.1016/J.SCITOTENV.2018.11.065>
- Seeberg-Elverfeldt, J., Schluter, M., Feseker, T., Kolling, M., 2005. Rhizon sampling of porewaters near the sediment-water interface. *Limnol. Oceanogr. Methods* 361–371.
- Semkin, R.G., Mierle, G., Neureuther, R.J., 2005. Hydrochemistry and mercury cycling in a High Arctic watershed. *Sci. Total Environ.* 342, 199–221.
<https://doi.org/10.1016/j.scitotenv.2004.12.047>
- Senn, D.B., Gawel, J.E., Jay, J.A., Hemond, H.F., Durant, J.L., 2007. Long-Term Fate of a Pulse Arsenic Input to a Eutrophic Lake. *Environ. Sci. Technol.* 41, 3062–3068.
- Serfor-Armah, Y., Nyarko, B.J.B., Adotey, D.K., Dampare, S.B., Adomako, D., 2006. Levels of

- arsenic and antimony in water and sediment from Prestea, a gold mining town in Ghana and its environs. *Water, Air, Soil Pollut.* 175, 181–192. <https://doi.org/10.1007/s11270-006-9127-9>
- Shotbolt, L., 2010. Pore water sampling from lake and estuary sediments using Rhizon samplers. *J. Paleolimnol.* 44, 695–700. <https://doi.org/10.1007/s10933-008-9301-8>
- Silke, R., 2013. Giant Mine Milling and Roasting Process, Yellowknife, NWT A Historical Summary 30.
- Simmler, M., Bommer, J., Frischknecht, S., Christl, I., Kotsev, T., Kretzschmar, R., 2017. Reductive solubilization of arsenic in a mining-impacted river floodplain: Influence of soil properties and temperature. *Environ. Pollut.* 231, 722–731. <https://doi.org/10.1016/j.envpol.2017.08.054>
- Sivarajah, B., Cheney, C.L., Perrett, M., Kimpe, L.E., Blais, M., Smol, J.P., 2020. Regional gold mining activities and recent climate warming alter diatom assemblages in deep sub-Arctic lakes. *Polar Biol.* <https://doi.org/10.1007/s00300-020-02635-0>
- Sivarajah, B., Korosi, J.B., Blais, J.M., Smol, J.P., 2019. Multiple environmental variables influence diatom assemblages across an arsenic gradient in 33 subarctic lakes near abandoned gold mines. *Hydrobiologia* 1. <https://doi.org/10.1007/s10750-019-04014-1>
- Smedley, P.L., Kinniburgh, D.G., 2002. A review of the source, behaviour and distribution of arsenic in natural waters. *Appl. Geochemistry* 17, 517–568. [https://doi.org/10.1016/S0883-2927\(02\)00018-5](https://doi.org/10.1016/S0883-2927(02)00018-5)
- Smith, E., Naidu, R., Alston, A.M., Donald, L.S., 1998. Arsenic in the Soil Environment: A Review. *Adv. Agron.* 64, 149–195. [https://doi.org/http://dx.doi.org/10.1016/S0065-2113\(08\)60504-0](https://doi.org/http://dx.doi.org/10.1016/S0065-2113(08)60504-0)
- Sø, H.U., Postma, D., Jakobsen, R., Larsen, F., 2012. Competitive adsorption of arsenate and phosphate onto calcite; experimental results and modeling with CCM and CD-MUSIC. *Geochim. Cosmochim. Acta* 93, 1–13. <https://doi.org/10.1016/j.gca.2012.06.021>
- Spence, C., 2006. Hydrological processes and streamflow in a lake dominated watercourse. *Hydrol. Process.* 20, 3665–3681. <https://doi.org/10.1002/hyp>
- Spence, C., Guan, X.J., Phillips, R., Hedstrom, N., Granger, R., Reid, B., 2009. Storage dynamics and streamflow in a catchment with a variable contributing area. *Hydrol. Process.* 24, 2209–2221. <https://doi.org/10.1002/hyp.7492>
- Spence, C., Kokelj, S.A., Kokelj, S. V., Hedstrom, N., 2014. The process of winter streamflow generation in a subarctic Precambrian Shield catchment. *Hydrol. Process.* 28, 4179–4190. <https://doi.org/10.1002/hyp.10119>
- Spence, C., Kokelj, S.V., Kokelj, S.A., McCluskie, M., Hedstrom, N., 2015. Evidence of a change in water chemistry in Canada's subarctic associated with enhanced winter streamflow. *J. Geophys. Res. Biogeosciences* 120, 113–127. <https://doi.org/10.1002/2014JG002809>
- Spence, C., Kokelj, S. V., Ehsanzadeh, E., 2011. Precipitation trends contribute to streamflow

- regime shifts in northern Canada. IAHS-AISH Publ. 346, 3–8.
- Spence, C., Woo, M.K., 2006. Hydrology of subarctic Canadian Shield: Heterogeneous headwater basins. *J. Hydrol.* 317, 138–154. <https://doi.org/10.1016/j.jhydrol.2005.05.014>
- Spence, C., Woo, M.K., 2003. Hydrology of subarctic Canadian shield: Soil-filled valleys. *J. Hydrol.* 279, 151–166. [https://doi.org/10.1016/S0022-1694\(03\)00175-6](https://doi.org/10.1016/S0022-1694(03)00175-6)
- Splithoff, H.M., Mason, R.P., Hemond, H.F., 1995. Interannual Variability in the Speciation and Mobility of Arsenic in a Dimictic Lake. *Environ. Sci. Technol.* 29, 2157–2161. <https://doi.org/10.1021/es00008a041>
- St. Onge, S.M., 2007. Impacts of arsenic and sulphur dioxide contamination from mining activities on forest health near Yellowknife, NWT. Carleton University.
- Stubley, M.P., Irwin, D., 2019. Bedrock Geology of the Slave Craton, Northwest Territories and Nunavut. Yellowknife, NT.
- Sun, J., Quicksall, A.N., Chillrud, S.N., Mailloux, B.J., Bostick, B.C., 2016. Arsenic mobilization from sediments in microcosms under sulfate reduction. *Chemosphere* 153, 254–261. <https://doi.org/10.1016/j.chemosphere.2016.02.117>
- Sun, Q., Ding, S., Wang, Y., Xu, L., Wang, D., Chen, J., Zhang, C., 2016. In-situ characterization and assessment of arsenic mobility in lake sediments. *Environ. Pollut.* 214, 314–323. <https://doi.org/10.1016/j.envpol.2016.04.039>
- Szkokan-Emilson, E.J., Watmough, S.A., Gunn, J.M., 2014. Wetlands as long-term sources of metals to receiving waters in mining-impacted landscapes. *Environ. Pollut.* 192, 91–103. <https://doi.org/10.1016/j.envpol.2014.05.009>
- Tanaka, T., 1988. Distribution of arsenic in the natural environment with emphasis on rocks and soils. *Appl. Organomet. Chem.* 2, 283–295. <https://doi.org/10.1002/aoc.590020403>
- Tanamal, C., Blais, J.M., Yumvihoze, E., Chan, H.M., 2020. Health risk assessment of inorganic arsenic exposure through fish consumption in Yellowknife, Northwest Territories, Canada. *Hum. Ecol. Risk Assess.* 0, 1–22. <https://doi.org/10.1080/10807039.2020.1799187>
- Tang, Y., Zhang, M., Sun, G., Pan, G., 2019. Impact of eutrophication on arsenic cycling in freshwaters. *Water Res.* 150, 191–199. <https://doi.org/10.1016/j.watres.2018.11.046>
- Tank, S.E., Striegl, R.G., McClelland, J.W., Kokelj, S. V, 2016. Multi-decadal increases in dissolved organic carbon and alkalinity flux from the Mackenzie drainage basin to the Arctic Ocean. *Environ. Res. Lett.* 11, 054015. <https://doi.org/10.1088/1748-9326/11/5/054015>
- Taylor, M., Lau, B.P., Feng, S.Y., Bourque, C., Buick, J.K., Bondy, G.S., Cooke, G.M., 2013. Effects of oral exposure to arsenobetaine during pregnancy and lactation in sprague-dawley rats. *J. Toxicol. Environ. Heal. - Part A Curr. Issues* 76, 1333–1345. <https://doi.org/10.1080/15287394.2013.854715>
- Thienpont, J.R., Korosi, J.B., Hargan, K.E., Williams, T., Eickmeyer, D.C., Kimpe, L.E., Palmer, M.J., Smol, J.P., Blais, J.M., 2016. Multi-trophic level response to extreme metal

- contamination from gold mining in a subarctic lake. *Proc. R. Soc. B Biol. Sci.* 283, 20161125. <https://doi.org/10.1098/rspb.2016.1125>
- ThomasArrigo, L.K., Mikutta, C., Lohmayer, R., Planer-Friedrich, B., Kretzschmar, R., 2016. Sulfidization of Organic Freshwater Floccs from a Minerotrophic Peatland: Speciation Changes of Iron, Sulfur, and Arsenic. *Environ. Sci. Technol.* 50, 3607–3616. <https://doi.org/10.1021/acs.est.5b05791>
- Ukonmaanaho, L., Nieminen, T.M., Rausch, N., Shoty, W., 2004. Heavy metal and arsenic profiles in ombrogenous peat cores from four differently loaded areas in Finland. *Water. Air. Soil Pollut.* 158, 277–294. <https://doi.org/10.1023/B:WATE.0000044860.70055.32>
- Van Den Berghe, M.D., Jamieson, H.E., Palmer, M.J., 2018. Arsenic mobility and characterization in lakes impacted by gold ore roasting, Yellowknife, NWT, Canada. *Environ. Pollut.* 234, 630–641. <https://doi.org/10.1016/j.envpol.2017.11.062>
- Vincent, W.F., MacIntyre, S., Spigel, R.H., Laurion, I., 2008. The physical limnology of high-latitude lakes, in: Vincent, W.F., Laybourn-Parry, J. (Eds.), *Polar Lakes and Rivers: Limnology of Arctic and Antarctic Ecosystems*. Oxford University Press, p. 346.
- Vonk, J.E., Tank, S.E., Walvoord, M.A., 2019. Integrating hydrology and biogeochemistry across frozen landscapes 3–6. <https://doi.org/10.1038/s41467-019-13361-5>
- Vopel, K., Hawes, I., 2006. Photosynthetic performance of benthic microbial mats in Lake Hoare, Antarctica. *Limnol. Oceanogr.* 51, 1801–1812. <https://doi.org/10.4319/lo.2006.51.4.1801>
- Wagemann, R., Snow, N.B., Rosenberg, M., Lutz, A., 1978. Arsenic in sediments, water and aquatic biota from lakes in the vicinity of Yellowknife, Northwest Territories, Canada: RN - Arch. Environ. Contam. Toxicol., v. 7, p. 169-191. *Arch. Environ. Contam. Toxicol.* 7, 169–191.
- Walker, S.R., Jamieson, H.E., Lanzirrotti, A., Andrade, C.F., Hall, G.E.M., 2005. The speciation of arsenic in iron oxides in mine wastes from the Giant gold mine, N.W.T.: Application of synchrotron micro-XRD and micro-XANES at the grain scale. *Can. Mineral.* 43, 1205–1244.
- Walker, S.R., Jamieson, H.E., Lanzirrotti, A., Hall, G.E.M., Peterson, R.C., 2015. The effect of ore roasting on arsenic oxidation state and solid phase speciation in gold mine tailings. *Geochemistry Explor. Environ. Anal.* 15, 273–291. <https://doi.org/10.1144/geochem2013-238>
- Walvoord, M.A., Kurylyk, B.L., 2016. Hydrologic Impacts of Thawing Permafrost-A Review. *Vadose Zo. J.* 15, vzj2016.01.0010. <https://doi.org/10.2136/vzj2016.01.0010>
- Walvoord, M.A., Striegl, R.G., 2007. Increased groundwater to stream discharge from permafrost thawing in the Yukon River basin: Potential impacts on lateral export of carbon and nitrogen. *Geophys. Res. Lett.* 34. <https://doi.org/10.1029/2007GL030216>
- Wang, S., Mulligan, C.N., 2006. Occurrence of arsenic contamination in Canada: Sources, behavior and distribution. *Sci. Total Environ.* 366, 701–721. <https://doi.org/10.1016/j.scitotenv.2005.09.005>

- Warnken, J., Ohlsson, R., Welsh, D.T., Teasdale, P.R., Chelsky, A., Bennett, W.W., 2017. Antimony and arsenic exhibit contrasting spatial distributions in the sediment and vegetation of a contaminated wetland. *Chemosphere* 180, 388–395. <https://doi.org/10.1016/j.chemosphere.2017.03.142>
- Wauthy, M., Rautio, M., Christoffersen, K.S., Forsström, L., Laurion, I., Mariash, H.L., Peura, S., Vincent, W.F., 2018. Increasing dominance of terrigenous organic matter in circumpolar freshwaters due to permafrost thaw. *Limnol. Oceanogr. Lett.* 3, 186–198. <https://doi.org/10.1002/lo2.10063>
- Weber, F.A., Hofacker, A.F., Voegelin, A., Kretzschmar, R., 2010. Temperature dependence and coupling of iron and arsenic reduction and release during flooding of a contaminated soil. *Environ. Sci. Technol.* 44, 116–122. <https://doi.org/10.1021/es902100h>
- WHO, 2011. Arsenic in drinking water: Background document for development of WHO guidelines for drinking water quality. Geneva, Switzerland.
- Willemsse, N.W., Van Dam, O., Van Helvoort, P.J., Dankers, R., Brommer, M., Schokker, J., Valstar, T.E., De Wolf, H., 2004. Physical and chemical limnology of a subsaline athalassic lake in West Greenland. *Hydrobiologia* 524, 167–192. <https://doi.org/10.1023/B:HYDR.0000036132.96154.01>
- Williamson, C.E., Saros, J.E., Vincent, W.F., Smol, J.P., 2009. Lakes and reservoirs as sentinels, integrators, and regulators of climate change. *Limnol. Oceanogr.* 54, 2273–2282. https://doi.org/10.4319/lo.2009.54.6_part_2.2273
- Wolfe, S.A., Kerr, D., Morse, P.D., 2017a. Slave Geological Province: An Archetype of Glaciated Shield Terrain, in: Slaymaker, O. (Ed.), *Landscapes and Landforms of Western Canada*. Springer, pp. 381–393. <https://doi.org/10.1007/978-3-319-44595-3>
- Wolfe, S.A., Morse, P.D., 2016. Lithalsa Formation and Holocene Lake-Level Recession, Great Slave Lowland, Northwest Territories. *Permafr. Periglac. Process.* <https://doi.org/10.1002/ppp.1901>
- Wolfe, S.A., Morse, P.D., Kokelj, S.V.S.V., Gaanderse, A.J., 2017b. Great Slave Lowland: The Legacy of Glacial Lake McConnell, in: Slaymaker, O. (Ed.), *Landscapes and Landforms of Western Canada*. Springer, pp. 87–96.
- Woodfine, D.G., Havas, M., 1995. Pathways of chemical recovery in acidified, metal-contaminated lakes near Sudbury, Ontario, Canada. *Water, Air Soil Pollut.* 85, 797–803.
- Woolway, R.I., Kraemer, B.M., Lenters, J.D., Merchant, C.J., O'Reilly, C.M., Sharma, S., 2020. Global lake responses to climate change. *Nat. Rev. Earth Environ.* 1, 388–403. <https://doi.org/10.1038/s43017-020-0067-5>
- Wrye, L.A., 2008. Distinguishing between natural and anthropogenic sources of arsenic in soils from the Giant mine, Northwest Territories and the North Brookfield mine, Nova Scotia. Queen's University.
- Xu, X., Chen, C., Wang, P., Kretzschmar, R., Zhao, F.J., 2017. Control of arsenic mobilization in paddy soils by manganese and iron oxides. *Environ. Pollut.* 231, 37–47. <https://doi.org/10.1016/j.envpol.2017.07.084>

- Yang, H., He, M., Wang, X., 2014. Concentration and speciation of antimony and arsenic in soil profiles around the world's largest antimony metallurgical area in China. *Environ. Geochem. Health* 37, 21–33. <https://doi.org/10.1007/s10653-014-9627-2>
- Yang, L., Donahoe, R.J., 2007. The form, distribution and mobility of arsenic in soils contaminated by arsenic trioxide, at sites in southeast USA. *Appl. Geochemistry* 22, 320–341. <https://doi.org/10.1016/j.apgeochem.2006.11.005>
- Yuan, Z.F., Gustave, W., Boyle, J., Sekar, R., Bridge, J., Ren, Y., Tang, X., Guo, B., Chen, Z., 2021. Arsenic behavior across soil-water interfaces in paddy soils: Coupling, decoupling and speciation. *Chemosphere* 269, 128713. <https://doi.org/10.1016/j.chemosphere.2020.128713>
- Zhang, C.P., Wu, P., Tang, C.Y., Xie, H.H., Zeng, Z.C., Yang, S.Z., 2014. Geochemical behavior of arsenic in reducing sulfidic sediments of reservoir contaminated by acid mine drainage. *Environ. Earth Sci.* 71, 4341–4351. <https://doi.org/10.1007/s12665-013-2828-7>
- Zogorski, J.S., Carter, J.M., Ivahnenko, T., Lapham, W.W., Moran, M.J., Rowe, B.L., Squillace, P.J., Toccalino, P.L., 2006. Volatile organic compounds in the nation's ground water and drinking-water supply wells, USGS, Circular 1292. <https://doi.org/10.1080/19443994.2014.925829>

Appendices

Appendix A: Supporting information for Chapter 3 - Arsenic in soils of the Yellowknife area: Regional distribution, attribution of source, and estimation of geochemical background

Sample homogeneity and analytical reproducibility

Grain size can have an important influence on soil concentrations of metal(loid)s, with concentrations typically increasing with a decrease in grain size due to larger available surface area for adsorption (Acosta et al., 2011). In this study, samples were not sieved and only gently ground prior to analysis to preserve the material as it would be encountered in the field. To test the influence of sieving on samples in this study, a subset of samples (N = 19) were split and one paired sample was sieved to < 2 mm and the other sample was not sieved. Results indicate comparable results between the sieved and unsieved portions of the samples (Figure A1).

There was a high degree of variability in field duplicates, with 72% of samples (N = 29) recording a relative percent difference (RPD) between the parent and duplicate sample > 20%. The lack of consistency in field duplicates is not surprising, since soil characteristics can vary substantially within a small area affecting soil chemistry. Additionally, several of the potential As-hosting minerals contain large amounts of As (i.e. As_2O_3 76 wt% As; and FeAsS 46 wt% As), therefore an uneven distribution of these As-rich but rare particles between samples would result in large differences in bulk As concentrations.

Analytical accuracy was assessed using repeated measurements (N = 44) of standard reference materials (SS-1 and SS-2, SCP Science, Québec, Canada; and MESS-3 and MESS-4, National Research Council Canada). The relative percent difference between standard and analytical values was < 12%, except for one SS-1 sample with an RPD of 23% (Jamieson et al. 2017). Details on all of this information are available in Jamieson et al. (2017).

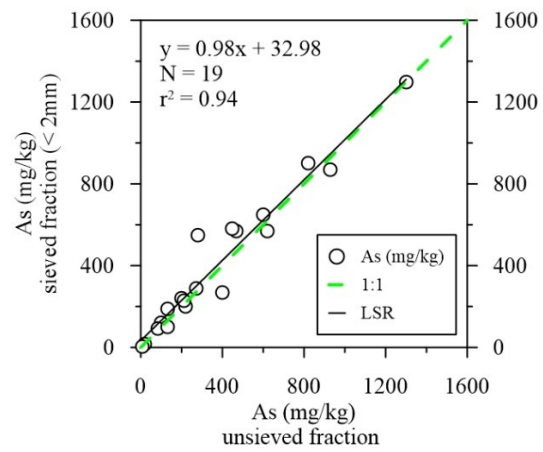


Figure A1 Comparison of As concentrations in sieved (< 2 mm) and unsieved samples from the Public Health layer.

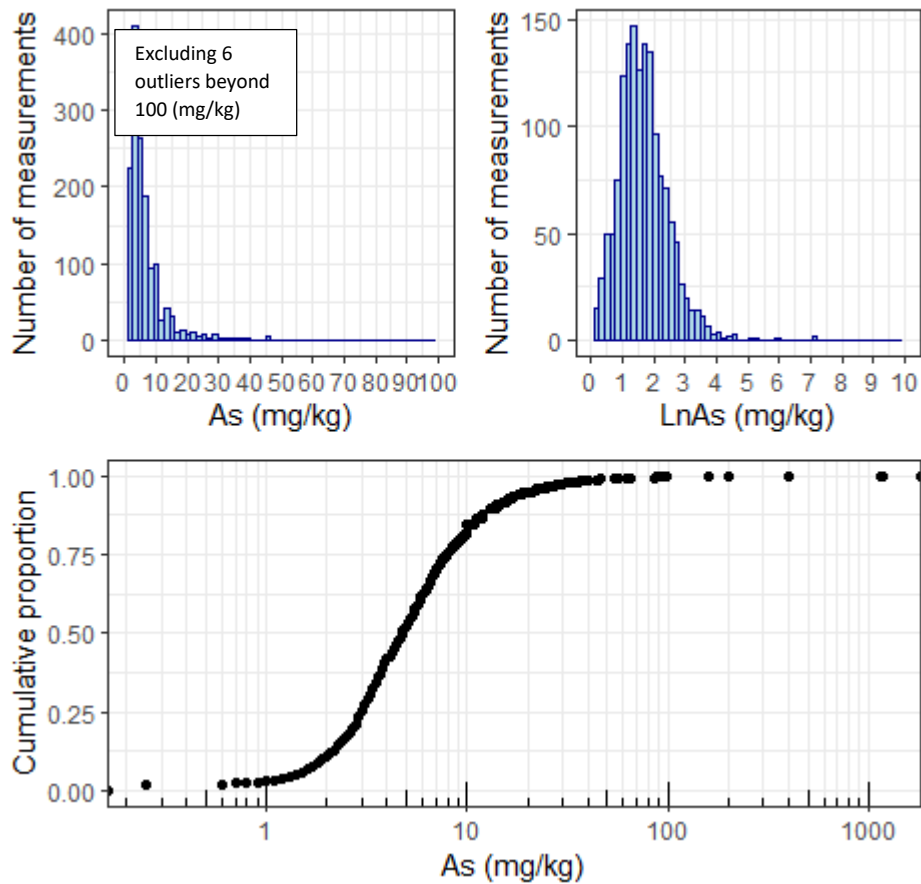


Figure A2 Arsenic distribution plots for Kerr and Knight (2005) data beyond 20 km from Yellowknife (N = 1490). Upper two plots represent histograms of normal and ln-transformed data. Bottom plot is a cumulative frequency plot for the untransformed data. The data are significantly different from a normal (Shapiro-Wilk test: $W = 0.08$, $p < 0.001$) and lognormal distribution (Shapiro-Wilk test: $W = 0.95$, $p < 0.001$).

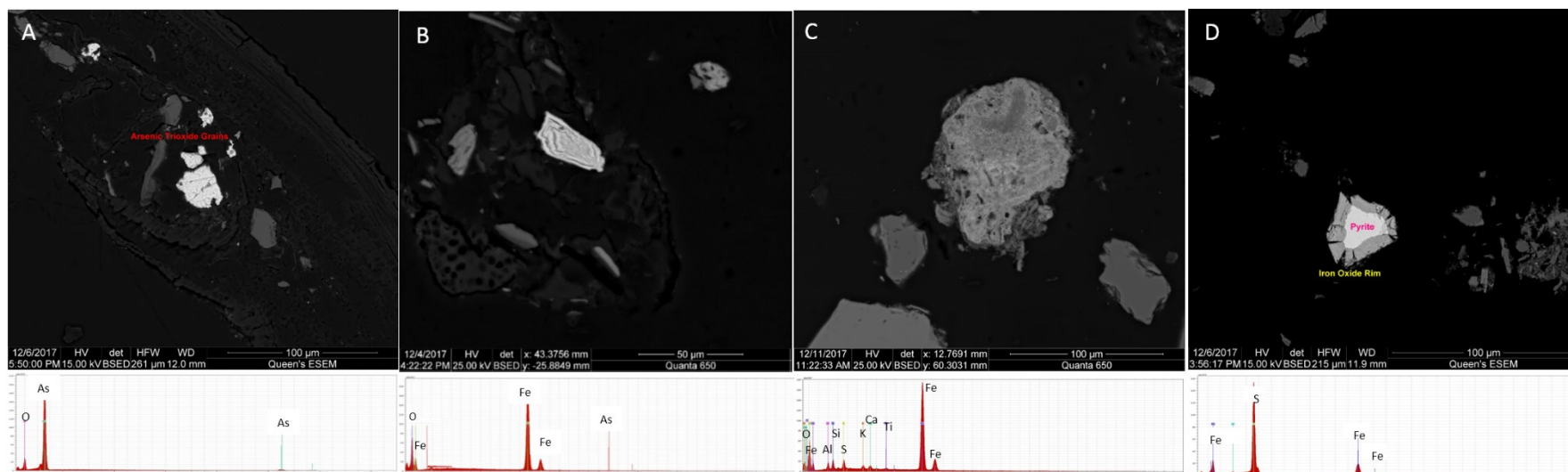


Figure A3 SEM images and EDS spectra for selected minerals discussed in this study, including: A) arsenic trioxide (BPR-OSC-93 PH); B) roaster generated Fe-oxide (sample INGT-OSG-46) (note no signal for As, since no As detected below 3 wt% As); C) authigenic Fe-oxyhydroxide (TX – OSC – 145 PH); and D) pyrite with oxidation rim (HW3 – 135 PH).

Table A1. Field and analytical methods from the independent till soil collection programs included in this study.

<i>Study</i>	<i>N</i>	<i>Soil type</i>	<i>Sampling interval</i>	<i>Sieved fraction</i>	<i>Digestion</i>	<i>Analytical method</i>	<i>Data source</i>
GSC Open File 7196	251	Till	Composite > 10 cm below surface	63 µm	<i>Aqua regia</i>	ICP-MS	Kjarsgaard et al. 2013
NTGS Open File 2017-03	60	Variable	> 15 cm below surface	N/A	<i>Aqua regia</i>	ICP-OES	Jamieson et al. 2017
NTGS Open File 2020-08	155	Till	Composite C-horizon > 10 cm below surface	63 µm	<i>Aqua regia</i>	ICP-MS	Normandeau 2020
GSC Open File 5015	1564	Till	Composite 10-70cm below surface	63 µm	N/A	INAA	Kerr and Knight, 2005

Table A2. Mineralogical information used for solid-phase arsenic mass distribution calculations

<i>As-hosting phase</i>	<i>Formula</i>	<i>Density (g/m³)</i>	<i>Wt. % As</i>	<i>Source</i>
Fe-oxyhydroxide	FeOOH	4500000	3.00	Walker et al. (2005); Schuh et al. (2018)
Mn-oxyhydroxide	MnOOH	4000000	3.00	Maitland (2019)
Realgar	AsS	3560000	70.03	Mineralogical Society of America (2000)
Pyrite	FeS ₂	5010000	0.68	Mineralogical Society of America (2000); Chryssoulis (1990)
Arsenic trioxide	As ₂ O ₃	3700000	75.74	Mineralogical Society of America (2000)
Arsenopyrite	FeAsS	6070000	46.01	Mineralogical Society of America (2000)
Fe-Ca arsenate		3920000	15	Bailey (2017)
Enargite	Cu ₃ AsS ₄	4450000	19	Mineralogical Society of America (2000)
Scorodite	FeAsO ₄ ·2H ₂ O	3290000	32	Mineralogical Society of America (2000)
Organics		3000000	3	Maitland (2019)

Table A3. Generalized linear model (GLM) results for influence of distance, direction and terrain unit on ln-transformed As concentrations in Public Health layer soils within 30 km of Yellowknife. The independent R^2 represents the unique contribution of that variable to the total, unadjusted R^2 of the GLM. See methods for additional details on the calculation of independent R^2 .

<i>Effect</i>	<i>p-value</i>	<i>F-value</i>	<i>Independent R²</i>
ln(Distance to Giant Mine)	< 0.0001	233.5	0.39
Normalized Direction	< 0.0001	21.5	0.06
Terrain unit	< 0.0001	14.3	0.08
	Total R^2 (unadjusted)		0.53
	Adjusted R^2		0.52

Table A4. Arsenic mineral distributions in Public Health layer soil samples as determined by SEM-MLA (see methods for details)

Sample	Lat	Long	Distance to Giant roaster (km)	Distance to Con roaster (km)	Total As (mg kg ⁻¹)	As distribution mass%										Total%
						Realgar	Fe Oxides - with As	Mn oxide with As (+Fe, Ca, Al)	A ₂ O ₃	Organics with As	Pyrite	Arsenopyrite	Scorodite	Ca-Fe arsenate	Enargite	
BPR-OSC-93PH	62.5068	-114.371	0.89	8.33	2300	2	1	0	96	1	0	0	0	0	0	100
G-WGM-14	62.4986	-114.384	1.43	7.46	2100	0.1	0	0.5	96.8	0.2	0.1	0.6	1.7	0	0	100
G-WGM-21	62.4982	-114.384	1.44	7.43	4700	0	2.5	3.8	83.2	3.8	0.7	0	6	0	0	100
G-WGM-17	62.4985	-114.384	1.44	7.45	1900	0	0	0	98.5	0.1	0	0.1	1.3	0	0	100
G-WGM-21-Dup	62.4982	-114.384	1.44	7.43	1900	0	0	0	99.4	0	0.1	0	0.5	0	0	100
BPR-OSC-01PH	62.4988	-114.384	1.45	7.49	1800	4.7	0.5	0	94.2	0.6	0	0	0	0	0	100
G-WGM-44	62.4986	-114.384	1.45	7.47	1900	0	0	2.9	96.9	0.1	0.1	0	0	0	0	100
G-WGM-23	62.4982	-114.384	1.45	7.43	1800	0	0	0	98.1	0.6	0	0.4	0.9	0	0	100
BPR-PSC-161PH	62.4965	-114.384	1.51	7.23	3400	0	0.2	0	95.8	0	0	4	0	0	0	100
BPR-PSC-160PH	62.4961	-114.385	1.56	7.20	1000	0	4	0	96	0	0	0	0	0	0	100
YK-20-Dup	62.5172	-114.376	1.93	9.50	800	0	0	0	96.7	0	0.7	0	2.6	0	0	100
YK-20	62.5172	-114.376	1.93	9.50	760	0	0	0	98.8	0.4	0.3	0	0.5	0	0	100
BPR-FCSC-14PH	62.4873	-114.391	2.39	6.29	500	0	0	0	97.5	0	0.1	0	0.1	2.3	0	100
NDILO-FCSC-25	62.4789	-114.33	2.86	5.53	280	0	6.8	85.6	0.26	0	0.5	0	6.69	0	0.15	100
NDILO-OSC-23	62.4753	-114.335	3.18	5.12	220	0	0.9	0.2	98.8	0	0	0	0	0.1	0	100
NDILO-OSC-23 D	62.4753	-114.335	3.18	5.12	220	0	2.6	0.2	88.2	0.3	0.8	0	2.1	5.8	0	100
YK67 OSC 06PH	62.4878	-114.298	3.41	7.15	62	0	3.1	0	96	0	0.5	0	0	0.4	0	100
YK-24	62.5359	-114.34	3.87	11.65	180	0	0	86.6	13.4	0	0	0	0	0	0	100
G-SIT-03	62.4734	-114.409	4.15	5.10	390	0	0.6	0	98.5	0.1	0.8	0	0	0	0	100
G-SIT-47	62.4726	-114.407	4.16	4.97	1100	0	0	3.3	94.6	0	0.1	2	0	0	0	100
G-SIT-27	62.4726	-114.409	4.21	5.00	3000	0	11.8	79.1	8.9	0.1	0.1	0	0	0	0	100
BPR-FENC-18PH	62.4732	-114.411	4.23	5.12	120	68.2	26	0	0	0	5.8	0	0	0	0	100
G-SIT-20	62.4722	-114.409	4.25	4.97	390	0.3	0	0	99.6	0	0.1	0	0	0	0	100
G-SIT-20-DUP	62.4722	-114.409	4.25	4.97	160	1.9	0	0	97.1	0	1	0	0	0	0	100
G-SIT-53	62.4719	-114.41	4.31	4.96	450	0	0	10.3	88.5	0	1.2	0	0	0	0	100
LL-06	62.4781	-114.43	4.57	6.06	290	0	0	0.7	99	0.1	0	0.1	0.1	0	0	100
ML-OSC-98PH	62.5383	-114.411	4.88	12.04	210	0	2.1	0	97.1	0.7	0.1	0	0	0	0	100
LL-04	62.4795	-114.441	4.99	6.52	450	0	0	0	100	0	0	0	0	0	0	100

Table A4 (cont'd). Arsenic mineral distributions in Public Health layer soil samples as determined by SEM-MLA.

Sample	Lat	Long	Distance to Giant roaster (km)	Distance to Con roaster (km)		As distribution mass%										Total%
						Realgar	Fe Oxides - with As	Mn oxide with As (+Fe, Ca, Al)	A ₂ O ₃	Organics with As	Pyrite	Arsenopyrite	Scorodite	Ca-Fe arsenate	Enargite	
ML-FCOSC-97PH D	62.5414	-114.41	5.16	12.38	400	0	4.9	0	93.2	1.9	0	0	0	0	0	100
DETR-FCSC-34PH	62.4594	-114.299	5.59	4.63	270	0	3.4	0	77.6	1.9	0.8	16.3	0	0	0	100
TX-FCSC-144	62.5571	-114.36	6.13	13.93	130	0	15.7	2.5	81.5	0.1	0.2	0	0	0	0	100
TX-FCSC-144D	62.5571	-114.36	6.13	13.93	130	0	10.2	8.7	80.1	0.3	0.7	0	0	0	0	100
TX-OSC-145	62.5574	-114.36	6.16	13.96	43	0	59	0.3	0.3	0.1	17.3	23	0	0	0	100
LL-01	62.4834	-114.475	6.40	7.97	380	0	0	2.9	78.7	16.3	2.1	0	0	0	0	100
CM-25	62.4439	-114.353	6.47	1.52	570	0	23.8	62.2	9.9	0.5	3.6	0	0	0	0	100
LL-OSC-120	62.5577	-114.399	6.55	14.09	59	0	0.7	0	99	0.3	0	0	0	0	0	100
CM-24	62.4397	-114.393	7.16	1.57	710	0	8	0.7	76.2	0.8	0.6	0.2	13.5	0	0	100
DETR-OSC-37PH	62.4404	-114.309	7.29	3.15	220	0	0.4	0	96.9	0	1.5	0.7	0	0	0.5	100
DETR-FCSC-38PH	62.4402	-114.31	7.30	3.10	46	0	0.3	2	94.3	0.5	0	2.9	0	0	0	100
CM-22	62.4364	-114.351	7.30	0.97	590	17.3	59.2	21.8	1.3	0	0.1	0	0	0	0.3	100
LL-OSC-106	62.5666	-114.402	7.54	15.08	200	0	14.7	0	85.1	0	0.2	0	0	0	0	100
CM-23	62.4363	-114.4	7.63	1.77	330	0	7.2	0	45.1	2.5	0.9	0	42.8	0	1.5	100
NWC3-OSG-86	62.5067	-114.507	7.69	10.98	620	0	4.6	0	92.8	1	0.2	0	0	1.4	0	100
NWC1-FCSC-82PH	62.5381	-114.488	7.82	13.34	250	0.5	8.1	0	84.5	2.6	0.1	4.2	0	0	0	100
LL-PSC-117	62.5686	-114.411	7.89	15.36	24	0	97.9	0	0	0	2.1	0	0	0	0	100
TX-OSC-151	62.5796	-114.362	8.63	16.43	72	0	98.9	0	0	0.4	0.7	0	0	0	0	100
TX-OSG-152	62.5797	-114.362	8.64	16.44	210	0	51.6	33.7	1.5	13.2	0	0	0	0	0	100
TX-OSG-152D	62.5797	-114.362	8.64	16.44	210	0	45.5	1.5	45.8	0	0.3	0	0	6.9	0	100
CM-18	62.4262	-114.395	8.66	1.58	270	0	6.2	3.9	80.4	0.6	1.4	0	4.1	3.4	0	100
TX-FCOSC-155	62.5817	-114.355	8.86	16.67	78	0	3	0	96.8	0	0.2	0	0	0	0	100
YK-78	62.4188	-114.314	9.51	3.10	11	0	0	0	78	2.7	7.7	0	11.6	0	0	100
YK-05	62.4451	-114.498	9.62	6.90	370	0	0	15	83.9	0	0	0	1.1	0	0	100
CM-08	62.4155	-114.398	9.84	2.41	540	1.90	0.30	1.50	91.10	0.30	0.40	0.80	1.60	2.10	0	100
Grace-05	62.4188	-114.437	10.12	3.88	440	0	3.4	9.4	0	2.6	37.6	0	47	0	0	100
VL-FCSC-108	62.5918	-114.438	10.80	18.15	120	0	3	0	96.8	0	0.2	0	0	0	0	100
Grace-01	62.418	-114.465	10.86	5.26	81	0	0	0	95	0.1	1.5	0	3.4	0	0	100

Table A4 (cont'd). Arsenic mineral distributions in Public Health layer soil samples as determined by SEM-MLA.

Sample	Lat	Long	Distance to Giant roaster (km)	Distance to Con roaster (km)		As distribution mass%										Total%
						Realgar	Fe Oxides - with As	Mn oxide with As (+Fe, Ca, Al)	A ₂ O ₃	Organics with As	Pyrite	Arsenopyrite	Scorodite	Ca-Fe arsenate	Enargite	
TX-20	62.38	-114.428	14.05	6.57	650	0	0	1	99	0	0	0	0	0	0	100
EAST2-FCSC-66	62.4492	-114.088	15.03	14.50	52	0	11.6	0	34.5	0	2.4	51.5	0	0	0	100
MASL-OSC-65	62.4015	-114.143	15.69	12.02	87	0	1.6	0	97.6	0	0.3	0	0.5	0	0	100
HOML-PSC-58	62.656	-114.303	17.34	25.13	19	0	91.1	0	0	5.3	3.6	0	0	0	0	100
IL-11	62.6592	-114.38	17.52	25.28	13	0	0	0	0	0.2	4.5	4.8	53.4	0	37.1	100
DUF-OSC-54	62.6527	-114.468	17.70	25.10	52	0	11	0	89	0	0	0	0	0	0	100
IL-01	62.6608	-114.386	17.72	25.48	120	0	0	0	32.1	0.5	3.9	46	10.4	0	7.1	100
SW3-PSC-89	62.4028	-114.627	17.73	13.77	30	0	92.5	0	0	1	6.5	0	0	0	0	100
TX-02	62.6577	-114.281	17.74	25.49	200	0	0	86.1	1.9	0	0.9	11	0.1	0	0	100
YK-59	62.6032	-114.662	19.26	24.33	13	0	0	0	97.5	0	2.5	0	0	0	0	100
YK-66	62.4307	-113.995	20.23	19.15	12	0	0	0	91.3	0	3.4	0	5.3	0	0	100
YK-54	62.3549	-114.643	21.98	16.57	1	0	0	0	0	38.8	5.2	0	56	0	0	100
YK-39	62.5522	-113.94	22.11	25.69	63	0	0	0	0	3.6	0.6	0	95.8	0	0	100
YK-69	62.3347	-114.082	23.38	18.24	8.9	0	0	3.2	60.5	1.4	25.5	0	6.3	0	3.1	100
YK-68	62.3345	-114.082	23.41	18.27	6.2	0	0	0	0	0.6	0.5	94.4	4.5	0	0	100
MIR-OSG-01	62.2736	-114.46	25.95	18.25	8.1	0	6.3	0	83.3	0	10.4	0	0	0	0	100
YK-63	62.7555	-114.328	28.22	36.04	40	0	0	91.5	0	0	4.6	0	3.9	0	0	100
YK-62	62.756	-114.328	28.29	36.10	5.6	0	0	0	78.2	3.5	7.5	8.7	2.1	0	0	100
YK-61	62.7565	-114.329	28.33	36.15	1.6	0	0	72.3	0	0.4	0	0	27.3	0	0	100
YK-01	62.5276	-114.944	30.27	31.51	18	0	0	83.9	0	1	1.4	0	13.7	0	0	100
YK-36	62.5146	-113.751	31.17	32.99	53	0	0	0	73.3	0	16.3	0	10.4	0	0	100
BPR-OSC-22PH					470	1.2	0	0	96	0	0	0	2.8	0	0	100
BERRY-OSG-63					84	0	60.8	0.8	26.8	0	1.6	10	0	0	0	100

References

- Anthony, J.W., Bideaux, R.A., Bladh, K.W., 2000. Handbook of Mineralogy. Nichols, M. (ed.), Mineralogical Society of America, Chantilly, VA 20151-1110, USA.
<http://www.handbookofmineralogy.org/>.
- Bailey, A.S. 2017. Characterization of Arsenic-Hosting Solid Phases in Giant Mine Tailings and Tailings Dust. Queen's University. MSc Thesis.
<https://qspace.library.queensu.ca/handle/1974/22810>.
- Chryssoulis S. 1990. Detection and quantification of “invisible” gold by microprobe techniques. In Proc. Symp. Gold 90, Soc. for Mining, Metall. Explor. Hausen D. M, Halbe D. N., Petersen, and E. U. Tafuri (eds.), pp. 323–331.
- Kerr, D.E., Knight, R.D. 2005. Till geochemistry, Slave Province, Northwest Territories and Nunavut. Geological Survey of Canada, Open File 5015.
- Kjarsgaard, B. A., Knight, R.D., Sharpe, D.R., Kerr, D.E., Cummings, D.I., Russell, H.A.J., Lemkow, D. 2013. Till Geochemistry Studies of the Thaidene Nene MERA Study area. In, Mineral and Energy Resource Assessment of the proposed Thaidene Nene National Park Reserve in the area of the east arm of Great Slave Lake, Northwest Territories. Wright, D.F., Ambrose, E J, Lemkow, D., Bonham-Carter, G (eds.). Geological Survey of Canada, Open File 7196, p. 313-337, <https://doi.org/10.4095/292459> (Open Access).
- Maitland, K. M. 2019. Arsenic concentrations and solid phase speciation in soils in the Yellowknife region. MSc. Thesis. Queen's University. 259 p.
<https://qspace.library.queensu.ca/handle/1974/799/discover>

- Normandeau, P.X. 2020. Indicator minerals and till geochemistry applied to volcanogenic massive sulphide (VMS) and other greenstone belt related deposits exploration in the Slave Geological Province, NT. NTGS Open Report 2020-008.
- Schuh, C.E., Jamieson, H.E., Palmer, M.J., and Martin, A.J. 2018. Solid-phase speciation and post-depositional mobility of arsenic in lake sediments impacted by ore roasting at legacy gold mines in the Yellowknife area, Northwest Territories, Canada. *Applied Geochemistry* 91 (April): 208–20. <https://doi.org/10.1016/j.apgeochem.2017.10.025>.
- Walker, S.R., Jamieson, H.E. Lanzirrotti, A., Andrade, C.F., and Hall, G.E.M. 2005. The speciation of arsenic in iron oxides in mine wastes from the Giant gold mine, N.W.T.: Application of synchrotron micro-XRD and micro-XANES at the grain scale. *The Canadian Mineralogist*, 43: 1205-1244.

Appendix B: Supporting information for Chapter 4 - Seasonal variation of arsenic and antimony in surface waters of small subarctic lakes impacted by legacy mining pollution near Yellowknife, NT, Canada

Summary of field sampling and analytical methods for regional lake surveys from Palmer et al. (2015) and the resampling of 31 lakes in this study.

Surface water samples were collected for a variety of chemical and physical analyses from 86 lakes in either September 2012 or September 2014 from a helicopter equipped with pontoons. Thirty-one lakes were resampled in March 2015 to assess seasonal differences in lake water chemistry across the region. Best efforts were made to consistently sample in the center of lakes. During the open water season, water samples were collected from approximately 30 cm below the surface in 250 mL polyethylene containers that had been rinsed three times with lake water. During the ice-covered season, water samples were collected from a 20-cm diameter hole that was augered through the ice. All ice shavings were removed from the hole with a clean spoon and samples were collected from approximately 15 cm below the ice surface in 250 mL polyethylene containers that had been rinsed three times with lake water. Following collection, water samples were stored out of direct sunlight in a cooler with ice packs and immediately delivered to a laboratory accredited by the Canadian Association for Laboratory Accreditation (CALA) for analysis. Water samples were analyzed for 15 physical and chemical variables, including: Ca, Cl, F, Mg, K, Na, SO₄, dissolved organic carbon, dissolved inorganic carbon, NO₃-N, NO₂-N, dissolved and total nitrogen, and dissolved and total phosphorous following standard methods (Clesceri et al., 1998). Water samples were also analyzed for 15 dissolved metal(loid)s by inductively coupled plasma - mass spectrometry (ICP-MS) following EPA method 200.8 (Creed et al., 1994). These samples were filtered immediately on arrival at the laboratory using a 0.45 µm filter and acidified with high

purity nitric acid (HNO₃). Although we refer to these results as the “dissolved” fraction of the metal(loid)s in the sample, it should be recognized that colloids may pass through the 0.45 μm filter and may be included in the “dissolved” ICP-MS results. All water chemistry data used in the analyses, tables and figures presented in Palmer et al. (2015) are presented in Appendix 1 of Palmer et al. (2015).

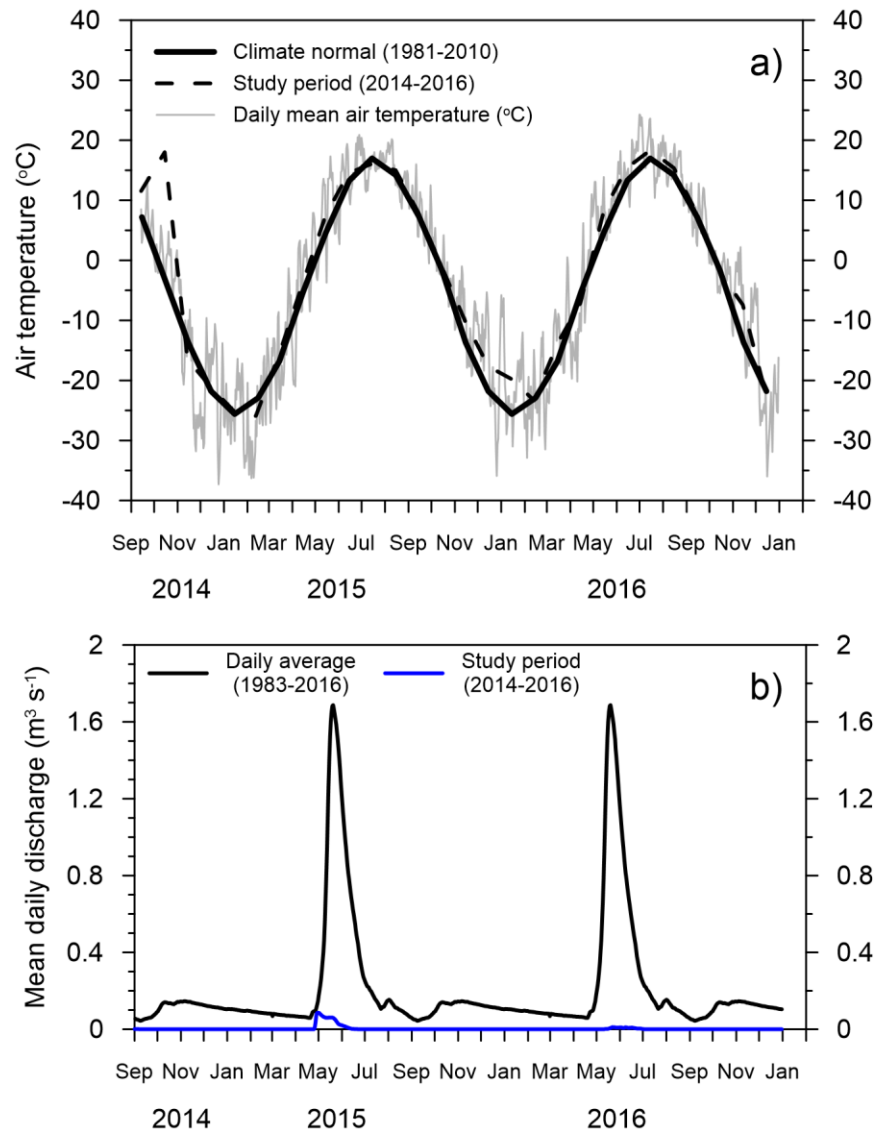


Figure B1: a) Air temperature at Yellowknife airport, including mean monthly air temperature from the climate normal (1981-2010) and the study period (September 2014 to December 2016), plus the mean daily air temperature during the study period. Data from Environment Canada (2018). b) Mean daily discharge at the outlet of Lower Martin Lake at Baker Creek for the entire hydrometric record (1983-2016) and the study period (September 1, 2014 to December 31, 2016). Data from Water Survey of Canada (2018).

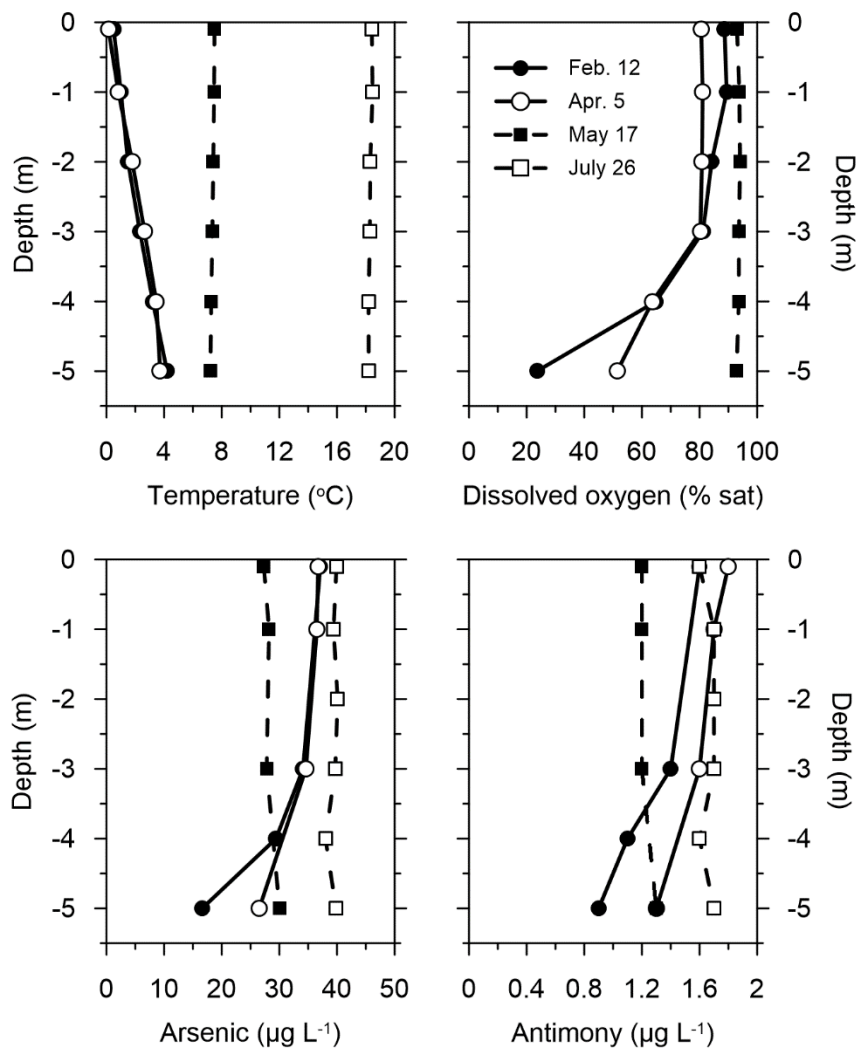
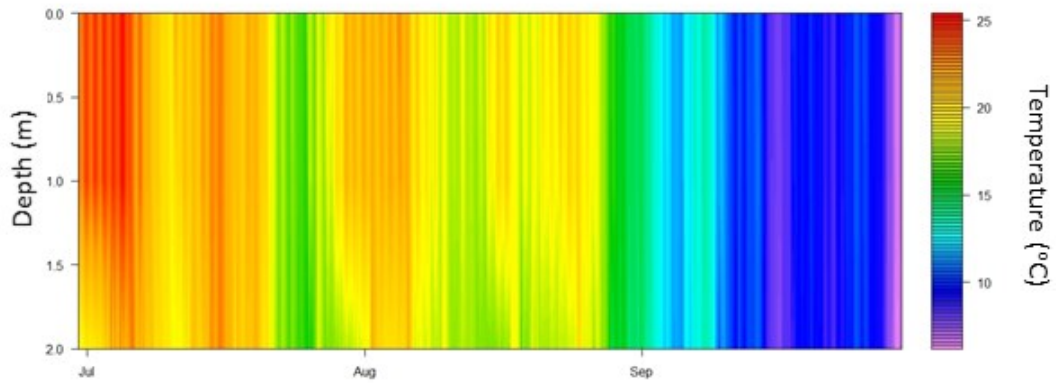


Figure B2: Physical and chemical properties of the water column in Long Lake during the ice-covered and open water season 2016. Note, depth to sediment surface at the sampling location is 5.5 m. Metalloid concentrations refer to the filtered fraction ($< 0.45 \mu\text{m}$) of the sample.

a)



b)

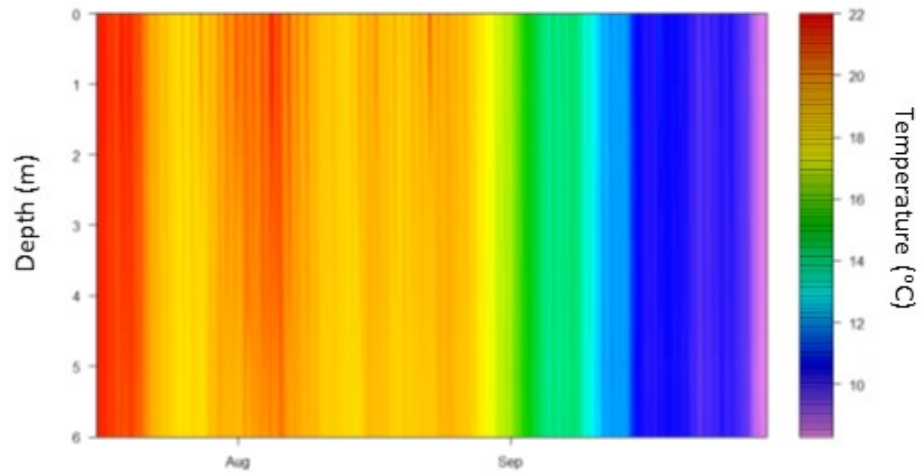


Figure B3: Summer water temperatures in: a) Handle Lake (June 30 – Sept. 29, 2016); and b) Long Lake (July 16 – Sept. 29, 2016). Water temperatures were recorded with iButton (iBCod L) temperature loggers (AlphaMach, Ste-Julie, QC) at depths of 1 and 2 m in Handle Lake and 1, 2, 3, 4, 5, and 6 m in Long Lake. Figures created with “rLakeAnalyzer” package in R v.3.4.1 (R core team, 2017).

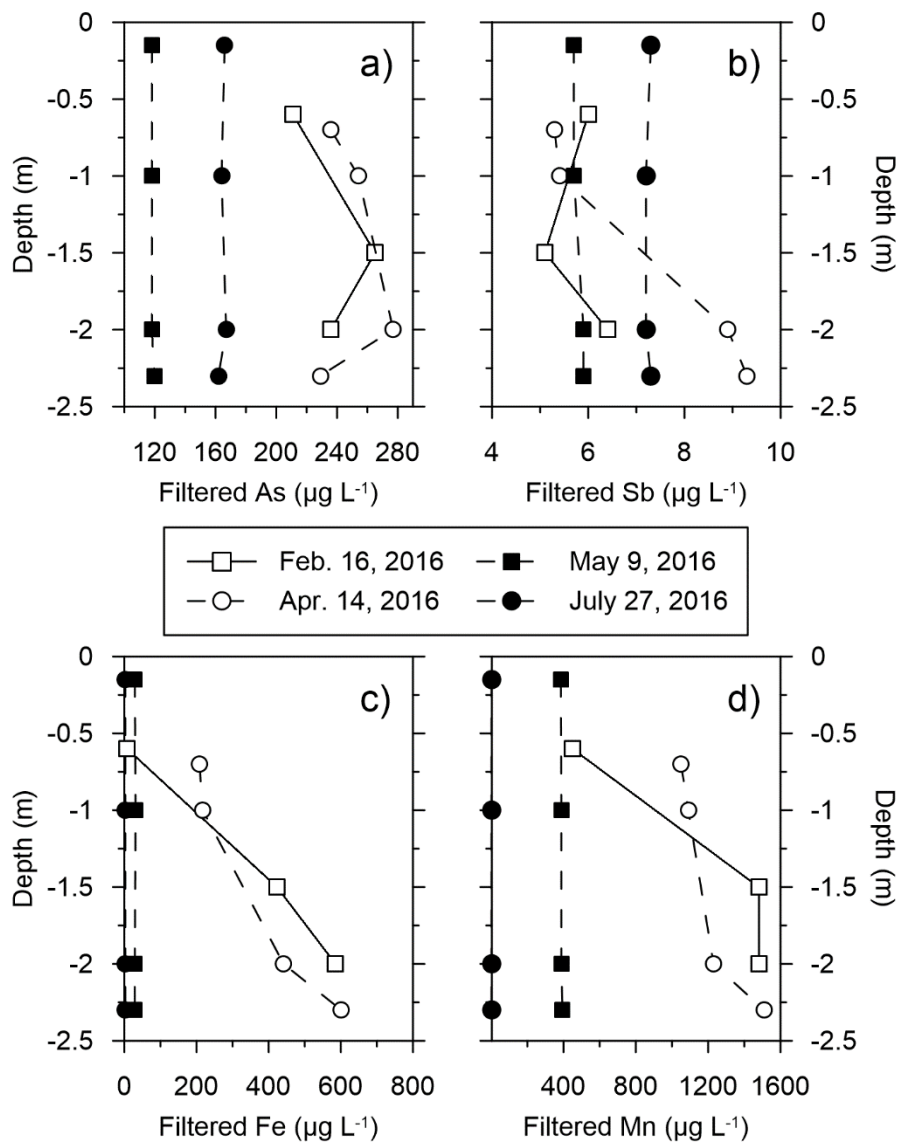


Figure B4: Water column profile concentrations of As, Sb, Fe and Mn in Handle Lake during open water and under ice conditions. Note, under ice sampling depths represent distance from the ice surface and the upper measurement was collected 10 cm below the base of the ice cover.

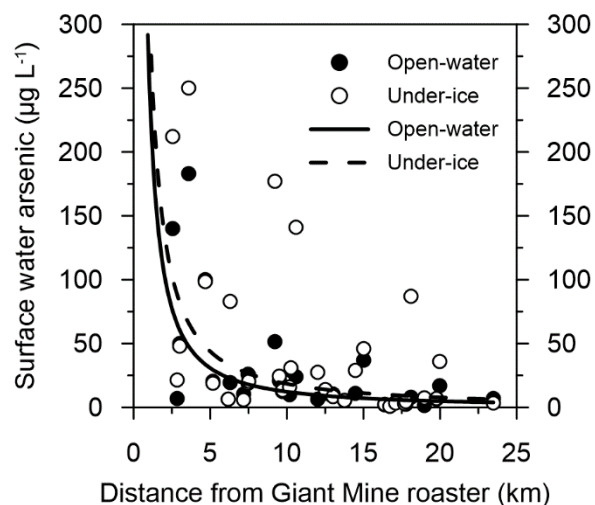


Figure B5: Concentrations of total As in filtered (< 0.45 µm) surface waters with distance from the historic Giant Mine roaster during the two regional lake water surveys undertaken in September (open-water) and March (under-ice). The models of best fit are represented by the following functions: open-water ($\ln(y) = -1.33 \ln(x) + 5.57$; $r^2 = 0.44$; $p < 0.001$; $N = 32$); and under-ice ($\ln(y) = -1.24 \ln(x) + 5.77$; $r^2 = 0.30$; $p < 0.001$; $N = 32$).

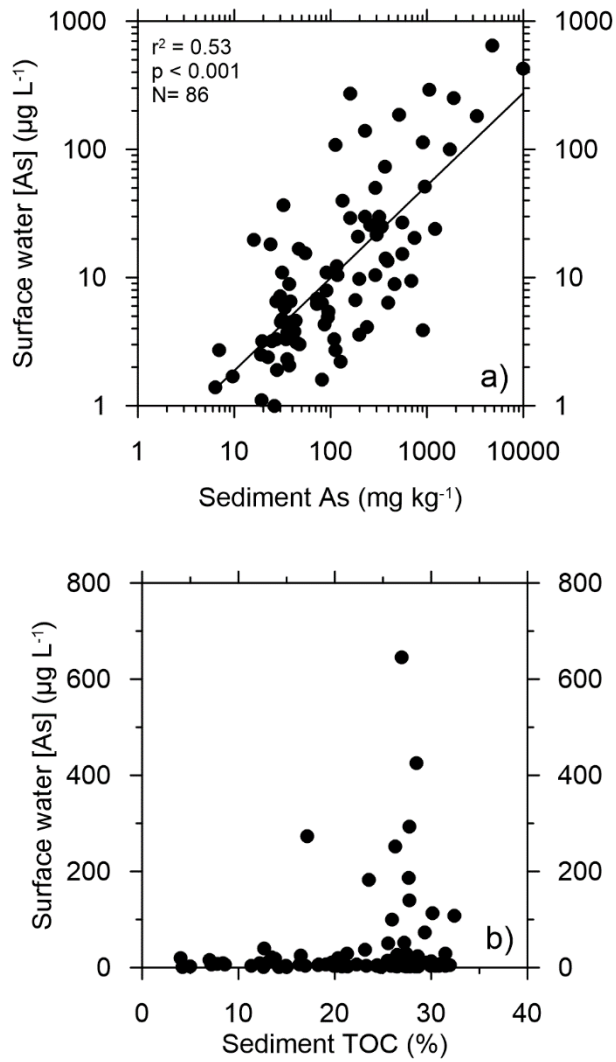


Figure B6: Relationships between surface water As (filtered $< 0.45 \mu\text{m}$) in the open water season and properties of near-surface sediments from the regional lake survey, specifically: a) sediment As concentrations; and b) sediment total organic carbon (TOC).

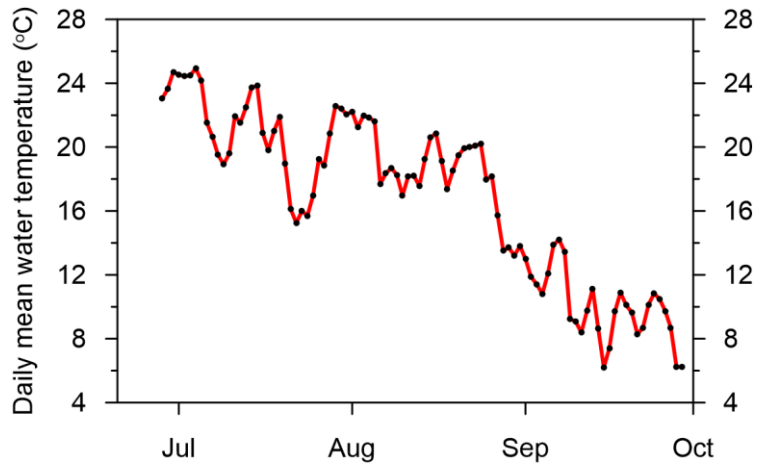


Figure B7: Daily mean water temperatures in BC-20, June 27, 2016 to September 30, 2016. Water temperature was recorded at 40 min intervals at 0.3 m depth with an iButton (iBCod L) temperature logger (AlphaMach, Ste-Julie, QC).

Table B1. Elemental concentrations of lake waters (prior to freeze up in September 2015) and of lake ice at the end of winter in April 2016. No white ice was observed at Handle Lake or Long Lake. Data for black ice are results from the depth-integrated sampling of the lake ice.

	BC-20	Handle	Lower Martin	Long Lake
<i>Thickness of ice layers (m)</i>				
White ice	0.12	-	0.19	-
Black ice	0.53	0.59	0.47	0.65
<i>Specific conductivity($\mu\text{S cm}^{-1}$)</i>				
White ice	207	-	129	-
Black ice	12.60	3.80	2.22	2.21
Lake water	408	262	154	427 ^a
[white ice] : [lake water]	0.51	-	0.84	-
Fraction of exclusion (black ice)	0.97	0.98	0.99	> 0.99
<i>Sum of major ions (mg L⁻¹)</i>				
White ice	49	-	30	-
Black ice	2.2	1.5	0.9	1.2
Lake water	87	59	36	141 ^b
[white ice] : [lake water]	0.56	-	0.83	-
Fraction of exclusion (black ice)	0.97	0.97	0.98	0.99
<i>Total unfiltered As ($\mu\text{g L}^{-1}$)</i>				
White ice	535	-	48	-
Black ice	9.7	2.7	0.95	0.79
Lake water	378	157	46	38 ^a
[white ice] : [lake water]	1.42	-	1.05	-
Fraction of exclusion (black ice)	0.97	0.98	0.98	0.98
<i>Total unfiltered Sb ($\mu\text{g L}^{-1}$)</i>				
White ice	4.3	-	1.6	-
Black ice	0.2	0.2	<0.1	0.1
Lake water	8.4	7.5	1.4	2.1
[white ice] : [lake water]	0.51	-	1.14	-
Fraction of exclusion (black ice)	0.98	0.97	0.96	0.95

^aFebruary 12, 2016

^bSeptember 30, 2016

Table B2. Results from nutrient and major ion analyses in surface waters from BC-20. Refer to the methods section in the text for details on the analytical procedures. MDL refers to the laboratory method detection limit.

	Site	Sample date	Ice thickness	TN ¹	DOC ²	TP ³	ChlA ⁴	pH	Ca	Cl	Mg	K	Na
<i>Units</i>			<i>m</i>	<i>mg L⁻¹</i>	<i>mg L⁻¹</i>	<i>mg L⁻¹</i>	<i>µg L⁻¹</i>		<i>mg L⁻¹</i>				
<i>MDL</i>				<i>0.06</i>	<i>0.5</i>	<i>0.002</i>	<i>0.01</i>		<i>0.1</i>	<i>0.7</i>	<i>0.1</i>	<i>0.1</i>	<i>0.1</i>
	BC-20	July 25, 2014	<i>N/A</i>	---	---	---	---	8.5	26.1	6.6	22.6	7.5	14.0
	BC-20	December 19, 2014	0.39	12.80	120	0.500	---	---	118.0	18.8	62.1	17.0	33.1
	BC-20	May 29, 2015	<i>N/A</i>	1.92	39	0.146	---	8.6	30.7	3.0	12.3	3.6	5.7
	BC-20	July 25, 2015	<i>N/A</i>	3.20	42	0.213	5.36	--	23.3	4.0	18.1	5.5	9.7
	BC-20	September 4, 2015	<i>N/A</i>	4.61	53	0.270	---	8.0	40.9	5.0	22.7	6.1	12.1
	BC-20	October 23, 2015	0.09	6.77	61	0.203	---	7.7	55.6	7.4	26.7	8.0	14.8
	BC-20	December 21, 2015	0.28	11.80	108	0.376	---	7.5	101.0	11.4	50.2	14.5	26.0
	BC-20	May 6, 2016	<i>N/A</i>	2.51	18	0.097	0.66	7.4	16.5	1.9	7.1	2.4	3.1
	BC-20	May 31, 2016	<i>N/A</i>	2.23	29	0.203	---	8.4	37.8	3.7	14.3	4.4	6.8
	BC-20	July 27, 2016	<i>N/A</i>	---	56	---	---	--	27.0	3.8	27.5	6.0	10.9
	BC-20	September 30, 2016	<i>N/A</i>	---	69	---	---	8.2	51.5	6.2	31.2	9.0	16.9

¹Total unfiltered nitrogen

²Dissolved organic carbon

³Total unfiltered phosphorous

⁴ChlorophyllA

Table B3. Results from nutrient and major ion analyses in surface waters from Handle Lake. Refer to the methods section in the text for details on the analytical procedures. MDL refers to the laboratory method detection limit.

Site	Sample date	Ice thickness <i>m</i>	TN ¹ <i>mg L⁻¹</i>	DOC ² <i>mg L⁻¹</i>	TP ³ <i>mg L⁻¹</i>	ChlA ⁴ <i>µg L⁻¹</i>	pH <i>pH</i> <i>units</i>	Ca <i>mg L⁻¹</i>	Cl <i>mg L⁻¹</i>	Mg <i>mg L⁻¹</i>	K <i>mg L⁻¹</i>	Na <i>mg L⁻¹</i>
<i>Units</i>												
<i>MDL</i>			0.06	0.5	0.002	0.01		0.1	0.7	0.1	0.1	0.1
Handle Lake	July 23, 2014	<i>N/A</i>	---	---	---	---	---	27.2	4.0	11.8	3.8	6.6
Handle Lake	December 19, 2014	0.35	2.85	24	0.091	---	---	38.1	5.4	15.4	5.0	8.5
Handle Lake	February 27, 2015	0.65	3.20	33	0.098	---	7.3	42.5	6.0	17.6	5.6	9.5
Handle Lake	May 29, 2015	<i>N/A</i>	1.72	36	0.065	---	8.6	29.6	4.4	12.0	3.7	6.3
Handle Lake	September 4, 2015	<i>N/A</i>	2.37	30	0.097	---	8.4	29.3	4.7	13.2	4.1	7.2
Handle Lake	October 29, 2015	0.10	2.59	32	0.093	---	8.0	33.9	5.8	14.1	4.5	7.8
Handle Lake	December 15, 2015	0.30	2.87	40	0.100	---	7.7	38.3	5.8	17.0	5.2	8.9
Handle Lake	February 16, 2016	0.51	3.13	36	0.101	---	7.6	42.7	6.7	19.7	6.0	10.1
Handle Lake	April 14, 2016	0.59	3.65	35	0.117	5.70	7.4	41.7	6.2	18.2	5.6	9.4
Handle Lake	May 9, 2016	<i>N/A</i>	2.41	26	0.088	0.80	7.7	31.0	4.7	13.4	3.7	6.7
Handle Lake	June 10, 2016	<i>N/A</i>	2.05	26	0.075	---	8.7	32.3	5.4	15.1	4.5	7.9
Handle Lake	July 27, 2016	<i>N/A</i>	---	26	---	---	8.5	35.0	5.5	19.2	4.4	7.9
Handle Lake	September 30, 2016	<i>N/A</i>	---	31	---	---	8.2	33.7	5.1	16.0	5.0	8.7

¹Total unfiltered nitrogen

²Dissolved organic carbon

³Total unfiltered phosphorous

⁴ChlorophyllA

Table B4. Results from nutrient and major ion analyses in surface waters from Lower Martin Lake. Refer to the methods section in the text for details on the analytical procedures. MDL refers to the laboratory method detection limit.

	Site	Sample date	Ice thickness	TN¹	DOC²	TP³	ChlA⁴	pH	Ca	Cl	Mg	K	Na
<i>Units</i>			<i>m</i>	<i>mg L⁻¹</i>	<i>mg L⁻¹</i>	<i>mg L⁻¹</i>	<i>µg L⁻¹</i>		<i>mg L⁻¹</i>				
<i>MDL</i>				<i>0.06</i>	<i>0.5</i>	<i>0.002</i>	<i>0.01</i>		<i>0.1</i>	<i>0.7</i>	<i>0.1</i>	<i>0.1</i>	<i>0.1</i>
	Lower Martin	August 15, 2014	<i>N/A</i>	---	---	---	---	---	12.8	4.0	4.5	1.3	3.3
	Lower Martin	February 27, 2015	0.6	3.61	29	0.050	---	6.9	25.2	5.9	7.9	2.4	5.9
	Lower Martin	April 8, 2015	0.84	4.12	31	0.052	---	7.0	29.5	6.7	8.9	2.9	6.4
	Lower Martin	October 29, 2015	0.10	1.87	28	0.032	---	7.8	18.8	5.2	5.7	1.8	4.5
	Lower Martin	February 16, 2016	0.45	2.31	31	0.041	---	7.2	24.8	5.7	8.1	2.6	6.1
	Lower Martin	April 14, 2016	0.66	3.16	32	0.045	---	7.0	27.2	6.5	8.6	3.0	6.2
	Lower Martin	May 6, 2016	0.4	0.57	6	0.013	2.00	7.1	3.7	1.0	0.9	0.4	0.8
	Lower Martin	May 31, 2016	<i>N/A</i>	1.57	23	0.033	---	---	16.8	4.1	5.3	1.5	3.9
	Lower Martin	July 27, 2016	<i>N/A</i>	---	26	---	---	---	18.2	4.5	9.1	1.6	4.1

¹Total unfiltered nitrogen

²Dissolved organic carbon

³Total unfiltered phosphorous

⁴ChlorophyllA

Table B5. Results from nutrient and major ion analyses in surface waters from Long Lake. Refer to the methods section in the text for details on the analytical procedures. MDL refers to the laboratory method detection limit.

	Site	Sample date	Sample depth <i>m</i>	Ice thickness <i>m</i>	TN ¹ <i>mg L⁻¹</i>	DOC ² <i>mg L⁻¹</i>	TP ³ <i>mg L⁻¹</i>	ChlA ⁴ <i>µg L⁻¹</i>	pH	Ca <i>mg L⁻¹</i>	Cl <i>mg L⁻¹</i>	Mg <i>mg L⁻¹</i>	K <i>mg L⁻¹</i>	Na <i>mg L⁻¹</i>
<i>Units</i>					<i>mg L⁻¹</i>	<i>mg L⁻¹</i>	<i>mg L⁻¹</i>	<i>µg L⁻¹</i>		<i>mg L⁻¹</i>	<i>mg L⁻¹</i>	<i>mg L⁻¹</i>	<i>mg L⁻¹</i>	<i>mg L⁻¹</i>
<i>MDL</i>					<i>0.06</i>	<i>0.5</i>	<i>0.002</i>	<i>0.01</i>		<i>0.1</i>	<i>0.7</i>	<i>0.1</i>	<i>0.1</i>	<i>0.1</i>
	Long Lake	April 8, 2015	0.15	1.0	0.79	10	0.012	---	7.7	39.9	72.6	15.4	3.8	32.3
	Long Lake	April 8, 2015	5.00	1.0	0.59	10	0.008	---	7.7	38.9	71.6	15.0	3.7	31.3
	Long Lake	Feb. 12, 2016	0.15	0.5	0.48	9	0.019	---	7.7	38.3	73.4	15.2	3.8	32.5
	Long Lake	Feb. 12, 2016	3.00	0.5	0.47	9	0.017	---	7.5	36.4	71.3	14.8	3.6	31.4
	Long Lake	Feb. 12, 2016	5.00	0.5	0.71	9	0.017	---	7.4	38.5	70.5	15.2	3.9	31.3
	Long Lake	April 5, 2016	0.15	0.65	0.48	9	0.014	4.03	7.7	39.2	72.4	14.9	3.8	32.3
	Long Lake	April 5, 2016	1.00	0.65	0.48	9	0.014	---	7.7	39.0	71.7	14.8	3.7	31.8
	Long Lake	April 5, 2016	3.00	0.65	0.49	9	0.015	---	7.7	38.0	70.7	14.5	3.6	31.4
	Long Lake	April 5, 2016	5.00	0.65	0.58	9	0.015	---	7.5	39.8	72.2	15.1	3.7	32.2
	Long Lake	May 17, 2016	0.15	<i>N/A</i>	0.44	8	0.015	3.32	7.8	32.5	61.2	12.1	2.9	26.8
	Long Lake	May 17, 2016	1.00	<i>N/A</i>	0.46	8	0.015	---	7.8	32.8	62.8	12.6	3.0	27.3
	Long Lake	May 17, 2016	3.00	<i>N/A</i>	0.44	8	0.016	---	7.8	31.8	60.4	12.2	2.9	26.3
	Long Lake	May 17, 2016	5.00	<i>N/A</i>	0.48	8	0.016	---	7.8	31.5	59.0	12.0	2.8	25.7
	Long Lake	July 26, 2016	0.15	<i>N/A</i>	---	7	---	---	8.2	34.9	61.9	16.0	3.0	27.6
	Long Lake	July 26, 2016	1.00	<i>N/A</i>	---	7	---	---	8.1	35.9	62.5	16.7	3.0	27.8
	Long Lake	July 26, 2016	2.00	<i>N/A</i>	---	7	---	---	8.1	36.6	64.0	17.1	3.2	28.4
	Long Lake	July 26, 2016	3.00	<i>N/A</i>	---	7	---	---	8.1	36.3	63.1	16.9	3.1	28.0
	Long Lake	July 26, 2016	4.00	<i>N/A</i>	---	7	---	---	8.1	33.1	56.9	15.6	2.7	25.4
	Long Lake	July 26, 2016	5.00	<i>N/A</i>	---	7	---	---	8.1	36.7	63.7	17.1	3.1	28.3
	Long Lake	Sept. 30, 2016	0.15	<i>N/A</i>	---	7	---	---	8.1	33.9	61.7	12.8	3.2	29.1

¹Total unfiltered nitrogen

²Dissolved organic carbon

³Total unfiltered phosphorous

⁴Chlorophylla

Appendix C: Supporting information for Chapter 5 - Hydrologic control on winter dissolved oxygen mediates arsenic cycling in a small subarctic lake

Comparison of porewater collection methods (Rhizons and dialysis arrays (peepers))

The high water content of lake sediments in Lower Martin Lake required the use of two different methods for sediment porewater collections. Dialysis arrays (peepers) were the preferred method, because larger sample volumes could be collected and there was no risk of drawing water from adjacent depth intervals. Peepers were used in late-winter 2018 and 2019 when the peepers could be fixed in place and there was no concern about the peepers sinking into the sediment during the deployment period. The Rhizon method (outlined in Methods) was used during the open-water season, since it was not possible to deploy peepers in the soft, water-rich sediments in the summer without the peepers sinking into the sediments. Figure C3 includes sediment porewater As data collected using both methods at the end of winter 2018. Porewater As concentrations were comparable for the two collection methods at depths 1 to 4 cm below the sediment boundary. There was disagreement between the peeper and Rhizon profiles in the upper sections of the profiles, likely because sediments porewaters were sampled using the Rhizon method > 2 weeks prior to when the peepers were deployed. As indicated in the manuscript, oxidation of the water column was initiated close to the sediment boundary in late-March to early April from benthic production of oxygen. Porewater chemistry collected using peepers reflects mean porewater conditions over a two-week period during this period of oxygen production. Consequently, porewater chemistry reflects an environment that was not in equilibrium. In contrast, porewaters collected with Rhizons represent conditions on the day of collection and were collected when reducing conditions persisted throughout the sediment profile.

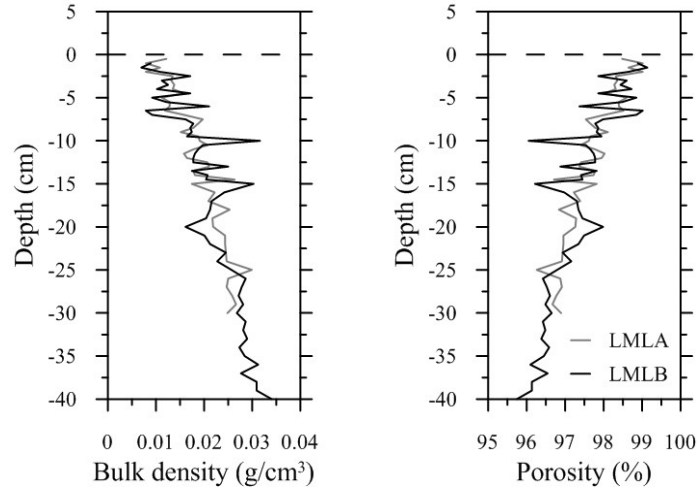


Figure C1: Bulk density and porosity in sediment core profiles from LMLA and LMLB collected September 2017. Porosity estimate based on particle density of 0.8 g cm^{-3} for organic matter. Water content (by weight) was $> 96\%$ in all core intervals for both cores.

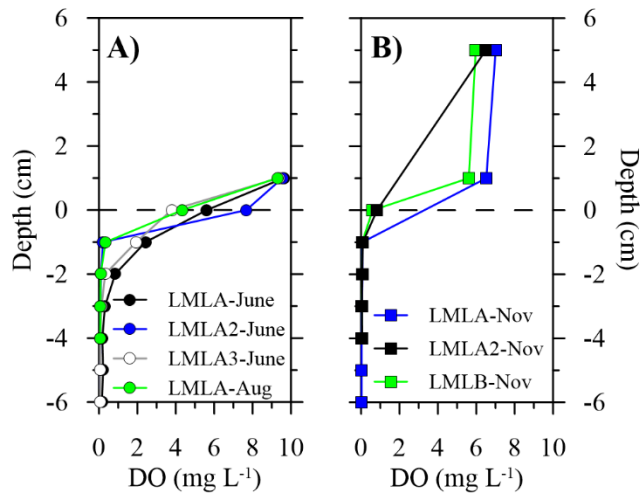


Figure C2.: Dissolved oxygen profiles in sediment porewaters and overlying waters in 2017 during: A) the open-water (June and August); and B) early winter (November) seasons. No oxygen was detected in late-winter sediment porewater profiles.

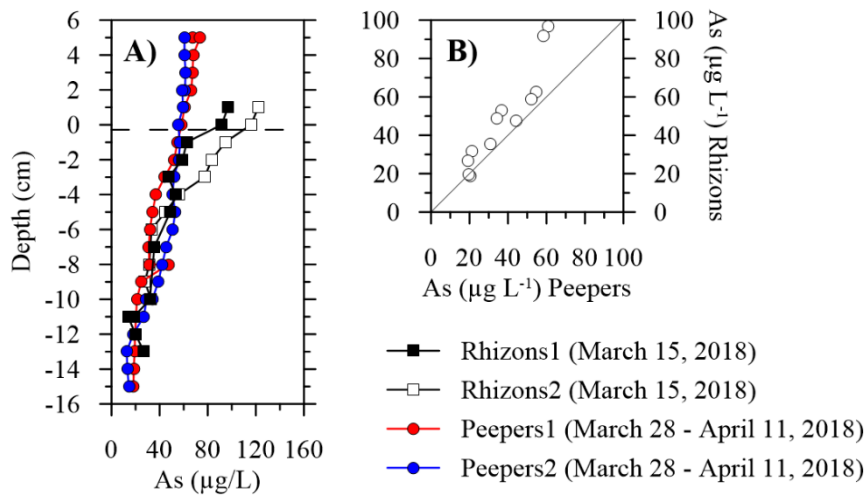


Figure C3: A) Porewater As concentrations in late winter 2018 using two different porewater collection methods (Rhizons and peepers). Note, peepers were deployed during a period when near-surface sediments started to oxidize. This is reflected by the poor association between solute concentrations in the upper portion of the profiles. B) Intercomparison between Rhizon and peeper porewater collection methods.

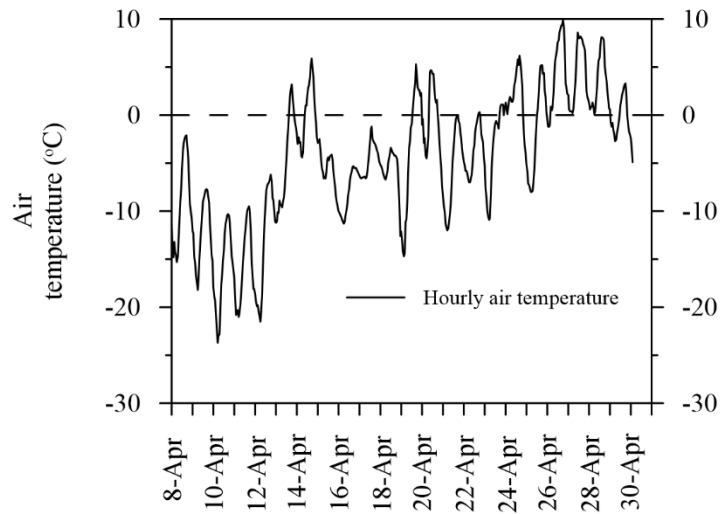


Figure C4: Hourly air temperature recorded at Yellowknife airport during spring 2018. Note, minimum daily air temperature remains above zero for an extended period starting on April 26 and is coincident with rapid snowmelt in the region. Data from Environment and Climate Change Canada (Climate station ID: 2204101) (ECCC, 2019a).

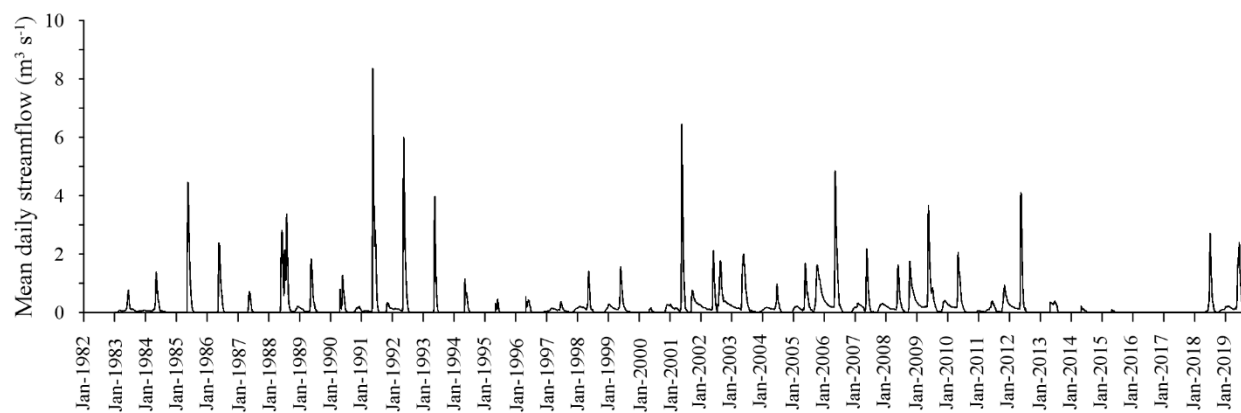


Figure C5: Stream hydrograph at the outlet of Lower Martin Lake, January 1983 to November 2019. Data from Water Survey of Canada station 07SB013 (ECCC, 2019b).

Table C1. Physical properties of Lower Martin Lake sediments (top and bottom of lake sediment cores) and end of winter ice thickness.

Sediment parameter	LMLA	LMLB
Bulk density (g cm ⁻³) (0-3 cm); (25-30 cm)	0.011; 0.026	0.010; 0.027
Water content (%) (0-3 cm); (25-30 cm)	98.5; 97.0	98.6; 96.9
Organic matter content (LOI) (%) (0-3 cm); (28-30 cm)	NA	76; 69
End of winter ice thickness (m) (2018;2019)	0.72; 0.86	0.70; 0.80

Table C2. Solid-phase arsenic mass distribution calculations

As-hosting phase	Total particles	Total particle area (μm^2)	Density (g/m^3) ^a	Wt.% As ^b	Thickness (μm)	Mass Distribution (%) ^c	Areal Distribution (%)
0-2 cm September 2017							
Fe and Mn-oxyhydroxide	174	1237	4280000	3.00	1	39	51
As-sulfide	14	85	3560000	70.03	1	52	3.5
Pyrite	49	1088	5000000	0.20	1	2.7	45
Arsenic trioxide	1	2	3870000	75.74	1	1.7	0.1
Arsenopyrite	2	6	6070000	46.01	1	3.8	0.2
Total	240	2418				100.00	100.00
0-2 cm April 2018							
Fe and Mn-oxyhydroxide	10	43.25	4280000	0.03	1	1.06	1.92
As-sulfide	51	199	3560000	70.03	1	95.11	8.88
Pyrite	60	2004	5000000	0.20	1	3.83	89.19
Total	112	2206				100.00	100.00
13-15 cm April 2018							
Fe and Mn-oxyhydroxide	23	157	4280000	3.00	1	0.30	0.86
As-sulfide	588	2599	3560000	70.03	1	97.36	14.20
Pyrite	481	15541	5000000	0.20	1	2.34	84.94
Arsenic trioxide	28	111	3870000	75.74	1	4.89	0.61
Total	1120	18408				100.00	100.00

^aFrom Mineralogical Society of America (2000)

^bFrom Schuh et al. (2018)

^cSee Methods in Chapter 5 for calculation of mass distribution

References

- ECCC. 2019a. Historical Canadian climate data. Extracted from the Environment and Climate Change Canada Historical Climate Data website (https://climate.weather.gc.ca/historical_data/search_historic_data_e.html) on December 4, 2019.
- ECCC. 2019b. Historical data from Water Survey of Canada station 07SB013. Extracted from the Environment and Climate Change Canada Historical Hydrometric Data web site (https://wateroffice.ec.gc.ca/mainmenu/historical_data_index_e.html) on December 14, 2019.
- Mineralogical Society of America. 2000. Handbook of Mineralogy, Volume IV. Mineral Data Publishing, Chantilly, VA.
- Schuh, C. E., H. E. Jamieson, M. J. Palmer, and A. J. Martin. 2018. Solid-phase speciation and post-depositional mobility of arsenic in lake sediments impacted by ore roasting at legacy gold mines in the Yellowknife area , Northwest Territories , Canada. *Appl. Geochemistry* **91**: 208–220. doi:10.1016/j.apgeochem.2017.10.025

Appendix D: Supporting information for Chapter 6 - Terrestrial and aquatic fluxes of arsenic in a subarctic landscape during years with contrasting hydrological conditions

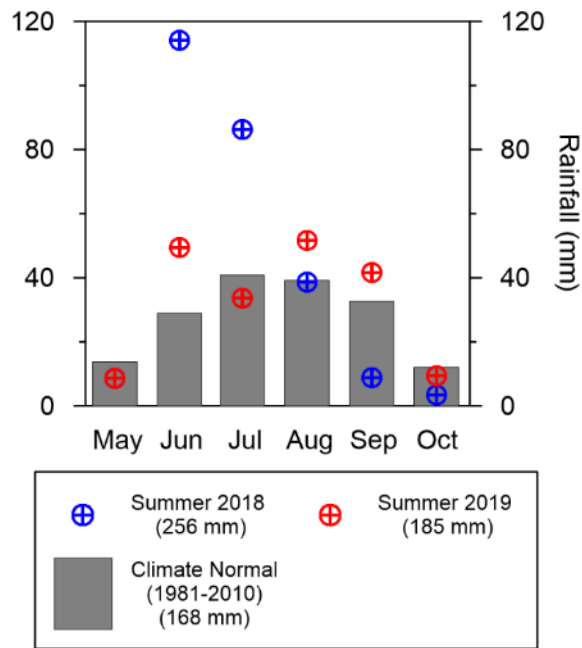


Figure D1: Monthly rainfall during the study period and for climate normals (1981-2010).

Table D1. Precipitation chemistry. Concentrations measured in $\mu\text{g L}^{-1}$ and reflect unfiltered samples.

	N	Date collected	As	Sb	Fe
Rain	2	June 28, 2018	All BDL (<0.2)	All BDL (<0.1)	All BDL (<5)
Snow	8	April 9, 2018	All BDL (<0.2)	All BDL (<0.1)	20(\pm 12)

Table D2. Seasonal As sedimentary fluxes ($\mu\text{g m}^{-2} \text{ day}^{-1}$) calculated as the residual from the watershed mass balance.

	2017-18	2018-19
Sept. - Nov.	0.8	-2.6
Nov. - April	703	94
April	-2294	-358
May	-2238	-509
June - Sept.	505	536
Annual mean	166	402

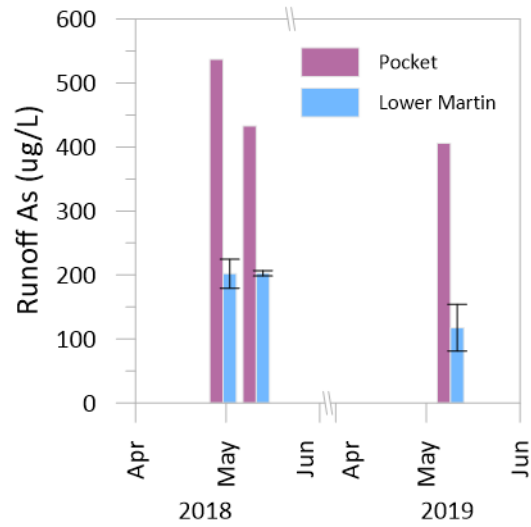


Figure D2: Relationship between runoff As chemistry at Pocket subcatchment and the Lower Martin Lake catchment. Lower Martin runoff samples were collected around the perimeter of the lake in May of 2018 and 2019. Runoff As at Lower Martin Lake was $2.7 (\pm 0.7 \text{ stdev})$ times lower than at Pocket Lake.

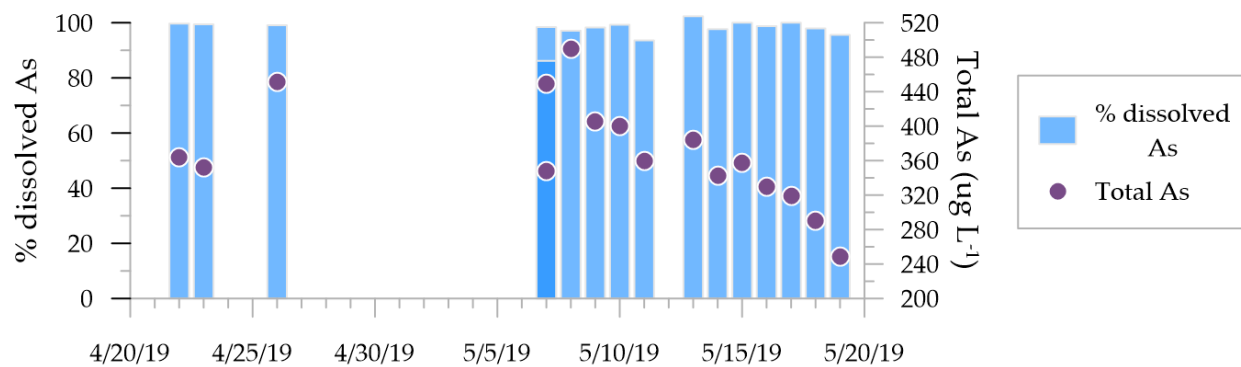
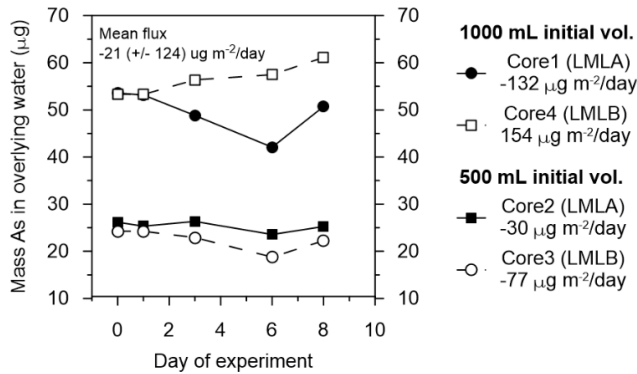
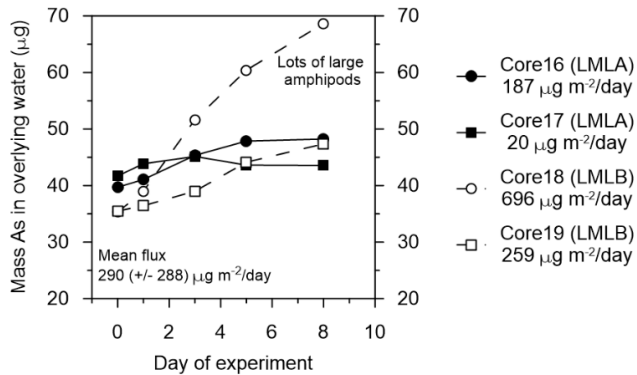


Figure D3: Total As ($\mu\text{g L}^{-1}$) and percentage of total As in the filtered fraction of surface runoff in 2019.

September 2017
(10°C)



July 2018
(19°C)



March 2018
(3°C)

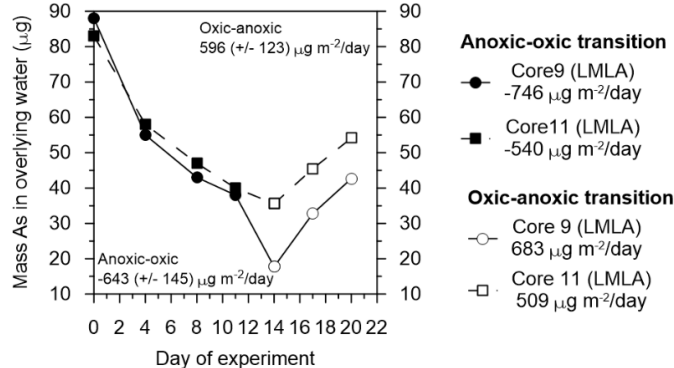


Figure D4: Daily As mass (μg) in the sediment incubation experiments. Overlying water conditions were well oxygenated in the September and July incubations (DO saturation > 30%). Oxygen conditions were manipulated in the March incubations. Overlying waters were anoxic ($< 0.5 \text{ mg L}^{-1} \text{ O}_2$) on initial collection of cores in March 2018 and were reoxygenated on Day 1 through removal of core caps. On Day 14 of the experiment the overlying water in the cores were purged of oxygen using high purity N_2 gas and remained below $0.5 \text{ mg L}^{-1} \text{ O}_2$ until the end of the experiment.

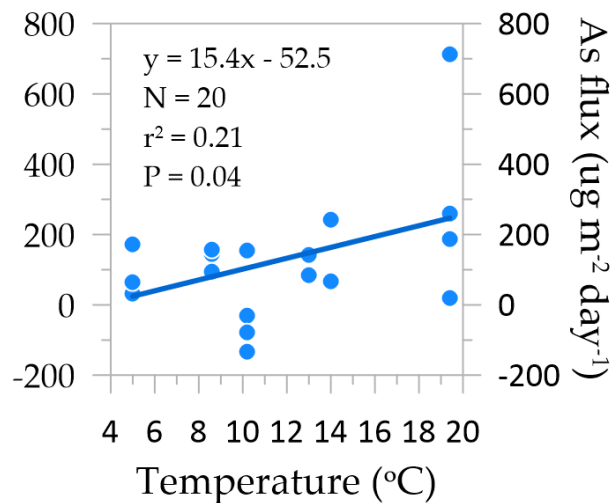


Figure D5: Arsenic flux – temperature relationships using individual flux measurements from diffusive flux model and incubations.

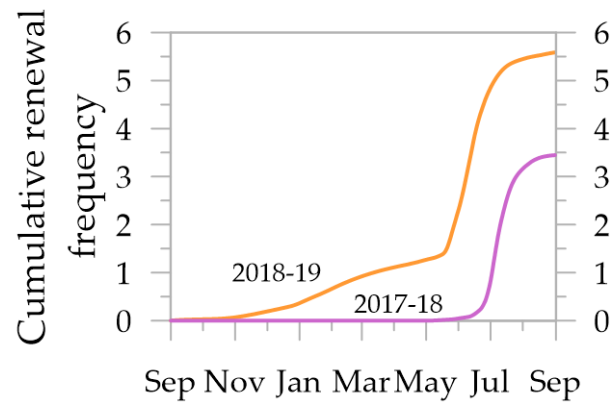


Figure D6: The cumulative lake water renewal frequency for Lower Martin Lake in the two study years. Renewal rate calculated as the ratio of cumulative discharge (m^3) at the outlet of Lower Martin Lake and the mean lake volume for the two study years.

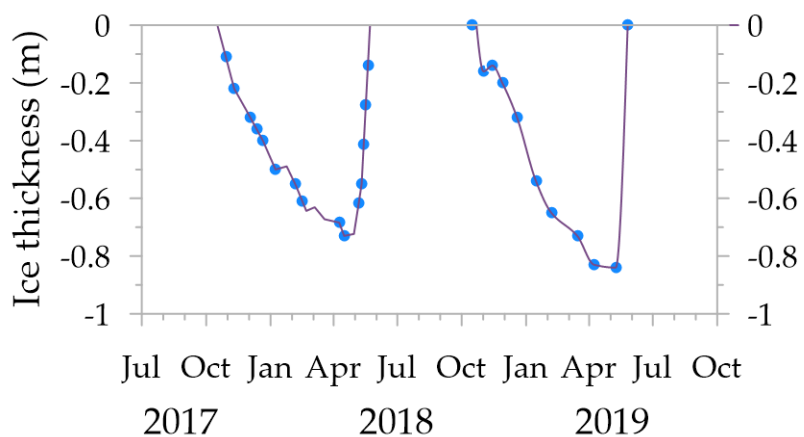


Figure D7: Lake ice thickness 2017-2019. Discrete ice thickness measurements are represented as points, and thicknesses between sampling depths, via cubic spline interpolation, are represented as the line.